SEQUENTIAL MICROBIAL-PHOTOCATALYTIC PROCESS FOR DEGRADATION OF NEONICOTINOID PESTICIDE

A Thesis
submitted in fulfillment of the requirement
for the award of degree of

DOCTOR OF PHILOSOPHY

IN

BIOTECHNOLOGY

TEENA SHARMA

Registration No. 900900019

DEPARTMENT OF BIOTECHNOLOGY
THAPAR UNIVERSITY, PATIALA-147004
PUNJAB (INDIA)

JUNE 2015

Dedicated to My Loving

Husband & Daughter

Abhishree

CERTIFICATE

This is to certify that the thesis entitled "***Sequential Microbial-Photocatalytic Process for Degradation of neonicotinoid Pesticide***" being submitted by Ms. Teena Sharma in fulfillment of the requirement for the award of the degree of Doctor of Philosophy in Department of Biotechnology, Thapar University, Patiala, is a record of candidate's own independent and original research work carried out by her under our supervision and guidance. The material embodied in this thesis has not been submitted in part or full to any other University or Institute for the award of any degree.

Dr. Anita Rajor
Associate Professor
School of Energy & Environment
Thapar University, Patiala-147004
Punjab (India)

Dr. Amrit Pal Toor
Professor
Dr. S.S.Bhatnagar UICET
Panjab University,
Chandigarh-160014 India

CANDIDATE'S DECLARATION

I, hereby declare that the work presented in the thesis entitled "***Sequential Microbial-Photocatalytic Process for Degradation of neonicotinoid Pesticide***" in fulfillment of the requirement for the award of the degree of Doctor of Philosophy being submitted to Department of Biotechnology, Thapar University, Patiala, is an authentic record of my own work carried out under the supervision of Dr. Anita Rajor from School of Energy & Environment, Thapar University, Patiala (India) and Dr. Amrit Pal Toor from Dr. S.S.B.UCIET, Panjab University, Chandigarh (India) . The matter embodied in this thesis has not been submitted in part or full to any other university or institute for the award of any degree in India or abroad.

Place: Patiala

Date:

Teena Sharma

(Teena Sharma)

ACKNOWLEDGEMENTS

God helps those who help themselves by being there with us and blessing us at all times provided we dare to dream and dare to achieve those dreams. First of all I thank the God almighty for giving me a breakthrough whenever I broke down and blessed me with whatever I have ever achieved.

I take this opportunity to thank my supervisors ***Dr. Anita Rajor*** *Associate Professor, School of Energy and Environment, Thapar University, Patiala, and* ***Dr. Amrit Pal Toor****, Dr.SSBUICET, PanjabUniversity,Chandigarh for providing me an opportunity to work under their guidance and supervision, assisting with all kinds of support, inspiration, wide counsel, constant encouragement, prudent advices, valuable suggestions, comments and patience throughout the Ph.D. work.*

I am profoundly obliged to ***Dr. Dinesh Goyal****, Professor and Head, Department of Biotechnology, Thapar University, Patiala for his good wishes and motivation.*

I would like to thank my doctoral committee members ***Dr. Dinesh Goyal****; and* ***Dr. Susheel Mittal*** *for their encouragement, constructive criticism and inspirations.*

The support of friends in every walk of life also acts as an essential component for success. A trustable friend all through the way, I am thankful to my friends ***Mr. Anoop, Mr. Kunal, Mr. Abhishek, Ms Taran, Ms Priyanka, Ms Kamal*** *and* ***Mr. Summit*** *for their support and lively discussions during the experimental work. A special thanks to* ***Mr. Inderpreet Singh Grover****, who has always helped me with his valuable advices, and guidance through all obstacles.*

I am really grateful to all the faculty members and my lab mates of the Department of Biotechnology Thapar University for enlightening me with their knowledge and inputs.

I would like to thank staff of the School of Energy and Environment, Thapar University, Patiala for the constant official help and cooperation.

Most of the results described in this thesis would not be possible without the help of Sophisticated Analytical Instrumentation Facility Panjab University, Chandigarh.

I feel a deep sense of gratitude for my parents and in-laws who have always showered unconditional love on me, encouraged and supported me in every aspect. They formed a part of my vision and taught me the good things that really matter in life.

For any successful accomplishment, the support and faith of near and dear ones is a must. I am totally indebted to my loving husband and my daughter ***Abhishree*** *for their love, patience, understanding and endurance during the whole tenure of the work.*

I gratefully acknowledge Department of Science & Technology, New Delhi for providing me financial support under DST WOS-A project.

Teena Sharma
(Teena Sharma)

LIST OF PUBLICATIONS/CONFRENCES

PUBLICATIONS

1. Teena Sharma, Amrit Pal Toor, Anita Rajor (2015). Photocatalytic degradation of imidacloprid in soil: Application of response surface methodology for optimization of parameters. RSC Advances, 5: 25059–25065.
2. Teena Sharma, Anita Rajor, Amrit Pal Toor (2015). Potential of *Enterobacter* sp. strain ATA1 on imidacloprid degradation in soil microcosm: Effects of various parameters. Environmental Progress and Sustainable Energy, DOI 10.1002/ep.12115
3. Teena Sharma, Anita Rajor and Amrit Pal Toor (2014). Isolation and Characterization of *Enterobacter* strain ATA1 Capable of Degrading Imidacloprid in Liquid by Co-metabolism. Bioremediation Journal, 18:227–235.

CONFERENCES

1. Teena Sharma, Amrit Pal Toor and Anita Rajor (2013) Photocatalytic degradation of insecticides on soil surfaces:A Review Advanced oxidation Processes (AOP), 21-23rd November 2013, Thapar University, Patiala
2. Teena Sharma, Anita Rajor and Amrit Pal Toor (2014) Biodegradation of imidacloprid by bacterium strain ATA1 isolated from Paddy field soil organized by Him Science Association, 17-18th May 2014, Shimla.
3. Teena Sharma, Amrit Pal Toor and Anita Rajor (2015) Photocatalytic degradation of imidacloprid on soil surfaces using TiO_2 and UV light (AOP), 25-28th September 2015. Munnar, Kerala.
4. Teena Sharma, Amrit Pal Toor and Anita Rajor (2015) Photocatalytic degradation of IMI in soil using Response surface methodology. National seminar on Sustainable Renewable Energy Generation, 25th March 2015, Panjab University, Chandigarh.

ABSTRACT

Imidacloprid (IMI) insecticide was selected from the neonicotinoid family on the basis of its intensive usage throughout the year for wheat and paddy crop in Punjab (India). Soil samples for isolation of bacteria were collected from paddy field and five bacterial strains (T1-T5) were isolated on enrichment media (NB) containing 50 mgL^{-1} of IMI. Out of these five, strain T1 and T5 exhibited the highest growth and further identified/characterized on the basis of morphological, biochemical, physiological characterization and phylogenetic analysis using 16S rRNA sequencing. Results showed that both of the isolates are a member of *Enterobacter sp.* and hereafter mentioned as ATA1 and ATA2. Phylogenetic tree were constructed for both isolates by neighbour joining method using GenBank-NCBI database. A close similarity of strain ATA1 was confirmed with *Enterobacter asburiae* JCM6051 (AB004744) with 98.1% gene sequence whereas strain ATA2 has shown 98% similarity with *Enterobacter hormaechei* ATCC 49162 strain (AZ508302). Both isolates were referred as *Enterobacter sp.* ATA1 and *Enterobacter sp.* ATA2. A significant growth shown by strain ATA1 as compared to strain ATA2 was further selected for degradation studies. Initially, tolerance to IMI at various concentrations (50-150 mgL^{-1}) in minimal media was performed and observed more growth for 50 mgL^{-1} as compare IMI=100 mgL^{-1} and 150 mg L^{-1}. Various co-metabolites (Maltose, Sucrose, Fructose, Lactose and Glucose) were used as additional source of carbon for both growth and degradation studies in minimal media broth. Among, these studied co-metabolites, glucose (0.1% w/v) found to show maximum growth, indicated its effective use as carbon source than the others. Co-metabolite degradation studies were performed in minimal media with glucose (MMG 0.1%) under the optimized concentration of IMI (50 mgL^{-1}) and glucose (0.1% w/v) and degradation of ~45% was confirmed at 3rd of incubation. No notable change was observed upto 15 days of degradation time. LC chromatogram analysis supported the results for its degradation and metabolites formation till 15 days of incubation. Microcosm study in soil was performed and various parameters (pH, inoculums size, initial concentration of imidacloprid and flooding of soil) were optimized under laboratory conditions. At variable pH = 1-11, highest degradation (68%) was percieved at pH = 7 after 15 days of incubation for fixed concentration of IMI (50 $mgkg^{-1}$ of soil). Effect of initial concentration of IMI (25-100 $mgkg^{-1}$of IMI) at pH = 7 showed that 50 $mgkg^{-1}$ of IMI lead to better degradation (74%) and hence considered as optimum. These results were further supported by GC-MS chromatograms where peak

height/peak area for IMI is least while using its concentartion = 50 $mgkg^{-1}$, revealing it to be an optimum amount. Highest degradation of IMI (74%) was obtained at inoculum size of 2×10^7 CFU g^{-1} soil and confirmation by GC-MS chromatograms.Influence of flooding/non-flodding conditions for degradtion of IMI, was studied and degradation was found to be more in non-flooded (60%) conditions as compared to flooded (50%). Identification of metabolites carrioed out through GC-MS analysis during microbial degradation of IMI. Six metabolites (I-1 to I-6) have been identified through their mass spectra.

Photocatalytic degradation studies were performed using TiO_2 as photocatalyst in soil. Photolysis and adsorption studies in soil confirmed insignificant change in the concentration of IMI when kept under dark for 18 h. Moreover, photolysis of IMI in soil also showed no notable change in its amount. Optimization of catalyst dose was done by varying TiO_2 amount from $0.1gkg^{-1}$ to $0.5gkg^{-1}$ and it was observed that degradation increases with increase in amount upto 0.3 gkg^{-1} and thereafter it decreases. This optimum TiO_2 dose was further used for optimizing other four experimental parameters namely UV light intensity, initial conc. of IMI, pH, and depth of soil using central composite design (CCD) based on response surface methodology (RSM).Analysis of experimental data was supported by Design-Expert Software (trial version 9.0.3.1, Stat-Ease, Inc., MN, USA). The 30 experimental set up obtained by RSM were experimentally performed and the obtained results have been plotted –ln(C/Co) vs. Time. For all the experiments, plots were straight line with regression values from 0.993 to 0.974, indicating that degradation of IMI followed the L-H kinetics and pseudo first order kinetics. Highest degradation of 83% was achieved (pH = 3, intensity of light = 30 Wm^{-2} and initial IMI = 10 mgL^{-1}) after 18 h of UV light irradiation and the corresponding apparent rate constant (k) was determined to be 15×10^{-4} min^{-1} followed by 9.3×10^{-3} min^{-1}.

Adequacy and significance of the studied model was verified by applying ANNOVA test with very low (<0.0001) probability value (P) for A (pH) and D (concentration of IMI) in comparison to other parameters B (intensity of light) and C (depth of soil). Additionally, adequacy of selected model (response surface reduced quadratic model) with real system was confirmed by analyzing the correlation between observed and predicted values. The response factor of calculated residual values showed that all data points lie close to straight line and within 95% confidence intervals line with mean values near zero confirming the good correlation between experimental and predicted values. Moreover, identification and probable mechanism involved for the formation of various intermediates during the photodegradation

of IMI with quantitative estimation of various ions (nitrate, nitrite, and chloride) was also carried out. Based upon the results obtained, a probable mechanism for conversion of one intermediate into another during decomposition of imidacloprid, and a stoichiometric mass balanced equation were being proposed.

Sequential studies were performed for microbial-photocatalytic (MP) and photocatalytic-microbial degradation processes (PM). It was found that residual amount of IMI after 15 day + 18 h of degradation in MP process (~2.6 mgL^{-1} = 96%) is significantly lower than that found in PM process (~7.0 mgL^{-1} = 87%) confirming betterment of former process. Results were further verified by time course analysis of common metabolite (m/z = 128 & 228) after LC-MS analysis. It was found that in case of MP process the metabolites became highest of their concentration in the initial 5 days of incubation and thereafter start degrading or inter-converting into other compounds. However, for PM process an opposite has been observed where the formation of these intermediates continues till 15 d + 18 h of degradation. These results confirmed the superiority of MP process comparative to PM process. In order to find out the optimum degradation time for mineralization of IMI, samples obtained after 5^{th} and 10^{th} day of microbial degradation were further subjected to the photocatalytic degradation under similar conditions and were analyzed for LC-MS spectrum. It was observed that more number of metabolite were formed (reflected by number of peaks) after 15 d + 18 h of degradation in relation with 5 d + 18 h and 10 d + 18 h. This clearly suggested that time of 15 d + 18 h is optimum for mineralization of IMI under the conditions specified in present study. However, not much significant difference in degradation of IMI was obseved after 10^{th} and 15^{th} day of incubation under the optimized conditions. Hence, LC-MS analysis was performed and results showed that despite of almost same degradation after 10^{th} and 15^{th} day the formation of metabolites is more in later. Therefore, it can be concluded that interms of mineralization 15^{th} day is better compared to 10th day.

TABLE OF CONTENTS

LIST OF TABLES

LIST OF FIGURES

LIST OF SYMBOLS/ABBERIVATIONS

Abbreviation	Word(s)
%	Percent
$^{\cdot}OH$	Hydroxyl Radical
°C	Degree celsius
µg	Micro gram
2,4,6-TCP	2,4,6-Trichlorophenol
2,4-DCP	2,4-dichlorophenol
2-CP	2-chlorophenol
Å	Angstrom
AOP	Advanced Oxidation Process
BET	Brunauer-Emmett-Teller
BLAST	Basic Local Alignment Search Tool
bp	Basepair
C	Catalyzer
CA	Cyanuric acid
CB	Conduction band
CCD	Central Composite Design
CFU	Colony Forming Units
Cl^-	Chloride
cm	Centimeter
COD	Chemical Oxygen Demand
d	Days
DNA	Deoxy Ribonucleic Acid
DT_{50}	Dissipiation Time
e^-	Electron
EDTA	Ehtylene Diamine Tetra Acetic acid
Eg	Band gap energy
ESI	Electrospray Ionization
eV	Electron volt
g	Gram
$g\ m^{-3}$	Gram per meter cube
g/L	Gram per litre
GC-MS	Gas Chromatography coupled with Mass Spectrum

H	Henry's Constant
h	Hour
h^+	Hole
H_2O	Water
H_2O_2	Hydrogen peroxide
H_2S	Hydrogen sulphide
HCH	Hexachlorocyclohexane
HPLC	High Performance Liquid Chromatography
I-1 to I-6	Identified photoproduced intermediates of imidacloprid
IC	Ion Chromatograph
IMI	Imidacloprid
K_{OC}	Soil Adsorption Coefficient
K_{OW}	Partition Coefficient
LC-MS	Liquid Chromatography Mass Spectrum
m^2g^{-1}	Meter square per gram
mg kg^{-1}	Milligram Per Kilogram
mgL^{-1}	Milligram Per Litre
min	Minute
mL	Milliliter
ml min^{-1}.	Milliliter Per Minute
MM	Minimal Media
MMG	Minimal Medium with Glucose
MP	Microbial followed by Photocatalytic
MPMC	3,4-xylyl N-methyl carbamate
MR	Methy red
MRM	Multiple Reaction Monitoring
NB	Nutrient Broth
NCBI	National Centre for Biotechnology Information
NHE	Normal Hydrogen Electrode
nm	Nanometer
NO_3^-	Nitrate
$O_2^{\bullet-}$	Superoxide radical
O_3	Ozone
OC	Organic Carbon
OD	Optical Density
Ox1	Oxidant
P	Available phosphorus

P25	Commercially available P25-TiO2
PCP	Pentachlorophenol
PCR	Polymerase Chain Reaction
PM	Photocatalytic followed by Microbial
PNP	p-nitrophenol
ppb	Parts Per Billion
ppm	Parts Per Million
RB	Reactive Black
Red1	Reducer
RNA	Ribonucleic Acid
rpm	Revolutions per minute
RSM	Response Surface Methodology
$S_2O_3^{2-}$	Thiosulfates
sec	Seconds
SIM	Sulfide Indole Motility
SO_3^{2-}	Sulfites
SO_4^{2-}	Sulfates
$t_{1/2}$	Half life
TiO_2	Titanium dioxide
USEPA	United State Environmental Protection Agency
UV	Ultra voilet
VB	Valance band
Vis	Visible
VP	Voges Proskauer
wt%	Weight Percentage
λ	Wavelength

1. INTRODUCTION AND LITERATURE SURVEY

1.1 Pesticides

Increased demand for food grains necessitates the production of vast amount of agricultural crops in each season. As a result, huge amount of agrochemicals such as pesticides are being used to increase the crops yield. Pesticides are the substances used to kill/repel/reduce or control some types of plant or animal (considered to be pests) to further enhance the production of crops (Estevez et al. 2008; Ahmed et al. 2001). Since, there are variations in the identity, physical and chemical properties of pesticides, therefore classification is necessary under their respective group. These substances are classified on the basis of their target organisms (herbicides, fungicides, insecticides etc.), chemical structure (organic and inorganic pesticides) and physical state (Drum, 1980). The chemical classification of pesticides is reported to be most useful classification in the field of pesticides due to its intimation of the efficacy, physical and chemical properties of the respective pesticides. Based upon the chemical nature of active ingredients, pesticides can be chemically classified into different groups namely; organochlorines, organophosphorous, carbamates, pyrethrin and pyrethroids (Buchel, 1983). Organochlorines are the first synthetic organic insecticides to be used in agriculture for the control of a wide range of insects. Some of the commonly used organochlorine pesticides includes DDT, lindane, endosulfan, aldrin, dieldrin and chlordane. Another class is organophosphorous insecticides, contains a phosphate group in its moiety, generally more toxic to invertebrates and vertebrates act as cholinesterase inhibitors that lead to a permanent destruction of acetylcholine neurotransmitter across a synapse. Some common examples of this family are: parathion, malathion, and diaznon. Carbamates are organic pesticides and are derived from carbamic acid. These insecticides possess high mammalian and insect toxicities. These insecticides works by inhibiting cholinesterase and differ from organophosphorous in terms of its species specificity and is reversible in nature (Drum, 1980). Some widely used members of this class are carbaryl, carbofuran and aminocarb. Pyrethroids are synthetically resembles to the naturally occurring pyrethrins which is an product of pyrethrum plant (*Chrysanthemum cinerariaefolium*). These pesticides are found to be potent poison which further causes threat to wildlife and also have a great influence on non-target organisms. These substances undergo many natural processes (harmful or beneficial) like adsorption, transfer, breakdown and degradation, when released into the

environment. Once they enter from the surroundings into food chain undergoes biomagnifications and their concentration is found to be increased at each level. For example, a study on residues of pesticides in vegetable, milk products, food products in various regions of Punjab district in India were performed and authors reported (Chahal et al.1997; Joia et al. 2001; Battu et al. 2004) persistence and storage of pesticides in the adipose tissues of human beings. The Irregular and indiscriminate application of these pesticides and their inefficient transfer to target organisms and acute toxicity even at low concentration had lead to the development and hence replacement of these existing pesticides with a new class of insecticides known as neonicotinoids.

1.1.1 Neonicotinoids

It is a relatively new class of synthetic organic insecticide, which are now widely used to control sucking insects (aphids, leafhoppers, whiteflies etc.) around the world. They have described to be ultimate alternatives to organophosphates and carbamates due to much lower application rate as compared to traditionally used insecticides (Schmuck et al. 2003). The global application of all the members of neonicotinoid family (~ 60 %) is considered as seed/soil treatment (Jeschke et al. 2011). This method of application of pesticide was considered to be a "safer" to minimize its impacts on nontarget organisms by reducing drift (Ahmed et al. 2001; Koch et al. 2005).

Generally, It has been found that the systemic activity of pesticides increases with increasing solubility due to consistency in the distribution of the active ingredient in the formulation (Koltzenburg et al. 2010) which further increased bioavailability of the pesticide (Pierobon et al. 2008). Most neonicotinoids are water-soluble and their solubility is dependent upon various factors such as pH, temperature and their physical state (PPDB, 2012). Due to moderate to high solubility of neonicotinoid, efficiency of these insecticides is confirmed to be more and further enhance the uptake of active ingredients. These systemic products were found to show more benefit as compared to other non-systemic products in terms of resistance to pest by treated plants (Dieckmann et al. 2010a). Moreover, members of this family of pesticides break down slowly in the environment, taken up by the plant to provide protection from insects as the plant grows. Neonicotinoids works by interfering with the transmission of stimuli in an insect's nervous system and the binding of the chemical with acetylcholine receptors results in paralysis and death of the insect (Iwaya & Kagabu, 1998).

Among variety of members in this family, the first nicotine-based insecticide, imidacloprid (IMI) was introduced into the USA by Bayer Crop Science in 1991. Imidacloprid [(*E Z*)-1-(6-chloro-3-pyridylmethyl)-*N*-nitroimidazolidin-2-ylideneamine (Fig. 1.1), registered globally in ~120 countries including India (Krohn and Helliponter, 2002) has the molecular formula $C_9H_{10}ClN_5O_2$ and molecular weight of 255.7 g/mol (Table1). This systemic chloronicotinoid insecticide is used for soil and seeds applications for the control of various insects namely aphids, thrips, whiteflies, termites, turf insects etc. High insecticidal activity at very low application rate makes IMI a promising insecticide which works (Yamamoto and Casida, 1999) by complete irreversible blockage of nicotinic acetylcholine receptors in central nervous system of insects.

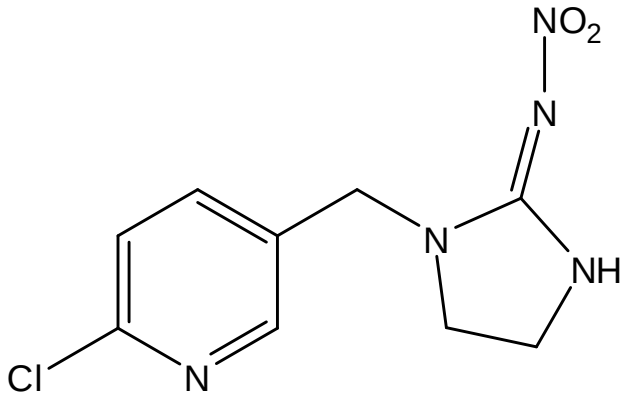

Fig. 1.1 Structural formula for Imidacloprid

Since, the behaviour of any pesticide results from the interactions between the chemicals with various components of the environment. Therefore, pesticides herein specifically IMI once applied can undergo various routes of dissipation in the environment. The major routes for dissipation include adsorption, transfer (runoff, leaching etc.,) and degradation (photodegradation, chemical degradation, and microbial degradation).

As, IMI possess variations in half life ($t_{1/2}$) from 27 to 229 days, following natural slow degradation process and transformed into some other heteroatoms containing intermediates that are sometimes reported to be more toxic than the parent compounds (Sarkar et al. 2001; Krohn and Hellpointner, 2002). Hence, IMI have been studied for its different modes of medium transformation in the various environmental components (air, water, plants and soil) including its breakdown to other molecules, referred here as fate, and is being discussed.

Table 1.1 : Physical and chemical properties of Imidacloprid

Physical-Chemical Property	Observations	Reference (s)
Appearance	Colourless crystals	Tomlin 2000
CAS number	138261-41-3	Tomlin 2000
Water Solubility	0.510-0.61 g/L @ 20°C	Krohn 1989, reviewed in Mulye 1995 Tomlin 2000
Half life ($t_{1/2}$)	27-229 days	Tomlin 2000
Melting Point	~144 °C	Tomlin 2000
Vapour Pressure	4×10^{-10} Pa @ 20°C	Tomlin 2000, EXTOXNET 1998
Henry's Constant (H)	1.0025×10^{-7} Pa m^3mol^{-1} @ 20°C	Mulye 1995
	2×10^{-10} Pa m^3mol^{-1} @ 20°C	Tomlin 2000
Partition Coefficient (K_{OW})	log P = 0.57 @ 21°C	Tomlin 2000
Soil Adsorption Coefficient (K_{OC})	262.0	Orme and Kegley 2003
	210	Nemeth-Konda et al. 2002
Ultraviolet Absorption	Absorption Wavelength (λ) (i) 211 nm ($\varepsilon = 1.378 \times 10^4$) (ii) 269 nm ($\varepsilon = 2.0545 \times 10^4$)	Wilmes 1988, reviewed in Mulye 1995

1.2 Metabolic fate of IMI in various components of environment

1.2.1 Fate in water

The persistence of IMI in water is dependent upon the various environmental factors such as exposure to light and its intensity, temperature, pH, presence and nature of microbes including the rate of its application and type of formulation. It has been reported that higher pH increases $t_{1/2}$ and thus persistence of IMI, while opposite trend was observed at low pH (Sarkar et al. 1999).Studies concerning with the breakdown of IMI suggested that hydrolysis of IMI could lead formation of metabolites namely imidacloprid-urea and 1-[(6-chloro-3-pridinyl) methyl]-2-imidazolidone (Zheng et al. 1999; Liu et al. 2006), further broken down into CO_2, nitrate (NO_3^-) and chloride (Cl^-). In a similar manner, a very recent report of Grover et al. (2014) also showed the formation of six metabolites and inorganic ions during the TiO_2 mediated photodegradation of IMI and signified that despite of its complete degradation, the mineralization was incomplete. The formation of metabolites was reported to be the cause for its incomplete mineralization. Roberts et al. (1999) reported the $t_{1/2}$ = 57 min during the irradiation (xenon lamp) of IMI contaminated water (pH =7), with formation of

nine metabolites. Among these metabolites five were found to be most prominent that includes a cyclic urea, cyclic guanidine derivative, an olefinic cyclic guanidine, and two fused ring products.

The rate of degradation of imidacloprid was found to vary with the pH, however the studies have showed conflicting results. For instance, Sarkar et al. (1999) reported increase in $t_{1/2}$ with increase in alkalinity ($t_{1/2}$ = 36.3 days at pH = 4 and 41.6 days at pH = 9). On contrary, authors indicated that imidacloprid could be more readily degraded under alkaline conditions (Yoshida, 1989, Mulye, 1995; Zheng and Liu, 1999). In an experimental study performed by Yoshida (1989), it was found that no hydrolysis products were detected at pH = 5 and pH = 7 at any sampling intervals. However, it transformed slightly at pH = 9 and the $t_{1/2}$ was calculated to be 346.5 days. This result is found to be in correlation with the results of USEPA (U.S. EPA 2005) where imidacloprid listed to be as stable at pH 5 and pH 7 and at pH = 9 its $t_{1/2}$ was reported to be 355 days. Thus, based upon these results it could be concluded that IMI is stable to the hydrolysis under environmentally relevant pH.

In the aqueous media, IMI is also reported to be metabolized by various microorganisms. Spiteller (1993) studied the degradation of IMI for 30 days using water and sediments that were collected from a pond. Radio-labeled IMI was applied to water initially @ 680 µg/L and at the end of the exposure ~ 67.6% of radioactivity was found to remain in the water column, where ~64.0% corresponds to IMI and rest was found as metabolites. However, in the sediment much less radioactivity (~29.3%) was detected and out of this ~20.4% was determined to correspond to IMI. Moreover, ~ 0.7% of the radioactivity was detected as CO_2 and less than 0.1% as other volatile metabolites. It was concluded that in 30 days, not much biodegradation found to occur with an estimated first $t_{1/2}$ = 129 days (Spiteller, 1993). Henneböle (1998) conducted his study with pond water and sediment in order to determine the effect of exposure of artificial light (xenon lamp) and sunlight on the degradation of imidacloprid. The $t_{1/2}$ of radio-labeled IMI was determined to be was determined < 14 days when applied at initial rate of 620 µg/L. Moreover, ~5.8% of IMI had been found to mineralize in 21 days, upon the exposure to sunlight, however under the artificial light the mineralization was determined to be ~9.8%. The $t_{1/2}$ of IMI is reported to be even less in case of mesocosm studies that were performed under natural conditions. For instance, Moring et al. (1992) reported $t_{1/2}$ = 1.4 days for imidacloprid, in an outdoor microcosm study. It was also signified in their report that IMI did not appeared to persist in sediment.

1.2.2 Fate of IMI in plants

After the application of IMI in soil, it is taken up by plant roots and translocated to various parts of the plants. Many studies have reported its persistence in plants (Rouchaud et al.1994; Alsayeda et al. 2008). Three major plant metabolites viz. imidazolidine derivative, the olefin metabolite and the nitroso-derivative were confirmed from various studies (Nauen et al. 1998; Mukharjee and Gopal, 2000) and found to more toxic than IMI itself. Upon its administration for seed treatment it gets absorbed by the seedling from the disintegrating seed coat. For instance in a French study (Laurent and Rathahao, 2003), seeds of sunflower plants were treated with IMI (1.0 mg/seed) and pollens produced by these grains were found to be contained by IMI at a concentration of 13.0 ppb. Westwood et al. (1998) found that the leaves of sugar beet seedlings contained an average of 15.2 ppm of IMI after treatment at a rate of 0.9 mg/seed.

1.2.3 Fate in soil

Processes that determines the behaviour and fate of insecticides in soil environment are sorption-desorption and degradation processes. These processes further affects IMI's persistence and the way of transportation (volatilized, or leached) to reach the target organisms. The effective persistence of pesticides in soil varies from a week to several years depending upon properties and structure of the constituents in the pesticide and availability of moisture in soil. Sorption process binds the pesticide molecules by the surface of soil, whereas desorption implies detachment of the molecules to the liquid medium. Hence, information regarding sorption-desorption processes of IMI are essential in predicting its fate in soil environment. Various results reported (Cox et al. 1998b; 2001; Fernandez et al. 2007; Liu et al. 2006; Ping et al. 2010) that IMI retention in soil is highly dependent on the amount of the pesticide applied, soil characteristics (soil texture, organic carbon content (OC), cation exchange capacity (CEC), pH and temperature) and physicochemical properties of the pesticide itself. A number of studies (Cox et al. 1998a ; Kamble and Saran, 2005; Oi, 1999) have determined increase in sorption rates with decrease in initial concentration of IMI and vice-versa, indicating greater potential for its mobility with increasing concentration. Sorption behaviour of IMI also found to be largely dependent on the soil OC content, where the soils with higher OC content showed higher sorption capacity and less potential mobility of IMI. Another important characteristic of soil is amount of organic carbon associated with cation exchange capacity in soil. Higher amount of organic matter and cation exchange

capacity increases adsorption and reduces leaching behaviour of IMI. Studies regarding effect of pH on adsorption have reported (Bansal, 2010; Pusino et al. 2003; Paszko, 2006) that adsorption was positively correlated with soil organic carbon and cation exchange capacity while negatively correlated with soil pH. Similar, trends were observed by Ping et al. (2010) and Bajeer et al. (2012) showed adsorption of IMI becomes higher under lower pH and/or lower temperature, while keeping other parameters constant.

Persistence of IMI is also measured in terms of its $t_{1/2}$ which is determined to be 27-229 days in soil and is found to be dependant (Scholz and Spiteller, 1992) upon factors like sorption, pH, and organic matter, type of formulation and vegetation cover. For example, $t_{1/2}$ of IMI after degradation was observed to be 48 and 190 days, in crop covered soils and bare soils respectively (Scholz and Spiteller, 1992). Some studies also revealed strong persistence of IMI in soil under standardized laboratory conditions and show unpredictable persistence under a range of field conditions (Krohn and Hellpointner, 2002) regarding its dissipation time. It is noted that the dissipation time, DT_{50} (i.e., the time required for half of it to dissipate) for IMI is in the order of 1-2 years (PMRA 2001) though some variations has already been reported in the literature on its dissipation times, half-lives and the potential for accumulation. Sabbagh et al. (2002) reported calculated half-lives for IMI ranged from 83 days to greater than a year while some of the evidences proved reduction in its dissipation times when applied to cropped fields, rather than fallow fields (Scholz and Spiteller, 1992; Krohn and Hellpointer, 2002). From the agricultural point of view, longer persistence of pesticides leading to accumulation of residues in soil that may result into the increased absorption of such toxic chemicals by living organisms. Hence, longer $t_{1/2}$ and over use of IMI led to their accumulation (Estevez et al. 2008; Ahamed et al. 2001) in the soil.

Thus, it is clear from the above discussion that the fate of IMI in various environmental components has resulted into its fragmentation into various metabolites and in some case it also leads to the formation of inorganic ions i.e., it undergoes mineralization. Such fate of IMI or any pesticide in soil could be caused by various degradation processes and are being discussed as follows.

1.3 Degradation of pesticide(s) in soil

The pesticides present in the soil has been reported to be degraded through many ways such as chemical degradation (Macrae and Alexender, 1965), physico-chemical (Vikelsoe and Johansen, 2000), microbial degradation (Topp et al. 1997) and degradation

using Advanced Oxidation Processes (AOP) (Bolton, 2001; Domenech et al. 2004) Among these various processes microbial degradation and AOPs are of special concern to the researchers and have been used for the degradation of many organic pollutants including pesticides.

1.3.1 Microbial degradation

Accumulation of pesticides and their degradation products present in the top soil not only influence the population of various soil microbes but also their biochemical activities like nitrification, ammonification, decomposition of organic matter and nitrogen fixation (Karunya and Reetha, 2012). Microorganisms play an important role in the metabolism of organic pollutants present in the soil (Alexander, 1965).

Microbial degradation is conversion of toxic compounds into non-toxic with the help of microorganisms (bacteria and fungi) as reported by Topp et al. (1997) and Shahgholi (2014). This type of degradation in soil is well known (Craigmill and Winterlin, 1985) to be influenced by many environmental factors that affect the course and the rate of pesticide degradation in soil. The most important factors are soil texture, bioavailability of pesticides, population and survival of microorganisms and their physiological status (Singh, 2008).

The content of organic matter and clay is reported (Gish et al. 1995; Sadeghi et al. 1998; Alletto et al. 2010) to have direct influence on leaching behaviour of pesticide in conventional tilled soil. Lesser the amount of organic matter, more easily would be the leaching and hence less time for the microbes to come in contact with the pesticide thereby reduces the degradation. The pH of soil also have a great influence on the process of degradation of pesticides, as it can alter the degree of adsorption of pesticide in soil, and conditions for the growth of microbes. These factors individually or collectively could changes the rate of degradation of the pesticide. It has been reported by Gavrilescu (2005) that rate of degradation increases with decrease in pH, however, opposite results has been reported by Walker et al. (2001) showing a more rapid degradation of isoproturon in soils at higher pH. The temperature of the soil also influences the degradation rates, which is further dependent on the nature of microbe involved in the degradation. Generally, rates of degradation for most of the reactions catalyzed by enzymes became almost double for every 10 °C increase in temperature (between 10–45°C). Thus, it is generally expected that with increase in soil temperature will tend to increase in degradation rate (Walker et al. 2001).

In addition to these mentioned parameters, the soil practices also reported to affect the population and survival conditions of the microbes that ultimately influence the degradation of pesticides. For instance, Mapa et al., (1986) described effect of different soil practices (such as soil tillage or organic amendments) on its structure by different mechanisms (aggregation of soil particles, creation of pore space) that in-turn affects the growth of micro flora. Tillage also affects soil organic carbon location, impounding and also water retention properties which further lead to different sorption and degradation properties (Alletto et al., 2008; Stenrød et al., 2006). However, contradictory results have been documented by some authors (Vieuble-Gonod et al. 2003; Mamy et al. 2011) concerning the effect of soil practices on degradation of pesticides.

Literature has shown that different microorganisms could be used either to transform pesticides or to degrade into small molecules. The microbial degradation of pesticides is controlled by the bio-availability of the pesticide to a pesticide-degrading microorganism and the activity of the microorganism (Anhalat et al. 2007). It has been reported that pesticide itself may act as adequate carbon source for some microorganisms present in the soil (Aislabie et al. 1995; Galli, 2002). Beside of above mentioned parameters affecting the degradation of pesticides, the ability of bacteria to degrade pesticide could also linked to the contact time with the compound i.e., the environmental situation in which they build up their physiological adaptability.

The main processes which are determined to be responsible for microbial degradation of pesticides are metabolism and co-metabolism. One or several interacting organisms metabolize the pesticide into inorganic components (like CO_2) during microbial degradation and complete their requirements (growth and energy) by mineralizing it. Metabolism of pesticides may involve a three-phase process. In first phase, metabolism takes place by various processes (oxidation, reduction, or hydrolysis) causing transformation of parent molecule in to a more water soluble and less toxic product. In second phase, further enhancement in water solubility occurs by conjugation of a pesticide/ metabolite with a sugar or amino acid. In the third phase, alteration of metabolites that are formed in second phase into secondary conjugates takes place and are also non-toxic in nature. This process are done by fungi and bacteria which produces intracellular or extra cellular enzymes (hydrolytic, peroxidases, oxygenases, etc) as reported by Ortiz-Hernández et al. (2011) and Van Eerd et al. (2003).

Another process for the metabolism of pesticides in the environment is governed by co-metabolism in which organisms grow at the expense of a co-metabolite to transform the pesticide in to metabolites without deriving any nutrient or energy for growth from the process. Metabolites formed duting their metabolism is generally less toxic than the pesticides itself and sometimes can be more toxic (Tixier et al. 2002).

Some bacterial isolates does not have the ability to survive on pesticides as sole source of energy and carbon, as they do not possess all the enzymatic tools to mineralize pesticides. For the removal of these pollutants from the contaminated soil, co-metabolism process is found to be more approachable biological process, when the pollutant does not support microbial growth (Duetz et al. 1994). It is the process by which compound is unexpectedly degraded by an enzyme or cofactor produced during microbial metabolism of another compound. This kind of degradation is benefitted over the bioremediation strategies, as the later can only stimulate a specific group of microorganisms for degrading contaminants of concern. Co-metabolic bioremediation has been used for more than last two decades for the decontamination of many organic recalcitrant molecules. It was reported (Janke and Fritsche, 1985) that the utilizable substrates (co-metabolites) provide energy, cofactors, or metabolites for the different cellular events involved in the transformation process. Liu et al. (2013) showed that products, and pathways for the IMI co-metabolic transformation using *S. maltophilia* CGMCC 1.1788 were similar in presence of both sucrose and succinate to those found when succinate was only used as utilizable substrate rather than to sucrose alone. Rojo (2010) even reported that *Pseudomonas* preferentially utilized succinate present in limited amount as compared to excess of sugar in the transformation solution.

Hence, microbial degradation has potential to degrade the pesticides and is benefitted by its low cost option for decontamination and destruction of pesticides and is efficient, economical and environmentally friendly technique (Hilarides et al. 1994; Lehto et al. 2000) Therefore, it can be used for the degradation of the neonicotinoids a relative newer class of pesticides.

1.3.1.1 Microbial degradation of neonicotinoids

This family of insecticides is comparatively resistant to the degradation than the other classes and therefore considered as biorefractory pesticide pollutants (Tomizawa and Casida 2005; Liu et al.2010). However, there are limited microbial species some of which have already been reported to transform neonicotinoid insecticides into simple compounds. Different type

of microbes such *Stenotrophomonas maltophilia* (Zhao et al. 2009), white rot fungus *phanerochaete sordida* (Wang et al, 2012), *Leifsonia sp.* (Yao et al. 2006) were reported to degrade the members (other than IMI) of this class of insecticides. Wang et al. 2013 isolated acetamiprid degrading bacteria *Pigmentiphaga sp.* AAP-1 from soil and observed that the isolate could utilize 100 mgL^{-1} of acetamiprid in 2.5 h. Zhou et al. 2013 investigated the degradation of thiamethoxam in soil enrichment culture and observed that this culture is capable of degrading 96% of applied amount of pesticide within 30 days. The degradation acetamiprid and thiacloprid were degraded by Liu et al. (2011) in sterilized and unsterilized soil and showed 94.0% and 98.8% of their degradation, respectively. Since, this microbial degradation involving various isolated microorganisms has shown that members of neonicotinoid family can be potentially degraded. Therefore, this process has also been employed for the degradation of imidacloprid, a relatively newer and extensively used neonecotinoids pesticide and is being discussed.

1.3.1.2 Microbial degradation of IMI

Very few studies on the degradation of IMI have been reported by using different bacterial strains. First report on imidacloprid degradation was given by Anhalt et al. (2007) and showed that isolated microorganism *Leifsonia* strain PC-21 degraded 37-58% of applied amount of IMI. The intermediates produced after degradation was identified as imidacloprid guanidine, imidacloprid urea and some unknown metabolites as well. Phugare et al. (2013) isolated the bacterium *Klebsiella pneumonia* strain BHC1 from the IMI contaminated agricultural soil which was capable to degrade upto 78% of IMI and the main intermediate formed is 6-chloronicotinic acid. Similarly, Madhuban et al. (2011) showed that 69% of microbial degradation of IMI (50 mgL^{-1}) within 20 days by using *Burkholderia cepacia* strain CH9 which was isolated from an agricultural field.

The effect of various physicochemical properties of soil on the degradation of IMI was also confirmed by different studies as favored by recent report of Hu et al. (2013) observed *Ochrobactrum* sp. strain BCL-1 capable of degrading ~67.67% of IMI (50 mg L^{-1}) within 48 h under optimized conditions of pH = 8 and 30°C. In acidic pH of 3 and 5, degradation of 12.01% and 18.39% were reported whereas with alkaline pH of 9 and 11, it was 32.74% and 23.16% respectively (Phugare et al. 2013). In addition to this, effect of temperature and initial concentration of IMI along with other pesticides were also reported in the literature (Deshpande et al. 2004; Jadhav et al. 2010). In an another recent report (Sharma

et al. 2014) it was observed bacterial cultures viz., *Bacillus aerophilus* and *Bacillus alkalinitrilicus* isolated from sugarcane field soil could efficiently degradation IMI and the corresponding $t_{1/2}$ were reported to be 13 and 16 days, respectively. Some studies also reflect the influence of soil nature and presence of other species on the degradation of IMI. Liu et al. (2011) showed only 22.5% of IMI could be degraded over a period of 25 days in unsterilized soil, while no degradation was observed after same time period in sterilized soil. The degradation products of imidacloprid were identified as olefin, nitroso or guanidine metabolites. A recent report (Shetti et al. 2014) showed that decreases in content of DNA, RNA, protein, glucose and growth of isolate *Bacillus weihenstephanensis* decreases the rate of degradation of IMI (256 mgL^{-1} to 256 μgL^{-1}). Pandey et al. (2009) reported transformation of IMI by using *Pseudomonas sp.* under microaerophilic conditions in the presence of an alternate carbon source. This insecticide was found to transform to nitrosoguanidine, desnitro and urea metabolites and a pathway regarding this transformation was proposed. In this report bacterial transformation of 'magic nitro' group which is responsible for the insect selectivity of neonicotinoid insecticides assumed to be reduced to nitrosoguanidine and aminoguanidine and then cleaved to the guanidine and urea derivatives (Tomizawa and Casida, 2003 & 2005; Ford and Casida, 2006). Capri et al. (2001), studied the degradation of IMI in Italian soils, found that its concentration decreased rapidly in the first 10 days followed by a slower decrease in the total amount recovered. Although, these results supported the contention that microbial degradation is an important pathway for transformation and sometimes mineralization of neonicotinoid and specifically IMI in soil. Yet the formation of various metabolites confirms that despite high percentage of degradation or degradation rate, mineralization is either slow or was not taken into account. In order to degrade IMI completely, a much efficient process is required. In this direction AOP is one of the concerned process which is being adopted by many researchers (Cernigoj et al. 2006; Toor et al. 2005) for the degradation of the many organic pollutants including pesticides.

1.3.2 Advanced oxidation Processes

Presently AOPs are considered as powerful technologies that are being widely used in treatment of various kinds of organic pollutants (Badriyha et al. 2007). These are found to be different from other processes as molecules are degraded rather than concentrated or transforming into different phases. The concept of AOP was recognized and well defined as "processes involving the generation of highly reactive oxidizing species able to attack and

degrade organic substances" (Glaze et al.1987; Huang et al. 1993). It is also reported (Domenech et al. 2004) to be a physico-chemical process with high efficiency, capable to produce profound changes in the chemical structure of the contaminants via the participation of hydroxyl radicals ($^{\bullet}OH$ radicals). Ascribed to the high oxidation ability of these radicals (Legrini et al. 1993; Rajeshwar, 1996; Goswami and Blake, 1996; Andreozzi et al. 1999; Huston and Pignatello, 1999; Joseph et al. 2000), AOPs has emerged to be of meticulous interest. However, few studies have suggested that in addition to the generation of $^{\bullet}OH$, other oxidising species can also be produced in AOPs (Anipsitakis and Dionysiou, 2003& 2004). The mechanism of AOP process is well known. The oxidation of organic molecules or pollutants takes place by radicals that are generated by hydrogen abstraction (eq. 1.1). This can further react with oxygen molecules forming peroxyradicals and initiate oxidative degradation chain reactions for the complete mineralization of the organic pollutants (Blanco, 2003).

$$RH + {}^{\bullet}OH \rightarrow RH^{\bullet} + H_2O \qquad (1.1)$$

The formation of these free radicals could takes place via either by photochemical or non-photochemical in AOPs. Among the different approaches in AOPs (ozonation and ozone related processes (O_3/H_2O_2, UV/O_3), electrochemical oxidation) the photocatalysis processes is considered as the most competent for removal of contaminants or for the degradation of various pesticides from the environment (Sahoo et al. 2011;; Scott and Ollis, 1995; Bandala et al. 2007b; Arancibia et al. 2002; Chiron et al. 2000; Ikehata and El-Din, 2005b; Ikehata and El-Din, 2006, Martínez-Huitle et al. 2008).

1.3.2.1 Photocatalysis

This process has been defined by Kisch (1989) as the acceleration of a photoreaction by a catalyzer. Photons, with their energy can affect the chemical bonds of a chemical compound by the cleavage of one or more covalent bonds in a molecular entity (Muller, 1994). The applications of photocatalytic degradation along with effects of various parameters on the rate of degradation of different pollutants have been reviewed and reported by Carey et al. (1976) and Starner et al. (2012). The photocatalysis is broadly divided into two categories namely Homogeneous (Fenton and photo Fenton-like processes) and heterogeneous photocatalysis (TiO_2/UV, ZnO/UV etc.).

1.3.3.1 Homogeneous photocatalysis

In this type of process, the reactants and the photocatalysts are found to be in the same phase and of environmental importance. This process plays an important role in purification of waste water and carried out under UV-light irradiation in presence of transition metal (higher oxidation state) and an oxidizer such as H_2O_2. In the course of this process, the formation of hydroxyl radicals takes place which upon reaction with a substrate lead to form various other organic radicals. Moreover, the presence of atmospheric oxygen the original form of the transition metal ion is restored i.e, it gets regenerated with the simultaneous formation of superoxide ions and peroxy radicals and radicals corresponding to the substrate.

The most commonly used homogenous photocatalysis includes ozone (O_3), the transition metal oxide and the photo-Fenton systems. The advantages of using these methods are (i) an environmentally-friendly reagent, (ii) relatively cost-effective process, (iii) degradation in sunlight and (iv) the reloading of the required $^{\cdot}OH$ for oxidation. However, this process also suffers from some disadvantage that are found to be necessity of low pH, use of iron as catalyst (in photo Fenton reactions) causing additional processing to remove it from the reaction.

1.3.3.2 Heterogeneous photocatalysis

Acceleration of the photoreaction in the presence of a catalyst (specifically semiconductor) when both catalyst and reaction medium are in difference phases, then the process is known as heterogeneous photocatalysis (Radwan, 2005). This began in 1972 with a revolutionary report of Fujishima and Honda (1972), where splitting of the water takes place into hydrogen and oxygen using titanium dioxide (TiO_2). This process includes a complex sequence of the reactions and consisted of number of steps (Hermann, 1999, Pirkanniemi and Sillanpaa, 2002), which were determined to be (i) mass transfer of the organic contaminant in the liquid phase to the TiO_2 surface (ii) adsorption of the organic contaminant onto the photon activated TiO_2 surface (iii) photocatalysis reaction for the adsorbed phase on the TiO_2 surface (iv) desorption of the intermediate from the TiO_2 surface and finally (v) mass transfer of the intermediate from the interface region to the bulk fluid. In order to initiate the reaction in heterogeneous photocatalysis, a semiconductor is required. Currently number of them are reported to be used in heterogeneous photocatalysis (Jansen and Letschert, 2000; Nagaveni et

al. 2004b ; Cernigoj et al. 2007), however for the purpose of photocatalytic degradation every semiconductor is not appropriate as described in the upcoming section.

1.3.3.2.1 Semiconductors used in heterogeneous photocatalysis

Over the last two decades the application of semiconductors has grown exponentially in the field of photocatalysis. The function of the semiconductor in photocatalysis is that upon absorption of an incident photon of appropriate amount of energy the formation of e^-/h pair takes place. The charge carriers thus produced gets transported to the surface of the semiconductor, captured by the surface adsorbed molecules and initiate the oxidation and reduction processes, simultaneously (Habisreutinger et al. 2013). Since, transportation of e^- between valance band (VB) and conduction band (CB) occurs only when the appropriate

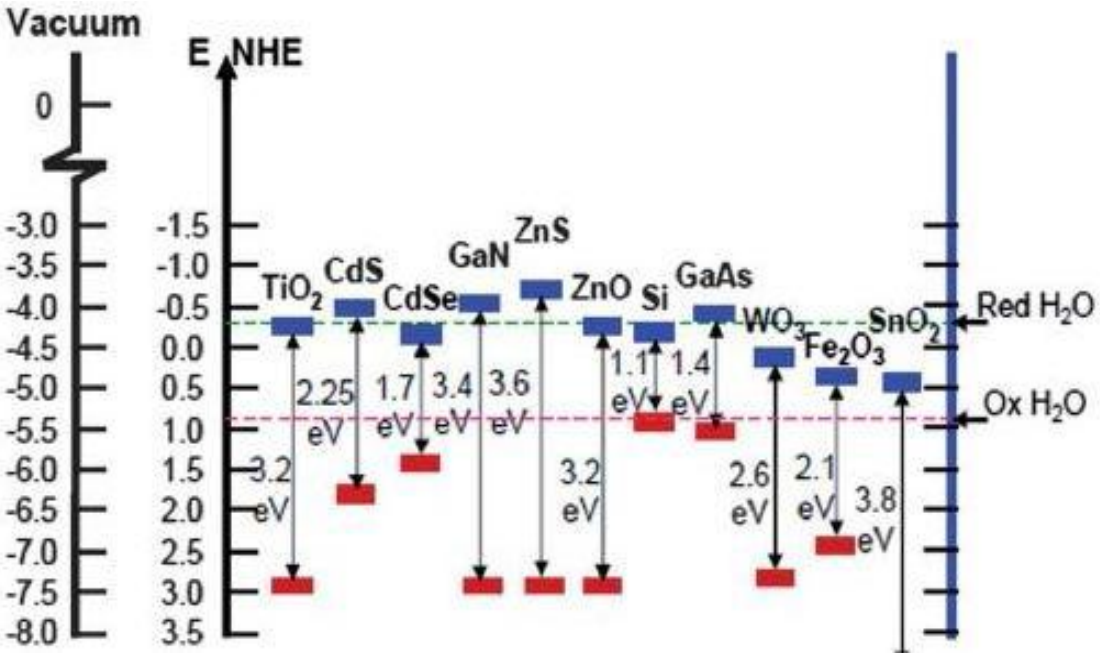

Fig. 1.2 Bandgaps and redox potentials of different types of semiconductors using the normal hydrogen electrode (NHE)

amount of energy/frequency is supplied. Hence, for a semiconductor to be an ideal photocatalyst, the top of VB must be separated from the bottom of the CB by about ~1.23 eV for promotion of redox reactions (Viswanathan, 2003). A number of semiconductors such as ZnO, CdS, CdSe, ZnS, WO_3, TiO_2 etc., have been explored for their photocatalytic properties (Pirkanniemi and Sillanpaa, 2002). The catalytic activity of semiconductor is also strongly depends on band edge positions i.e., positions of VB and CB and for some of the semiconductors it is given in Fig. 1.2. Among varieties of available semiconductors, TiO_2 is

most effective and commonly used photocatalyst (Blake, 2000; Blanco et al. 2007; Oller et al. 2006) which is being credited to biologically and chemically inertness and has been used in number of applications including degradation of organic pollutants. It is used as a brightener, desiccant, reactive and most widely used level is as photocatalyst in the field of energy and environmental applications (Sharma and Lee, 2013). In principle, TiO_2 with a wide band gap (~3.2 eV) in the UV range can utilize not more than 5% of the total solar energy coming on the surface of the earth.

The most popular photocatalyst configuration used on laboratory scale is commercially available Degussa P-25 TiO_2 and is reported to be most photoactive as revealed by many reports (Kumar and Bansal, 2012 & 2013; Toor et al. 2006). The effectiveness or efficiency of Degussa P25 TiO_2 could be explained on the basis of (i) reasonably well defined crystal phases (Anatase : rutile :: 70 : 30), (ii) high BET surface area (55 ± 15 m^2g^{-1}) (iii) particle size in nano regime (30-50 nm) and appropriate position of VB (3.0 eV vs NHE) and CB (-0.2 eV vs NHE) with respect to oxidation potential of many organic molecules. Another benefit of using TiO_2 as photocatalyst (Murray 2006) is its regeneration using UV light, and is so reusable.

1.4 Mechanism/reactions of TiO_2 photocatalyst

The mechanism (Fig. 1.3) of a photocatalytic process is well known (Bernardini et al. 2010; Naldoni et al. 2013; Sinha et al. 2009; Kansal et al. 2014; Arriaga et al. 2010; Sood et al. 2014; Nakata and Fujishima, 2012) and is observed when a photocatalyst absorbs UV and/or visible (Vis.) light irradiation from sunlight or an illuminated light source having energy equal to or more than the band gap energy of TiO_2. The negative charged e^- in the VB of the photocatalyst is excited to the CB resulting in the formation of h^+ in the VB and is referred as "photo-excited" state of TiO_2 (eq. 1.2). After photoexcitation, the excited e^-/h^+ pairs can recombine and/or get trapped into meta-stable surface states and thereby releasing the input energy as heat, without any chemical effect. However, upon separation and transportation of these excited charges to different reactive sites, various chemical reactions with adsorbed species (eq. 1.2-1.7) could be perceived. The photogenerated h^+ (+2.8 V vs NHE) reacts with adsorbed water molecules to form hydroxyl radicals (•OH). Meanwhile, e^- in the CB (-0.5 to -1.5 V vs NHE) participates in reduction processes that converts the adsorbed molecular oxygen to oxidative superoxide radical ($O_2^{\bullet-}$) (Litter, 1999; Chen and Mao,2007; Kansal et

al.2014;) and/or reduce various organic compounds. Both of these photoproduced species being oxidative can decompose the nearby absorbed organic molecules.

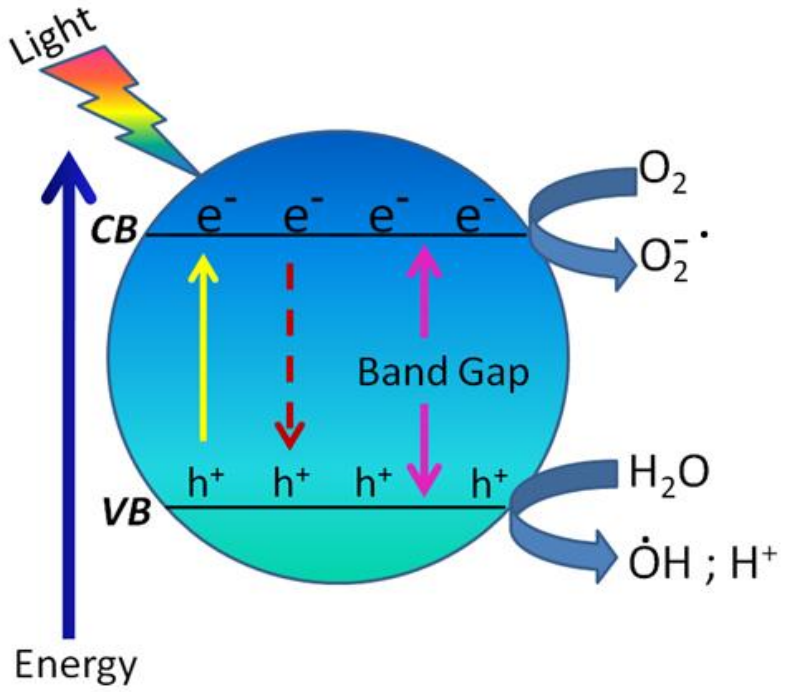

Fig. 1.3 Mechanism of TiO_2 photocatalysis

$$TiO_2 + h\nu \rightarrow TiO_2 (e^- + h^+) \quad (1.2)$$

Two oxidation reactions have been observed on TiO_2 surface:

Electron transfer from adsorbed substrate (organic pollutants),

$$TiO_2 (h^+) + RX_{ad} \rightarrow TiO_2 + RX_{ad}^{\bullet +} \quad (1.3)$$

Electron transfer from adsorbed solvent molecule

$$TiO_2 (h^+) + H_2O_{ad} \rightarrow TiO_2 + HO_{ad}^{\bullet} + H^+ \quad (1.4)$$

$$TiO_2 (h^+) + OH_{ad}^- \rightarrow TiO_2 + HO_{ad}^{\bullet} \quad (1.5)$$

More HO^- radicals adsorbed at the particle surface, due to high concentration of H_2O molecules (iii and iv) and emerge to be of greater importance in oxidative degradation processes. Molecular oxygen is responsible for accepting species in the electron- transfer reaction from the conduction band of the photocatalyst to oxygen.

$$e^- + O_2 \rightarrow TiO_2 + O_2^{\bullet -} \quad (1.6)$$

The addition of electron acceptors like (H_2O_2) can considerably enhances the rate of photodegradation (iv),

$$TiO_2 (e^-) + H_2O_2 \rightarrow TiO_2 + HO^{\bullet} + OH^- \quad (1.7)$$

These photoproduced charge carriers and in-turn produced chemical species being highly oxidative in nature are capable to degrade the pesticides, were used in many studies as discussed later.

1.5 Photocatalytic degradation of pesticides

A great number of pesticides which are reported to be bio-recalcitrant and non-biodegradable in nature were not considered to undergo biological process for their degradation (Khodja et al., 2001). Hence, photocatalysis using TiO_2 have been used for treatment of pesticide contaminated environment (Peyton et al. 1982; Glaze et al. 1987; Miller et al. 1988; Carey, 1990; Legrini et al. 1993; Masten and Davies, 1994; Benitez et al. 1995; Casero et al. 1997). Since, TiO_2 is inexpensive and nontoxic, oxidation and reduction occur simultaneously on each irradiated particles and requires no conventional reagents. Therefore, it is enormously used as photocatalyst for detoxification of pesticides and is well documented in different environmental components such as water and soil.

1.5.1 TiO_2 mediated photocatalytic degradation of pesticides in water

A wide range of pesticides could be efficiently degraded using TiO_2 without the formation of harmful by products (Jansen and Letschert, 2000; Asahi et al. 2001; Khan et al. 2002; Yu et al. 2002; Ihara et al. 2003; Sivalingam et al. 2003). Herrmann et al. (1999) investigated the photocatalytic degradation of organo- phosphorous insecticides and depicted the identification of intermediates as well as the degradation pathways. Similar, studies were conducted on the degradation of phosphamidon in water using two different photocatalysts (ZnO and TiO_2) and out of these two, TiO_2 was reported (Rabindranathan et al.2003) to be more effective, though the degradation leads to complete mineralisation in both cases. Emmanualle et al. (2003) investigated photocatalytic degradation of six herbicides in the aqueous solutions using TiO_2 to find out the influence of various parameters and observed adsorption as an important factor for degradation. Four water soluble pesticides have been studied by Malato et al. (2002a) at pilot scale and it was observed that both degradation (90%) and mineralization could be achieved by TiO_2 photocatalysis.

Muzkat et al (1992) studied photocatalytic mineralisation of xenobiotics in contaminated rinse water from agricultural sprayers and well-water. They concluded that $t_{1/2}$ of malathion (100 ppb to 50 ppm) after photomineralisation was less than 1 h in the presence of TiO_2 as photocatalyst. Photocatalytic degradation studies of many other

pesticides have been reported (Doong and Chang, 1997) and it was observed that rate of degradation of pesticides depends upon their nature. Photocatalytic oxidation of lindane in water using TiO_2 catalyst showed that 99.9% of it can be degraded in 5 h and the various photoproduced intermediates were identified and observed (Balanco and Malato, 2001;Guillard et al. 1996). These photoproducts were classified in to various categories i.e chlorocyclohexanes, chlorocyclohexenes, chlorobenzenes, chlorophenols, chloropropanes, chloropropanones and the pentachlorocyclohexanone isomer. Zaleska et al. (2000) studied the photocatalytic degradation of DDT in water over TiO_2 catalysts and found that highest efficiency for supported TiO_2. Peris et al. (1993) investigated the degradation of carbary using a continuous flow of TiO_2 slurry under UV-light and anticipated that a multistep degradation proceeds involving the attack of the substrate by ·OH radicals.

Tanaka et al. (1995) studied photocatalytic degradation of 3,4-xylyl N-methyl carbamate (MPMC) and other carbamate pesticides in aqueous TiO2 suspensions. They also proposed a degradation mechanism along with formation of oxygenated aliphatic intermediates. Photodegradation of acidified aqueous solutions of atrazine was studied (Texier et al. 1999) in the presence of TiO_2 and $Na_4W_{10}O_{32}$ under UV light. Both catalysts were proved to be efficient even though the mechanisms of degradation were found to be different. Photodegradation of the herbicide 3,4-dichloropropionamide in aqueous TiO_2 suspensions was examined by Pathirana et al. (1997) and found that the degradation was found to occur via dechlorination within 5 h. Optimization of various parameters (pH values, catalyst dosages, light intensities, dissolved oxygen levels etc.) were reported (Ku and Jung, 1998) for the degradation of monocrotophos in aqueous solution by UV/TiO_2. It was found that rate of degradation was more in acidic conditions than alkaline conditions. In the case of paraquat and diquat, the rate of degradation ion was reported to be dependent on the pH as well as the type of the catalyst (Florencio et al. 2004).

Coleman et al. (2007) studied the effect of different kinds of TiO_2 on 1, 4-dioxane removal. They found that TiO_2 photo catalysis with both UV and solar light is effective in degrading 1,4-dioxane. Maheshwari et al. (2013) evaluated adsorption kinetics ciprofloxacin hydrochloride of at different temperature and initial concentration of ciprofloxacin hydrochloride.

1.5.2 Photocatalytic degradation of pesticides in soil using TiO_2 as photocatalyst

Extreme and enormous agricultural methods in due course of time lead to accumulation of pesticides in high concentrations in soil. In recent years, TiO_2 photocatalysis, has been extensively applied not only in waste water treatment and aqueous media (Valente et al.2009; Devi et al.2009; Lhomme et al. 2007; Tamimi et al.2006) but also utilized for *in situ* soil treatment (Higarashi and Jardim2002; Villaverde et al.2007). *In situ* treatment of glyphosate in soil was performed (Xu et al. 2011) using $Fe_3O_4/SiO_2/TiO_2$ photocatalyst and results showed that degradation efficiency of glyphosate reaches 89% in 2 h by using photocatalyst dosage of 0.4 g/100 g (soil). Soil thickness was reported to be an important factor for the photocatalytic degradation of glyphosate. Photocatalytic degradation of the pesticide diuron was done to evaluate the potential use of this technology for *in situ* remediation under laboratory conditions (Higarshi and Jardim, 2002). In this study, spiked soil samples of diuron were exposed to solar light to optimize the different parameters that were found to have influence on the kinetics of the pesticide degradation. Results have shown that photocatalytic treatment using TiO_2 in the presence of solar light to be very efficient in the destruction of diuron in the top 4 cm of contaminated soil and even low loads (0.1%). A similar performance of TiO_2 was observed for the degradation of carbetamide (Muszkat et al.1995). Verma et al.(2013) studied degradation of malathion and found maximum degradation at 3.0 g/L of catalyst dose of TiO_2 and pH=6 on fixed concentration of pesticide.

Photocatalytic degradation of hexachlorocyclohexane (-HCH) was performed by Xu et al. (2007) using both TiO_2 and montmorillonite composite as photocatalysts in soils under UV-light irradiation. The results indicated that the photocatalytic activities of the composite photocatalysts varied with the amount of TiO_2. Moreover, the composite TiO_2 has shown more photocatalytic than the pure P25 with the its same mass. In addition, effect of pH and dosage of composite photocatalysts on the degradation of -HCH was investigated and various intermediates were identified and characterized as pentachlorocyclohexene, trichlorocyclohexene, and dichlorobenzene.

Wang et al. (2007) investigated photodegradation of p-nitrophenol (PNP) on soil surface to explore the photochemical remediation of soil polluted by nitrophenols. Spiked soil samples were irradiated by UV light with and without the addition of TiO_2. Enhanced PNP photodegradation was observed by adding TiO_2 from the range of 0.5–2 wt%. Soil pH, humic acid and soil moisture were found to be important factors which influence the rate of PNP

photodegradation. Increase in soil moisture significantly increased the degradation whereas humic acid reduced the degradation rate. Different degradation rates were observed with change in soil pH and higher degradation efficiencies were observed under alkaline condition. The process of photodegradation of some other herbicides and fungicides, such as trifluralin, carboxin, oxycarboxin, mecoprop, dichlorprop, chlorimuron-ethyl,atrazine and bensulfuron-methyl, has also been observed in soil and the results indicated that photodegradation is one of the important pathways for their degradation in soil. (Romero et al. 1998; Hustert et al. 1999; Choudhury and Dureja, 1997; Balmer et al. 2000; Gong et al., 2001; Si et al. 2004).

Thus, the above literature clearly depicts that the photocatalysis involving TiO_2 as photocatalyst provides an effective pathway for the degradation of pesticides and hence used for the degradation of IMI and is now being described as follows.

1.5.3. TiO_2 assisted photocatalytic degradation of IMI

As stated earlier that IMI has been extensively used in agriculture fields since two decades, therefore accumulated in the various components of environment. Moreover, the high solubility of IMI in water also makes it of special concern to the environment as it can easily runoff from the agricultural fields to the nearby water sources and thereby contaminates them. This is reflected by the ground water monitoring project conducted by Bayer Corporation (1998) on Long Island, NY, that showed presence of IMI (0.1 ppb to 1.0 ppb) in an agricultural well. A recent study by Starner and Goh (2012) showed the presence of IMI in 89% of the water samples collected from rivers, creeks and drains in California. About 19% of these samples were found to have IMI exceeding its permissible limit (1.05 ppb) as prescribed by United States Environmental Protection Agency. Much higher concentrations of IMI (upto 200 ppb) were found to be present in groundwater, streams and ditches of the Netherlands as document by Van Dijk, (2013). Ascribed to leaching behaviour and high water solubility of IMI, various studies were carried out to find out its degradation in water and identification of its metabolites formed.

Kitsiou et al. (2009) studied the photocatalytic degradation of IMI using TiO_2 in aqueous solution and compared the results with other two processes. It was found that TiO_2 assisted degradation of IMI under UV-light performs better than the other two and lead to more number of metabolites which were identified by GC-MS analysis. In a pilot scale experiment Malato et al. (2001) identified the technical feasibility, mechanisms, and

performance of degradation of aqueous IMI and found that TiO_2 could mineralize (95%) it in 450 min. Zabar et al. (2012) reported disappearance of IMI along with two other pesticides (thiamethoxam and clothianidin) using immobilised TiO_2 on glass slides. It was shown that all the three pesticides degrade (97%) within 2 h and followed first order kinetics. Despite of such high degradation, the percentage of mineralization ($9.1 \pm 0.2\%$ for imidacloprid, $14.4 \pm 2.9\%$ for thiamethoxam and $14.1 \pm 0.4\%$ for clothianidin) was very low.

Feng et al., (2013) prepared a series of La-doped TiO_2 and showed that $20\%H_3PW_{12}O_{40}/0.3\%La\text{-}TiO_2$ possessed the best photocatalytic activity for degradation of IMI. The degradation conversion of imidacloprid reached 98.17% after 60 min irradiation by using this catalyst. The degradation of IMI corresponded with first-order kinetic reaction, and the $t_{1/2}$ of the degradation of IMI was 9.35 min under the optimal conditions. Redlich et al. (2007) studied degradation of imidacloprid in aqueous solution under stimulated solar irradiation and found its $t_{1/2}$ to be 3 days. Some identified intermediates were found to be more persistent ($t_{1/2}$ upto 660 days) than IMI itself towards their decomposition. However, Liu et al. (2006) reported its $t_{1/2}$ = 30 min when its aqueous solution was irradiated under UV-light in presence of P25.

Thus, it is clear from the literature that neither individual microbial degradation nor photocatalytic degradation has lead to the complete (100%) dissipation/mineralization of IMI in soil. Hence, another remediation strategy for destructive elimination of IMI and its metabolites from environment is required. An alternative for destructive removal of the IMI and its metabolites could be the microbial treatment combined with pre/post treatment of photocatalytic oxidation that could reduce its recalcitrant metabolites.

1.6 Sequential microbial and photocatalytic degradation of pesticides

Photodegradation and biodegradation are observed to be major degradation processes which can clean up the environment as described previously. Many studies have been reported (Scott and Ollis, 1995) regarding oxidation of organic compounds to lose their toxicity before their degradation using microbes to achieve mineralization. Despite the fact that photocatalysis is less time consuming for the treatment of pesticides, one of their major problem is cost as compared to other conventional processes (Sarria et al. 2002).

In order overcome the problems regarding biological process and photocatalysis, coupling both of these processes where biological degradation can act as either pre or post treatment could be an alternative to minimize time and operational cost (Scott and Ollis,

1995; Benitez et al. 1995; Felsot et al. 2003). In this coupling process the aim of the photocatalytic degradation is not only to convert the pesticide into the toxic intermediates, but to provide the intermediates that should be less toxic than parent and to be completely removed by biological processes (Zeng et al. 2000; Sarria et al. 2002; Esplugas et al. 2004; Goi et al. 2004). Some studies have reported the use of photodegradation process as a pretreatment or post-treatment of a biological process (Beltran, 2004, Lapertot et al. 2006b). Very few works on the application of this kind of coupled methodologies are available in literature corresponds to TiO_2/UV oxidation (Jafari et al. 2012; Gonzelez et al.,2010;Tamer etal.,2006 & 2007). However, it seems to be well documented for other processes such as by ozonation (Marco et al., 1997; Helble et al., 1999; Yeber et al., 1999; Beltran et al., 1999; Benitez et al., 2001; Ledakowicz et al., 2001; Amat et al.,2003) or by H_2O_2/UV (Adams and Kuzhikanni, 2000; Ledakowicz et al., 2001; Chan et al.,2004) for degradation of organic molecules other than pesticides.

Chan et al. (2004) examined the sequential oxidation of atrazine under different experimental conditions which resulted into deisopropylatrazine, deethylatrazine and deethyldeisopropylatrazine as major intermediates. It was also observed that addition of H_2O_2 could significantly enhance the degradation of atrazine into ammeline, ammelide and cyanuric acid (CA) intermediates/products. Further degradation of CA was carried out by a newly isolated CA-degrading bacterium, *Sphingomonas capsulata*. The photochemical pretreatment integrated with microbial degradation lead to the complete degradation and detoxification of atrazine.

Decolorization and degradation of Reactive Black 5 azo dye was investigated (Jafari et al. 2010) using biological, photocatalytic (UV/TiO_2) individually and in a combined manner. Complete decolorization of the dye with 200 mg/L in less than 24 h was achieved by the application of *Candida tropicalis* JKS2. Mineralization of RB5 solution (50 mg/L) was obtained after 80 min by photocatalytic process (0.2 g/L TiO_2). However, this process was not efficient for the removal of the dye at high concentrations (≥ 200 mg/L). In a two-step combined treatment process, biological treatment followed by photocatalytic degradation, the peak in corresponding to it significantly disappeared after 2 h illumination with 60% COD removal achieved in the biological step. The combined process was observed to be more effective than individual biological and photocatalytic process, mainly reported in wastewater treatment and degradation of pesticides in aqueous media.

Shah, (2013) investigated the decolorization and degradation of Reactive Black 5 azo dye by biological, photocatalytic (UV/TiO_2) and combined processes. Treatment of the synthetic medium containing RB5 *by Pseudomonas aeruginosa* ETL-2211 indicated complete decolorization of the dye (with 200 mg/L) in less than 24 h but degradation of the aromatic rings did not occur during the biological treatment. In case of photocatalytic process (0.2 g/L TiO_2) of 50 mg/L RB5 solution, mineralization was obtained after 80 min, however, the process was not effective in the removal of the dye at high concentrations (≥ 200 mg/L). A combined treatment process, namely, biological treatment followed by photocatalytic degradation, was assessed and it was found that absorbance peak in UV region significantly disappeared after 2 h illumination and about 60% COD removal in the biological step. It is suggested that the combined process is more effective than the photocatalytic and biological treatments.

Gonzalez et al. (2010) studied the degradation of 2-chlorophenol (2-CP), 2,4-dichlorophenol (2,4-DCP), 2,4,6-richlorophenol (2,4,6-TCP) and pentachlorophenol (PCP) via biological, photocatalytic (AOP) and in sequential manner. Biodegradation of chlorophenols was done by using white-rot fungus *Trametes pubescens*, while in photocatalysis TiO_2/UV was used. In the biological degradation, highest degradations (94.6% to 37.8%) was obtained when the reaction medium was supplemented with glucose as co-factor, ranging from degradation activity for 2-CP > 2,4-DCP > PCP > 2,4,6-TCP. In photodegradation, the obtained range was 82.0% to 24.0% following order 2-CP > 2,4,6-TCP > 2,4-DCP > PCP. Combining both of these in sequential manner gave 100% degradation for all the tested chlorophenols.

Despite the availability of good number of reports using sequential processes for better performance towards the dissipation of organic pollutants, efforts to use the same for removal of pesticides have been rarely attempted in water but remain unexplored in soil.

1.7 Gap in the Proposed Research Area

Thus, it is clear from the above literature survey that much work has been done for the photocatalytic degradation of imidacloprid in aqueous medium but the literature seems to remain silent for its photocatalytic degradation in soil. A verity of microbes has been studied for the degradation of IMI. However, the reports seem to be rarely documented for its degradation by a microbe which present soil is having history of same pesticide that was isolated and then used for the same purpose. Most of the studies only consider removal of

IMI i.e., its degradation, but the role of heteroatoms present in it towards the formation and stability of its metabolites and final form in which they appear in soil is also not well reported. Moreover, the existing literature only specifies that either microbial degradation followed by photocatalytic or its vice versa has been implemented for the degradation of pesticides in water. However, the use these processes both individually and comparatively was not attempted for the degradation of pesticides in the soil.

1.8 Objectives of the proposed work

The main objectives of the proposed work are listed as follows:

1. Isolation of neonicotinoid degrading bacteria from contaminated soil.
2. Optimization of conditions for maximum degradation of pesticide by bacteria.
3. Optimization of conditions for maximum photocatalytic degradation using TiO_2.
4. Studying sequential microbial-photocatalytic degradation of pesticide with optimum parameters.

2.0 MATERIALS AND METHODS

This chapter includes various materials and methods used for the isolation, identification and characterization of bacterial isolates. It also describes the optimization of various parameters required for the maximum microbial (in broth and soil) and photocatalytic degradation (using TiO_2) of imidacloprid and techniques that were used to extract and analyze its residual amount, metabolites and inorganic ions (nitrate, nitrite and chloride).

2.1 Materials Used

Technical grade Imidacloprid (purity 99%) was obtained as gift sample from Bayer crop science, India. All solvents (acetonitrile, methanol and ethyl acetate) used in the experiments were of HPLC grade and purchased from Merck India (P) Ltd. De-ionized water used for preparing stock solution of imidacloprid, sulphuric acid, sodium hydroxide, hydrochloric acid, anhydrous sodium sulphate, and all other chemicals used for minimal media (MM) preparation and for characterization purposes were of high analytical grade and obtained from Loba Chemi, India. Enrichment media (other MM) were purchased from HIMEDIA. Titanium dioxide (Degussa P25, average particle size of 30-50 nm, anatase: rutile :: 80:20) catalyst was obtained from Evonik Industries formerly Degussa corporation, India.

2.2 Methodology

2.2.1 Preparation of stock solution of imidacloprid

A stock solution of IMI (500 mgL^{-1}) was prepared by dissolving 250 mg of it in 500 ml of solvent (water and acetonitrile) by stirring on magnetic stirrer. This stock solution was further diluted to obtain the IMI solution of desired concentration.

2.2.2 Soil samples for isolation and degradation study

The soil samples (5-10 cm deep) for the isolation of bacteria were collected from paddy fields at Rakhra village Patiala (District), Punjab (India), with a history of 9-10 years of utilization of imidacloprid for the isolation of bacteria and soil samples were collected from Thapar University campus, Patiala, Punjab (India) with no pesticide history for the degradation studies. Prior to any experiment, soil sample was dried, homogenized, sterilized (for degradation studies only) and its physicochemical characteristics was determined accordance to standard methods.

2.2.3 Physicochemical characterization of soil

Various physicochemical parameters (pH, Organic carbon, available phosphorous, bulk density, water holding capacity, permeability, moisture content and soil texture) were analysed as per reported standard methods and is being describe herein:

2.2.3.1 pH

It was determined as per the method of Jackson (1967), by using soil : water :: 1 : 2. A lot of 10 g of soil was placed in a 100 ml beaker and 20 ml of distilled water was added, stirred well for 5-10 min and kept undisturbed for 2 h followed by stirring again. Then pH was measured using calibrated (using buffers of pH 4.0, 7.0 and 9.2) pH meter (Cyberscan pH 510).

2.2.3.2 Total organic carbon

It was performed as per the method given by Walkey and Black (1965).

Reagents

1. 1N Potassium Dichromate solution: $K_2Cr_2O_7$ = 49.04 g/liter
2. 0.5 N Ferrous Ammonium Sulphate: 198.0 g of salt per litre of solution.
3. Diphenylamine indicator: 0.5 g of diphenylamine in a mixture of 20 ml water and 100 ml concentrated sulphuric acid.
4. Concentrated sulphuric acid.
5. Orthophosphoric acid (85%) and sodium fluoride (NaF).

Procedure

1. 1 g of soil was taken in a 500 ml conical flask followed by the addition of 10 ml of 1N $K_2Cr_2O_7$. The flasks were swirled for mixing the soil and reagent.
2. Concentrated H_2SO_4 (20 ml) was added, shaked and the flask was allowed to stand undisturbed (30 min) and thereafter 200 ml of distilled water was added.
3. To this mixture, Orthophosphoric acid (10 ml), NaF (0.5 g) and diphenylamine indicator (1 ml) was added.
4. The contents thus obtained were titrated with freshly prepared ferrous ammonium sulphate solution (0.5 N) till the colour changes from blue-violet to green. A blank was also run without soil.

Calculations:

$$\text{Organic carbon (\%)} = \frac{10\,(B-T) \times 0.003 \times 100}{B \times \text{Wt. of soil}}$$

Where, B is the volume of ferrous ammonium sulphate solution required for blank titration and T is the volume of ferrous ammonium sulphate solution required for soil sample titration.

2.2.3.3 Available phosphorus

Available phosphorus (P) in the soil samples was estimated as per the method given by Olsen et al. (1954).

Reagents

1. 0.5 M sodium bicarbonate ($NaHCO_3$) extracting solution: 84 g of $NaHCO_3$ was added in distilled water and the volume was made up to 2 L followed by adjustment of its pH = 8.5 with 1M or 1N NaOH.
2. Reagent A: 12.0 g of ammonium molybdate in 250 ml distilled water and 0.2908 g of antimony potassium tartarate in 100 ml distilled water was added to 1000 ml of 2.5 M H_2SO_4, mixed thoroughly and volume made up to 2 L with distilled water.
3. Reagent B (freshly prepared): 1.058g of ascorbic acid in 200 ml of reagent A and mixed.
4. Sulphuric acid (2.5 M): 140 ml of concentrated H_2SO_4 diluted to 1L.
5. Stock Standard P solution (50 ppm P): 0.2917 g KH_2PO_4 dissolved in water to a final volume of 1 L.
6. Working Standard P solution (1 ppm): 20 ml of (50 ppm P) solution diluted to 1L**.**

Procedure

1. 2.5 g soil was placed in a 100 ml Erlenmeyer flask followed by the addition of 50 ml extracting solution.
2. The solution was kept on a shaker for 30 minutes and filtered through Whatman No. 42 filter paper.
3. 10 ml aliquot of the filtrate was transferred to a 100 ml beaker and then addition of 1 ml of 2.5 M H_2SO_4, 15.5 ml of distilled water, 8 ml of Reagent B and another 15.5 ml of distilled water was done.
4. A blank was prepared as above said. For the standard curve: 0, 2, 5, 10, 15 and 20 ml of standard solution was placed in 50 ml volumetric flasks separately. Ten ml of extracting solution , 1.0 ml of 2.5 M H_2SO_4, 8 ml Reagent B was added and the final volume was

made upto 50 ml. The P concentrations of these solutions were 0.04, 0.1, 0.2, 0.3 and 0.4 ppm respectively. After 10 minutes, the P concentration was read at 882 nm.

Calculations:

P in soil (ppm) = P in extract (ppm) x 20 (the standard soil to solution ratio).

2.2.3.4 Water holding capacity

It was measured as per the method given by Black et al. (1965).

Apparatus

Circular brass boxes (keen boxes) of 5.6 cm internal diameter and 1.6 cm depth were taken which had 0.75 mm holes spaced 4 mm apart at the bottom. Each box was fitted with a brass lid.

Procedure

1. Soil samples were collected, sieved and dried at 105°C in an oven.
2. A filter paper strip of the size of the base of the keen box was cut.
3. The filter disc was weighed and placed in a petridish contain water to measure the moisture absorbed by the filter paper.
4. The disc was placed at the bottom of the keen box and weighed followed by filling of the box with soil. Each time the box was tapped to make a approximate uniform soil column.
5. The box containing soil was weighed and kept in a petridish containing water for overnight saturation.
6. The box was removed the next day, wiped and weighed followed by overnight drying at 80º C in the oven in order to obtain constant weight.
7. The box containing oven-dry soil was weighed finally at room temperature.

Calculations:

Weight of box+ filter paper = W1

Weight of the box +oven dry soil = W2

Weight of the box+ soil after moistening = W3

Weight of dry soil = W2-W1

Weight of moisture absorbed = W3-W2

$$\text{Water holding capacity of the soil} = \frac{(W3-W2)-(W2-W1)}{W2-W1} \times 100$$

2.2.3.5 Bulk Density

It was measured as per method given by Black et al.(1965).

Procedure

1. Collected the soil sample by removing unnecessary material from the upper layer of the soil.
2. Soil samples were dried at 105°C for 24 h till constant weight was achieved.
3. Weighed the empty specific gravity bottle
4. Filled the soil samples in bottle and recorded the volume.

Calculations:

Weight of empty bottle = W1

Weight of bottle and soil = W2

Weight of soil = W2-W1

Volume of the soil = V ml

$$\text{Bulk density of the soil/fly ash} = \frac{W2-W1}{V\ (cm^3)}\ gm^{-3}$$

2.2.3.6 Soil moisture content

Moisture content of the soil samples were done by using method as per Black 1965.

Procedure

1. Weighed aluminum tin, recorded its weight and then tared the weighing balance.
2. The soil sample (10 g) was placed in the tin and recorded its weight as wet soil.
3. Placed the sample in the oven 105^{o}C, and dried it for 24 hours till constant weight.
4. Recorded this weight as weight of dry soil.
5. Repeated step 4 until there was no difference between any two consecutive measurements of the weight of dry soil.

Calculations:

The moisture content in dry weight basis may be calculated using the following formula:

$$\text{(Soil moisture content) } \Theta_d = \frac{\text{(dry wt. of empty tin) - (wt. of tin with soil)}}{\text{(wt. of wet soil)}} \times 100$$

2.2.3.7 Permeability Test

Coefficient of permeability of a soil was determined using constant head method (ASTM D2434-68 standard)

Planning and Organization

1. Preparation of the soil sample for the test
2. Finding the discharge through the specimen under a particular head of water.

Procedure

1. 2.5 kg soil sample was taken from a thoroughly mixed air dried or oven dried soil.
2. The initial moisture content of sample was determined and kept in the air tight container.
3. Added required quantity of water to get the desired moisture content and mix the soil thoroughly.
4. Weighed the empty permeameter mould and clamp it between the compaction base plate and extension collar after greasing inside.
5. The assembly was placed on a solid base and filled with sample and compacted.
6. Excess soil was removed after completion of a compaction
7. The weight of mould with sample was find out and placed the mould with sample in the permeameter to saturate it.

Calculations:

Coefficient of permeability for a constant head test is given by:

$$k = \frac{qL}{Ah}$$

Where; k = coefficient of permeability in cm/sec

q = Discharge cm^3/sec

L = Length of specimen in cm

A = Cross sectional area of specimen in cm^2

h = Constant head causing flow in cm^2

2.2.3.7 Soil Texture Analysis

Soil texture for paddy field soil and Thapar field soil were performed according to Chopra and Kanwar (1991)

2.2.4 Growth media used for isolation and degradation studies

Nutrient broth (NB) was used as enrichment media for the growth of IMI degrading bacteria having various components as listed in Table 2.1 and pH of media was maintained to 6.8 ±0.5, adjusted by using 0.1N HCl and/or 0.1 N NaOH. All the components of growth medium were sterilized (121 °C, 15 psi for 15 min) in an autoclave before use.

Table 2.1 Composition of Nutrient broth Media

Component	Amount (gL^{-1})
Peptone	0.5
NaCl	0.5
Beef/yeast extract	0.3
Agar	15.0 g

The acclimatization of the isolated bacterial colonies for screening of their tolerance to IMI was carried out in MM which was composed of various constituents as listed in Table 2.2. The pH (7 ±0.5) of the media was adjusted by using 0.1N HCl and/or 0.1 N NaOH.

Table 2.2 Composition of Minimal Media

Component	Amount (gL^{-1})
Sucrose	10
K_2HPO_4	2.5
KH_2PO_4	2.5
$(NH_4)_2HPO_4$	1
$MgSO_4.7H_2O$	2
$FeSO_4.7H_2O$	0.01
$MnSO_4.4H_2O$	0.007
Agar	15 g

2.2.5 Preparation of Petriplates

The sterilized media (NB and MM) was poured in UV-light sterilized petri plates and was allowed to solidify (24 h) under the aseptic conditions in laminar air flow bench. After the solidification of media, these plates were kept in an inverted position (24 h) at an ambient temperature for sterility test.

2.2.6 Isolation of Imidacloprid (IMI) Tolerant Bacteria

2.2.6.1 Isolation of IMI Bacterial Isolates

Isolation of bacterial was done on enrichment media (NB) using serial dilution spread plating technique (Cappuccino and Sherman, 1989) as explained below:.

1. Initially soil sample (2 gm) was suspended in 100 ml of NB media, spiked with 50 mgL^{-1} of IMI and kept for incubation on rotary shaker at 37± 0.1 $^{\circ}C$ for 48 h.
2. Thereafter, an aliquot of 100 µl was spread on NA plates using serial dilution technique and incubated further at 37 $^{\circ}C$ for 48 h.
3. The resulting colonies were selected on the basis of colour morphology and sub cultured on same medium till pure colonies were obtained.
4. The isolates thus obtained (hereafter termed as T1-T5) were further screened on minimal media containing imidacloprid (50 mg L^{-1}) to find out their ability to use IMI as carbon source.
5. These isolated colonies were individually re-streaked on same agar media (streak plate method) to get the pure isolates and stored at 4 ºC till further use.

The growth of bacterial isolates (T1-T5) was evaluated by using IMI (50 mgL^{-1}) as sole source of carbon in 100 ml of MM. Isolates were inoculated in different MM flask and incubated at 37 ^{o}C. The growth of these isolates was monitored by measuring the absorbance @ 600 nm (section 2.2.10.6.1) after regular intervals of time (1 d) till 28 days. Among these isolates T1 and T5 have shown better growth (discussed later in section 3.1) and were selected for further characterization while only T1 was chosen for degradation study of IMI.

2.2.6.2 Identification and Characterization of T1 and T5 Bacterial Isolates

These bacterial isolates (T1 & T5) were identified/characterized on the basis of morphological, biochemical, physiological characterization and phylogenetic analysis using 16S rRNA sequencing.

2.2.6.2.1 Morphological Characterization

The bacterial isolates were morphologically identified on the basis of colony color, form, margin, elevation on agar medium, type of surface growth, clouding and sedimentation in broth medium. It was done by both macroscopically and microscopically.

2.2.6.2.1.1 Macroscopic Characteristics

The bacterial isolates initially grown in liquid minimal medium were diluted (serial dilution technique) and spread on MM agar plates and incubated at 37 °C in inverted position for 48 h. After incubation the macroscopic characteristics were observed and recorded (Table 2.3). Shape of the colony on agar plate was observed in terms of circular, irregular, filamentous or spindle. The colony colour was observed (white, orange, yellow or translucent, opaque, shiny etc.) and elevation was confirmed by holding plate to the side as flat, raised, convex etc. Various characteristics in the form of surface growth, sedimentation and clouding were observed by inoculating isolates in MM broth. The growth was checked after incubation at 37 °C for 48 h @120 rpm on orbital shaker.

Table 2.3 Macroscopic observations of bacteria on agar plate

S. No.	Characterization/Property	Observation to be recorded
1	Form/shape	Circular, Irregular, Filamentous or Spindle
2	Colony color	White, Orange, Yellow Or Translucent, Opaque etc.
3	Margin	Smooth/Entire, Lobate, Undulate or Filamentous
4	Elevation	Flat, Raised, Convex etc.

2.2.6.2.1.2 Microscopic Characteristics

Type of strain was determined by Gram staining method and performed accordingly to the method described by Cappuccino and Sherman (1999).

Gram Staining

Phenotypically it is the first step for identifying an unknown bacterial isolate. According to cell wall structure it can broadly divided into two groups viz., gram positive and gram negative. It is well known that appearance of purple colour during gram staining indicates the gram-positive cells having a thick peptidoglycan layer. However, appearance of pink colour indicates the gram-negative cells with a thin peptidoglycan layer.

Procedure

1. A thin smear of bacterial culture was made on clean glass slide, air dried and heat fixed.

2. Smear was then covered with crystal violet (primary stain) for 30 sec and then washed gently with distilled water.
3. Gram's iodine (mordant) was applied on the smear for 30 sec and washed with distilled water.
4. Slides were flooded with decolorizer (95% ethyl alcohol) drop wise until no more purple color was flown from the smear (approximately for 10-20 sec). After that the slide was washed with distilled water.
5. Smear was flooded with Safranin (counter stain) for 30 sec and washed with distilled water.
6. Extra water from stained slides was dried by blotting paper then air dried and examined microscopically under 40X and 100X for cell morphology and colour.

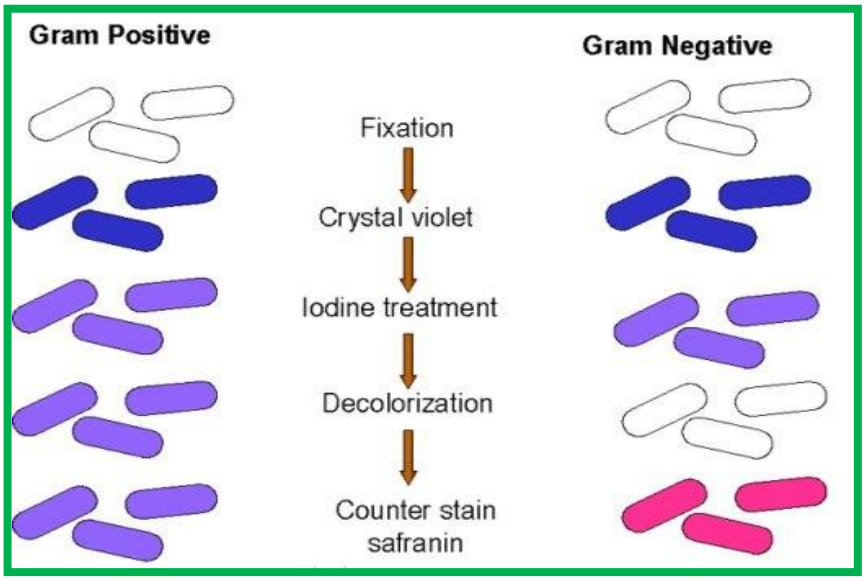

Fig. 2.1 Change in colour during Gram staining process in bacterial cell

2.2.6.2.2 Biochemical Characterization

Various tests such as hydrogen sulphide (H_2S) formation, motility, methyl red-Voges Proskauer, citrate, starch, gelatin hydrolysis, catalase, pectin, carbohydrate and amino acid utilization were performed as per reported methods (Aneja, 2008). The positive test (+) showed growth of the isolate in corresponding medium, while negative results (-) signifies absence of growth of isolate. The bacterial isolates showing weak positive results denoted by w/+.

2.2.6.2.2.1 H_2S production

This analysis indicates the reduction i.e., hydrogenation of either inorganic compounds viz., thiosulfates ($S_2O_3^{2-}$), sulfites (SO_3^{2-}) or sulfates (SO_4^{2-}) or sulphur possessing amino acids (cystine, cysteine and methionine) during metabolism by bacteria. The formation of hydrogen sulphide can be identified by incorporating H_2S indicator to the culture medium, which are salts of either ferrous (Fe^{+2}) or lead (Pb^{+2}) and gives visible insoluble black precipitates. This analysis was performed on sulfide indole motility (SIM) agar medium (Table 2.4).

Table 2.4 Constituents of SIM agar medium

Component	**Amount (gL^{-1})**
Peptone	30.0
Beef extract	3.0
Ferrous ammonium sulfate	0.2
Sodium thiosulfate	0.025
Agar	15
pH	7.3

Initially, the medium was dissolved in distilled water, poured in glass test tubes and autoclaved. Thereafter, bacterial isolates (T1 and T5) were inoculated into the agar test tube by means of stab inoculation (approximately 1-2 cm deep in agar) and incubated at 35 ± 2 °C for 48 h. After incubation, the tubes were observed for the presence/absence of black coloration along the line of stab inoculation. The positive test for H_2S production was shown by the appearance of black coloured insoluble precipitates of ferrous sulphide.

2.2.6.2.2.2 Motility test

This analysis signifies the mobility of bacteria in liquid or semi solid medium which is possessed due to the presence of locomotory organs namely flagella, cilia, pseudopodia or by special fibrils that provide gliding form of motility and was carried out on SIM agar medium (Table 2.4). Similar to H_2S analysis (*section 2.2.6.2.2.1*), test tubes were prepared and after inoculation observed for the culture growth together with the stab inoculation deep inside the agar or dispersion of the culture away from the stabbed area. The negative result was indicated by the growth of culture in a distinct zone along the stab.

2.2.6.2.2.3 Methy red-Voges Proskauer (MR-VP) test

This test is used to differentiate two types of bacteria that (i) produces large amount of organic acid (formic, acetic, lactic, succinic, etc.) as stable end products and (ii) produces ethanol/acetoin, and are non-acidic end product. Methyl red-Voges Proskauer analysis was executed by inoculating the bacterial isolates in two different test tubes (one for MR test and other for VP test) having MR-VP broth (Table 2.5) The inoculated tubes were then incubated. After the culture growth, ~5 drops of methyl red was added to one of the test tube, while to the another VP reagents (12 drops of 5% w/v ethanolic solution of α-naphthol; 2-3 drops of 40% w/v aqueous solution of KOH) were added. After this, test tubes were kept for 15-20 min and were observed for any change in colour i.e., for positive/negative results and are abbreviated as MR+, MR-; VP-, VP+. Opposite results were obtained for MRVP test, i.e. MR+, VP- or MR-, VP+.

Table 2.5 Composition of MR-VP broth

Component	**Amount (gL^{-1})**
Peptone	7.0
Glucose	5.0
Potassium phosphate	5.0
pH	6.9

2.2.6.2.2.4 Citrate test

To screen the bacterial isolates on the bases of their ability to utilize citrate as carbon and energy source, this test was performed. Utilization of citrate depends upon production of citrase enzyme by bacteria that breaks down the citrate into oxaloacetic and acetic acid. This changes the pH of the medium and indicated by change in color of the growth medium containing bromothymol blue pH indicator. Simmon's citrate agar medium (Table 2.6) was used to perform this test in which components of the medium were dissolved in distilled water, transfered in test tubes and autoclaved. After this, the tubes were put in an inclined position to form agar slants. Inoculation of the bacterial culture was done into the agar test tube by means of streaking (zig zag position) and further incubated at 35 ± 2 °C for 48 h. After 48 h, the inoculated slant was compared with the control and observed for change in

colour of the medium. The tubes where the bacteria utilizes citrate showed blue colour (a positive test) while no change in color (green color) indicated negative test.

Table 2.6 Composition of Simmon's citrate agar medium

Composition	Amount (gL^{-1})
Ammonium dihydrogen phosphate ($NH_4H_2PO_4$)	1.0
Dipotassium phosphate (K_2HPO_4)	1.0
Sodium chloride (NaCl)	5.0
Sodium citrate	2.0
Magnesium sulfate ($MgSO_4.7H_2O$)	0.2
Bromothymol blue	0.8
Agar	15.0
pH	6.9

2.2.6.2.2.5 Starch hydrolysis test

On the basis of the ability of the bacterial isolate to produce amylase enzyme to degrade the starch, this test was exhibited. Starch, a complex polysaccharide composed two constituents – amylase and amylopectin. Starch hydrolysis test was carried out by preparing starch agar medium plates (Table 2.7). Bacterial culture was inoculated by spread plating or streak plating technique and these inoculated plates were incubated at 35±2 °C for 48 h.

Table 2.7 Composition of starch agar medium

Composition	Amount (gL^{-1})
Starch (soluble)	20.0
Peptone	5.0
Beef extract	3.0
Agar	15.0
pH	7.0

After incubation bacterial growth was observed and the agar plates were flodded with iodine solution (Iodine + KI mixture). The area where bacterial growth was observed showed a clear

zone indicated the amylolytic activity (a positive test) whereas no clear zone (blue color of the medium) indicated negative test.

2.2.6.2.2.6 Catalase test

Catalase test was used to detect the production of catalase enzyme by bacteria to protects the cell from the toxic by-products of oxygen metabolism i.e. hydrogen peroxide (H_2O_2), a potent oxidizing agent. This test was performed by growing the culture on trypticase soy agar slants (Table 2.8). Inoculation of bacterial cell was done using streak inoculation and incubated at 35 ± 2 °C for 48 h. One uninoculated tube was kept as a control. After incubation, the agar slants (inoculated and uninoculated) were filled (2 cm above the slant) with 3% H_2O_2 solution. Extensive bubble formation indicated the positive test whereas no bubble formation indicated the negative test.

Table 2.8 Composition of trypticase soy agar medium

Composition	Amount (gL^{-1})
Trypticase	15.0
Phytone	5.0
Sodium chloride (NaCl)	5.0
Agar	15.0
pH	7.3

2.2.6.2.2.7 Gelatin hydrolysis test

This test was used to screen the hydrolysis of gelatin (a protein) by bacterial isolate which is used as source of carbon and energy for their growth. Hydrolysis of gelatin into amino acids was done by proteolytic exoenzyme, known as gelatinase, and is produced by bacteria when grown on semi-solid medium containing gelatine. It was performed by using gelatin agar medium (Table 2.9). Gelatin agar tubes were prepared and inoculated by bacterial isolate using stab inoculation that were incubated at 35 ± 2 °C for 48 h. One of the uninoculated tube was kept as a control. After incubation the tubes (inoculated and uninoculated) were placed in refrigerator (4°C) for 15-30 min. After the bacterial growth the agar tubes showing liquid medium even after cooling at 4 °C gives positive test, whereas the solidification of medium after cooling gives negative test.

Table 2.9 Composition of gelatin agar medium

Composition	Amount (gL^{-1})
Gelatin	40.0
Peptone	20.0
Sodium chloride (NaCl)	5.0
Dipotassium phosphate (K_2HPO_4)	2.5
pH	6.8 ± 0.2

2.2.6.2.2.8 Pectin hydrolysis test

Pectin substances are considered as primary constituents of plant tissues and composed of complex carbohydrates (galacturonic acid). This test was carried out to identify the pectinase (pectin hydrolyzing enzyme) producing bacteria on solid agar medium. This test was performed on pectin agar medium (Table 2.10) where ingredients of the medium were dissolved in distilled water, autoclaved and poured in petriplates. Inoculation of the culture was done by spot inoculation or streak inoculation on agar plates and incubated at 35 ± 2 °C for 48 h in an inverted position.

Table 2.10 Composition of pectin agar medium

Composition	Amount (gL^{-1})
Pectin	10.0
Sodium nitrate ($NaNO_3$)	2.0
Potassium chloride (KCl)	0.5
Magnesium sulfate ($MgSO_4.7H_2O$)	0.5
Dipotassium phosphate (K_2HPO_4)	1.0
Ferrous sulfate ($FeSO_4.\ 7H_2O$)	0.01
Agar	20.0
pH	6.0

After incubation the agar plates were flooded with 1% hexadecyltrimethyl ammonium bromide reagent. The reagent precipitated the unhydrolyzed pectin gave white opaque colour

to the medium. A clear zone around the bacterial growth was observed indicating the pectin hydrolysis by pectinase enzyme.

2.2.6.2.2.9 Carbohydrate utilization test

Carbohydrates are the organic molecules composed of carbon, hydrogen and oxygen and act as source of carbon and energy for the growth of microbes. This test was performed on MM at pH = 7 (Table 2.11). The carbohydrate i.e., sucrose in this medium was replaced by different available carbohydrates (glucose, lactose, mannitol, xylose, fructose, maltose). The liquid medium (broth) flasks (containing different carbohydrates) were prepared and inoculated with bacterial culture. The inoculated flasks along with respective carbohydrate control (uninoculated) were incubated at 35 ± 2 °C @ 120 rpm for 48 h. The presence (denoted as +), absence (denoted as -) and weak growth (denoted by w/+) was assessed by comparative analyzing the inoculated tubes with control (uninoculated) tubes.

Table 2.11 Composition of carbohydrate minimal medium

Composition	Amount (gL^{-1})
Carbohydrate*	10
Di-potassium phosphate (K_2HPO_4)	2.5
Potassium dihydrogen phosphate (KH_2PO_4)	2.5
Diammonium phosphate dibasic ($(NH_4)_2HPO_4$)	1
Magnesium sulfate heptahydrate ($MgSO_4.7H_2O$)	2
Ferrous sulfate heptahydrate ($FeSO_4.7H_2O$)	0.01
Manganous sulfate ($MnSO_4.4H_2O$)	0.007
pH	7

* Carbohydrate: Glucose, Lactose, Mannitol, Xylose, Fructose, Maltose

2.2.6.2.2.10 Amino acid utilization test

Amino acids are the building blocks of peptides and proteins. These acids act as carbon and nitrogen source for the growth of large number of bacteria, fungi and yeasts which metabolize them by the process of catabolism. This test was carried out on MM having pH = 7 (Table 2.12). The carbon source in this medium (i.e. sucrose) was replaced by different available amino acids (such as glycine, tyrosine, valine, arginine, serine, tryptophan, alanine, leucine and threonine). The liquid medium (broth) flasks (containing different amino acids)

inoculated with bacterial culture along with respective amino acids as control (uninoculated) were incubated at 35±2 °C @ 120 rpm for 48 h. The presence (denoted as +), absence (denoted as -) and weak growth (denoted by w/+) was assessed by comparative analyzing the inoculated tubes with control (uninoculated) tubes.

Table 2.12 Composition of amino acid minimal medium

Composition	Amount (gL^{-1})
Amino acid*	10
Di-potassium phosphate (K_2HPO_4)	2.5
Potassium dihydrogen phosphate (KH_2PO_4)	2.5
Diammonium phosphate dibasic ($(NH_4)_2HPO_4$)	1
Magnesium sulfate heptahydrate ($MgSO_4.7H_2O$)	2
Ferrous sulfate heptahydrate ($FeSO_4.7H_2O$)	0.01
Manganous sulfate ($MnSO_4.4H_2O$)	0.007
pH	7

*Amino acid: Tyrosine, Valine, Arginine, Serine, Alanine, Leucine and Phenylalanine

2.2.6.2.3 Physiological Characterization

This characterization includes the growth of bacterial isolate under different saline (0-20% NaCl content), temperature (20-55°C) and pH (3-11) conditions in both enrichment (Table 2.1) and MM (Table 2.2). The growths of isolates were measured under different conditions in terms of optical density by UV-vis spectrophotometer (*section 2.2.10.6.1).* Incubation conditions for salinity and pH was 35 ± 2 °C @ 120 rpm for 48 h.The imidacloprid degrading isolates T1 and T5 growth at optimum parameters range were further identified (Table 2.13) .

Table 2.13: Range of different parameters for physiological characterization

Character	**Range of different parameters**
Salinity	0, 2, 4, 6, 8, 10, 12, 14, 16, 18, 20% NaCl
Temperature	25, 28, 35, 37, 45, 50, 55 °C
pH	3, 5, 6, 7, 8, 9, 10, 11

2.2.6.2.4 Phylogenetic Analysis

The 16S rRNA gene sequencing was performed by Xcelris Labs Limited, Ahmedabad (India). DNA was isolated from bacterial strain T1 and T5 using QIAamp DNA Purification Kit

(Qiagen). After isolation of DNA the quantitative assessment was performed on Nanodrop spectrophotometer at 260 and 280 nm (1 O.D. @ 260 nm wavelength = 50 µg DNA per ml). However, its purity was estimated on the basis of ratio of optical density (260 : 280 nm), where ratio = 1.8-2.0 indicates the high purity of DNA. The concentration of DNA was calculated using the formula.

$$\text{Concentration of DNA (mg/mL)} = \text{OD@ 260 nm} * 50 * \text{dilution factor}$$

Quality and purity of DNA were verified by agarose gel electrophoresis having agarose = 0.8% w/v in 0.5X TAE (pH = 8.0) buffer. Ethidium bromide (1%; EtBr) was added @ 10µl /100ml. The wells were charged with 5µl of DNA preparations mixed with 1µl gel loading dye (6X). Electrophoresis was carried out at 80V for 30 min at room temperature. DNA from the isolates was visualized under UV using gel documentation system and the DNA was used further for polymerase chain reaction (PCR). Amplification of 16S rRNA gene fragment was done by PCR method from genomic DNA by using universal bacterial primers 8F (AGA GTT TGA TCC TGG CTC AG) and 1492R (ACG GCT ACC TTG TTA CGA CTT). Table 2.14 shows the composition of reaction mixture for PCR and the reaction was carried out in Eppendorf Thermal Cycler for 30 cycles (Fig. 2.2). Amplified PCR product was checked by using gel electrophoresis. PCR product (5 µL) of each isolate was mixed with 1 µl of 6X gel loading dye and electrophoresed on 1.2 % agarose gel containing ethidium bromide (1% solution @10 µl/100 ml) at constant 5V/cm for 30 min in 0.5 X TAE buffer.

Table 2.14 Composition of reaction mixture for PCR

Component	Quantity (µL)	Final concentration
DNase-RNase free water	7.50	--
2X PCR master mix (Fermentas)	12.50	1X
Forward primer (10 pmole/ µL)	1.00	10 pmole
Reverse primer (10 pmole/ µL)	1.00	10 pmole
Diluted DNA (30 ng/µL)	3.0	--
Total	25.00	--

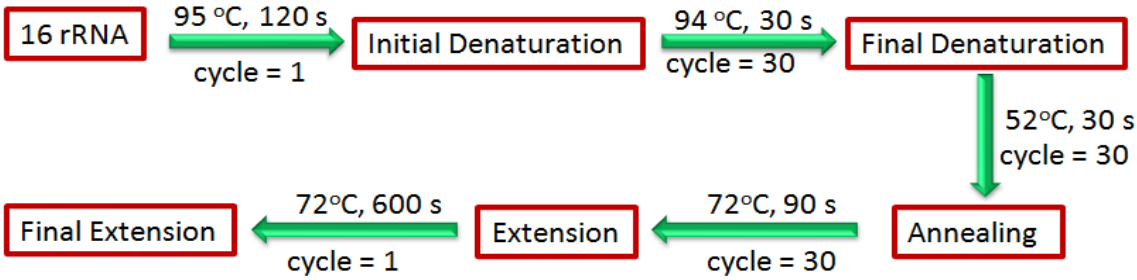

Fig. 2.2 Steps and conditions for PCR

2.2.6.2.4.1 Sequencing of 16S rDNA (purified) gene segment and sequence analysis

It was performed using BigDye® Terminator v3.1 Cycle sequencing kit (Applied Biosystems, USA) as recommended by manufacturer. The purified sequencing reaction mixtures were subjected for electrophoresis in an automated ABI 3730xl Genetic Analyzer (Applied Biosystem, USA).

The 16S rRNA gene sequence of the bacterial strains (T1 and T5) were processed manually, analyzed at NCBI (National Centre for Biotechnology Information) server (http://www.ncbi.nlm.nih.gov) using BLAST tool and compared to the corresponding neighbor sequences from the GenBank-NCBI database. Multiple alignment of both the strains were performed with related *Enterobacter* species (from GenBank-NCBI database) using Multalin program (Corpet, 1988) and phylogenetic tree was constructed by the neighbor joining method (Saitou and Nei, 1987). Evolutionary distance matrices for the neighbor joining method were calculated using the algorithm of Kimura's two-parameter model (Kimura, 1980). The topology of the phylogenetic tree was evaluated by performing a bootstrap analysis with 1000 replicates. The GenBank/EMBL/DDBJ accession numbers for the 16S rRNA gene sequence of the bacterial strains and related *Enterobacter sp.* were collected and phylogenetic tree were constructed in MEGA 5. The 16S rRNA sequences for T1 and T5 were submitted to GenBank-NCBI, provided with the accession numbers and named *Enterobacter sp.* ATA1 and *Enterobacter sp.*ATA2 respectively.

2.2.7 Optimization of growth conditions for isolate ATA1

2.2.7.1 Tolerance studies

Bacterial isolate ATA1 was subjected to various concentrations of IMI (50, 100 and 150 mg L^{-1} respectively) in MM, and its Growth was monitored by taking absorbance at 600nm in an UV-vis. spectrophotometer (*section 2.2.10.6.1)* for 28 days.

2.2.7.2 Influence of various carbon sources

Various co-metabolites (1% w/v of individual lactose, glucose, fructose, maltose and sucrose) were added in 100 ml of MM, inoculated with an aliquot of culture ATA1 (1ml =1.6 OD) from enrichment medium, incubated at 37 $^{\circ}$C, monitored after regular interval for 7 days by measuring the absorbance at 600 nm using UV-Vis. spectrophotometer (*section 2.2.11.1).*

2.2.7.3 Enumeration of viable cell count

Growth of isolated strain ATA1 was confirmed by enumerating viable cell count with and without (control) adding IMI. An aliquot of 24 h old grown culture from nutrient broth was inoculated in MM with optimised amount of glucose (0.1% w/v, termed as MMG) as co-metabolite containing different concentrations of IMI (50, 100 and 150 mgL^{-1}). Bacterial culture (1 ml) withdrawn at regular interval was serially diluted (0.85% w/v saline water), spread in duplicate on nutrient agar plates and incubated at 37 $^{\circ}$C. Colonies were counted immediately after inoculation and after every 24 h for 7 days.

2.2.8 Co-metabolic Degradation of Imidacloprid

Isolate ATA1 to be assayed for their degradation of imidacloprid was first grown in NB medium and further an aliquot of 48 h old culture (2 ml) transformed into MMG medium with imidacloprid (50 mgL^{-1}), incubated at 37°C, extracted and analysed at regular interval of time for 15 days.

2.2.8 .1 Extraction of Imidacloprid from minimal medium

Sample (5 ml) obtained after degradation was extracted by ethyl acetate (3 x 5 ml). The combined extract was allowed to pass through anhydrous sodium sulphate, evaporated to dryness over gentle stream of N_2 gas. The residues thus obtained were redisolved in 1 ml of acetonitrile and stored at 4 $^{\circ}$C till analyzed by using LC-MS technique (*section 2.2.11.2).*

2.2.9 Microbial degradation of Imidacloprid in soil

2.2.9.1 Collection and preparation of soil for microcosm study

The soil samples for microbial degradation studies were collected from Thapar university campus, Patiala (Punjab), India (section2.2.2). Microcosm consists of 50 g soil spiked with IMI concentration of 50 mg kg^{-1} in beaker. For inoculums preparation strain ATA1 was grown in MMG (1% glucose w/v) medium at 37 $^{\circ}$ C on rotary shaker for 30 h followed by induction with IMI and grown further for 5 h. After this, the cells were harvested by

centrifugation at 10,000 rpm for 10 min at 4° C. Cells were washed three times and quantified by the dilution plate count technique. For experiments, bacterial cells (2×10^8 cells ml^{-1}) were used and added in IMI spiked soil in microcosm. In another set of beakers, minimal medium (un-inoculated) was added as control. Culture were thoroughly mixed in soil, and incubated at 37° C for 20 days under sterile conditions. Sterile distilled water (3 ml) was sprayed to maintain the moisture conditions after every 3 days. Appropriate amount of soil samples (2 g) were removed at different time interval and analyzed for IMI concentration.

2.2.9.2 Optimization of conditions for inoculums preparation

For the inoculums preparation, it is important to optimize the conditions such as carbon source (*section 2.2.7.2*), temperature and pH of the medium. In order to study the effect of different temperatures, strain ATA1 was subjected in minimal media with 1% glucose (w/v) to different temperature (20 ± 0.5 °C, 37 ± 0.5 °C, 45 ± 0.5 °C and 50 ± 0.5 °C). Effect of pH was also evaluated in minimal media containing 1% (w/v) glucose as carbon source by adjusting the pH of minimal media (range of pH 1-11).The samples were kept for incubation at 37 °C on rotary shaker at 120 rpm. It was monitored and analysed as described in *section 2.2.11.1*.

2.2.9.3 Influence of various parameters for biodegradation of imidacloprid in soil

Optimization of different parameters for degradation of imidacloprid in soil was done by varying one parameter at a time while keeping others constant. Initially pH was optimized and it was done by adjusting pH of soil (ranges from1-11) using 0.1N NaOH or 0.1N HCl at least two times till the values get stabilized. Thereafter, IMI spiked soil (50 mg kg^{-1}) was incubated with the bacterial cells 2×10^8 colony forming units per gram of soil (cfu g^{-1}) at 37 °C for 20 days.

Later on the inoculums size was optimized by diluting the strain ATA1 with different cell densities of $2x10^8$, $2x10^7$, $2x10^6$, $2x10^5$ cfu g-1 of soil using plate count method (Singh et al. 2004) and mixed in IMI spiked soil with optimum pH = 7. The Un-inoculated soil served as control.

Under the optimum conditions of pH and inoculum size, the soil were spiked with different concentration of IMI (25, 50, 75 and 100 mg kg^{-1}) were incubated at 37 °C for 20 days to achieve maximum degradation. Finally under all abovementioned optimized parameters, two sets of beaker containing 50 g of IMI spiked soil (50 mg kg^{-1}) were used to

find out effects of flooded and non-flooded conditions on degradation rate. In one set 4 ml of minimal medium containing 2 x 10^7 cfu g^{-1} bacterial cells was added (inoculated) and 4 ml of minimal medium without bacterial cells act as control (uninoculated). In another set for both inoculated and uninoculated spiked soil, additional 50 ml of minimal medium were mixed to represent the flooded conditions. Both sets were incubated at 37 $^{\circ}$C for 20 days.

Samples withdrawn after regular interval of 5, 10, 15 and 20 days were extracted (*section 2.2.9.4*) and analysed using HPLC (*section 2.2.11.3*) and GC-MS (*section 2.2.11.3*) technique.

2.2.9.4 Extraction of imidacloprid from soil

The soil samples (2 g) were extracted with acetonitrile (10 ml) by sonication for 15 min in an ultrasonic water bath (EN 60 US, tank size 12''×6"×6", 100W, 33 ± 3 KHz), stirred for 1 h and kept overnight for settlement . Thereafter, extract solution (10 ml) was separated from the soil by centrifugation (5000 rpm, time = 10 min) and soil sample remained in centrifuge tube was washed twice with acetonitrile (5 ml). The extract solution thus obtained was filtered (0.22 µm Millipore syringe filter), evaporated to dryness with gentle steam of N_2 gas and redisolved in acetonitrile (2 ml) and stored at 4 ^{o}C till analysis.

2.2.10 Photocatalytic degradation of Imidacloprid in Soil

2.2.10.1 Soil Sample collection

The soil samples were collected as per method (*section 2.2.9.1),* autoclaved (121°C, 3 × 30 min) and stored in the dark till use.

2.2.10.2 Lab scale photoreactor set-up

Adsorption and photodegradation studies (with and without TiO_2) were performed in UV reactor made up of wooden chamber (136 cm x 40 cm x 73 cm) equipped with six UV lamps (Phillips, 20W) with such an arrangement that height of the soil samples with respect to UV light can be varied (Fig. 2.3 a & b) as reported previously (Toor et al. 2005) by our group. The internal temperature of the chamber was maintained by using exhaust fan. Soil samples petriplates were covered with transparent sheet to avoid evaporation losses. Temperature of soil sample petriplates was maintained by circulating the water below it. Intensity of UV light intensity was measured using Eppley radiometer (model no. 33013, TUVR, USA).

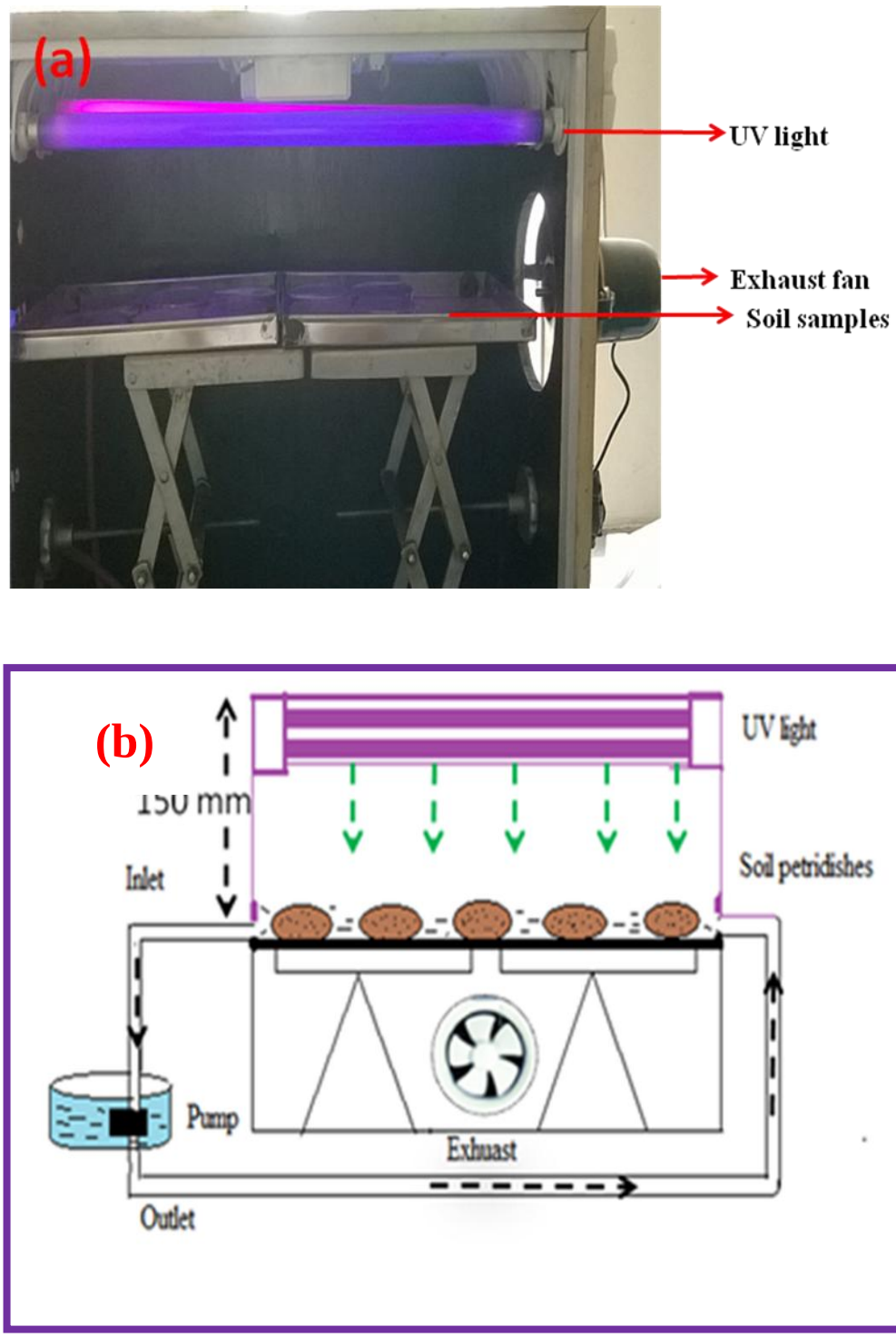

Fig.2.3 Diagram of Actual (a) and Schematic (b) lab scale set up

2.2.10.3 Dark adsorption and photolysis studies

The adsorption studies (with and without TiO_2) were performed in dark without using the UV-light. For this, the soil samples were spiked with 50 mg kg^{-1} of acetonitrile solution of IMI, mixed thoroughly for 3-5 h and dried by evaporating the solvent. The known amount of soil (5 g) was evenly spread on glass petriplates (90 mm of diameter), forming a layer of 0.2

cm estimated from soil bulk density and petriplate area. During adsorption studies, samples were withdrawn at regular time intervals for 18 h and analyzed by UV-Vis. spectrophotometer. The photolysis (without TiO_2) of IMI in soil was also studied by the similar procedure as for dark adsorption except the samples were place in a UV-reactor (Fig. 2.3 a& b) equipped with six UV-lamps (Phillips, 20W) that were switched on.

2.2.10.4 Experimental design and data analysis

Four variables pH, initial concentration of IMI, intensity of UV light and depth of soil were investigated by implementing stoichiometric approach using Central Composite Design (CCD) based on RSM. Analysis of experimental data was supported by Design-Expert Software (trial version 9.0.3.1, Stat-Ease, Inc., MN, USA) (Sakkas et al. 2010; Lu et al. 2011b). The 30 combinations obtained by software (Table 2.16) were experimentally performed as per method described in *section 2.2.10.5*.

The obtained results from these experiments were compared with the predicted ones by using ANNOVA which confirms the adequacy of the quadratic model.

2.2.10.5 Photocatalytic degradation of IMI in UV-light

For photocatalytic degradation, initially catalyst dose of TiO_2 was optimized in IMI spiked soil. It was performed by mixing various amount of TiO_2 (1-5% w/w) in the soil samples (50 mg kg^{-1}) by stirring for 3 h. Excess water was evaporated by keeping samples in oven at 40 °C. Known amount of samples (5 g) were kept in UV chamber for irradiation (18 h) and withdrawn at regular interval of time. The obtained samples were further extracted (*section 2.2.9.4*) analyzed via UV-vis. spectrophotometer (*section 2.2.11.1*).

In order to study the influence of other parameters such as pH (3-11), soil depth (0.2-1.0 cm), intensity of UV-light (10-30 Wm^{-2}) and initial concentration of IMI (10-90 mgL^{-1}), IMI degradation studies were performed at the optimized dose of TiO_2 (3% w/w). Optimization of pH was done by adjusting pH of soil (1, 3, 5, 7, 9 and 11) using 0.1N NaOH or 0.1N HCl at least two times till the values get stabilized. Soil depth was varied by changing the amount of soil (5-25g) at fixed dimensions of petriplates (*section 2.2.10.3*). For initial concentration of IMI optimization, samples were spiked with different concentration of IMI (25, 50, 75 and 100 mg kg^{-1}) in soil. Different Intensity of UV light in reactor chamber was achieved by varying the height of lab jack from 10 to 30 Wm^{-2} corresponding to the average intensity of UV light radiation available in sunlight. Samples were irradiated,

extracted (section *2.2.9.4*) and analyzed using UV-vis spectrophotometer (*section 2.2.11.1*) and LC-MS technique (*section 2.2.11.2*). The evolution of the heteroatoms present in the IMI to inorganic ions after photocatalytic degradation was quantitatively estimated using ion chromatograph (*section 2.2.11.5*).

2.2.11 Techniques used for analysis

The various metabolites formed after the degradation of IMI were analyzed by using various techniques

2.2.11.1 UV-Visible Spectrophotometer

UV–vis. spectrophotometer (HITACHI U-2800, Japan) was used to analyze growth of the isolates and degradation of IMI samples. The absorbance for growth of isolate was measured at λ_{max} = 600 nm and for the IMI at λ_{max} =270 nm. From standard solutions, calibration curves were prepared and concentrations of experimental solutions were thus determined.

2.2.11.2 LC-MS analysis

Liquid Chromatograph coupled with Mass Spectrometer (LC-MS) was used for the qualitative determination of the various metabolites of IMI that are found during its degradation. It was performed by injecting 10 µl in LC-MS (Waters) linked with a Micromass Q-Tof system equipped with Terra column C18 (250 × 4.6 mm, 5 µm), at 20°C. The acidified (0.1% formic acid) mobile phase (acetonitrile: water:: 80 : 20) was iso-cratically flow at a rate of 0.2 ml/min. Mass analysis was performed with a Z-spray source for positive electrospray ionization (ESI) using multiple reaction monitoring (MRM) scan mode.

2.2.11.3 High Performance Liquid Chromatography (HPLC)

The reaction solution obtained after degradation of IMI was analyzed by HPLC (Agilent LC 1120) technique in reverse phase, at ambient temperature using C-18 column (BDS, Qualigens) of dimensions 250 mm × 4.6 mm, and particle size of 5 µm. The constant flow (1 ml/min) of the mobile phase (acetonitrile : water :: 80:20) was maintained by binary pump. A 20 µl of reaction sample was manually injected which was analyzed at λ = 270 nm.

After analysis the reaction sample the absorbance (for UV-Vis.) or peak area of peak corresponding to IMI was determined and the following equations were used to calculate residual amount (eq. 1) and hence corresponding degradation (eq. 2) of IMI:

$$\text{Residual amount (mg } L^{-1}) = \frac{\text{Absorbance/peak area of (standard - sample)}}{\text{Absorbance/peak area of standard}} \times \text{Concentration of standard}$$

$$\text{Degradation (in \%)} = \frac{\text{(Concentration of Standard- Residual Amount)} \times 100}{\text{Concentration of Standard}}$$

2.2.11.4 Gas chromatograph (GC, 45X GC) coupled with Mass Spectrometer (MS, MS-Scion-45P)

The identification of the various metabolites formed during microbial degradation of IMI in soil was performed using GC-MS technique. Reaction solution (3 ml) of IMI obtained after degradation were prepared by filtering (cellulose filter 0.22 µm) and then evaporating to dryness over gentle steam of N_2 gas. Residue was dissolved in ethyl acetate (1 ml) and injected (1µl) to HP-5MS column (15m × 0.25 mm × 0.25 µm) with flow rate of 1ml/min of Helium gas. The injector and transfer line were isothermally kept at 250 °C and 275 °C, respectively. The oven was programmed from 60 °C (5 min hold) to 240 °C@6 °C.

2.2.11.5 Ion chromatograph (IC)

Quantification of inorganic anions (nitrate, nitrite and chloride) produced has been estimated by injecting 100 µl of the sample into Ion chromatograph equipped with a Waters 501pump, a Waters 431 conductivity detector, and ion pack (50 mm × 4.6 mm) column using methanol: water :: 60:40 as mobile phase @ 0.6 ml min^{-1}.

2.2.12 Sequential degradation of Imidacloprid

It was performed by combining the photodegradation of imidacloprid as pre- and post-treatment with the microbial degradation. Therefore, two types of degradation process were followed:

2.2.12.1 Microbial degradation followed by photocatalytic degradation (MP)

This process was carried out by initially degrading the IMI via microbial and then subjecting for the photocatalytic degradation (Fig. 2.4).

2.2.12.2 Photocatalytic degradation followed by Microbial degradation (PM)

This process was carried out by initially degrading the IMI via photocatalytically and then subjecting for the microbial degradation (Fig. 2.5). The individual degradation in both of these processes was performed as described in detail herein:

2.2.12.3 Microbial degradation

It was performed by spiking 1000 g of sterilized soil under optimum conditions as described in section *2.2.9.3.*

2.2.12.4 Photocatalytic experiments

Photocatalytic degradation of IMI in sterilized soil (1000 g) sample was performed under optimum parameters as described in section *2.2.10.5*.

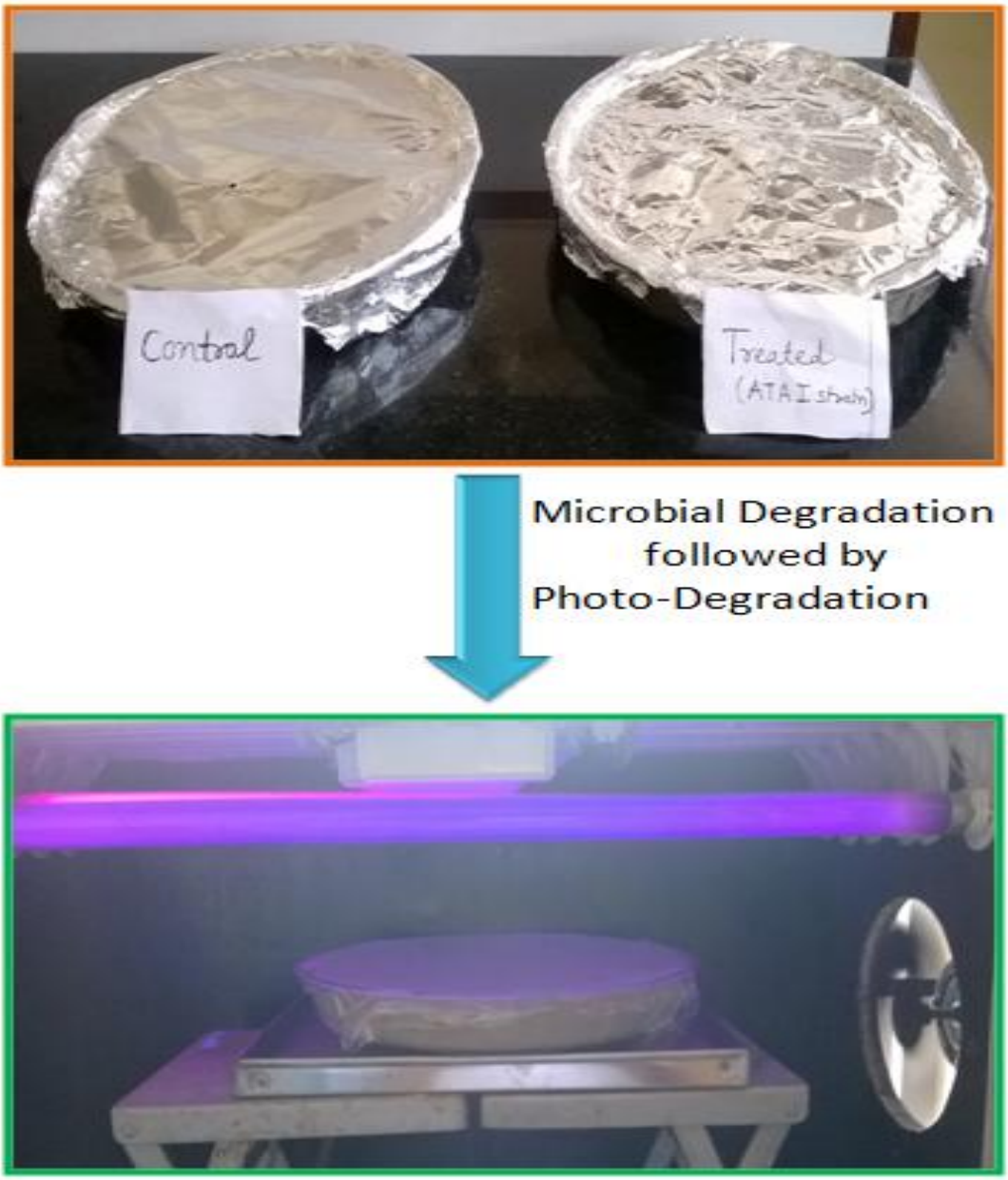

Fig. 2.4 Experimental setup for MP degradation process

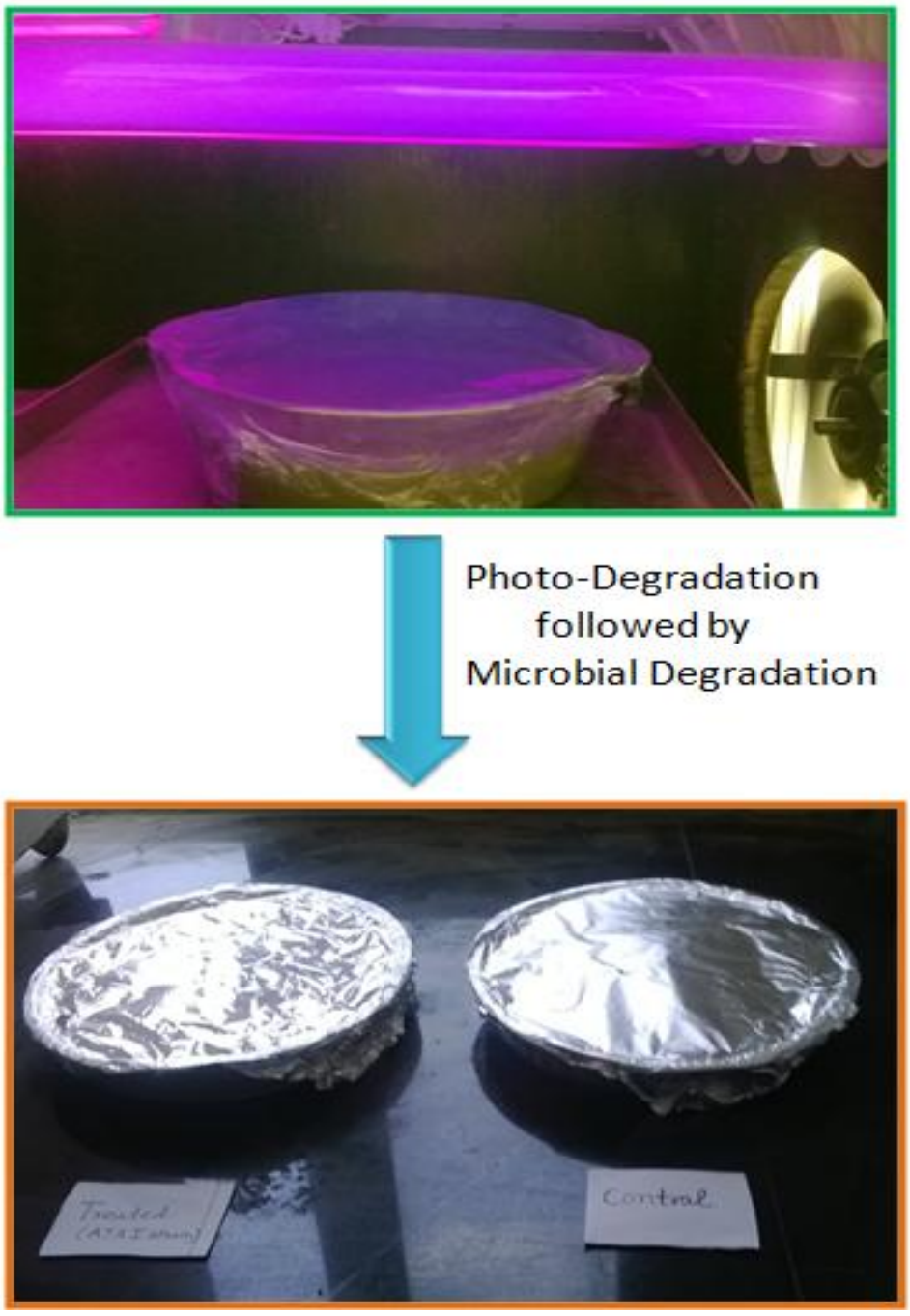

Fig 2.5 Experimental setup for MP process

2.2.12.5 Analysis of metabolites of IMI formed after MP and PM process

It was carried out by extracting soil samples (*section 2.2.9.4*) at various time intervals using LC-MS technique (*section 2.2.11.2*).

3.0 RESULTS AND DISCUSSION

3.1 Isolation and screening of imidacloprid degrading bacteria from paddy field soil samples

Five different bacterial strains (T1-T5) were isolated from paddy field soil having a history (10 years) of IMI application as insecticide. Initially, isolation was done in enrichment medium containing 50 mgL^{-1}

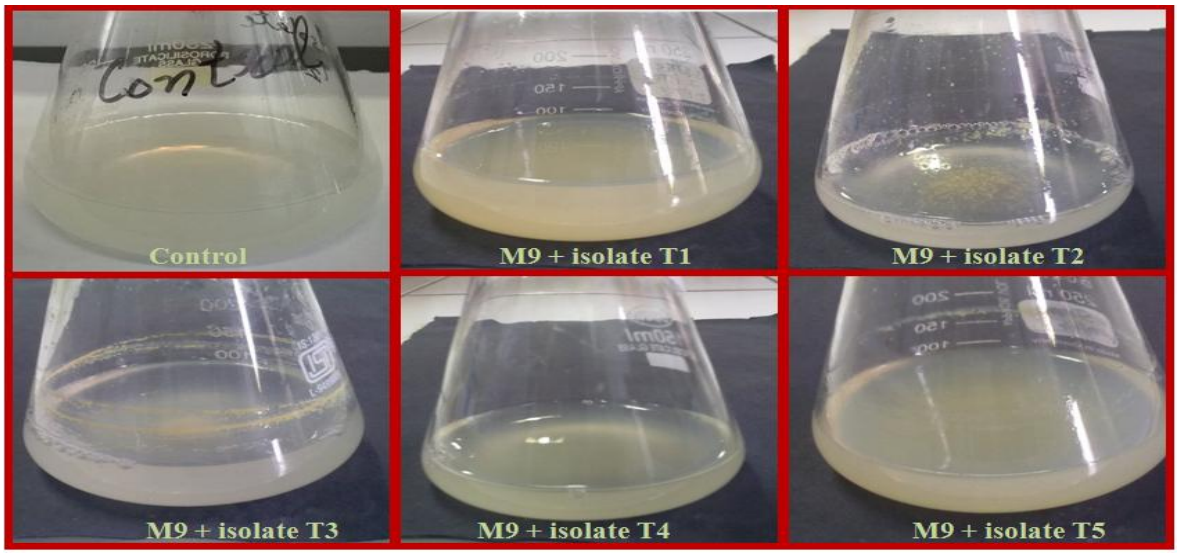

Fig.3.1 Growth of isolates T1 –T5 in minimal media before (control) and after inoculation

IMI concentrations, whereas secondary enrichment was done in minimal medium at its same concentration. These obtained isolates were further sub-cultured (3-4 times) on the same medium (both solid and liquid) in-order to study their efficiency for degradation of IMI. It was found that among the five isolates, strain T1 exhibited the highest growth followed by T5, in minimal media under the laboratory conditions (*section 2.2.6.1*) which is visualised (Fig. 3.1) and confirmed by time course study (Fig. 3.2) by observing the absorbance @ 600 nm. Therefore, these two strains have been selected for their various characterizations (morphological,

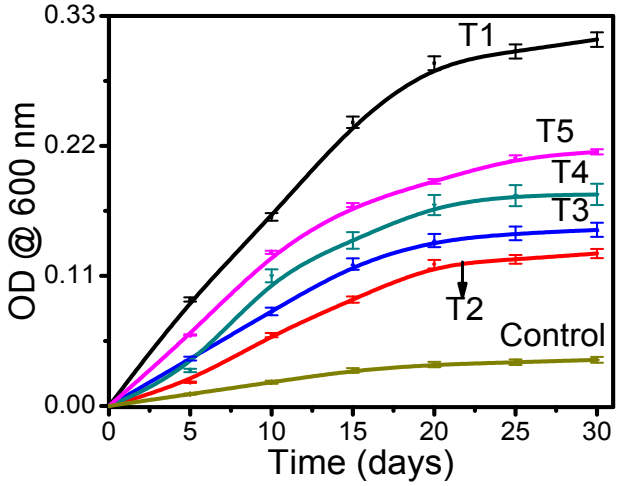

Fig 3.2 Growth of bacterial isolates in minimal media at various time intervals

biochemical, physiological and phylogenetic) and to study the degradation of IMI, as disused in forthcoming sections.

3.2 Identification and Characterization of imidacloprid degrading bacteria

3.2.1 Morphological Characterization

Morphological identification of bacterial isolates (T1 and T5) was performed on the basis of their colony colour, surface, form, margin along with elevation in an agar medium and via. gram straining (Table 3.1). These strains were identified to be gram negative having rod shape and non-motile in nature (Fig. 3.3 a & b).Moreover, these two isolates were found possess convex shaped with regular margin. On agar plate strain T1 was observed white and opaque with smooth surface whereas strain T5 was yellow and opaque with shiny smooth surface (Fig. 3.3 c & d).

Table 3.1 Morphological characterization of bacterial isolates T1 and T5

Morphological Test	T1	T5
Gram Straining	-ve	-ve
Shape (Rod/Cocci)	Small rods	Small rods
Colour	White & opaque	Yellow & opaque
Margin	Regular	
Elevation	convex	Convex
Surface	smooth	Shiny & Smooth

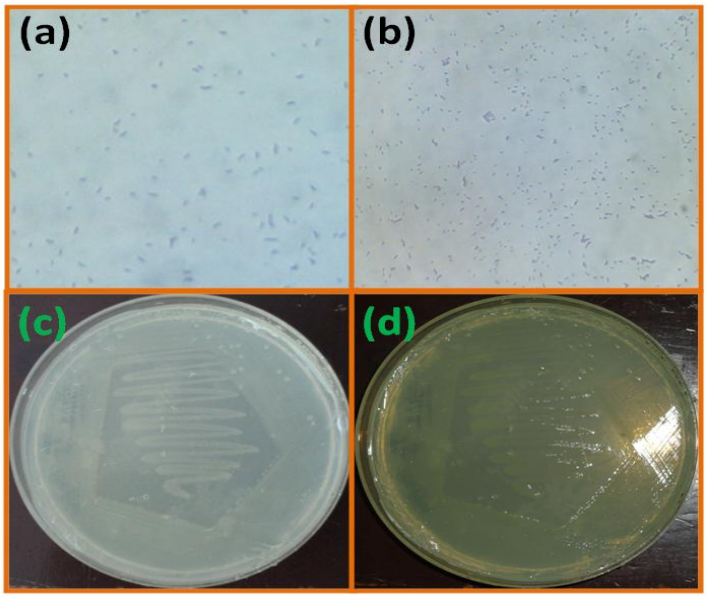

Fig. 3.3 Gram straining of isolate T1 (a) and T5 (b) and morphology of isolates T1 (c) and T5 (d) obtained from imidacloprid degrading enrichment culture in MM

3.2.2 Biochemical Characterization

Various tests required for the biochemical characterization of these isolates were performed and results obtained are summarized in Table 3.2. It was found that strain T1 was not able to hydrolyze starch, while opposite results have been found for strain T5. In this test, iodine reacted

with starch and produced dark blue coloration in the medium for isolate T5, whereas clear zone around the bacterial growth indicated amylolytic activity for T1. Both isolates were not able to hydrolyze pectin due to absence of an enzyme pectinase and showed negative results. Upon growth of these isolates on Simmon's citrate agar medium, a clear change in colour from green to blue visualized (Fig. 3.4 a) revealed citrate is being utilized by these strains. Both isolates (T1 & T5) have shown positive test for citrate utilization as indicated by the blue colour of the medium whereas no change (green colour) in the colour of the medium indicated negative test. This is because in the absence of glucose or lactose some microorganisms are capable of using citrate as carbon source and both isolates have not utilized citrate. For catalyse enzyme activity, Isolates T1 and T5 have shown positive results by breaking down the H_2O_2 into water (H_2O) and oxygen (O_2) as given by equation 3.1.

$$2\ H_2O_2 \xrightarrow{\text{Catalase}} 2H_2O + O_2 \qquad \ldots\ldots 3.1$$

The bubble formation due to evolution of O_2 indicated positive results for both isolates (Fig. 3.4b). In gelatine hydrolysis test for isolate T1, positive results was indicated by liquefaction of the gelatine agar medium due to the formation of gelatinase enzyme while for isolate T5 negative results were confirmed by solidification of the gelatin agar medium. For methyl red test, isolates T1 and T5 retained red colour by addition of methyl red as indicator (due to formation of acid) confirmed positive test for both. However for voges Proskauer test, no colour changes depicted negative test for them.

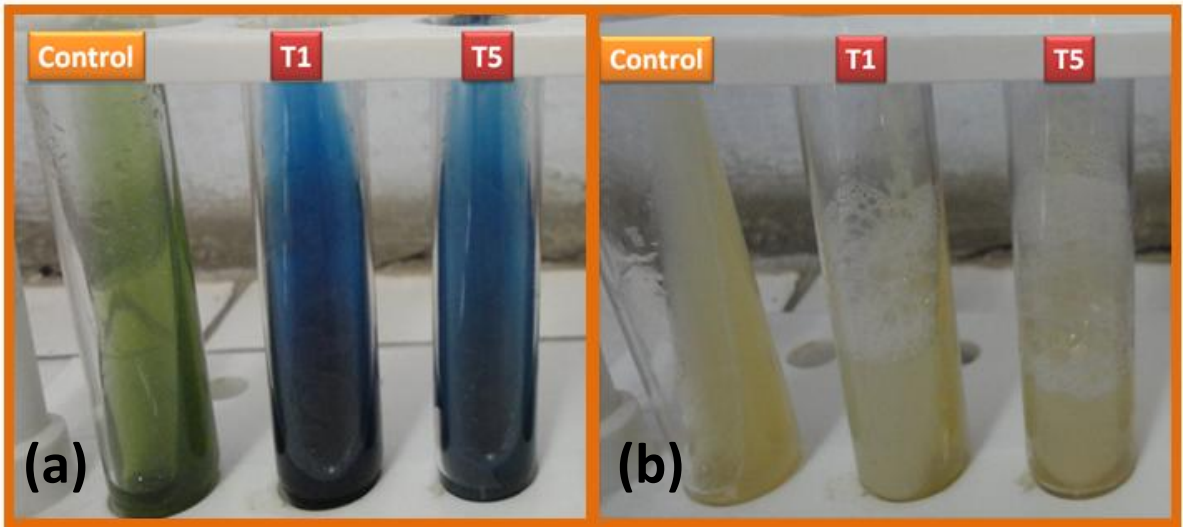

Fig. 3.4 (a) Citrate utilization test and (b) catalase test of isolates T1 and T5

It was found in carbohydrate utilization test that isolate T1 could consume all the carbon sources (glucose, Sucrose, Xylose, maltose, mannitol and fructose) whereas T5 has shown opposite results in relation with T1 for mannitol, xylose and maltose. On contrary to this, both of the isolates showed similar results for amino acid utilization test. The above mentioned results showed that T1 isolate is having more affinity to utilize all carbohydrate as compared to T5.

Table 3.2 Biochemical characterization of bacterial isolates

Biochemical Test	**T1**	**T5**	**Biochemical Test**	T1	T5
Starch Hydrolysis Test	**-**	**+**	**H_2S Production Test**	**-**	**-**
Gelatin Test	**+**	**-**	**Motility Test**	**-**	**-**
Catalase Test	**w/+**	**+**	**Methyl Red Test**	**+**	**+**
Lipase Test	**w/+**	**+**	**Voges- Proskauer Test**	**-**	**-**
Pectin Test	**-**	**-**	**Citrate Utilization Test**	**+**	**+**
Carbohydrate utilization					
Glucose	+	**+**	**Xylose**	**+**	**-**
Sucrose	**+**	**+**	**Fructose**	**+**	**+**
Mannitol	**+**	**-**	**Maltose**	**+**	**-**
Amino acid Utilization					
Tyrosine	**-**	**-**	**Phenylalanine**	**-**	-
Valine	**-**	**-**	**Leucine**	**-**	**-**
Arginine	**+**	**+**	**Threonine**	**-**	**-**

- = Test is positive, + = Test is positive and w = weak

3.2.3Physiological Characterization

Physiological characterizations of bacterial isolates were also performed by inoculating the isolates T1 and T5 in minimal media at different salt concentration (NaCl 0-20%) temperature (18-50° C) and pH (5-11) range and are summarized in Table 3.3. It was found that that optimum range for pH, temperature and salinity tolerance were 6-8, 37-44^{0}C and 3% for isolate T1 and 6-7, 35-45^{0}C and 3% for isolate T5, respectively. These results (morphological, biochemical and physiological characterization) showed that both of the isolates are a member of *Enterobacter sp.*

and are found to be in good correlation with previous reports of Brenner et al. (1986), Stephan et al. (2007) and Kampfer et al. (2005) showing similar biochemical analysis for *Enterobacter asburaie, Enterobacter turicensis* and *Enterobacter radicincitans* respectively. These two isolates belonging to *Enterobacter* sp. are referred thereafter as strain ATA1 and ATA2.

Table 3.3 Physiological Characteristics of isolate T1 and T5

Character	Isolate T1	Isolate T5
Salinity tolerance (% NaCl)	<4% in minimal medium	<4% in minimal medium
Temperature range (°C)	37-44	35-45
pH range	6-7	6-7

3.2.4 Phylogenetic Analysis

The phylogenetic analysis of imidacloprid degrading isolates ATA1 and ATA2 was done using 16S rRNA technique and by constructing phylogenetic tree. Forward (8F) and reverse (1492R) universal primers were used to generate the sequences of 16S rRNA gene and the resulting sequence was processed further by aligning the same for the formation of consensus sequence for both isolates. Length of consensus sequence of strain ATA1 and ATA2 have been found to be 1408 MP and 1406 MP respectively.

The 16S rRNA gene sequences of strain ATA1 and ATA2 were compared with other 16S rRNA gene sequences of reference strains of *Enterobacter sp.* from National Centre for Biotechnology Information (NCBI) database using BLAST. The strain ATA1 has shown close similarity with a cluster containing strains *Enterobacter asburiae* JCM6051 (AB004744) with 98.1% gene sequence simmlarity, *Enterobacter ludwigii* (AJ853891) with 97.9% gene sequence similarity, and Strain ATA2 has shown 98% similarity with both *Enterobacter hormaechei* ATCC 49162 strain (AZ508302) and *Enterobacter cloacae* strain 279-56 (J251469) respectively.

Phylogenetic tree for both strains were constructed by neighbour joining method (Fig. 3.5 & 3.6) using GenBank-NCBI database. Results obtained from the phylogenetic analysis suggested that isolate ATA1 formed a clade with Enterobecter asburaie strain JCM6051(AB004744) with a bootstrap value of 60% and similarly isolate ATA2 formed a clade with *Enterobacter cloacae strain 279-56* (J251469) with bootstrap value of 99% repectively.

The 16S rRNA gene sequence of isolates was deposited in the Gen Bank database and assigned accession no.JX233483.1 and JX233484.1 respectively.

Consensus sequence for isolate T1 (1408 MP)

GCGGGGCAAGACTGGTACAGTACCTTAGCTACTTTACCGGCGAGCGGCGGACGGGT
GAGTAATGTCTGGGAAACTGCCTGATGGAGGGGGATAACTACTGGAAACGGTAGCT
AATACCGCATAACGTCGCAAGACCAAAGAGGGGGACCTTCGGGCCTCTTGCCATCA
GATGTGCCCAGATGGGATTAGCTAGTAGGTGGGGTAACGGCTCACCTAGGCGACGA
TCCCTAGCTGGTCTGAGAGGATGACCAGCCACACTGGAACTGAGACACGGTCCAGA
CTCCTACGGGAGGCAGCAGTGGGGAATATTGCACAATGGGCGCAAGCCTGATGCAG
CCATGCCGCGTGTATGAAGAAGGCCTTCGGGTTGTAAAGTACTTTCAGCGGGGAGG
AAGGTGTTGAGGTTAATAACCTCAGCGATGACGTTACCCGCAGAAGAAGCACCGGC
TAACTCCGTGCCTAGCAGCCGCGGTAATACGGAGGGTGCAGCGTTAATCGGAATTA
CTGGGCGTAAGCGCACGCGGGCGGTCTGTCAAGTCGGATGTGAAATCCCCGGGCTC
ACCTGGGAACTGCATTCGAAACGGGCAGGCAGAGTCTTGTAGAGGGGGGTAGAATT
CCAGGTGTAGCGGTGAATGCGTAGAGATCTGGAGGAATACCGGTGGCGAAGGCGGC
CCCCTGGACAAAGACTGACGCTCAGGTGCGAAGCGTGGGGAGCAAACAGGATTAGA
TACCCTGGTAGTCCACGCCGTAAACGATGTCGACTTGGAGGTTGTGCCCTGAGGCGT
GGCTTCCGGAGCTAACGCGTTAAGTCGACCGCCTGGGGAGTACGGCCGCAAGGTTA
AAACTCAAATGAATTGACGGGGGCCCGCACAAGCGGTGGAGCATGTGGTTTAATTC
GATGCAACGCGAAGAACCTTACCTACTCTTGACATCCAGAGAACTTTCCAGAGATGG
ATTGGTGCCTTCGGGAACTCTGAGACAGGTGCTGCATGGCGTCGTCAGCTCGTGTTG
TGAAATGTTGGGTTAAGTCCCGCAACGAGCGCAACCCTTATCCTTTGTTGCCAGCGG
TCCGGCCGGGAACTCAAAGGAGACTGCCAGTGATAAACTGGAGGAAGGTGGGGATG
ACGTCAAGTCATCATGGCCCTTACGAGTAGGGCTACACACGTGCTACAATGGCGCAT
ACAAAGAGAAGCGACCTCGCGAGAGCAAGCGGACCTCATAAAGTGCGTCGTAGTCC
GGATTGGAGTCTGCAACTCGACTCCATGAAGTCGGAATCGCTAGTAATCGTAGATCA
GAATGCTACGGTGAATACGTTCCCGGGCCTTGTACACACCGCCCGTCACACCATGGG
AGTGGGTTGCTAAGAAGTAAGCTAGGTAGCTTAAACCATTCCGGGGGACGGCCCCC
T

Consensus sequence for isolate T5 (1406 MP)

CAAAGCTTAGTATTAATAAACCGTATCCCCTTTACCGTGCAAGCGGCGGACGGGTAG
AGTAATGTCTGGGAAACTGCCTGATGGAGGGGGATAACTACTGGAAACGGTAGCTA
ATACCGCATAACGTCGCAAGACCAAAGAGGGGGACCTTCGGGCCTCTTGCCATCAG
ATGTGCCCAGATGGGATTAGCTAGTAGGTGGGGTAACGGCTCACCTAGGCGACGAT
CCCTAGCTGGTCTGAGAGGATGACCAGCCACACTGGAACTGAGACACGGTCCAGAC
TCCTACGGGAGGCAGCAGTGGGGAATATTGCACAATGGGCGCAAGCCTGATGCAGC
CATGCCGCGTGTATGAAGAAGGCCTTCGGGTTGTAAAGTACTTTCAGCGGGGAGGA
AGGTGTTGAGGTTAATAACCTTCAGCGATTGACGTTACCGCAGAAGAAGCACTGTGC
TAACTCCGTGCCCAGCAGCCGCGGTAATACGGAGGGTGCCAGCGTTTATCGGAATTA
CTGGGCGTAAAGCGCACGCAGGCGGTCTGTCAAGTCGGATGTGAAATCCCCGGGCT
CAACCTGGGAACTGCATTCGAAACTGGCAGGCTAGAGTCTTGTAGAGGGGGGTAGA
ATTCCAGGTGTAGCGGTGAAATGCGTAGAGATCTGGAGGAATACCGGTGGCGAAGG
CGGCCCCCTGGACAAAGACTGACGCTCAGGTGCGAAAGCGTGGGGAGCAAACAGG
ATTAGATACCCTGGTAGTCCACGCCGTAAACGATGTCGACTTGGAGGTTGTGCCCTG
AGGCGTGGCTTCCGGAGCTAACGCGTTAAGTCGACCGCCTGGGGAGTACGGCCGCA
AGGTTAAAACTCAAATGAATTGACGGGGGCCCGCACAAGCGGTGGAGCATGTGGTT
TAATTCGATGCAACGCGAAGAACCTTACCTACTCTTGACATCCAGAGAACTTAGCAG
AGATGGATTGGTGCCTTCGGGAACTCTGAGACAGGTGCTGCATGGCGTCGTCAGCTC
GTGTTGTGAAATGTTGGGTTAAGTCCCGCAACGAGCGCAACCCTTATCCTTTGTTGC
CAGCGGTTCGGCCGGGAACTCAAAGGAGACTGCCAGTGATAAACTGGAGGAAGGTG
GGGATGACGTCAAGTCATCATGGCCCTTACGAGTAGGGCTACACACGTGCTACAAT
GGCGCATACAAAGAGAAGCGACCTCGCGAGAGCAAGCGGACCTCATAAAGTGCGTC
GTAGTCCGGATTGGAGTCTGCAACTCGACTCCATGAAGTCGGAATCGCTAGTAATCG
TAGATCAGAATGCTACGGTGAATACGTTCCCGGGCCTTGTACACACCGCCCGTCACA
C CATGGGAGTGGGTTATAGTGTATGCTACTCGTGAGCTTCTAAGACTAAACA

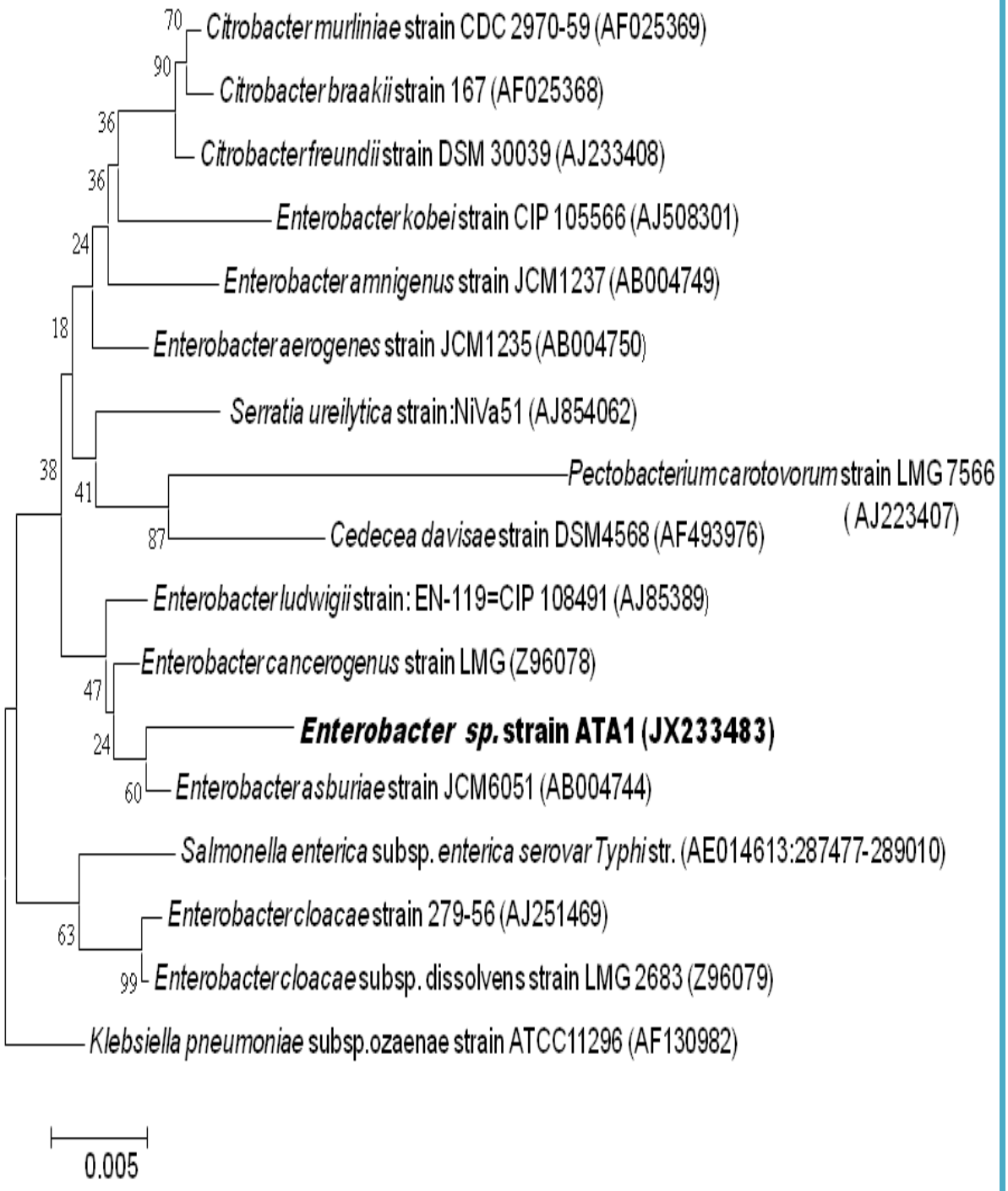

Fig. 3.5 Phylogenetic tree based on 16S rRNA gene sequences of isolate ATA1 and closely related strains of *Enterobacter* species, constructed using the neighbour-joining method. GenBank accession numbers are given in parentheses. Bootstrap values are shown at the branch points. The scale bar indicates 0.005 substitutions per nucleotide positions

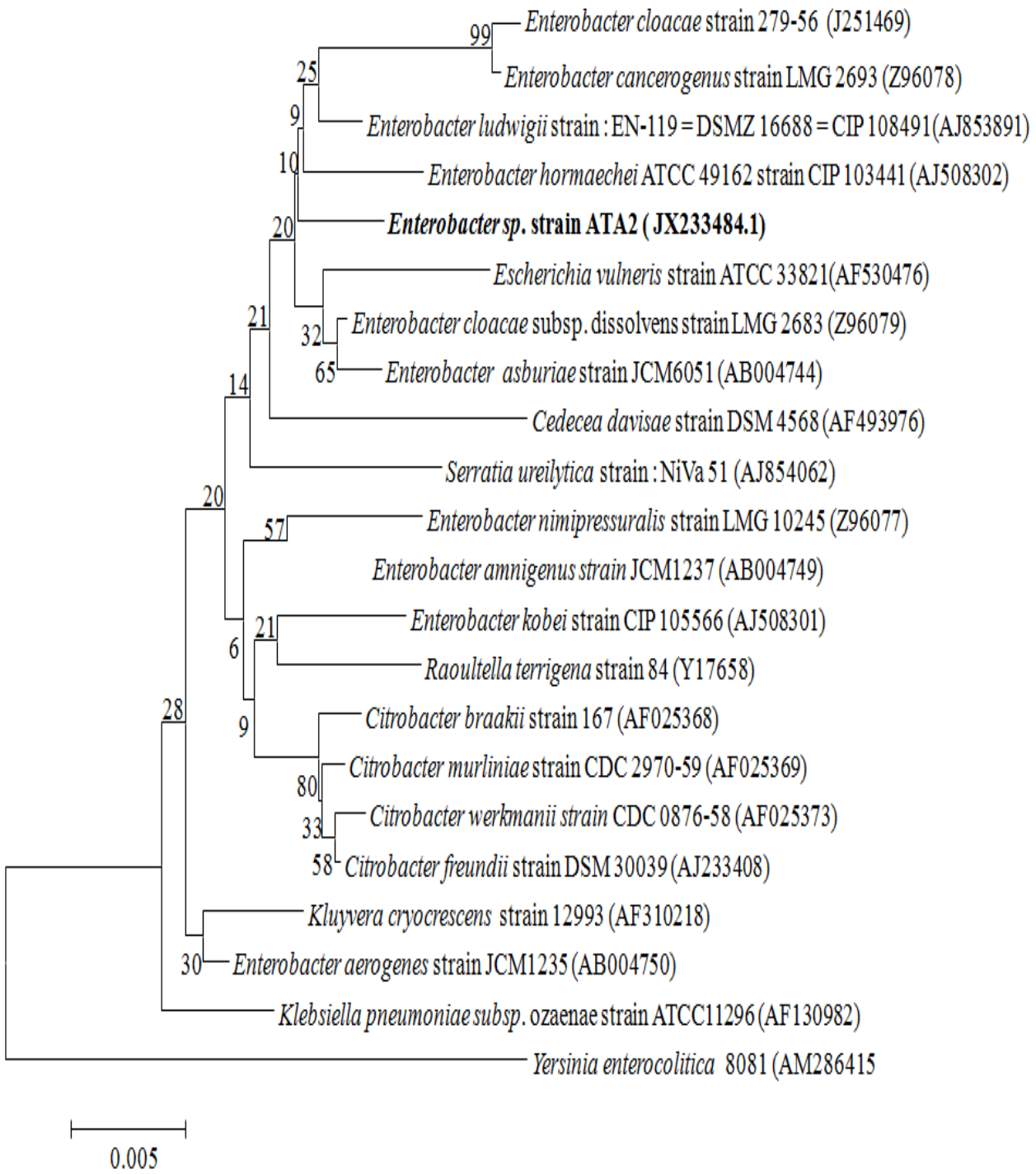

Fig. 3.6 Phylogenetic tree based on 16S rRNA gene sequences of isolate ATA2 and closely related strains of *Enterobacter* species, constructed using the neighbour-joining method. GenBank accession numbers are given in parentheses. Bootstrap values are shown at the branch points. The scale bar indicates 0.005 substitutions per nucleotide positions

3.3 Preliminary Investigations

Initial studies performed for degradation of IMI showed that *Enterobacter sp.* strain ATA1 has better efficiency to grow and degrade IMI as compare to *Enterobacter sp.* strain ATA2 as observed from Fig. 3.2. Therefore, strain ATA1 was used for degradation studies.

3.4 Tolerance of ATA1 for IMI

The bacterial isolate *Enterobacter sp.* strain ATA1 was studied for its tolerance at various concentration of IMI (50-150 mgL^{-1}) in minimal media and the obtained results are shown in Fig. 3.7. It can be seen that during initial 7 days of incubation of ATA1 with different concentration of IMI, no notable change in its growth was observed. Thereafter, significant change in the growth of ATA1 at IMI = 50-100 mgL^{-1} was observed that continued till 25 days of incubation and later on becomes almost constant. On contrary, at IMI = 150 mgL^{-1} almost no growth for strain ATA1 in-comparison to control was observed. This could be ascribed to the genotoxic effect of IMI on present bacterial strain and is supported by the results of Shetti and Kaliwal, (2012) showing increase in concentration of IMI renders the growth of *Brevundimonas sp.* MJ15. Similarly Asghar et al. (2006); Kulkarni and Kaliwal, (2012) have reported that with increase in concentration of pesticides (other than IMI), increases the stress induced proteins of *E.coli.* The obtained results are found to better than the previous reported strains viz., *Leifsonia* sp. strain PC-21 (Anhalat et al. 2007) having tolerance up to 25 mgL^{-1} of IMI over a period of 28 days whereas degradation of IMI (25 mgL^{-1}) was found to be 25-45% using various bacterial species (*Bacillus sp., Brevibacterium sp., Pseudomonas putida F1, Bacillus subtilis and Rhizobium sp.)* reported by Sabourmoghaddam et al. (2014).

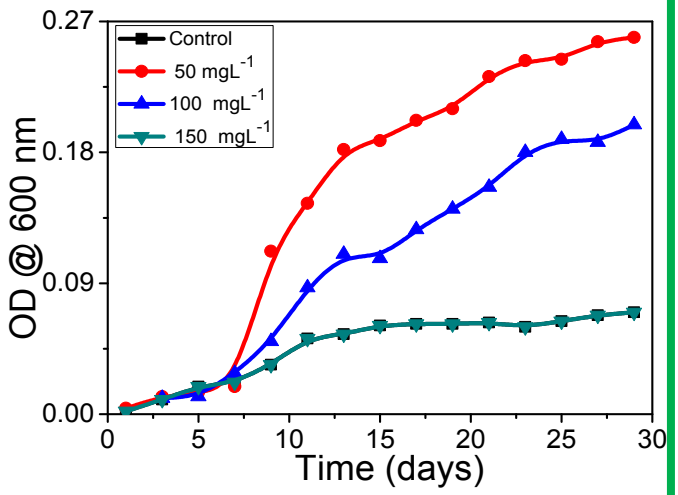

Fig. 3.7 Effect of different concentrations of Imidacloprid (50 ppm, 100 ppm and 150 ppm) on the growth of strain ATA1

3.5 Effect of Carbon Sources on Bacterial Strain Growth

Since, the use of IMI as sole source of carbon showed no notable growth of ATA1in MM, therefore additional carbon sources (Maltose, Sucrose, Fructose, Lactose and Glucose) i.e., co-metabolites were used. Growth of *Enterobacter* sp. strain ATA1 was studied in minimal broth media (Fig.3.8) containing 50mgL^{-1} of imidacloprid with all co-metabolites (individually). It was observed that growth of ATA1 was linear for all carbon sources (except for lactose) till 15 h, thereafter abruptly increases upto 20th h and became saturate till 30th h. Among these studied co-metabolites, glucose showed maximum growth, indicating that it can be effectively used as carbon source than the others. This could be ascribed to the fact that strain ATA1 first converts other carbon sources into glucose and thereafter utilize them for growth. Therefore, it can be concluded form these results that glucose is an appropriate additional carbon source followed by maltose, fructose, sucrose and lactose for degradation of IMI. These results are found to be in good correlation with the report of Anhalat et al. (2007) showing D-glucose as better source for the growth of *Leifsonia* sp. strain PC-21.

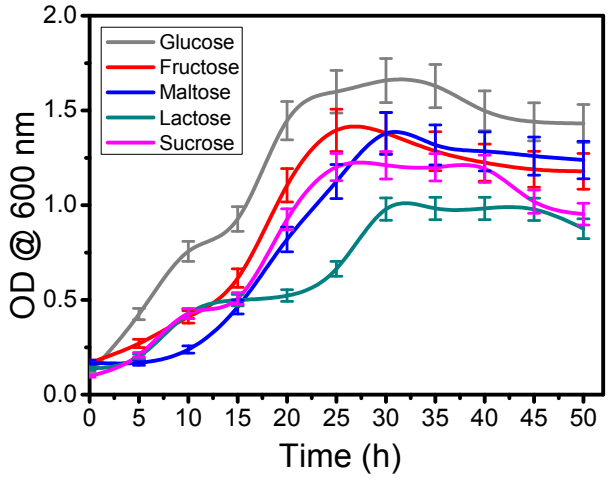

Fig. 3.8 Effect of carbon sources on the growth of *Enterobacter* sp. strain ATA1

3.6 Enumeration of viable cell count

As it has been observed in the present study that addition of glucose as co-metabolite facilitates the growth of ATA1. Therefore, various concentrations of IMI (50-150 mgL^{-1}) were used in presence of glucose (0.1% w/v), to study (Fig.3.9) the viable cell count of ATA1. The highest growth of ATA1 was observed in control on 4th day accredited to the absence of IMI. Moreover, it was also established that up to 4 days of initial incubation of ATA1 with different concentrations of IMI, an increase in the growth of ATA1 was perceived and the viable cell counts were determined to be 180×10^7 and 165×10^7 cfu per ml for 50 and 100 mgL^{-1},

respectively. However, at a concentration of 150 mgL^{-1}, the bacterial count showed resistance and inhibited throughout the incubation time. After 4 days of incubation, declination in the growth of strain ATA1 was observed and at 10^{th} day it becomes stagnant. These results indicate that higher concentration of IMI becomes toxic for the growth of microorganisms, resulting longer acclimation period to induce degradative enzymes of isolate ATA1. As a result, longer lag phase was observed at higher concentration of IMI and indicates that the toxic effect of IMI is dose dependent (Digrak and Kazanici, 2001; Ismail and Shamsuddin, 2005). Moreover, the present co-substrate is initially utilized by the isolate to stimulate microbes for production of enzymes which helps in degradation of IMI, as supported by Johansen et al. (1999); Bollag and Liu, (1990) for different xenobiotics. It has been also been documented (Shetti et al. 2012) that microorganisms (*Brevundimonas sp.* MJ15) became resistant to toxic chemicals with the production of specific degrading enzymes further supporting the present observation. These results are found to further in accordance with the previous reported work of Hindumathy and Gayathri, (2013) showed inhibition in the growth of the bacterial population in the 3^{rd} week of plantation in chloropyrifos contaminated soil. This may be due to toxic effect of pesticide itself or production of some secondary metabolites.

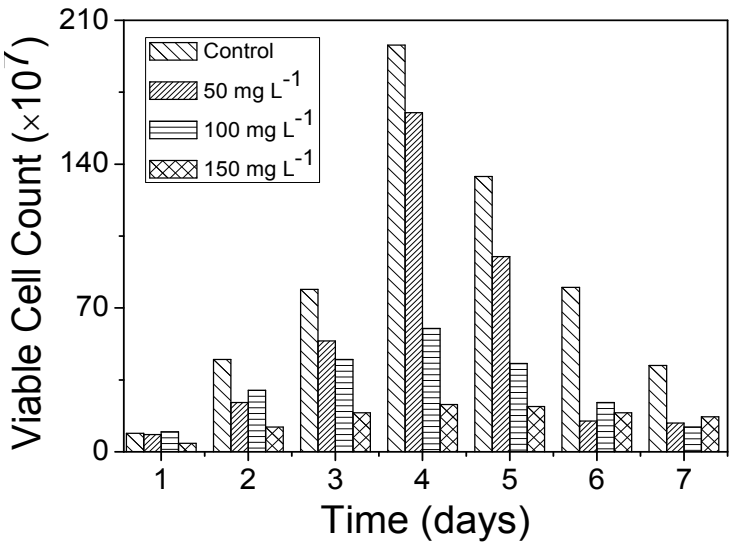

Fig. 3.9 Growth of strain ATA1 in the Presence of various concentration of Imidacloprid

3.7 Co-metabolic Degradation

As the optimized concentration of IMI was determined to be 50 mgL^{-1} in presence of glucose (0.1% w/v) as co-metabolite, therefore further degradation studies were performed under these conditions. It was found via., LC (Fig.3.10) chromatogram that after initial 3-days of degradation, the decrease in peak height/peak area was observed comparative to standard IMI (50 mg L^{-1}). Thereafter, with increase in degradation time (upto 15 days) no notable change in

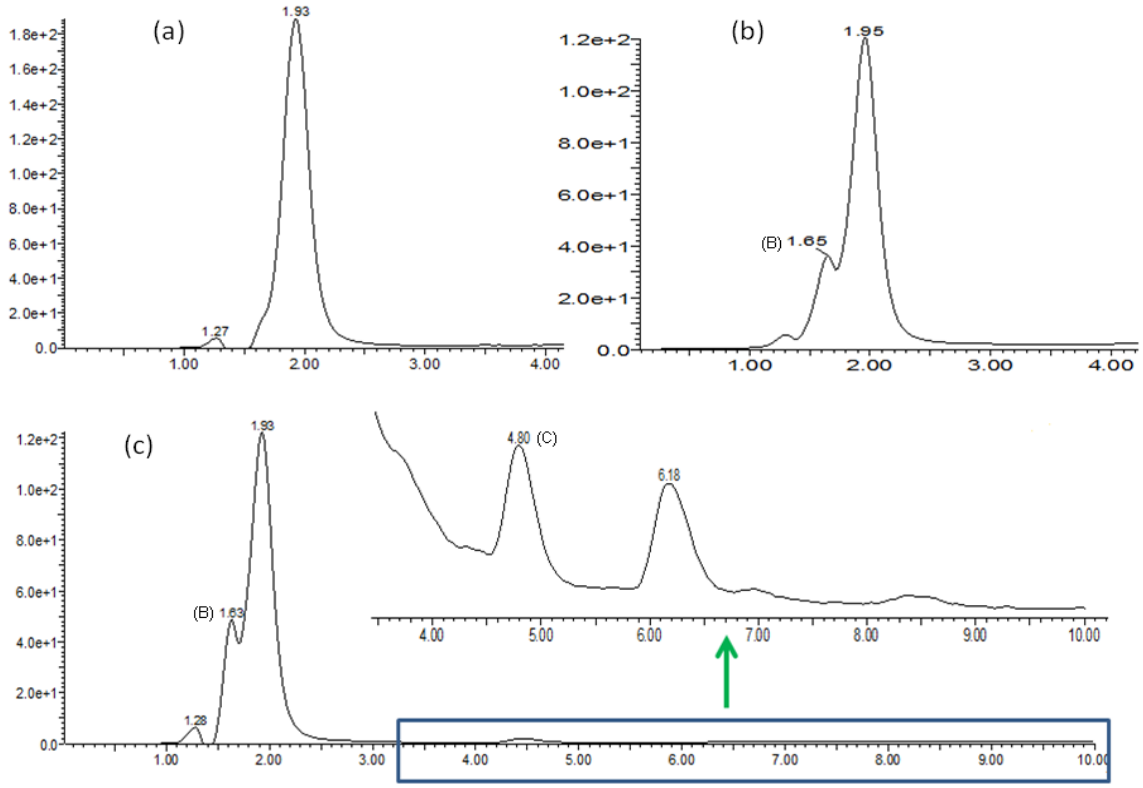

Fig. 3.10 LC Chromatograms of (a) Imidacloprid standard (b) at 3rd day of degradation (c) at 15th day of degradation. The arrow indicates the retention time of various intermediates of imidacloprid

same was observed, revealing that a maximum degradation perceived in a time period of initial 3-4 days. The time course (Fig.3.11) co-metabolic degradation of IMI in presence and absence of ATA1 showed that in presence of strain, both growth and corresponding degradation of IMI were comparative higher than that found only in control (without bacterial strain). Initially a lag period of ~30 h is found to be necessary for the cells growth in presence of IMI and glucose in comparison to without co-metabolite that requires several days for the same. The percentage of IMI degraded (~44%) by ATA1 in presence of glucose (0.1% w/v) became stagnant after initial three days of incubation and this trend continued thereafter. These results confirmed that co-metabolic degradation of IMI in presence of glucose induce degradative enzymes in strain ATA1. Additionally, added glucose by serving as carbon sources provided nutrition to ATA1 that may relieves toxicity effect of IMI and hence decreased the adaptation time for the bacterial strain. It is also believed here that in co-metabolic degradation, co-substrate may provide energy

and co-factors for different cellular activities, that may afford the energy or reduction equivalents (NADPH) required for aromatic ring hydroxylation (Wang et al. 2010). Since, it was being reported by Liu et al. (2013) that sucrose as a utilizable substrate enhances the co-metabolism by *Stenotrophomonas maltophilia* CMGCC 1.1788 for production of 5-hydroxyimidacloprid from IMI. Yun et al. (2009) also confirmed microbial degradation of 3-chlorobenzoate using glucose as co-metabolite.

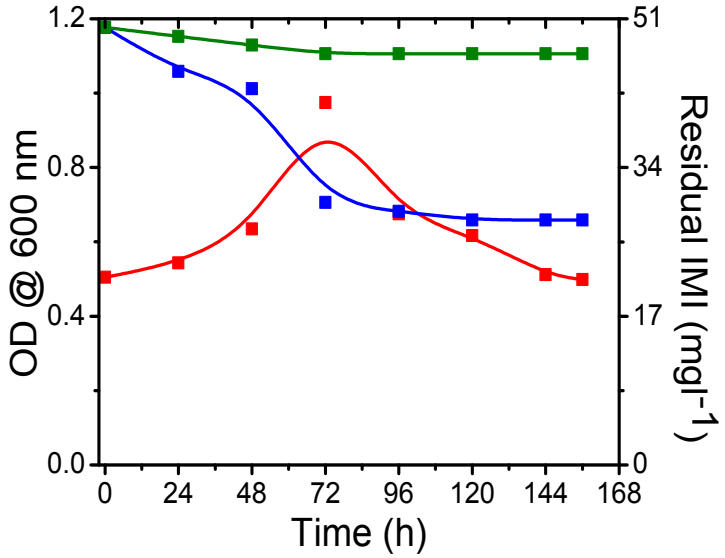

Fig. 3.11 Imidacloprid degradation and cell density in M9 medium with glucose (MMG) as co-substrate

3.8 Analysis and Identification of Imidacloprid Degrading Products

As we have observed in the LC chromatogram (Fig.3.10) that during co-metabolic degradation of IMI by strain ATA1, various new peaks were appeared (during 15 days of incubation) indicating the formation of intermediates/metabolites of IMI. The identification of these intermediates was performed by their respective mass spectrum (Fig. 3.12 a&b). It has been found that IMI (R_t = 1.9 min, m/z = 256) disintegrated into imidacloprid urea (R_t= 1.67 min, m/z = 212) and 4-hydroxy imidacloprid (R_t = 4.8 min, m/z =271). Initially, after 3 days of microbial degradation, one major metabolite imidacloprid urea has been found (Fig. 3.12 a). However, after 15 days of degradation process an additional metabolite 4-hydroxy imidacloprid was formed. Although, some more metabolites were produced after 15 days of microbial degradation (corresponding to various peaks in LC), yet remained unidentified in present study. Anhalat et al. (2007) reported imidacloprid-guanidine, imidacloprid-urea and some unknown metabolites during biodegradation period of imidacloprid by *Leifsonia* sp. strain.

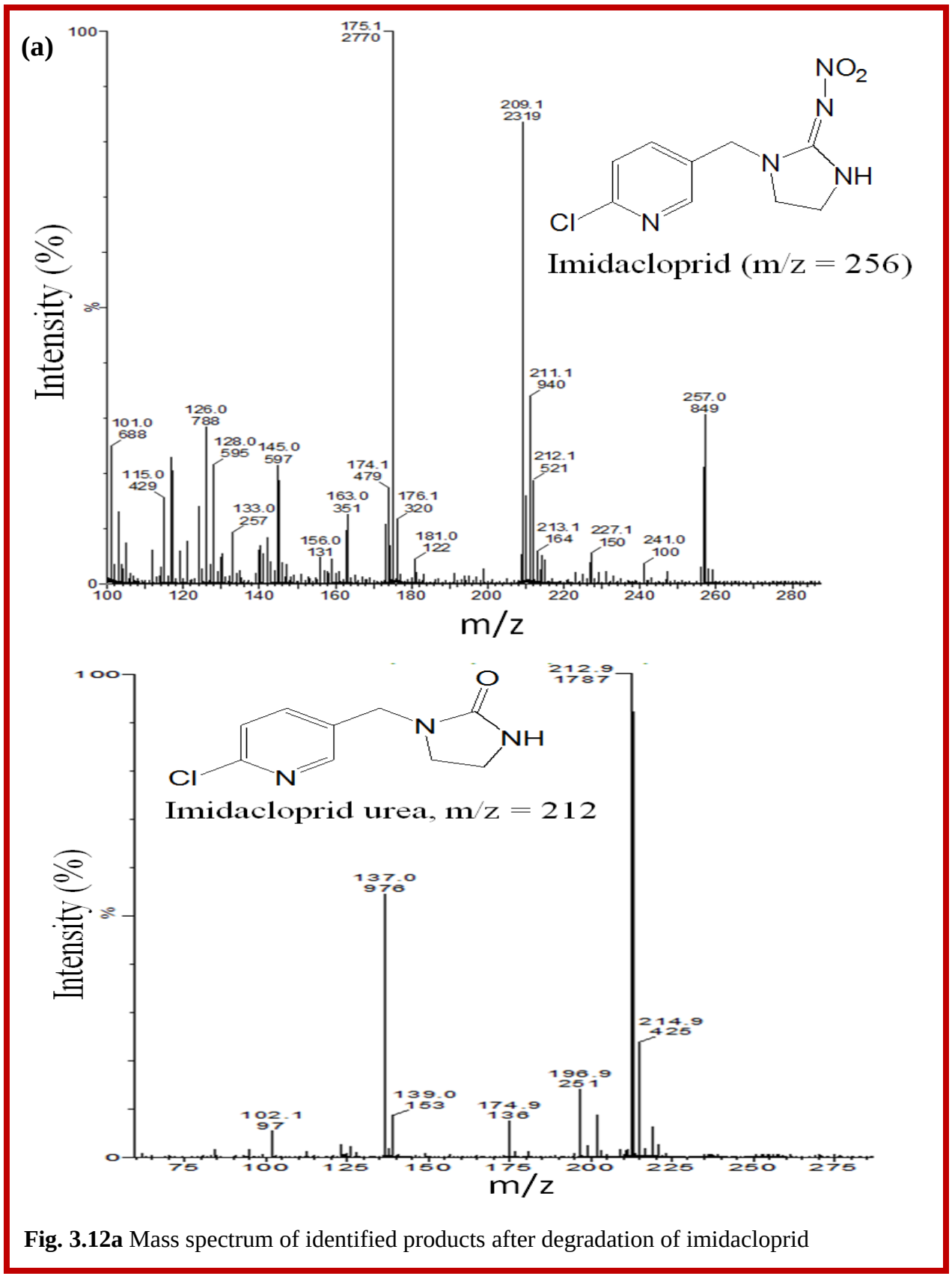

Fig. 3.12a Mass spectrum of identified products after degradation of imidacloprid

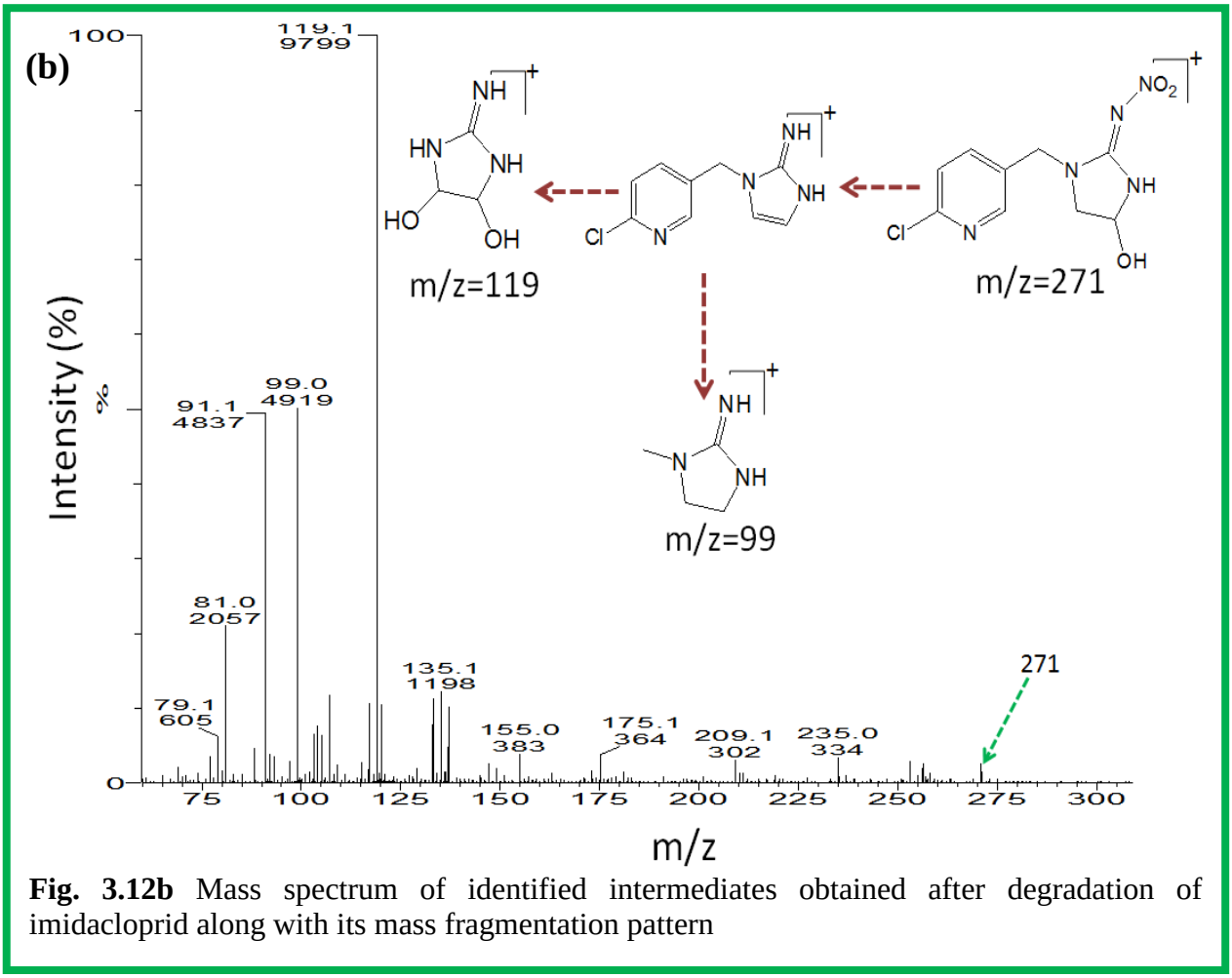

Fig. 3.12b Mass spectrum of identified intermediates obtained after degradation of imidacloprid along with its mass fragmentation pattern

3.9 Biodegradation of IMI in soil

The heterogeneity of microorganisms in heterogeneous soil structure plays an important role for microbial processes and the persistence of pesticides (Strong et al.1998). Soil sample used for isolation and for degradation studies were collected from paddy field and Thapar campus, respectively. These soil samples were analyzed for their physic-chemical characterization namely pH, total organic carbon, phosphorus, bulk density, permeability, moisture content, water holding capacity and texture. The obtained results are summarized in Table 3.4. The soil samples examined were found to be slightly alkaline in nature with almost similar soil texture and OC content.

Table 3.4 Physicochemical characterization of soil samples

S. No.	Parameters	Experimental soil	Paddy field soil
1	pH	7.5	8.2
2	Total Organic Carbon (%)	0.3	0.2
3	Available Phosphorus (%)	0.0023	0.008
4	Bulk Density (gcm^{-3})	2.0	1.34
5	Permeability (cm/sec)	$1.2x10^{-3}$	$2.15x10^{-3}$
6	Moisture Content (%)	1.23	4
7	Water Holding Capacity	20	46
8	Texture	Sandy loam	Loamy sand

3.10 Effect of various parameters on biodegradation of IMI in soil

Although, the pH of soil was determined to be ~7 and was found to comply with the pH used for the degradation of IMI in MMG, yet before studying the degradation of same in soil, pH along with other parameters (pH, inoculums size, initial concentration of imidacloprid and flooding of soil) were optimized. It should be important to mention here that the before adding the strain ATA1 the inoculums was prepared under the optimized conditions (Temp. = 37 °C; pH = 7, glucose as co-metabolite = 0.1% w/v) as explained previously (*section 2.2.9.2*).

3.11 Effect of soil pH on imidacloprid degradation

The time course analysis (Fig. 3.13) was performed to study the influence of pH (1-11) on the degradation of IMI (50 $mgkg^{-1}$ of soil) by HPLC (Fig. 3.14). It

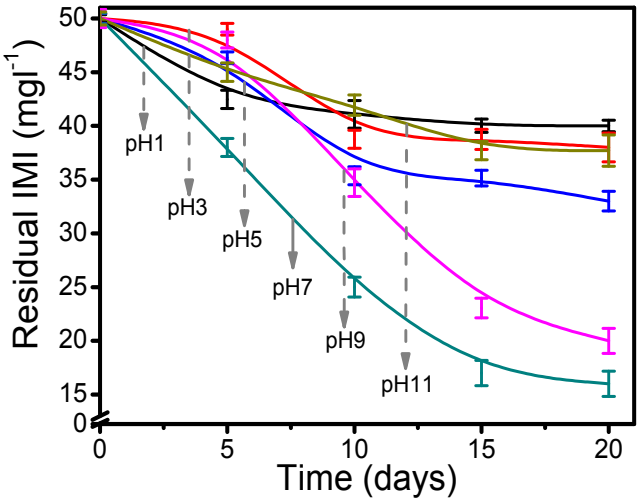

Fig. 3.13 Effect of soil pH on degradation of imidacloprid. Error bars represents the standard error of three replicates

can be clearly seen that, maximum degradation was found at pH = 7, which was determined to be ~50% for initial 5 days of incubation therefater increased to 68% for 15 days of incubation and hence became almost constant. However, ~34% and ~60% degradation of IMI was achieved at pH = 5 and pH = 9 for same time of duration. In highly acidic (pH = 1 & 3) and alkaline (pH = 11) conditions the degradation was merely 20-25%. Thus, pH 7 was determined to be optimum for maximum degradation of IMI in soil and can be ascribed to the better bioavailability of IMI together with optimal biotic activity of bacterial cells at this pH. These results are in good correlation with the reports of Bending et al. (2003) and Hong et al. (2007) where neutral conditions were found to be better for the degradation of isoproturon and fenitrothion and via. *Sphingomonas sp.* and *Burkholderia sp. FDS-I* respectively.

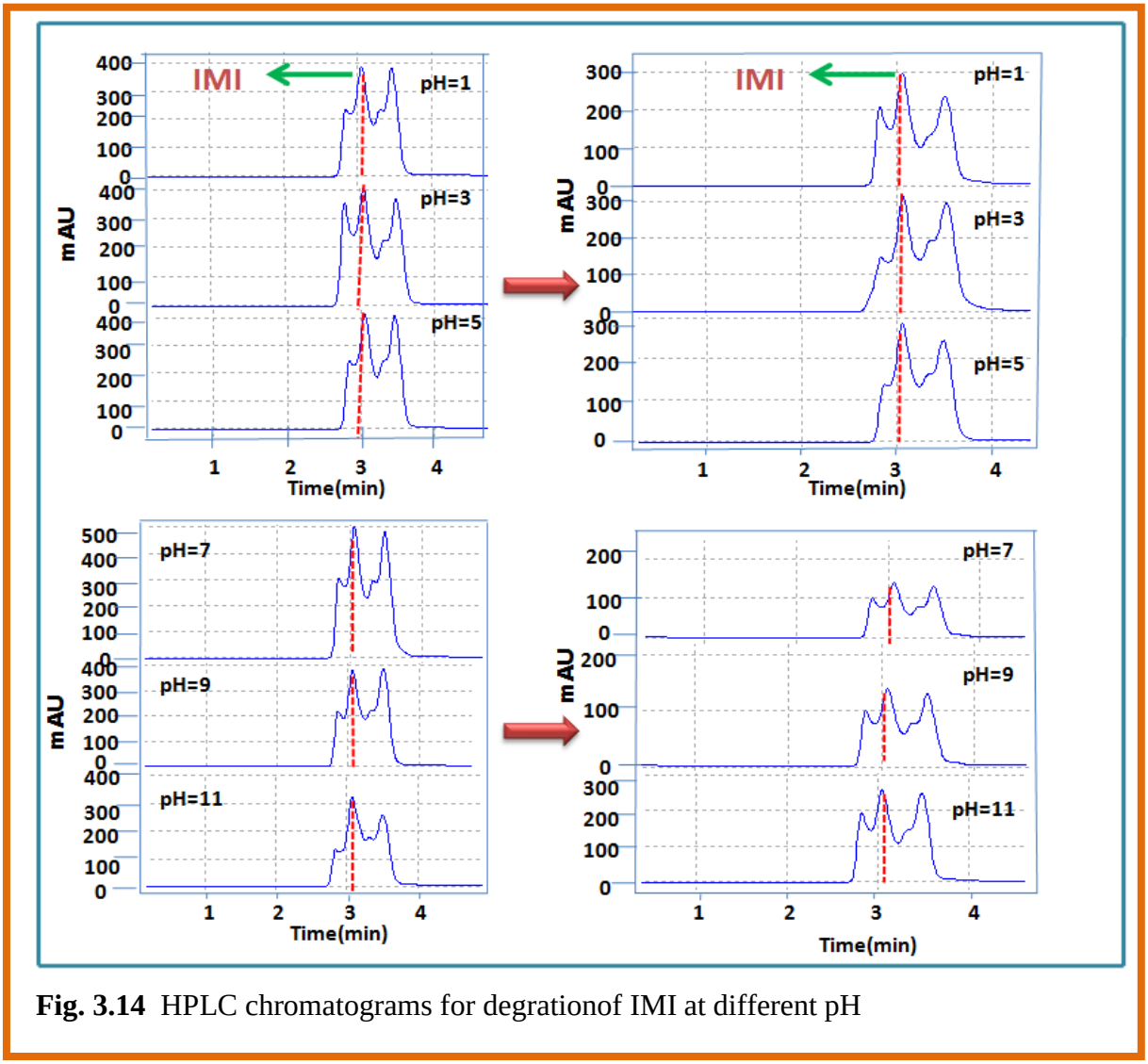

Fig. 3.14 HPLC chromatograms for degrationof IMI at different pH

3.12 Effect of initial concentration of IMI on degradation

Under the optimized condition of soil pH, studies related to effect of initial concentration of IMI towards its degradation were performed and the obtained results are shown in Fig. 3.15. The time course study for influence of initial concentration of IM showed that at 25 mgkg^{-1} strain ATA1 was able to degrade ~80 % of IMI. However, by increasing twice the concentration of IMI i.e., 50 mgkg^{-1} soil, degradation rate became almost ~ 74% for the same time of incubation. Moreover, not much differnce in degradation (~ 6%) of IMI in soil was obseved by doubling its concentration, therefore 50 mg kg^{-1} dose of IMI was considered as optimum. Further increase in concentration of IMI (75-100 mgkg^{-1}) resulted into a sharp decrease in degradation as well as for production of its metabolites as observed upto 20 days of incubation. These results were supported by GC-MS chromatograms (Fig. 3.16) showing that peak height/peak area for IMI (Rt =11.6 min) was least while using its concentartion (50 mgkg^{-1}), revealed it to be an optimum amount. Such trends could be accredicted to the fact that

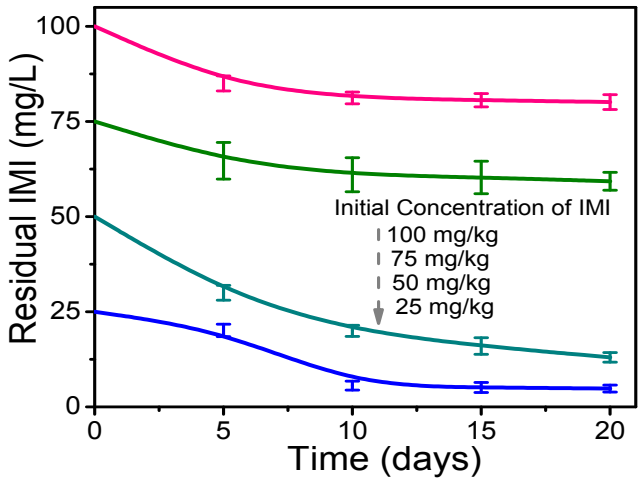

Fig. 3.15 Effect of initial concentration on the degradation of imidacloprid. Error bars represents the standard error of three replicates

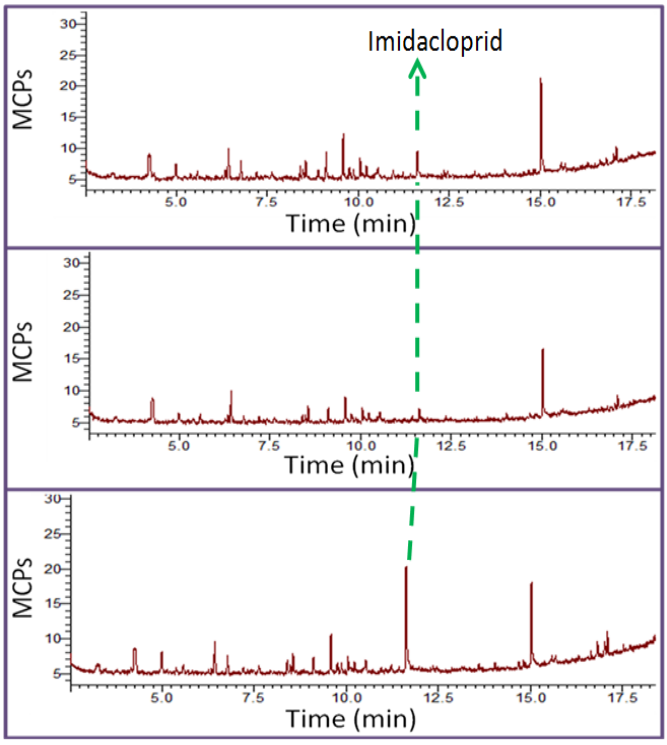

Fig. 3.16 GC chromatographs for initial concentration of imidacloprid (a) 25 mg kg^{-1} (b) 50 mgkg^{-1} (c) 75 mgkg^{-1} at 20 days of incubation

varriation in concentration of pesticide causes inflation in the degradative activity of microorganisms. The inhibition in the degradation rate at very high concentrations of IMI could be explained on basis of need for greater numbers of bacteria to initiate rapid degradation as confirmed by Karpouzas and Walker, (2000) for dissipation of organophosphates in soil. It has been reported (Nishino and Spain, 1993) that gene expression for degradation of aromatic compounds is inducible rather than constitutive at higher concentration of pesticides.

3.13 Effect of inoculum size on IMI degradation

Figure 3.17 depicts the effect of inoculum size on the degradation of IMI. It is found here that that addition of 2×10^5 CFU g^{-1} soil has negligible effect on the degradation of IMI, since ~9 % degradation was observed even after 20 days of incubation. It was also visulised that increase in inoculum size causes increase in degradation of IMI, and became highest for 2×10^7 CFU g^{-1} soil (74%). However, with further increase in the same to 2×10^8 CFU g^{-1} the degradation of IMI decreased to 61% indicating 2×10^7 CFUg^{-1} soil as an optimum cell density for degradation.

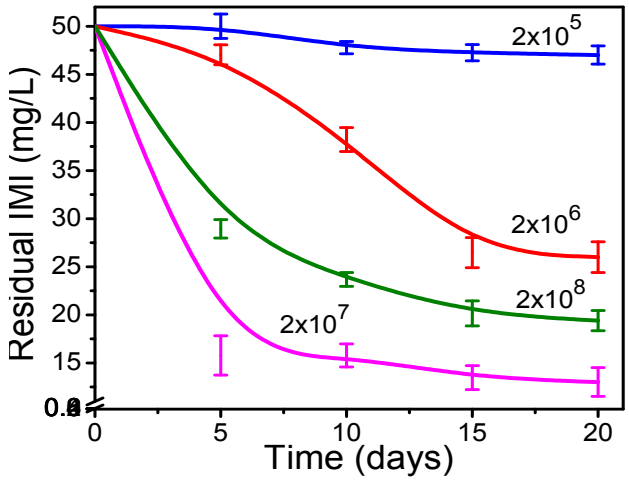

Fig. 3.17 Effect of inoculum size on degradation of imidacloprid. Error bars represents the standard error of three replicates

These results found to correspond with the GC-MS chromatograms (Fig. 3.18) indicating 2×10^7 CFU g^{-1} to be an optimum inoculum size. Moreover, under the optimum conditions of pH and initial concentration of IMI, the highest degradation with 2×10^7 showed 74% of degradation in initial 5 days of incubation.Thus, it clearly revealed that highest and fast activity was achieved at 2×10^7 CFU g^{-1} in relation to other inoculum sizes under similar experimental conditions. It was suggested by Chen and Alexander (1989) that an acclimation period during degradation of xenobiotics reflects the time required for multiplication of microbial population to a certain level which rapidly degrades xenobiotics. Similar results for different bacterial strains (other than ATA1) and for other pollutants have been performed and showed that there optimal size of inoculants as native microorganism is necessary for successful bioremediation (Awasthi et al.

2000; Comeau et al. 1993; Miethling and Karlson, 1996; Ramadan et al.1990; Rousseaux et al. 2001; Singh et al.2006).

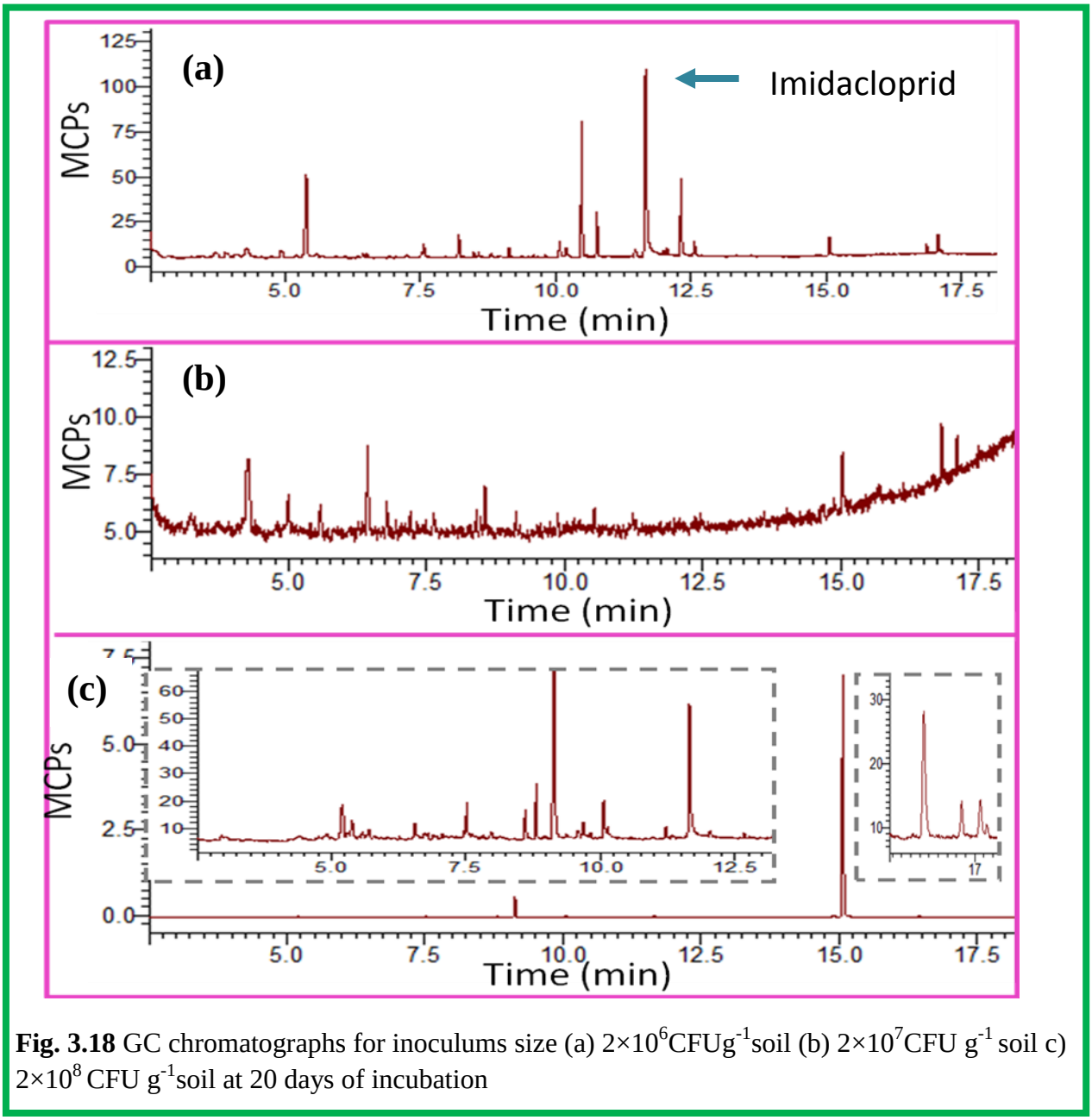

Fig. 3.18 GC chromatographs for inoculums size (a) 2×10^{6}CFUg^{-1}soil (b) 2×10^{7}CFU g^{-1} soil c) 2×10^{8} CFU g^{-1}soil at 20 days of incubation

3.14 Imidacloprid degradation in flooded and non-flooded soil

In order to study the influence of flooding/non-flodding conditions for degradtion of IMI, soil samples were flooded with minimal medium. It was found (Fig. 3.19) that in initial 5 days of incubation, there was no difference in degradation rate but on 10th day it became drastically

significant as IMI was degraded more efficiently in non-flooded (60%) conditions as compared to flooded (50%). Later on i.e., after 15 days the degradation became linear. Since, degradtion rates in non-flooding conditions exceeds by ~10% to that of flodding conditions therfore is suggested here that present strain can be even useful in water logged soils . A great influence of flooding on herbicide persistence in soil was confirmed by Accinelli et al. (2005), while an opposite effect was observed for metolachlor under flooding conditions. Awasthi et al. (2000) also reported faster degradation of endosulfan in wet soil as compared to flooded soil.

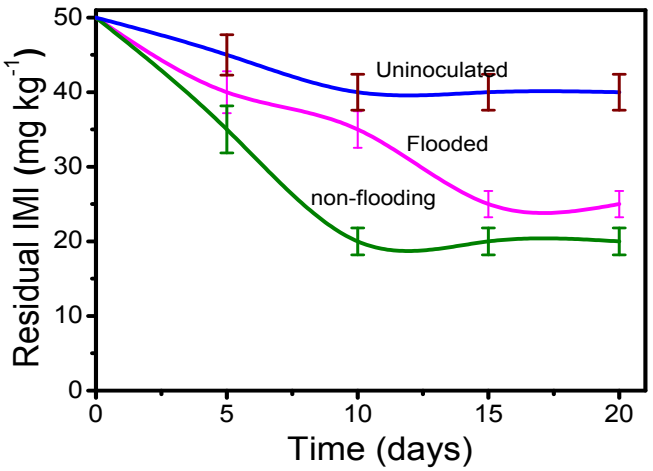

Fig. 3.19 Effect of Flooding on the degradation of IMI. Error bars represents the standard error of three replicates

3.15 Metabolites production from IMI degradation

Since, aerobic oxidation of organic compounds are often reported to convert parent molecule into other compounds inspite of the complete mineralization.Therefore, GC-MS analysis was carried out to identify the metabolites of IMI (Fig. 3.20). Among variety of metabolites formed, six have been identified (Fig. 3.21-3.23), marked as I-1 to I-6 through their mass spectra and their structures are shown in their respective mass spectrums.

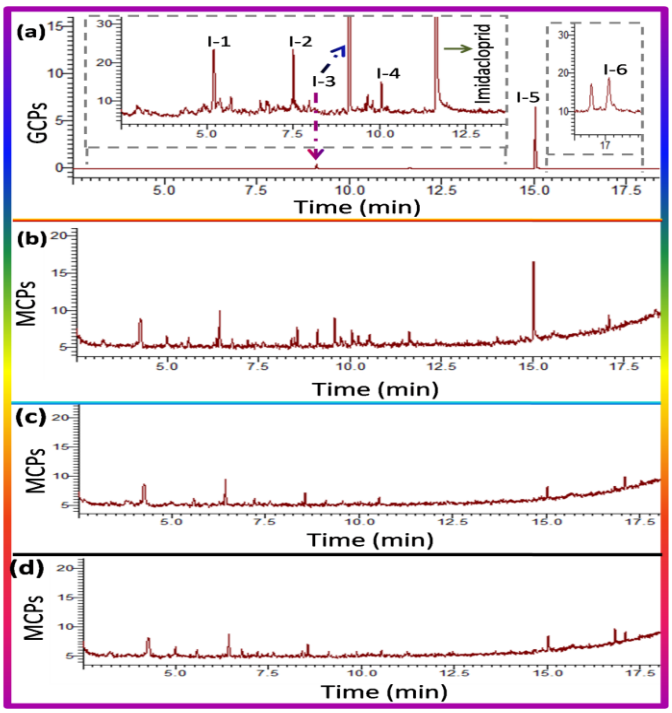

Fig. 3.20 GC Chromatographs of degradation of IMI under optimized conditions; (a) pH (b) initial concentration of IMI (c) inoculum size (d) flooding of soil. Inset corresponding enlarged view, numbers represents the identified intermediates

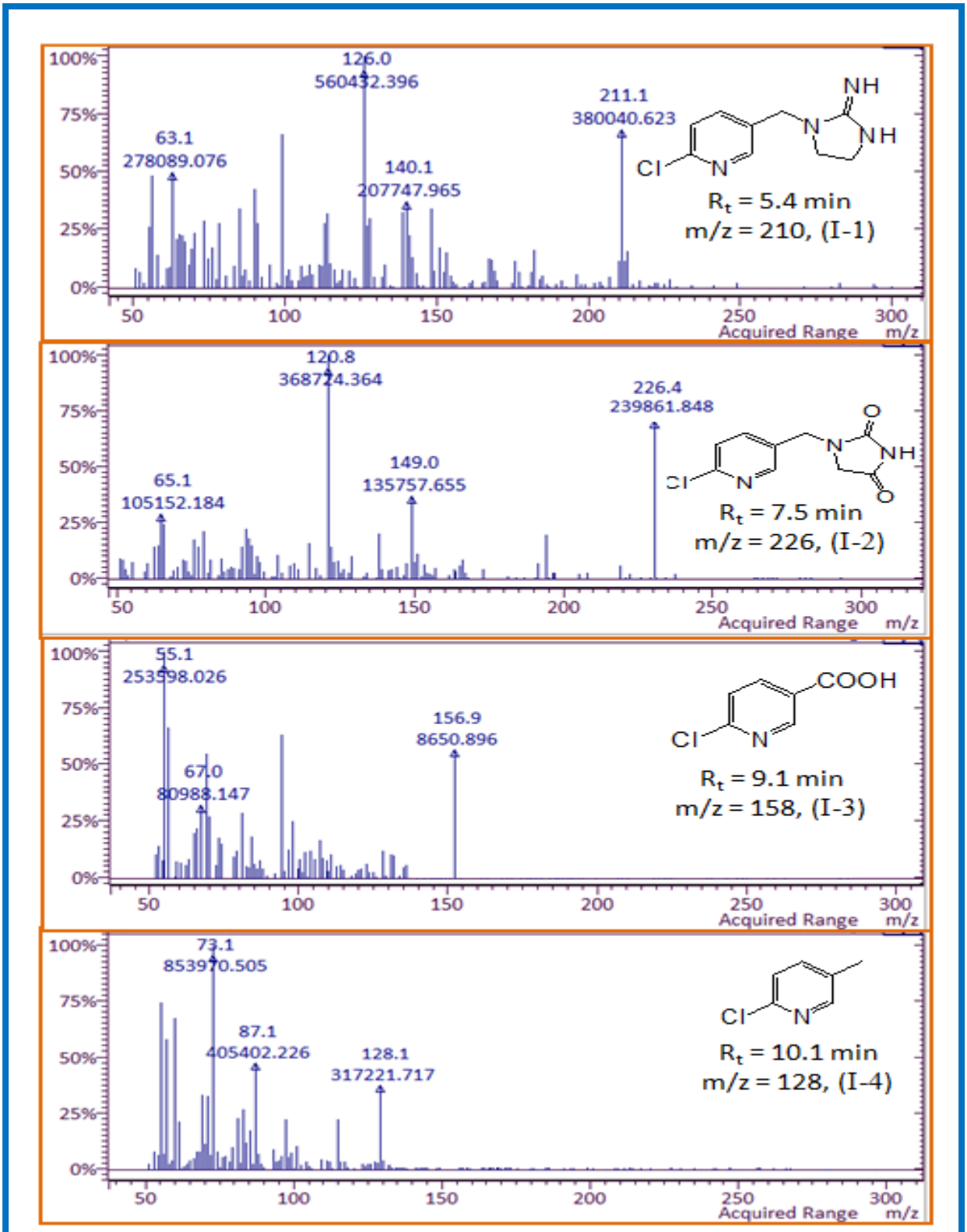

Fig. 3.21 Mass spectrum for identified intermediates of imidacloprid

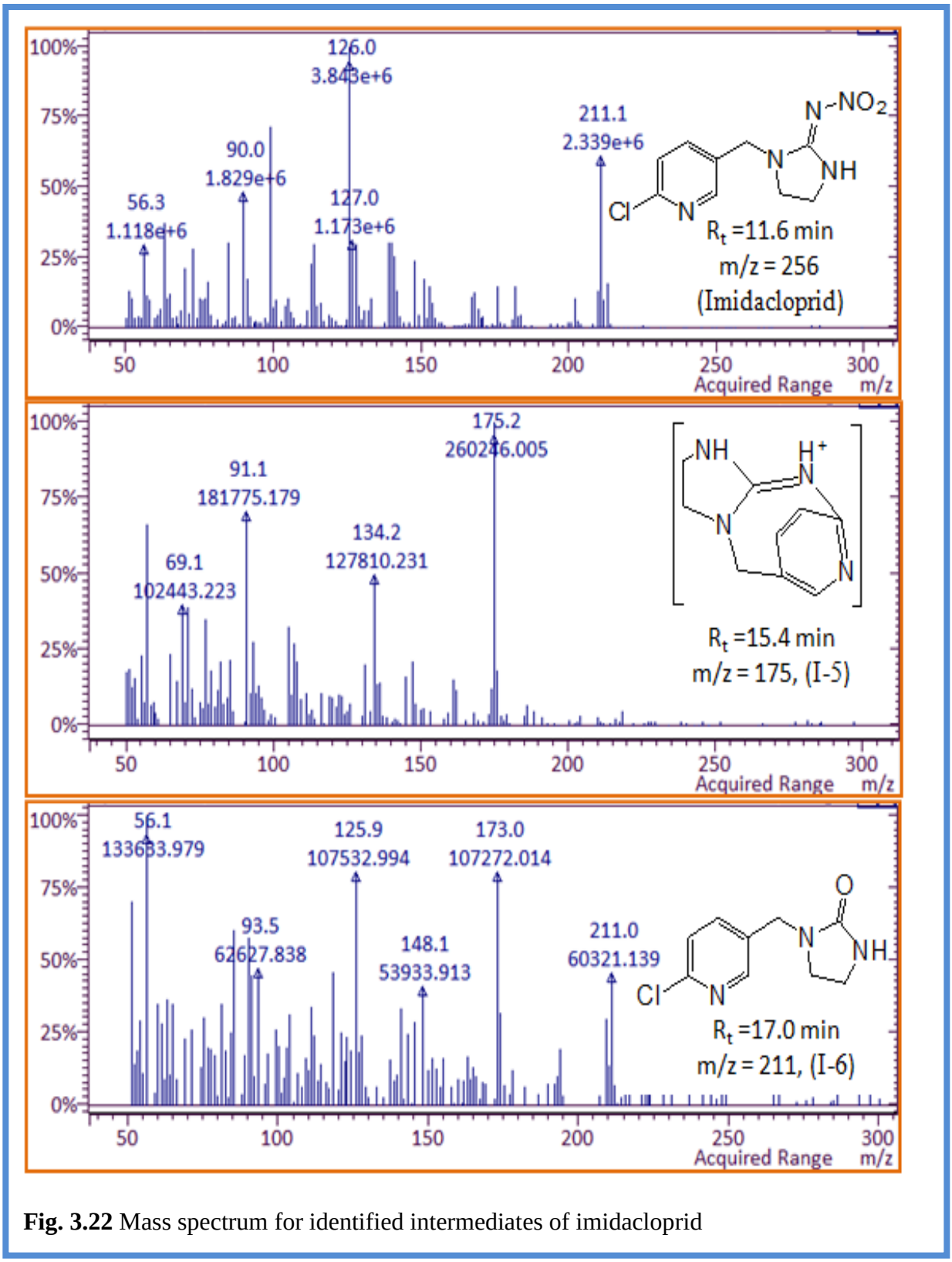

Fig. 3.22 Mass spectrum for identified intermediates of imidacloprid

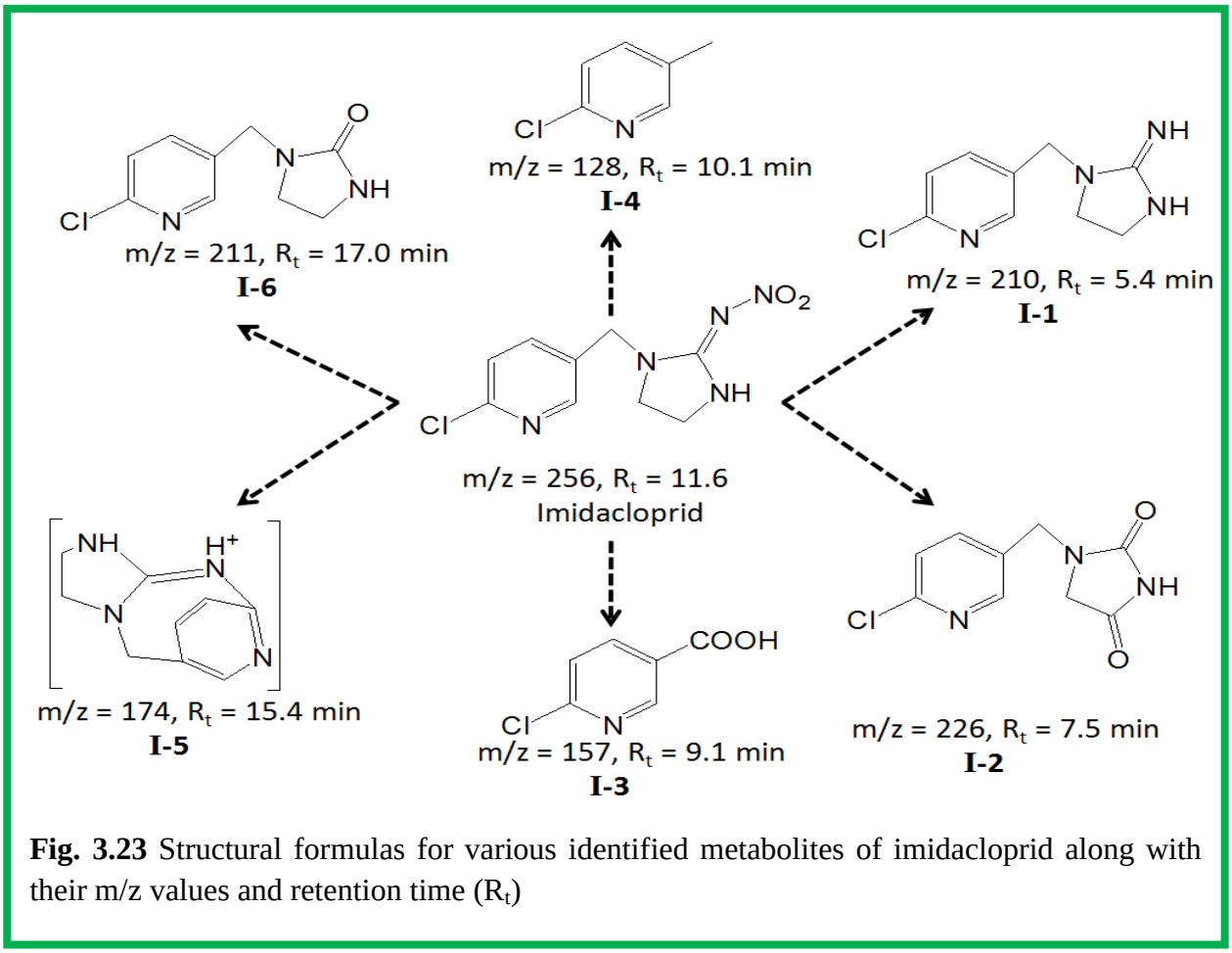

Fig. 3.23 Structural formulas for various identified metabolites of imidacloprid along with their m/z values and retention time (R_t)

In soils IMI degrades mainly via three different routes (i) hydroxylation of the imidazolidine ring leading to 5-hydroxyl IMI and subsequent removal of water to form the olefin metabolite (ii) reduction of the nitro group to form the nitrosimine compound and loss of this group with the formation of the guanidine metabolites (iii) loss of nitro group to form guanidine IMI and further oxidation to form urea IMI as reported recently by Sharma et al. (2014) and Grover et al. (2014). Moreover, the presence of various metabolites which is reflected through their respective peak height/areas is also considered as a probable cause for the slow degradation of IMI. It was seen that after 15 days of incubation and under the optimized conditions (Fig., 3.20, initial concentration, pH and inoculum size) the peak area/peak height of IMI was significantly lower than those of others. In our study two metabolites of imidacloprid named as I-1 (m/z=210) and I-5 (m/z=174) are formed due to loss of NO_2, Cl and NO_2 and is also reported by Thuyet et al. (2010). The formation of identified metabolites is in good correlation with the previous study of Pandey et al. (2009) where bacterium *Pseudomonas sp*. 1G, isolated from soil was used for

microbial degradation of IMI. Specifically, two of identified metabolites (IMI guanidine and urea) have also been reported to recover after degradation of IMI (37–58% of 25 mgL^{-1} over 4 weeks) in broth using *Leifsonia* sp. strain PC-21 (Anhalat et al.2007).

3.16 Photocatalytic degradation of IMI using P25-TiO_2

The degradation of IMI using ATA1 has found to exhibit incomplete microbial degradation and hence incomplete mineralization, as reflected by formation of its various metabolites in the present study. Therefore, to achieve higher degradation/mineralization of IMI, TiO_2 mediated photocatalytic degradation of same was carried out in soil. For this purpose the commercially available Degussa P25-TiO_2 (surface area = 50 ± 15 m^2g^{-1}, particle size = 30-50 nm and anatase : rutile :: 70:30) which was reported (Sharma and Lee, 2013) to have very profound efficiency for degradation of many organic pollutants was applied. Prior to study the degradation of IMI, its stability was verified by the photolysis (UV-light without TiO_2) experiment. Moreover, the adsorption studies for IMI in soil at different pH (without TiO_2) and at an optimized pH with TiO_2 were also performed before proceeding towards its photocatalytic degradation.

3.16.1 Dark adsorption studies of IMI in soil with and without TiO_2

The adsorption of any pesticide in soil is well known to influence its persistency/ability to pollute the other environmental sources. Therefore, it is necessary to study adsorption effect before carrying out the degradation of the pesticide or any other environmental contaminant. In this direction, the experimental studies were performed in order to evaluate aforementioned parameter for IMI degradation. These studies were performed (with and without TiO_2) by stirring the IMI spiked soil samples in dark and the sample were analyzed after regular time intervals (*section 2.2.10.2).* Since, the physico-chemical studies for soil showed its pH ~ 7, therefore adsorption of IMI on soil in dark was initially studied at this pH. It was observed that during initial 3 h of dark studies, adsorption of IMI on soil was perceived and thereafter became saturated till 18 h.

This clearly showed that time of 3 h was enough to attain the equilibrium between adsorption and desorption of IMI in the soil. It was also confirmed from the present study that change in the concentration of IMI was not significant when kept under dark for 18 h ascribed to its adsorption in soil. As pH has significant effect on adsorption of pollutants, therefore the same

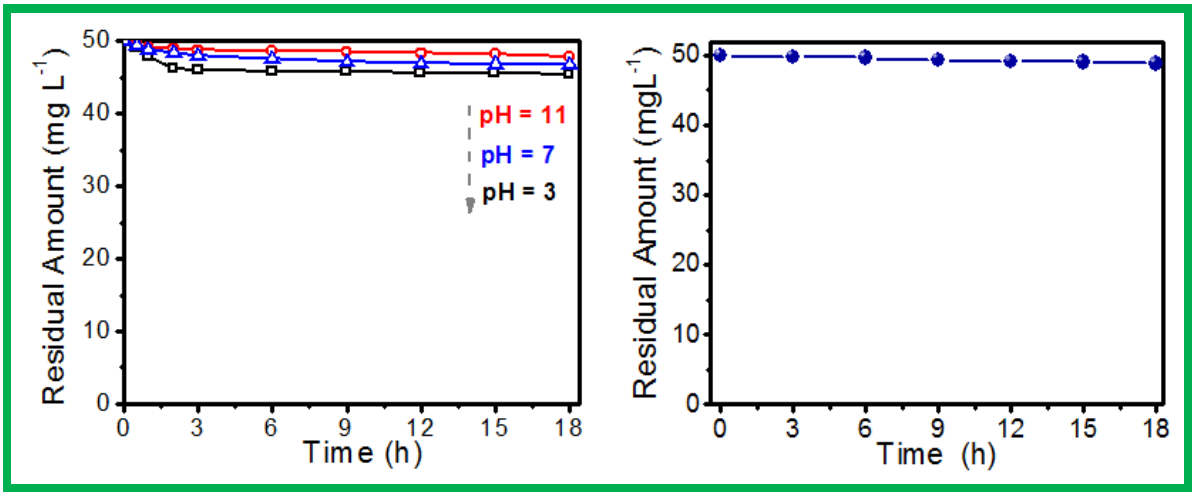

Fig. 3.24 Time course adsorption studies of IMI on soil surfaces (a) different pH without TiO_2 and (b) With TiO_2 at pH = 3

study for IMI at different pH (3 and 11) in soil was performed (Fig. 3.24 a). The results showed that adsorption of IMI in soil was ~5% at pH = 11 which increases up to ~9% at pH = 3. This could be ascribed to the proto-nation of imdazole ring and is in good agreement with the work of Jodeh et al. (2014) where same was reported to be a cause for decrease in sorption of IMI in alkaline silty clay soil. As catalyst is considered to be an important factor that influences the rate of reaction, so before studying the degradation of IMI, the adsorption of IMI on TiO_2 was also carried out (Fig. 3.24 b). It was observed that there was no notable difference in the adsorption of IMI on TiO_2 in comparison to without catalyst. Moreover, photolysis of IMI in soil was also carried out and concluded no significant change in its amount even after 18 h of UV-light irradiation (Fig. 3.25). This clearly depicts the stability of IMI molecule and is in accordance with the very recent report of Grover et al. (2014) where its $t_{1/2}$ is reported to be 40-60 days. Further photolysis was compared with photocatlytic degradation and it was observed

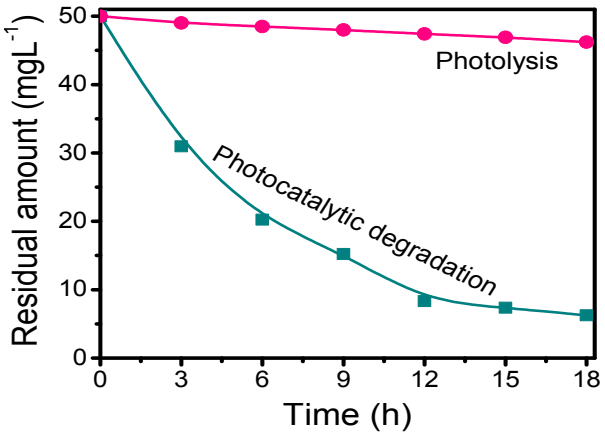

Fig. 3.25 Study for degradation of imidacloprid by photolysis and photodegradation

that in comparison to photolysis, residual amount of IMI was very less signified the importance of photocatalytic degradation.

3.16.2 Effect of TiO_2 catalyst dose

Since, catalyst dose is well known to influence the rate of photocatalytic reaction therefore, the amount of TiO_2 was initially optimized for degradation of IMI and the obtained results are shown in Fig. 3.26 a&b. It was observed that as the amount of TiO_2 (0.1-0.5 gkg^{-1}) was varied in the IMI contaminated soil, the degradation increased upto 0.3 gkg^{-1} of TiO_2 dosage. However, further increase in its dose caused decreased in the photodegradation of IMI and the results were verified by plotting catalyst dose vs. degradation. It can be clearly visualized (Fig. 3.26 b) that maximum photocatalytic degradation of IMI (~ 80%) was achieved by using 0.3 gkg^{-1} of TiO_2 revealing it to be an optimum catalyst dose. These variations in degradation efficiency with different catalyst dose could be explained by the fact that with increase in the amount of catalyst, number of active sites on the photocatalyst surface increases, causing an increase in the number of $^{\bullet}OH$ radicals which actually participate in IMI degradation. However, beyond an optimum TiO_2 dose, the light penetration to it declines resulting decrease in formation of excited charge carriers and hence oxidative hydroxyl and superoxide radicals (Malato et al. 2001; Muhamad 2010). Consequently, decrease in degradation rate of IMI was observed.

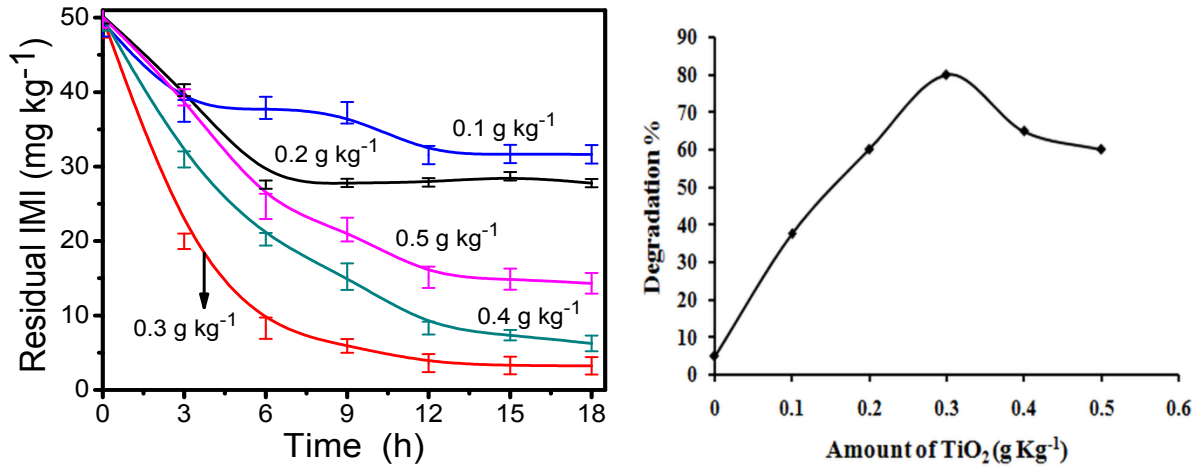

Fig. 3.26 (a) Time course study for photocatalytic degradation of imidacloprid using various TiO_2 amounts and (b) optimized amount of TiO_2 dose.

The photocatalytic oxidation of the organic substrates is dependent upon many other parameters such as initial concentration of reactant, pH of reaction media, intensity of light and depth of

light penetration. These, aforementioned parameters need to be optimized to achieve the maximum photocatalytic degradation of the substrate. In order to optimize all these parameters, a large number of experimental data has to be achieved which are not only difficult to perform but also gives the data that would be too complex to analyze. Hence, to avoid the same, a theoretical model was used. In this direction Response Surface Methodology (RSM) based upon Central Composite Design (CCD) is reported (An et al. 2011) to be an adequate model as it is an efficient experimental strategy for determination of optimal conditions.

3.16.3 Selection of various parameters for optimization and Response Surface Modeling

RSM is a method of collection of statistical and mathematical techniques used to optimize certain processes where response of interest is affected by various parameters following analysis of variance for identifying significant parameters. A mathematical equation representing the relationship between a single response and control factors can be obtained by this model. In the present study four important parameters viz., initial concentration of IMI, pH of soil, intensity of UV-light and depth of soil were selected as factors for optimizing the performance and reducing the operation cost for photocatalytic degradation of IMI. Stoichiometric approach was carried out by CCD based on RSM and the photocatalytic degradation efficiency was selected as response. Analysis of experimental data was supported by Design-Expert Software (trial version 9.0.3.1, Stat-Ease, Inc., MN, USA) (Sakkas et al. 2010; Lu et al.2011b).

Table 3.5 Factors and Levels used in 30 factorial design study

Variables	Symbol	-2 (-ὰ)	-1	0	+1	+2 (+ὰ)
		Coded level				
pH value	***A***	3	5	7	9	11
Intensity of light(Wm^{-2})	***B***	10	15	20	25	30
Depth of soil (g)	***C***	5	10	15	20	25
Imidacloprid conc.(mgL^{-1})	***D***	10	30	50	70	90

These selected variables were firstly converted to dimensionless ones A (pH), B (Intensity of light), C (depth of soil), and D (initial concentration) with coded values at levels:- -α,1,0,+1,+α as shown in Table 3.5. The experimental design came from RSM had concluded 30 experiments based upon various parameters pH, intensity of light, depth of soil and initial concentration of IMI (Table 3.6) were performed further.

Table 3.6 Experimental data in central composite design of photocatalytic degradation of imidacloprid

Run	pH (A)	Intensity of light Wm^{-2} (B)	Amount of soil g (C)	Initial conc. of imidacloprid mgL^{-1} (D)	R1(%) (Experimental)
1	7	20	15	50	52
2	3	20	15	50	60
3	7	20	15	50	52
4	7	30	15	50	63
5	3	10	25	10	49
6	7	10	15	50	47
7	11	10	5	90	19
8	3	10	5	10	63
9	7	20	25	50	44
10	3	30	5	90	55
11	3	30	5	10	83
12	11	30	25	10	50
13	11	30	5	10	55
14	11	30	25	90	27
15	3	10	5	90	49
16	3	30	25	90	34
17	7	20	15	50	54
18	7	20	15	50	53
19	3	30	25	10	66
20	7	20	15	50	54
21	11	30	5	90	45
22	7	20	15	90	45
23	3	10	25	90	41
24	7	20	5	50	62
25	7	20	15	10	60
26	7	20	15	50	53
27	11	10	25	90	14
28	11	10	5	10	42
29	11	10	25	10	21
30	11	20	15	50	42

3.16.4 Effect of various parameters on photocatalytic degradation of IMI

30 experiments obtained from RSM design setup (Table 3.6) were performed and analyzed. Experiments were performed at pH = 3, 7 and 11 by varying intensity of light, soil depth and initial concentration of IMI. C/C_0 Vs time graphs were plotted for all these 30 experiments.

In Fig. 3.27a, degradation was studied at pH =11 for initial concentration of 10 mg L^{-1} for 1 cm soil depth at intensity of 10 Wm^{-2} and 30 Wm^{-2} and was observed that degradation was more at higher intensity. Then experiments were performed at pH = 11, intensity of light = 10 Wm^{-2}, initial concentration of IMI = 10 mgL^{-1} by varying the soil depth and it was found that degradation decreases as soil depth increases (Fig. 3.27b). Further at pH = 11, experiments were performed (Fig. 3.27c) for soil depth of 1 cm and 10 Wm^{-2} light intensity and for different initial concentration of IMI and it was concluded that degradation decreases as the concentration of IMI increases.

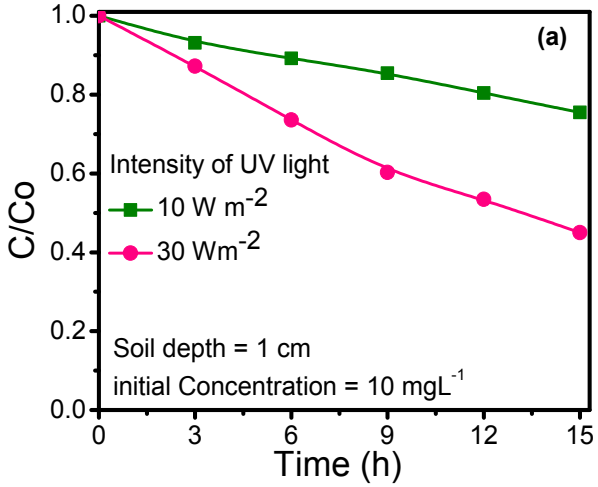

Fig. 3.27a Kinetic analysis for degradation of imidacloprid at pH = 11

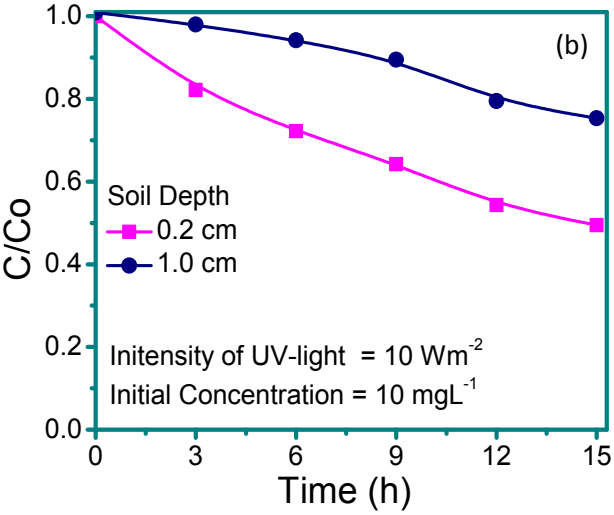

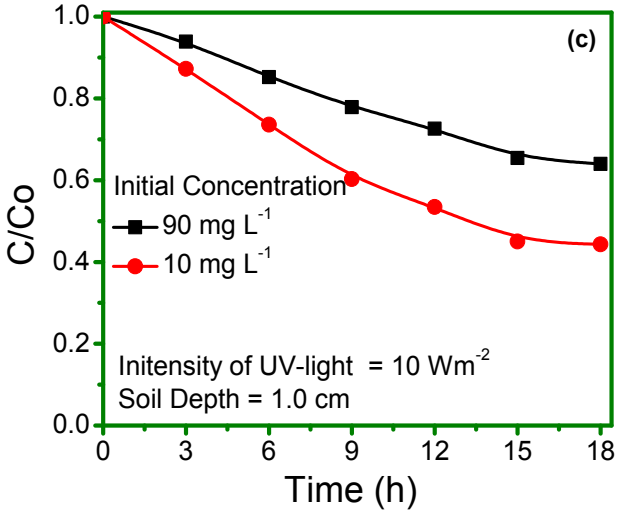

Fig. 3.27 b &c Kinetic analysis for degradation of imidacloprid at pH = 11

At pH = 3, experiments at different parameters range were also carried out to find out photocatalytic degradation of IMI. It was found (Fig. 3.28a) that by decreasing intensity of light, degradation also decreases at soil depth of 1 cm and initial concentration of 10 mgL^{-1} of IMI in soil. For the intensity of 10 Wm^{-2} and initial concentration of 10 mg L^{-1}, degradation of IMI was observed to be decreased as the soil depth increased (Fig. 3.28b).Fig 3.28 c depicted decreased in rate of degradation of IMI with increased in the concentration of IMI for 90 mgL^{-1} and 10 mgL^{-1} in soil at soil depth= 0.2 cm and intensity of light= 30 Wm^{-2}.

At pH=7 (Fig. 3.29 a, b & c), three experiments were performed and it was found that by varying intensity of light, soil depth and intial concentration of IMI, trend for the degradation of IMI was similar to pH= 3 and 11.

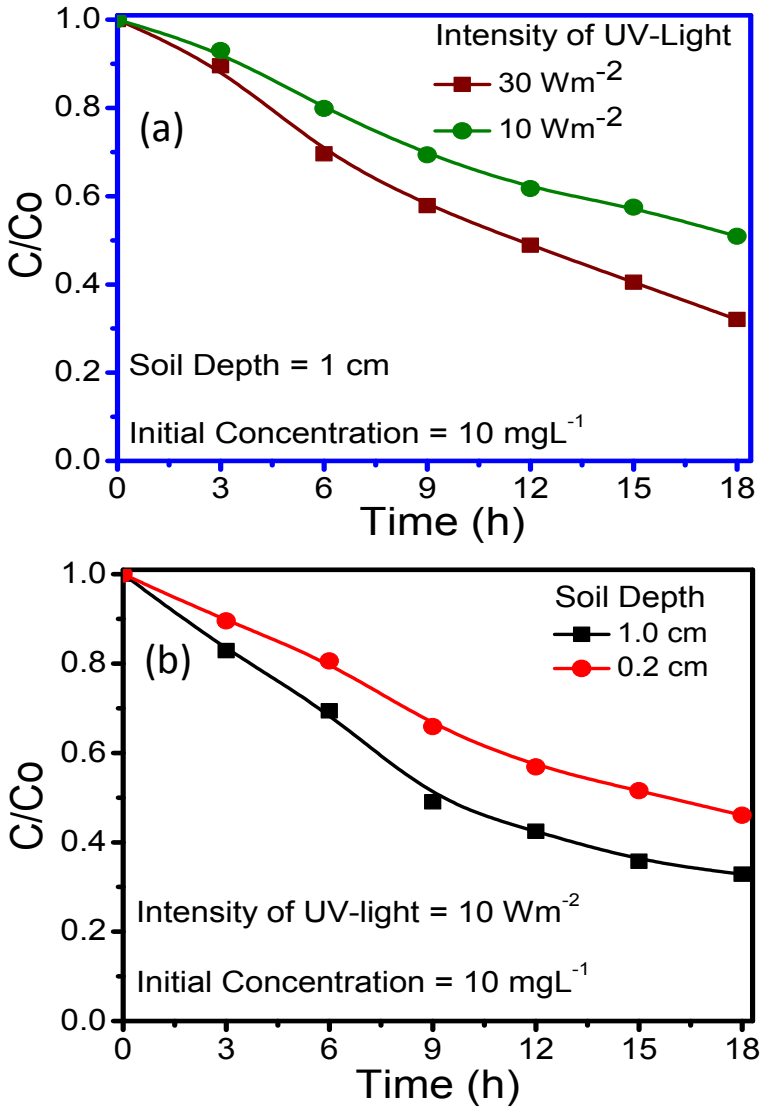

Fig. 3.28 a&b Kinetic analysis for degradation of imidacloprid at pH = 3

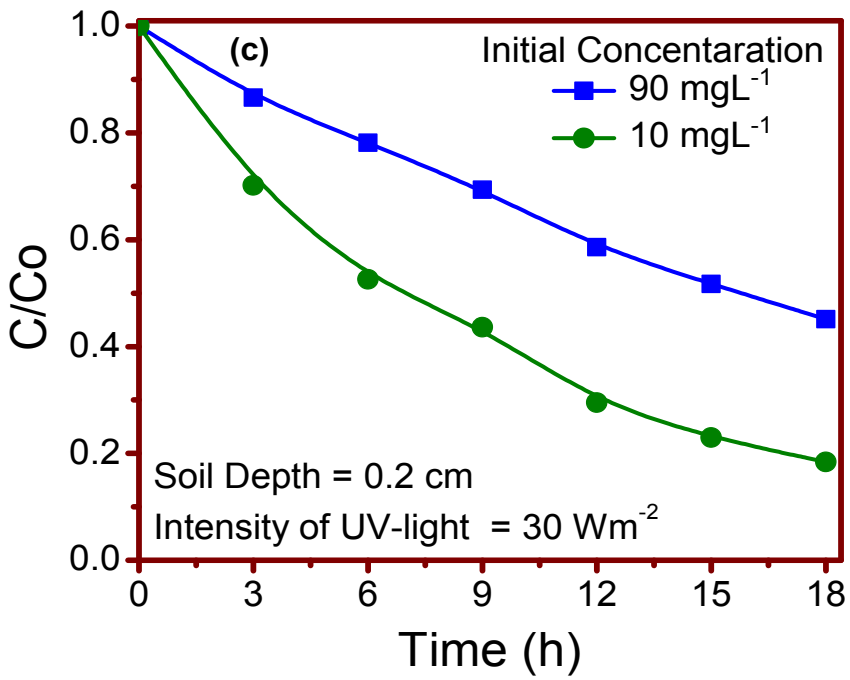

Fig. 3.28 c Kinetic analysis for degradation of imidacloprid at pH = 3

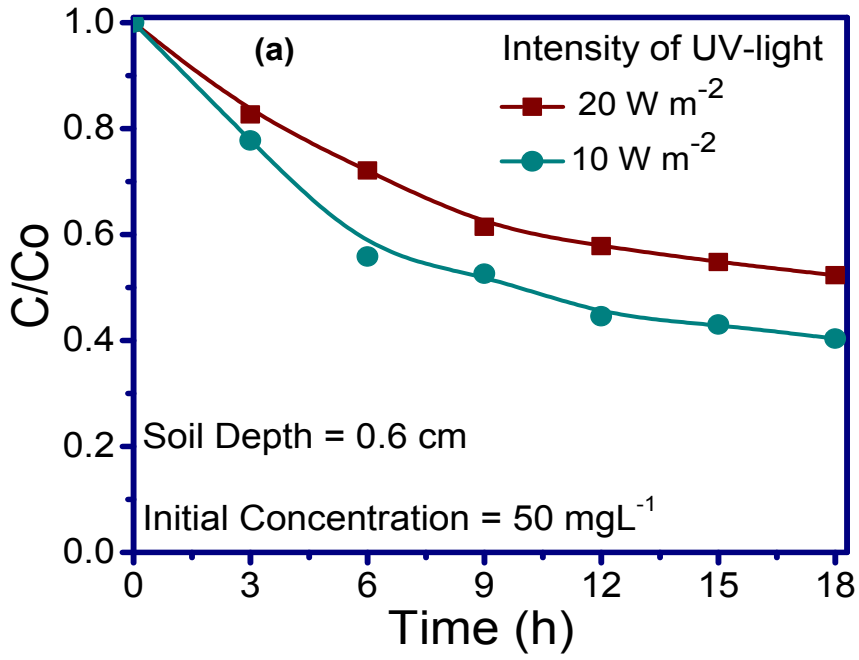

Fig. 3.29 a Kinetic analysis for degradation of imidacloprid at pH = 7

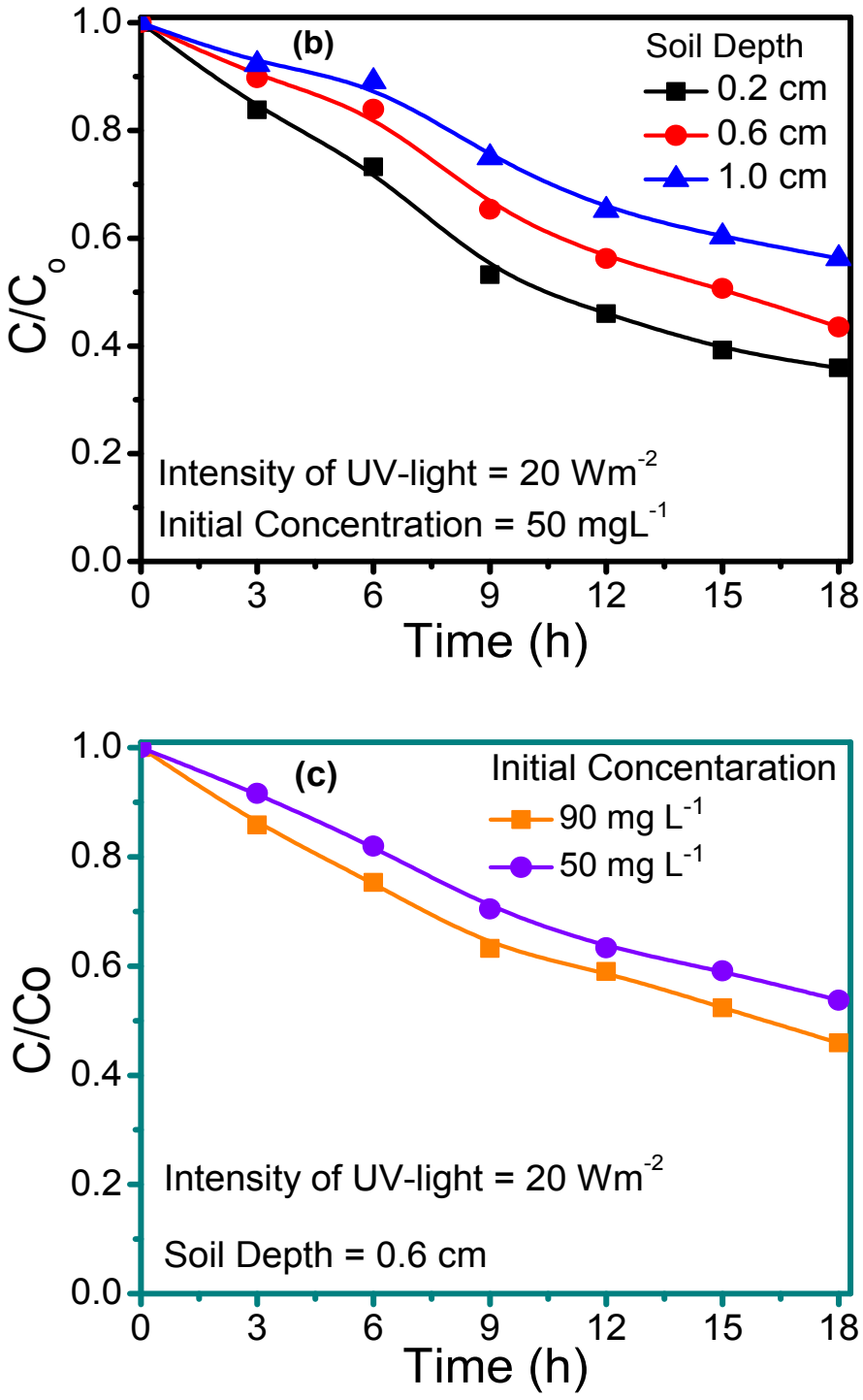

Fig. 3.29 b&c Kinetic analysis for degradation of imidacloprid at pH = 3

3.17 Kinetic studies for IMI degradation

From the kinetic point of view, it is more appropriate to characterize oxidation kinetics for the degradation of the molecules, since it gives the real measure of the oxidation rate during the advanced oxidation reaction. Moreover, the photocatalytic oxidation kinetics of many organic compounds is fitted to Langmuir–Hinshelwood (L–H) model as:

$$\frac{dc}{dt} = \frac{k_t k_c}{1 + k_c} \qquad \text{…….(3.2)}$$

Where, k is the reaction rate constant, K is the equilibrium adsorption constant, C the substrate concentration at any time t (Saien et al. 2008). According to this model, the rate of disappearance of reactant is only the product of an apparent rate constant and the Langmuir adsorption term, and thus mass transfer phenomena does not have any control to the overall kinetics of the photodegradation. In case of low concentration of reacting substrate this equation simplifies to apparent first order kinetics:

$$-\ln(C/Co) = k_a Kt = kt \qquad \text{……..(3.3)}$$

Where k is apparent rate constant which can be obtained by plotting –ln(C/Co) vs. time of irradiation for the 30 experiments suggested by RSM model were performed as discussed in *section 3.16* for different parameters and shown in Fig. 3.30-3.44. It can be clearly seen that plots are straight line for all the experiments with regression varying between 0.993 to 0.974, indicating that degradation of IMI under the specified conditions (inset Fig. 3.30-3.37) followed the L-H kinetics and pseudo first order kinetics. The values of apparent rate constant were found for all experimental results and shown in Table 3.7. The highest value of apparent rate constant (k) 15 x 10^{-4} min^{-1} was observed at pH = 3, intensity of light = 30 W m^{-2} and initial IMI = 10 mg L^{-1}, followed by 9.3 x 10^{-3} min^{-1}, revealed the former as an optimum conditions for photocatalytic degradation of IMI (83%) in soil.

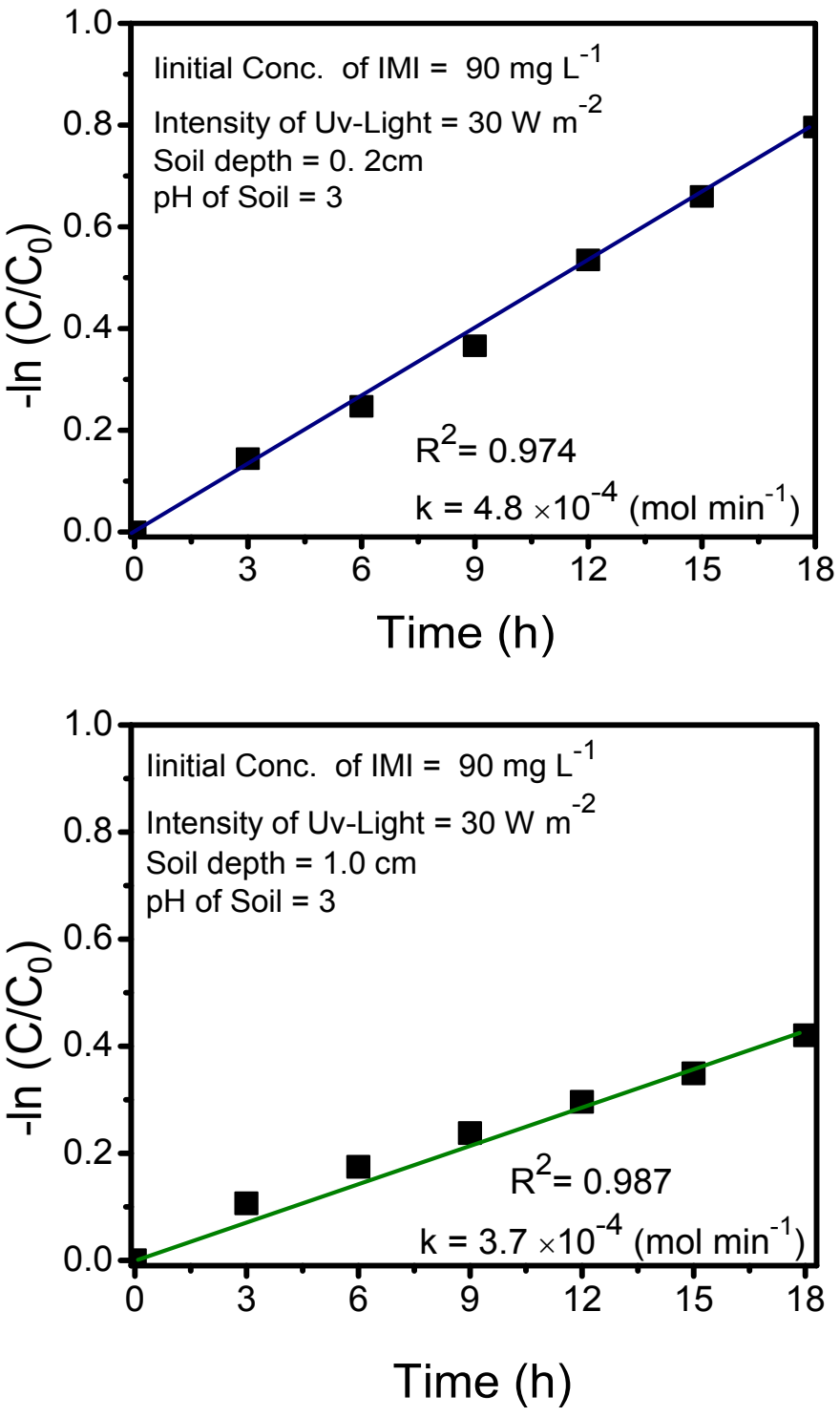

Fig. 3.30 Kinetic study for degradation of imidacloprid under different reaction conditions

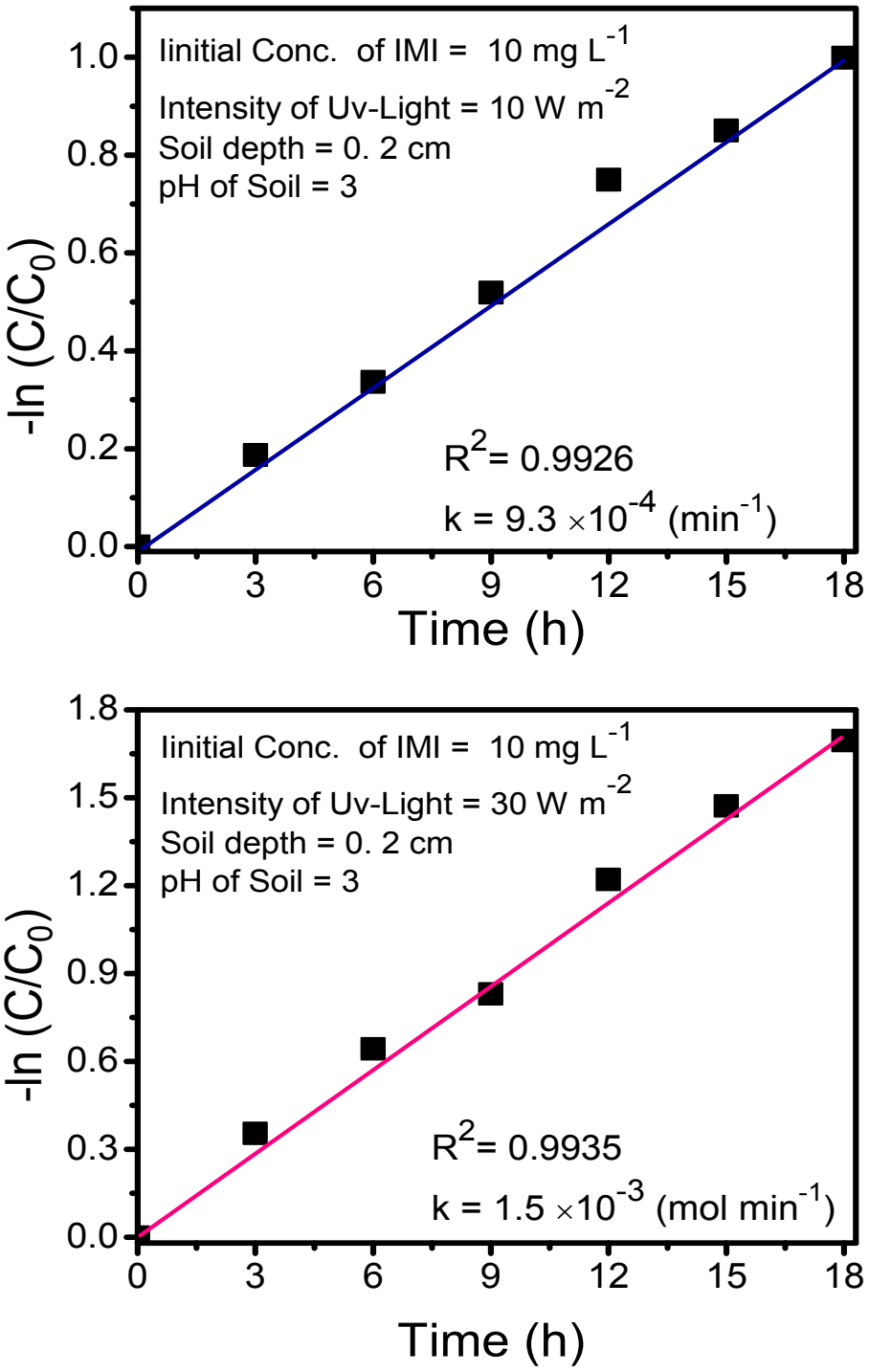

Fig. 3.31 Kinetic study for degradation of imidacloprid under different reaction conditions

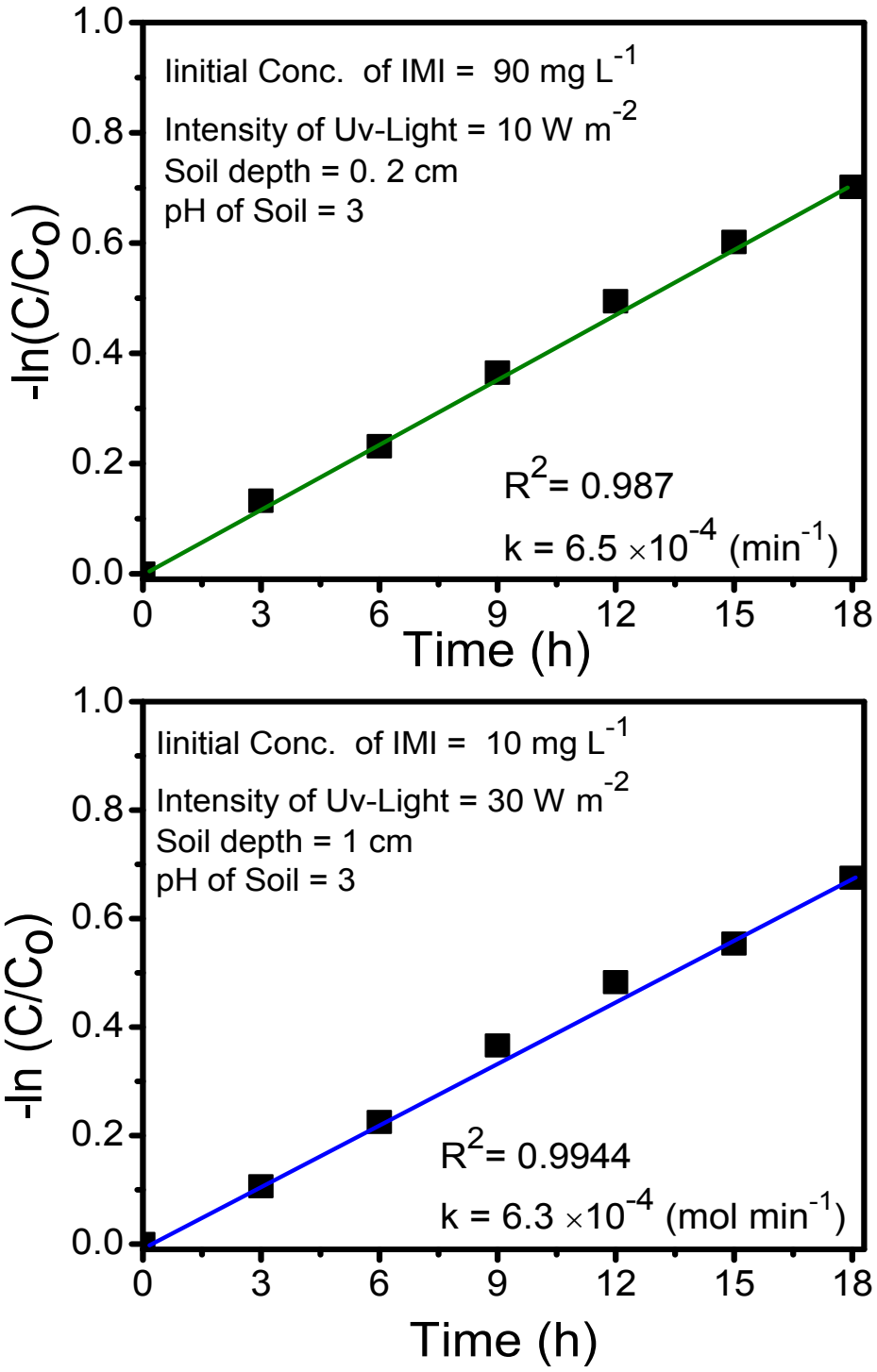

Fig. 3.32 Kinetic study for degradation of imidacloprid under different reaction conditions

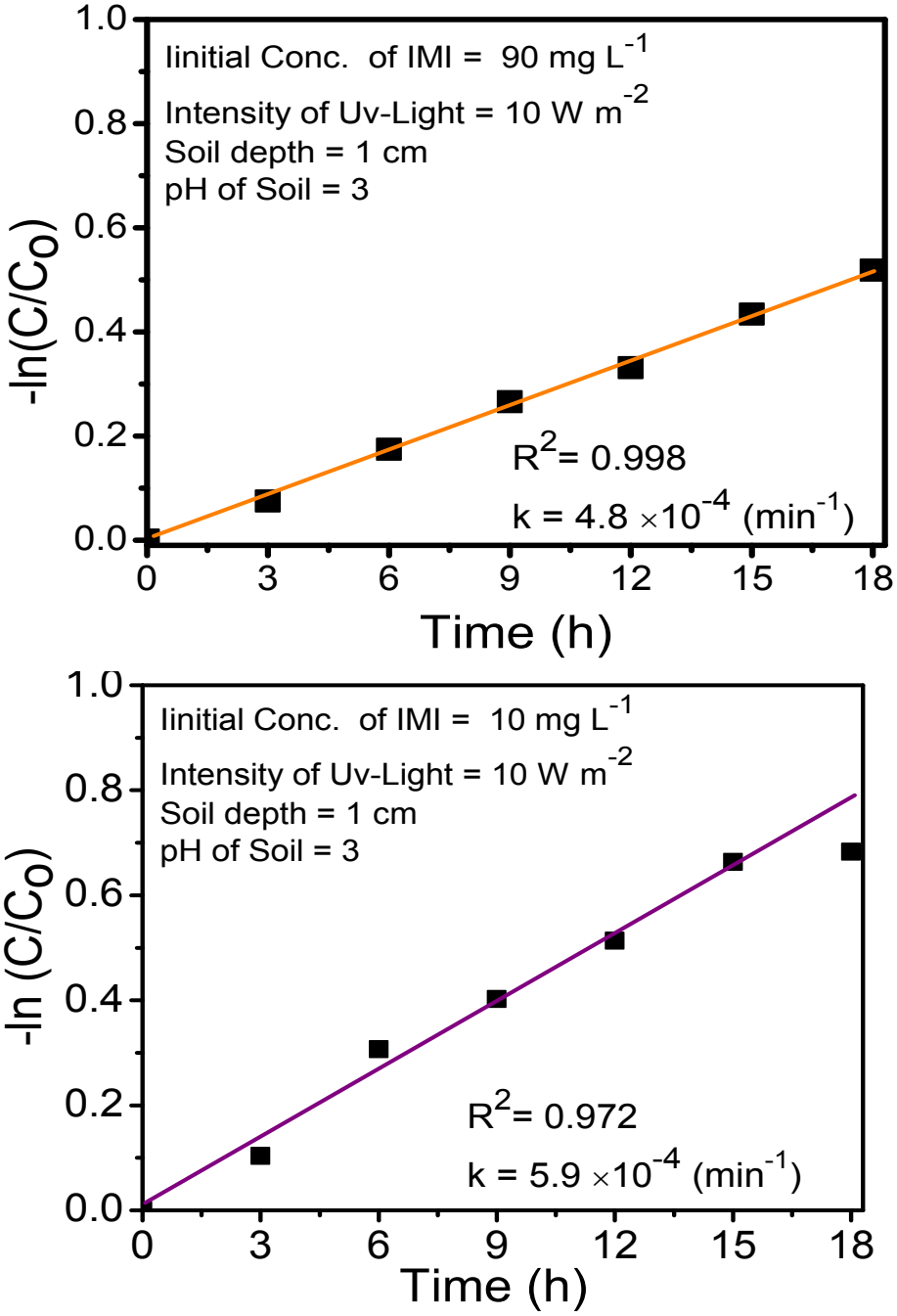

Fig. 3.33 Kinetic study for degradation of imidacloprid under different reaction conditions

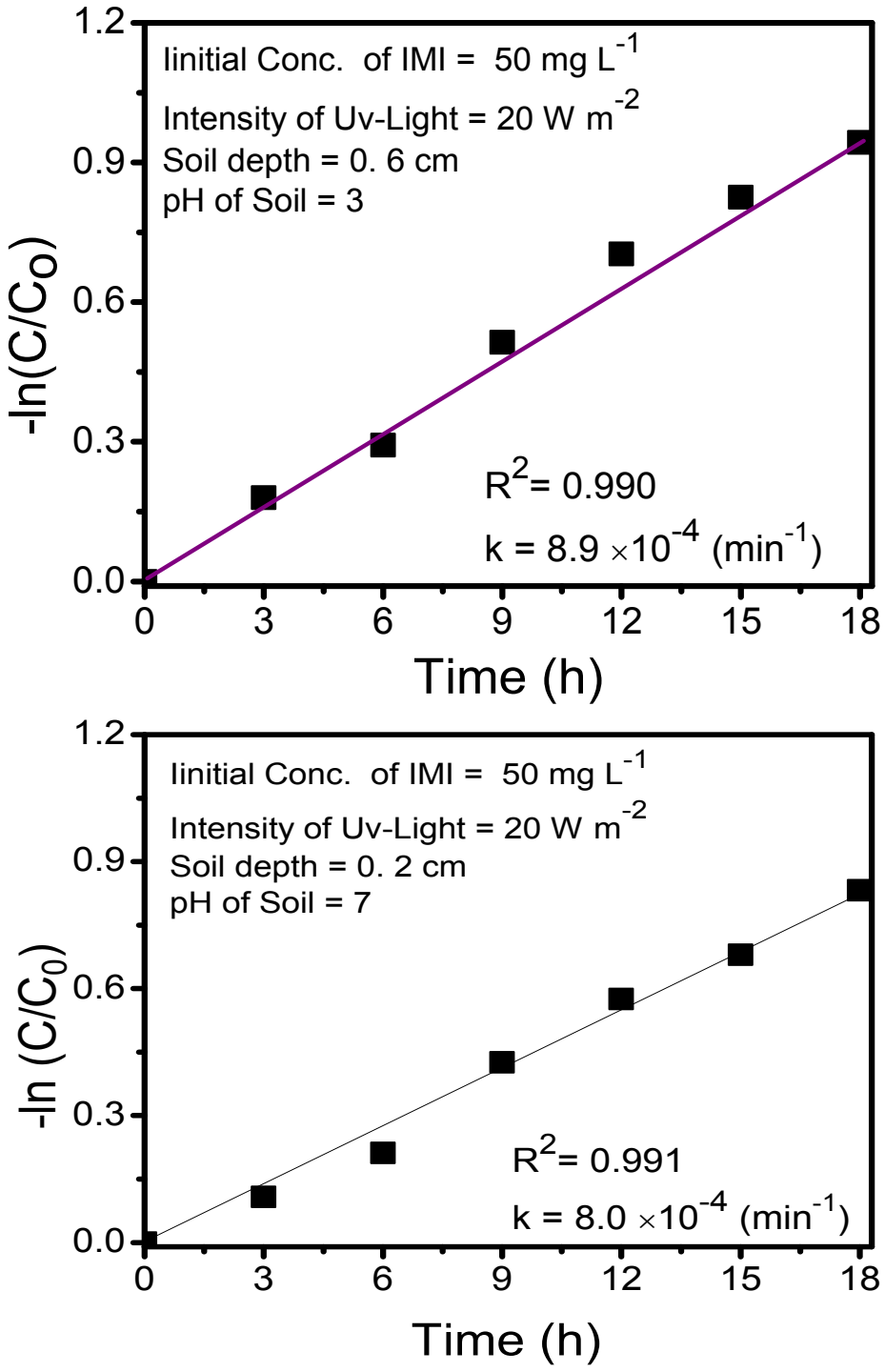

Fig. 3.34 Kinetic study for degradation of imidacloprid under different reaction conditions

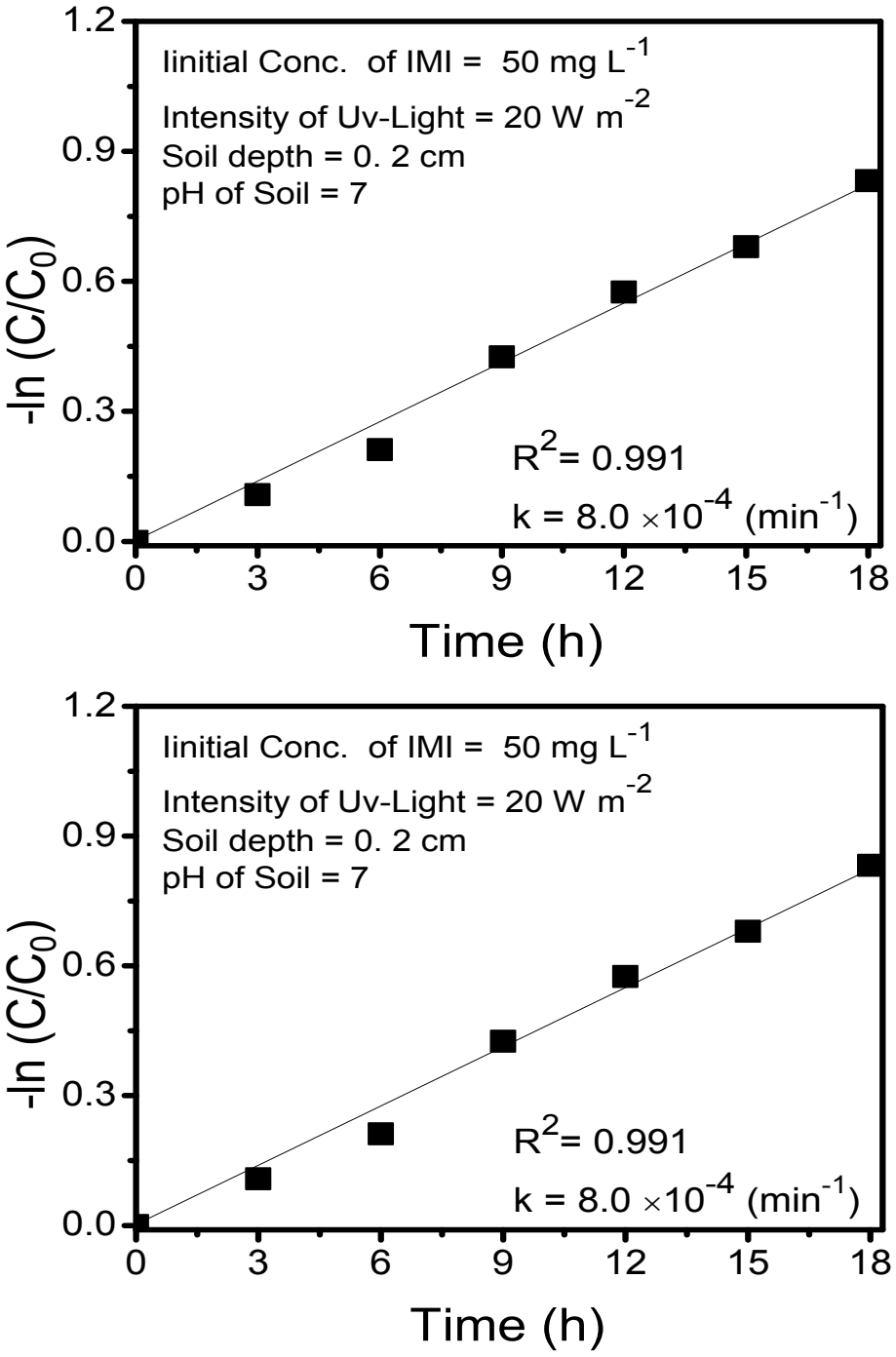

Fig. 3.35 Kinetic study for degradation of imidacloprid under different reaction conditions

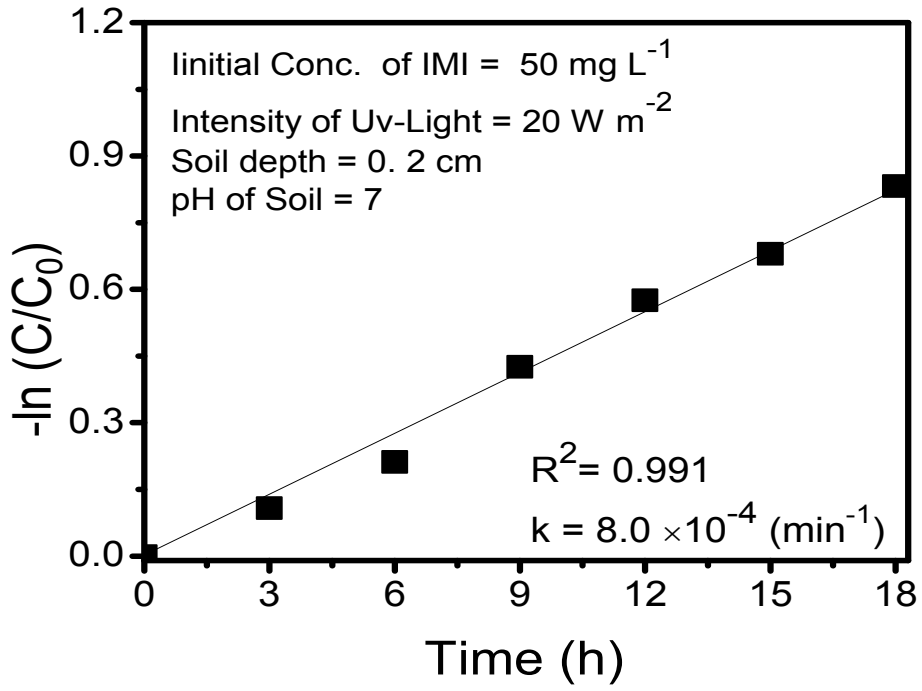

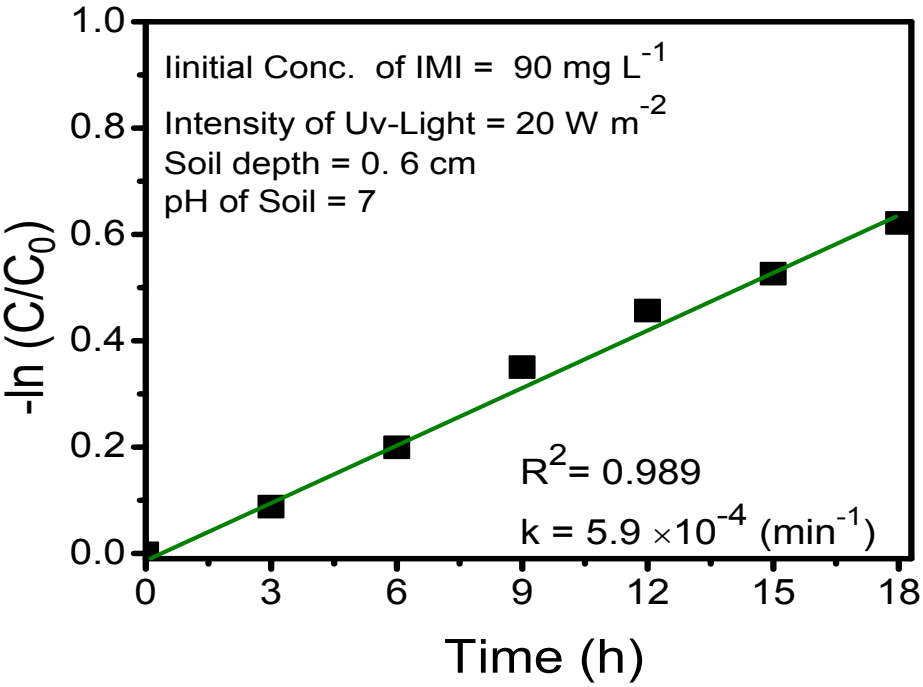

Fig. 3.36 Kinetic study for degradation of imidacloprid under different reaction conditions

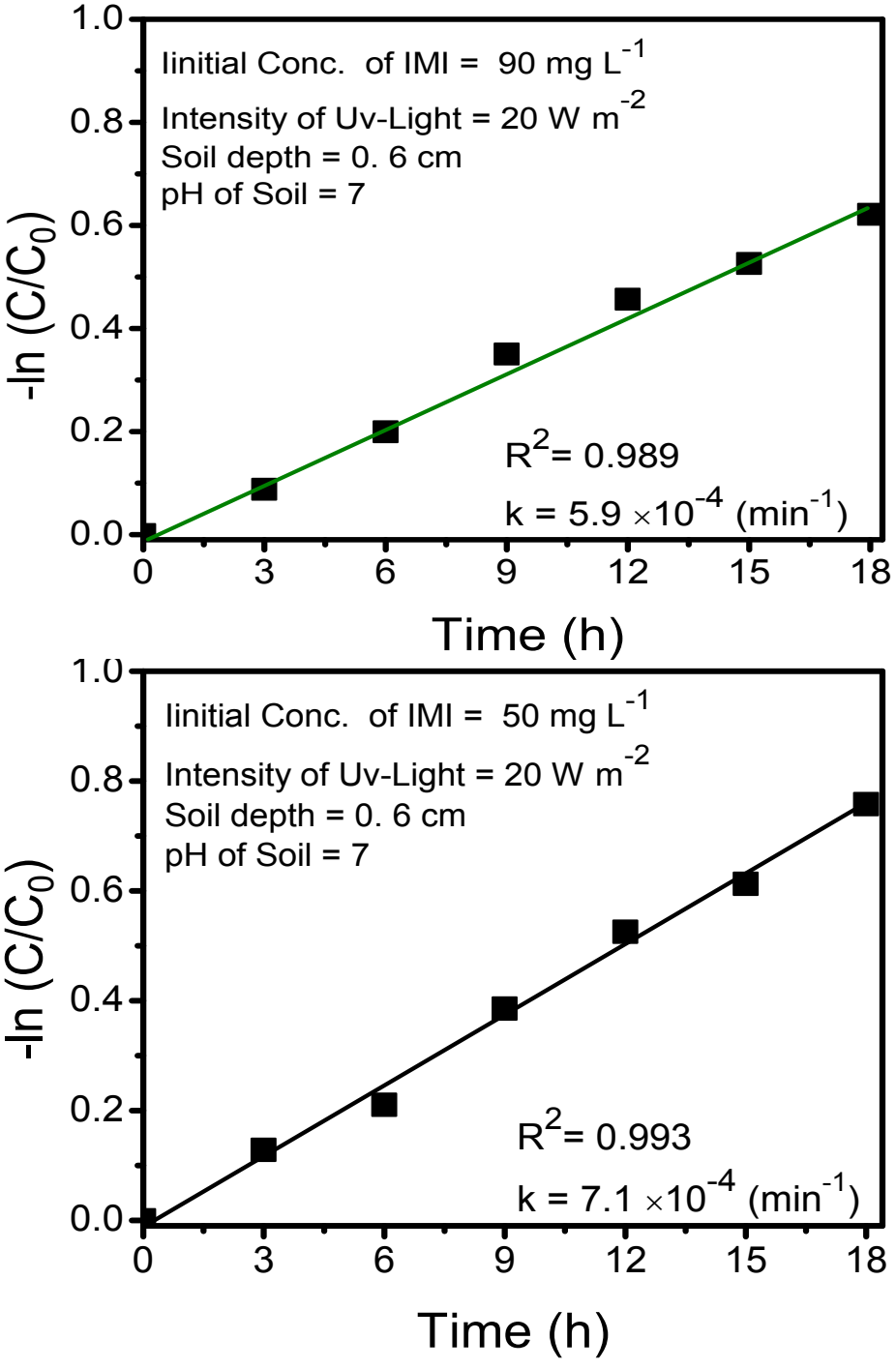

Fig. 3.37 Kinetic study for degradation of imidacloprid under different reaction conditions

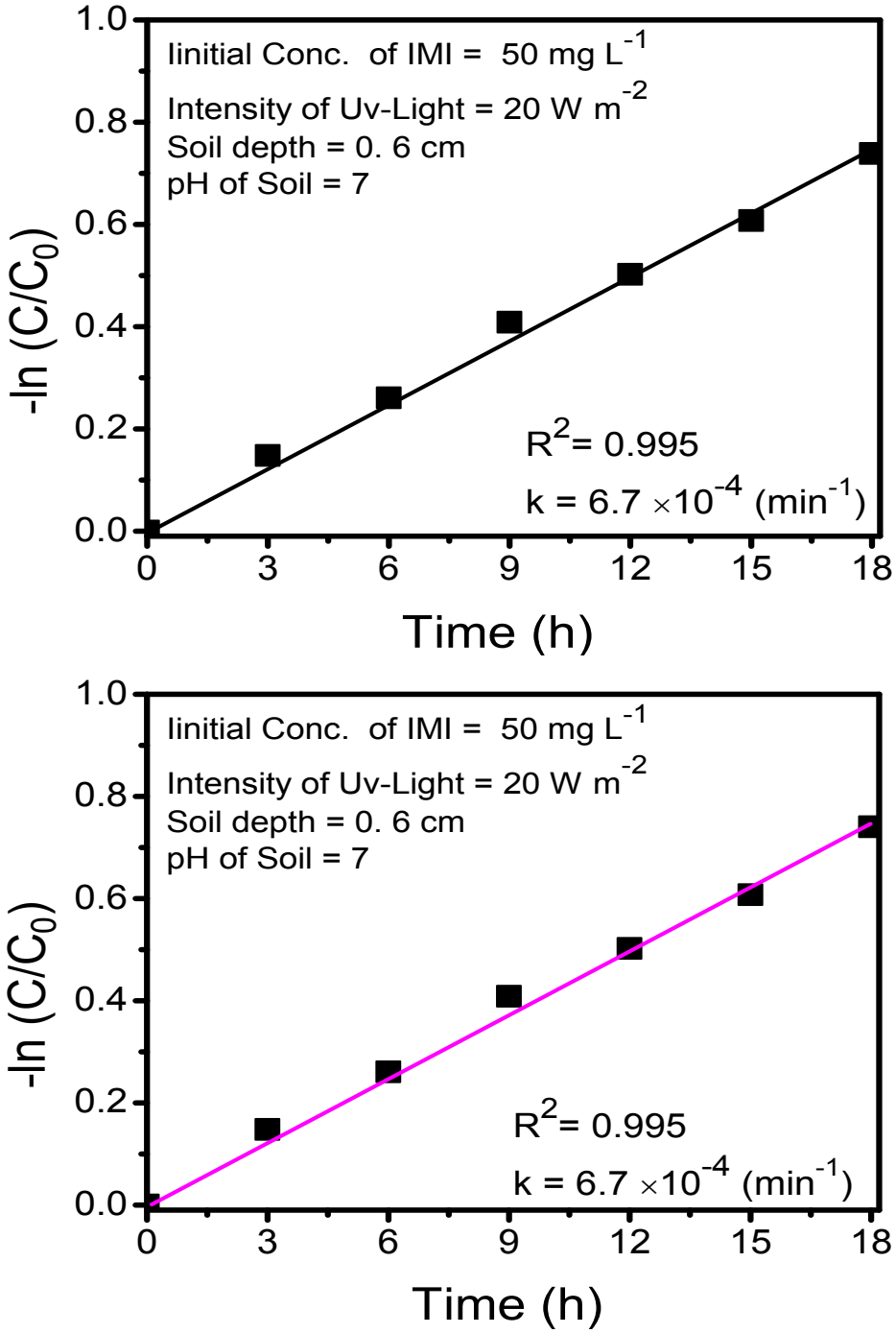

Fig. 3.38 Kinetic study for degradation of imidacloprid under different reaction conditions

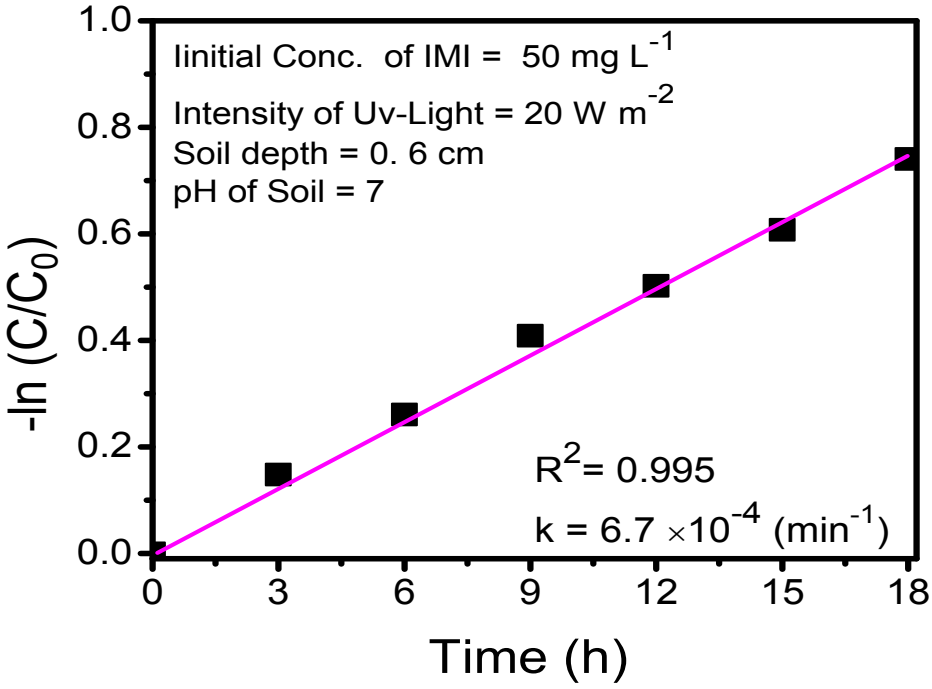

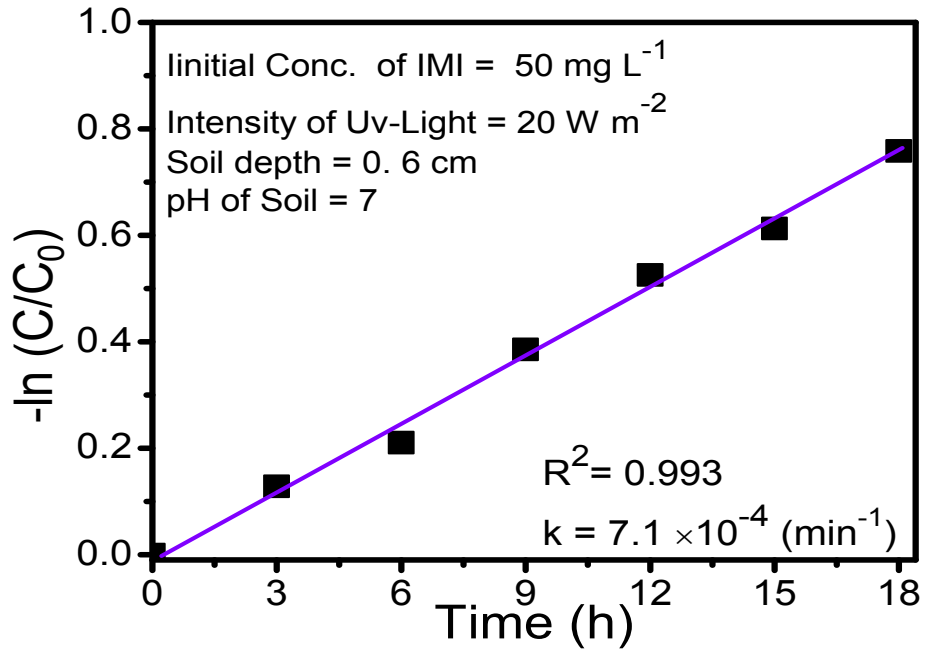

Fig. 3.39 Kinetic study for degradation of imidacloprid under different reaction conditions

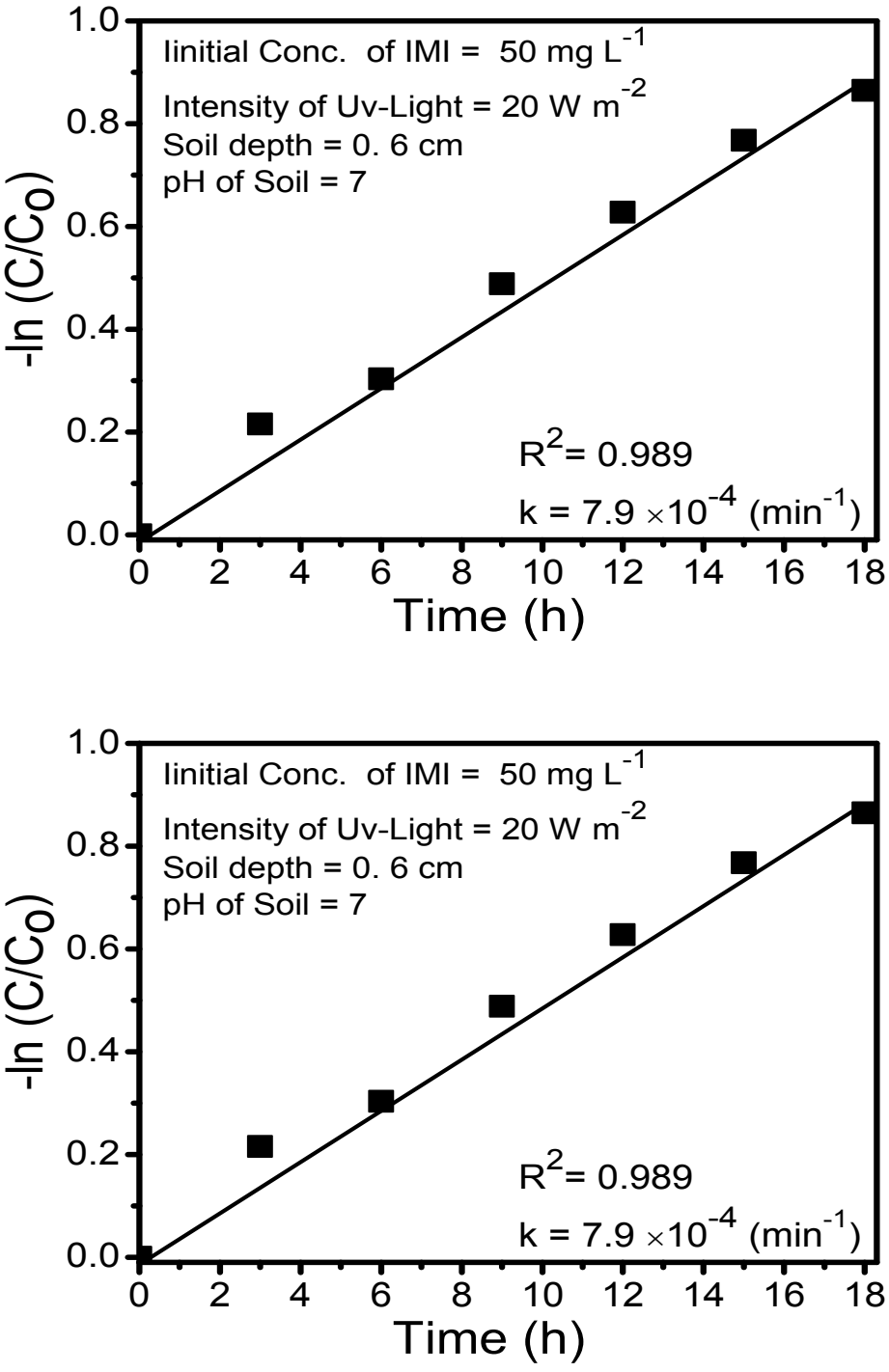

Fig. 3.40 Kinetic study for degradation of imidacloprid under different reaction conditions

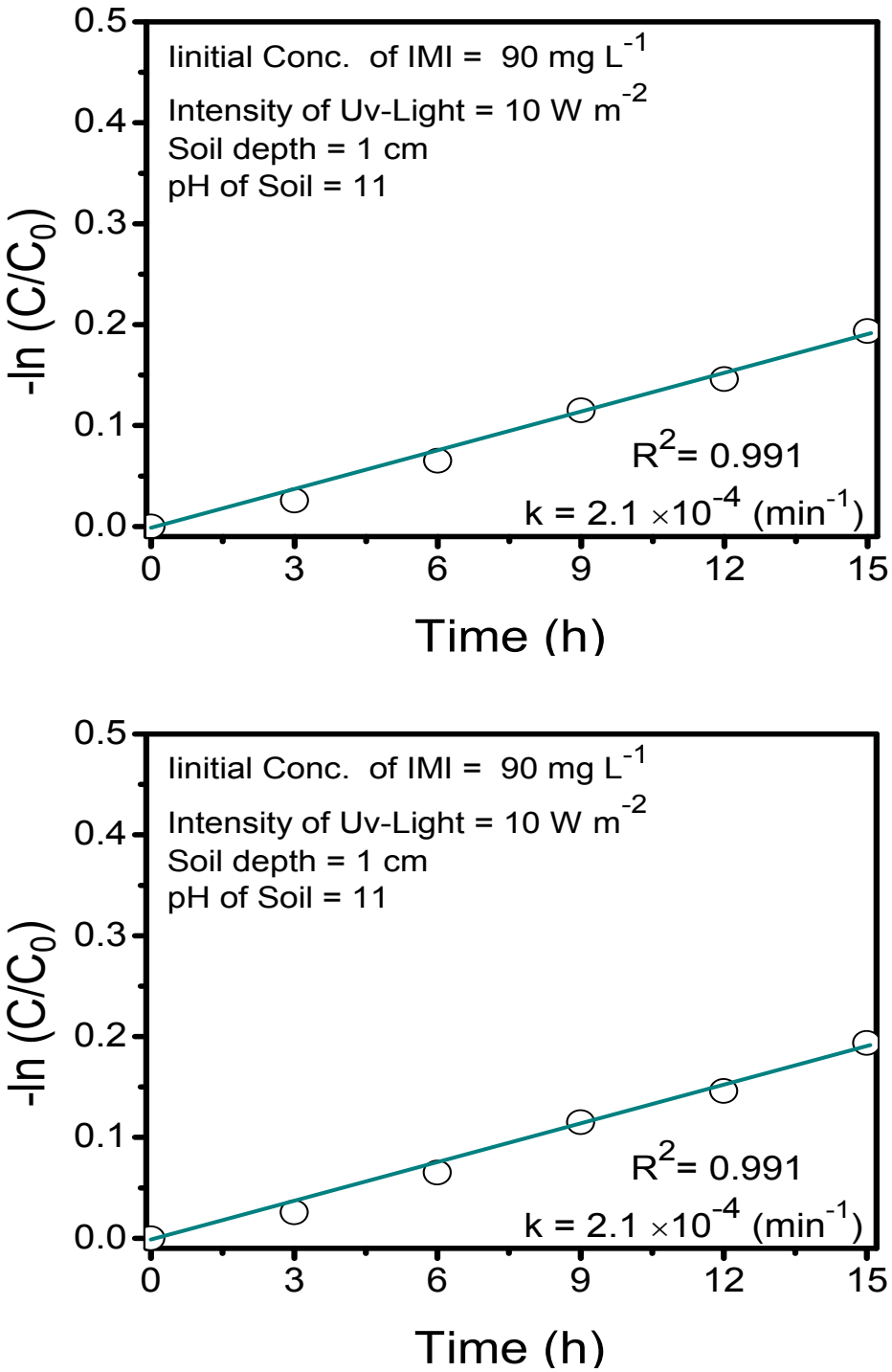

Fig. 3.41 Kinetic study for degradation of imidacloprid under different reaction conditions

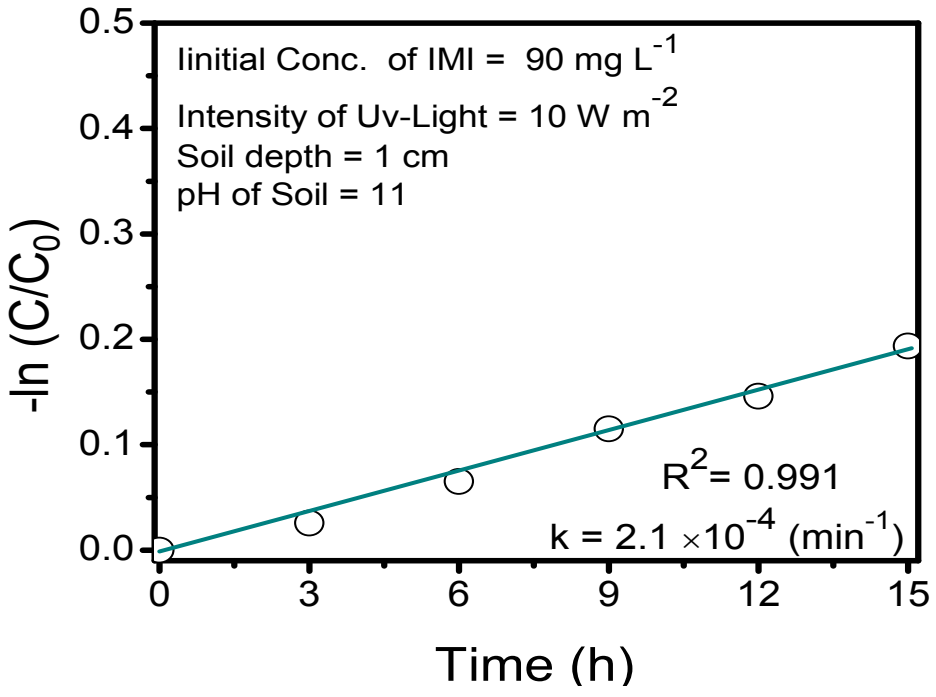

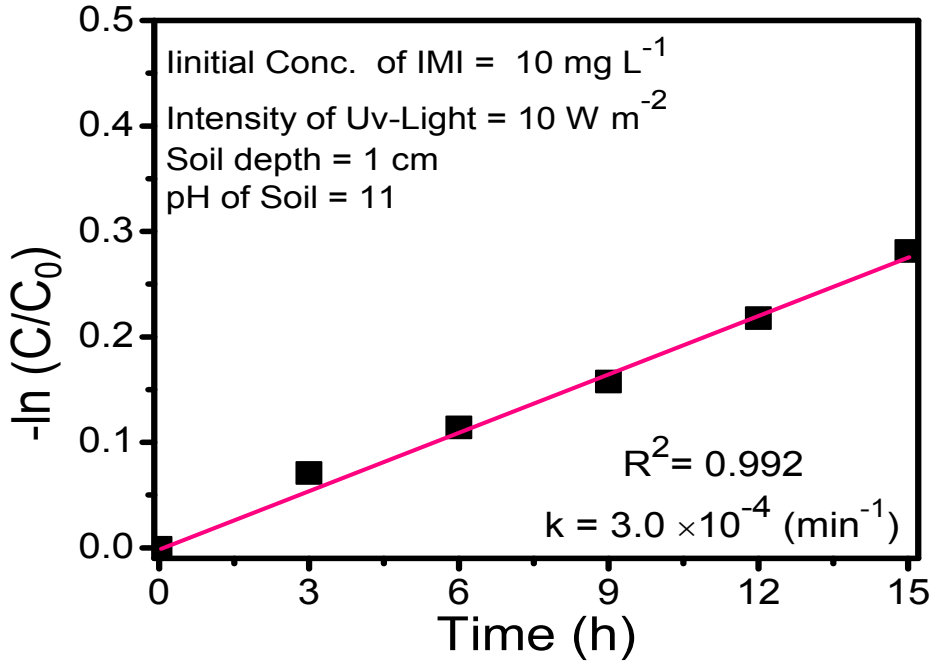

Fig. 3.42 Kinetic study for degradation of imidacloprid under different reaction conditions

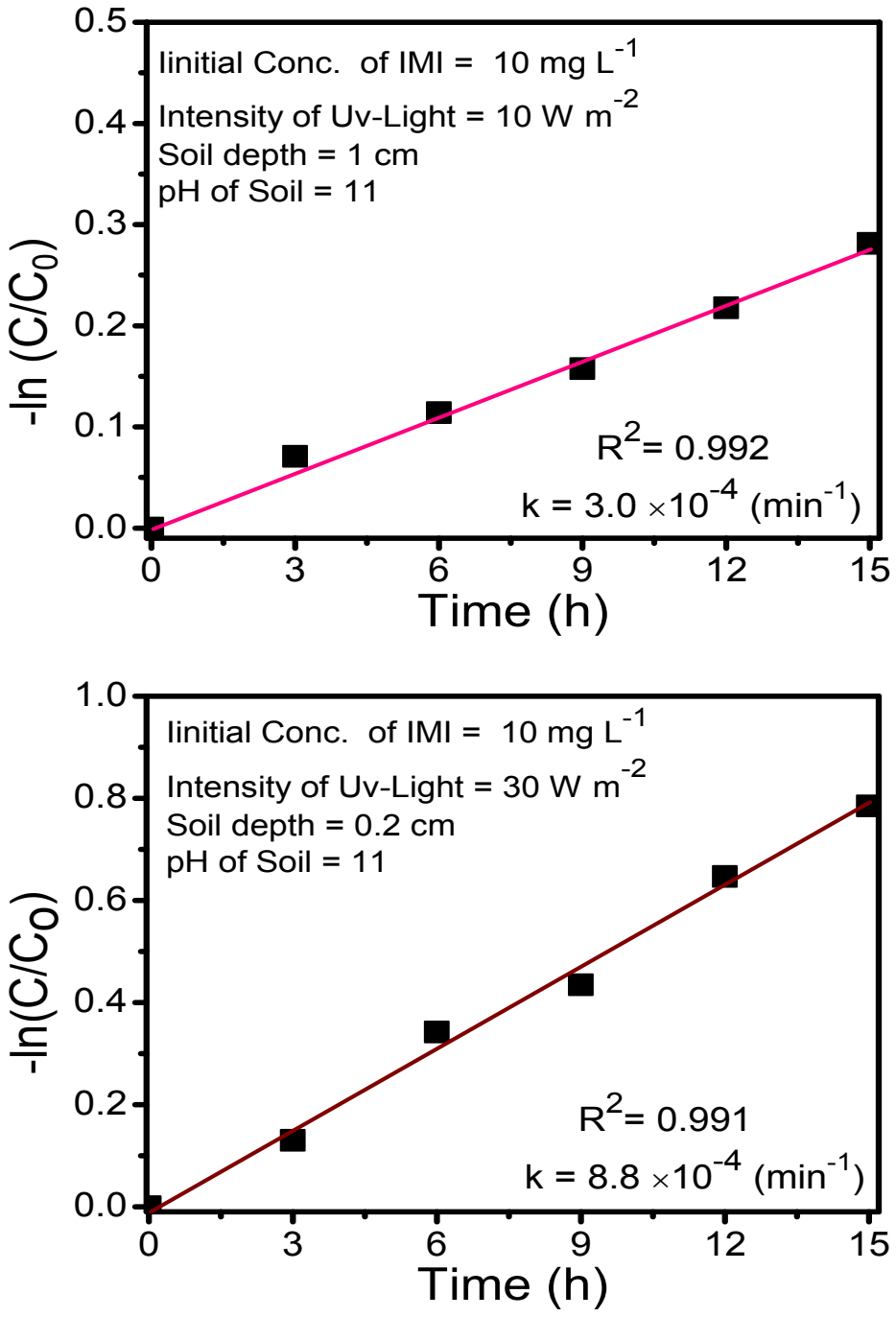

Fig. 3.43 Kinetic study for degradation of imidacloprid under different reaction conditions

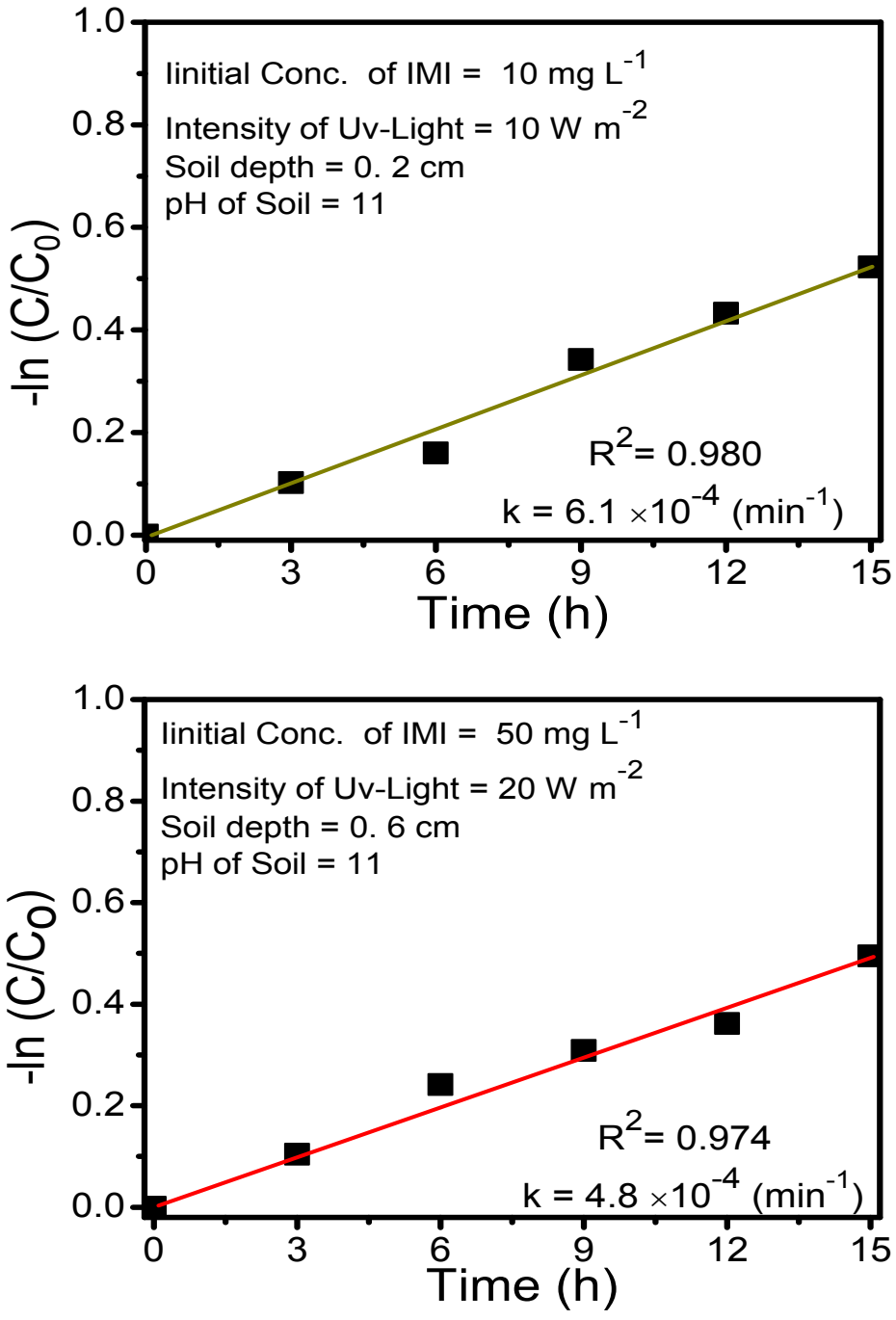

Fig. 3.44 Kinetic study for degradation of imidacloprid under different reaction conditions

Table : 3.7 Apparent rate constants for 30 experimental design set up

S. No	pH	Initial Concentration (mgL^{-1})	Intensity (Wm^{-2})	Soil depth (cm)	k ($\times 10^{-4}$ min^{-1})
1		90	30	0.2	4.8
2		90	30	1.0	3.7
3		10	30	0.2	15
4		10	10	0.2	9.3
5	3	90	10	0.2	6.5
6		10	30	1.0	6.3
7		90	10	1.0	4.8
8		10	10	1.0	5.9
9		50	20	0.6	8.9
10		50	20	0.2	8.0
11		50	20	0.2	6.0
12		50	30	0.6	9.0
13		50	20	1.0	5.5
14		90	20	0.6	5.9
15	7	20	10	0.6	8.5
16		50	20	0.6	7.1
17		50	20	0.6	6.7
18		50	20	0.6	6.7
19		50	20	0.6	7.0
20		50	20	0.6	7.1
21		50	20	0.6	7.9
22		90	30	1.0	4.7
23		90	10	1.0	2.1
24		90	10	0.2	3.1
25		90	30	1.0	7.5
26	11	10	10	1.0	3.0
27		10	30	1.0	7.3
28		10	30	0.2	8.8
29		10	10	0.2	6.1
30		50	20	0.6	4.8

3.18 CCD Model and residual Analysis

According to the RSM results, polynomial modeling was performed on the responses of the corresponding coded values of the four different process variables. The comparison of the

experimental values was done against the predicted responses by this model for the degradation efficiencies of IMI in soil as shown in Table 3.8.

Table 3.8 Experimental and predicted data in central composite design of photocatalytic degradation of imidacloprid

Run	pH (A)	Intensity of light Wm^{-2} (B)	Amount of soil g (C)	Initial conc. of imidacloprid mgL^{-1} (D)	R1(%) (Experimental)	R2 (%) (Predicted)
1	7	20	15	50	52	49
2	3	20	15	50	60	59
3	7	20	15	50	52	49
4	7	30	15	50	63	56
5	3	10	25	10	49	52
6	7	10	15	50	47	41
7	11	10	5	90	19	23
8	3	10	5	10	63	67
9	7	20	25	50	44	42
10	3	30	5	90	55	59
11	3	30	5	10	83	86
12	11	30	25	10	50	54
13	11	30	5	10	55	59
14	11	30	25	90	27	31
15	3	10	5	90	49	53
16	3	30	25	90	34	37
17	7	20	15	50	54	49
18	7	20	15	50	53	48
19	3	30	25	10	66	69
20	7	20	15	50	54	49
21	11	30	5	90	45	49
22	7	20	15	90	45	40
23	3	10	25	90	41	44
24	7	20	5	50	62	56
25	7	20	15	10	60	58
26	7	20	15	50	53	49
27	11	10	25	90	14	17
28	11	10	5	10	42	46
29	11	10	25	10	21	24
30	11	20	15	50	42	39

It has also been found here that amount of IMI photo-catalytically degraded (83%) complies with the theoretically determined (86%), not only for the optimized conditions but for all the experiments. Based upon these results a theoretical co-relation between these parameters could be expressed as follows:

R = +64.69562 -1.20421 pH + 1.41174 Intensity- 0.36298 soil + 0.010786 conc.-0.098242 pH Intensity- 0.11836 pH soil -0.042773 pH conc.- 0.024414 soil Intensity-0.014629 Intensity conc.+ 2.30469E-003 soil conc. +6.67969E-003 pH Intensity soil+ 2.48047 E-003 pH Intensity conc. + 1.52344E-003 pH soil conc. -8.98438E- 005 Intensity soil conc. -7.42188E -005 pH Intensity soil conc.

In the above expression, R is the response variable for degradation efficiency of imidacloprid. In order to further verify the adequacy and significance of the studied model the most important ANNOVA test for the evaluation of data was applied. It can be depicted from Table 3.9, the probability value (P) for A (pH) and D (concentration of IMI) are very low (<0.0001) in comparison to other parameters B (intensity of light) and C (depth of soil).

Table 3.9 Response surface model regression coefficients and P-value for responses

Term	Variable	Regression coefficients	P
pH value	*A*	-10.28	<0.0001
Intensity of light	*B*	7.39	0.0002
Depth of soil	*C*	-7.06	0.0003
Imidacloprid conc.	*D*	-8.89	<0.0001
pH value× Int. of light	*AB*	2.81	0.0971
pH value× depth of soil	*AC*	0.69	0.6704
Int. of light× depth of soil	*BC*	1.19	0.4652
Int. Of light× IMI conc.	*BD*	-0.81	0.6155
pH value ×IMI conc.	*AD*	-2.56	0.1275
Depth of soil× IMI conc.	*CD*	0.31	0.8462
pH value× Int. of light× depth of soil	*ABC*	1.19	0.4652
pH value× Int. of light× IMI conc.	*ABD*	2.19	0.1883
pH value× depth of soil × IMI conc.	*ACD*	0.06	0.9690
Int. of light× depth of soil × IMI conc.	*BCD*	-2.44	0.1456
pH value× Int. of light× depth of soil × IMI conc.	*ABCD*	-1.19	0.4652

Since, in the ANNOVA analysis it is being well known that factors with very low value of probability have more significance than the higher ones. Hence, the variables A and D were found to have much significant effect than the B and C for the photocatalytic degradation of IMI. Additionally, adequacy of selected model with real system was confirmed by analyzing the

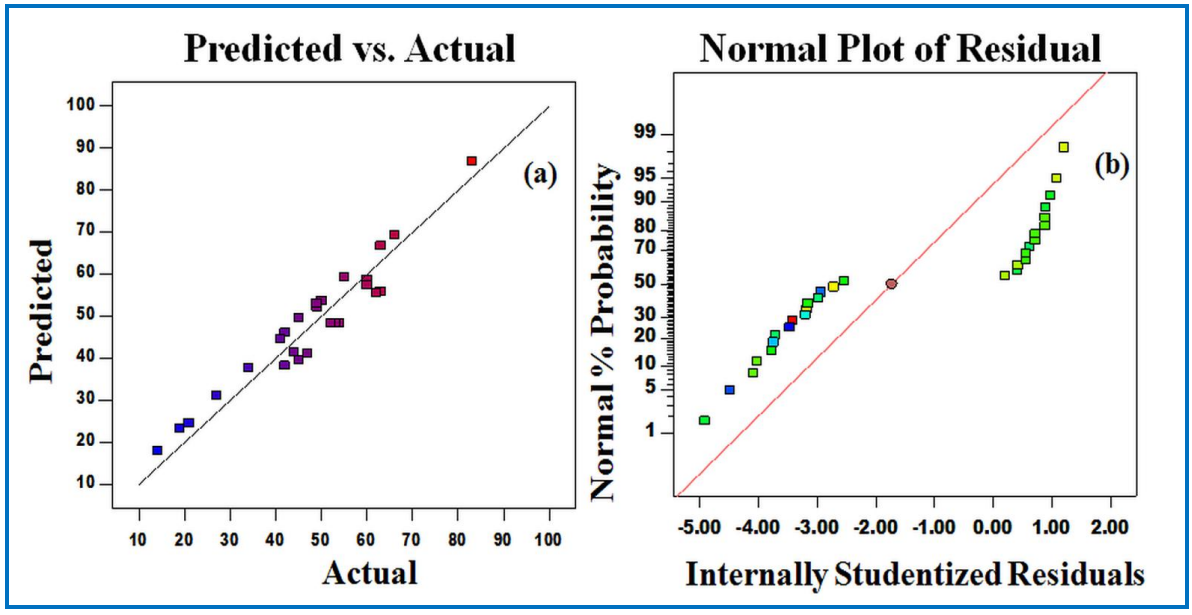

Fig. 3.45 (a) Experimental and calculated values for degradation of imidacloprid and (b) internally studentized residuals plot during photocatalytic process.

correlation between observed and predicted values. The parity between experimental and predicted values is given in Fig. 3.45a where the experimental data has been reasonably fitted well within ±10 %. The response factor of calculated residual values were plotted and shown in Fig. 3.45b which depicts that all data points lie close to straight line and within 95% confidence intervals line with mean values near zero.

The plot of studentized residuals vs. Predicted values was plotted to check the constant error (Fig. 3.46). It can be seen that

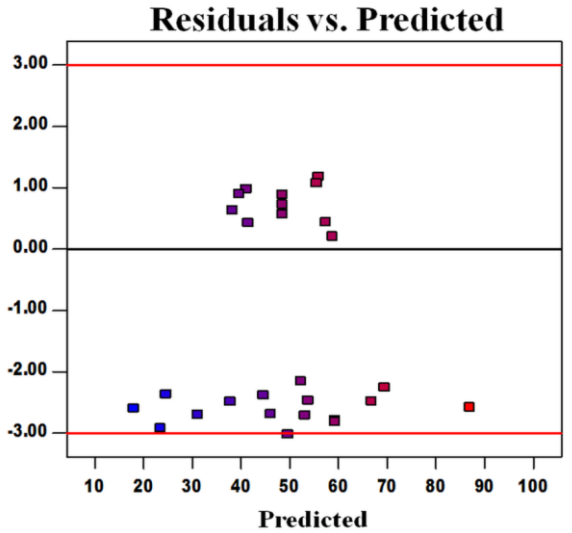

Fig. 3.46 The internally studentized residual plots

there is no specific pattern followed by the points i.e., the points are randomly distributed along the horizontal line from -3 to +3 and are considered as the top and bottom outlier detection limit. This random distribution of data points indicated that linear model is well fit for the degradation of IMI under the experimental conditions. Moreover, such type of distribution for data points also reflects that variance for these experimental results would be less and constant, indicated the preciseness in the obtained results with the constant error.

3.18.1 Effect of variables as response surface plots

In order to achieve insight about the impact of each variable, the three-dimensional (3D) plots for the predicted responses were formed. From these plots, the potential relation between any of the two parameters (pH, soil depth, initial concentration of IMI and intensity of light) effect collectively on photocatalytic degradation efficiency can be analyzed. The response surface (Fig. 3.47) for pH and initial concentration of IMI (at constant light intensity and soil depth) revealed that with decrease in both of above said parameters, photocatalytic degradation of IMI increased. This is reflected by increase in intensity of red colour from green one. Moreover, the highest amount of IMI degraded experimentally (83%) was found to be in good correlation to that determined from this 3D response surface plot (86%), further supporting experimental observations of present study.

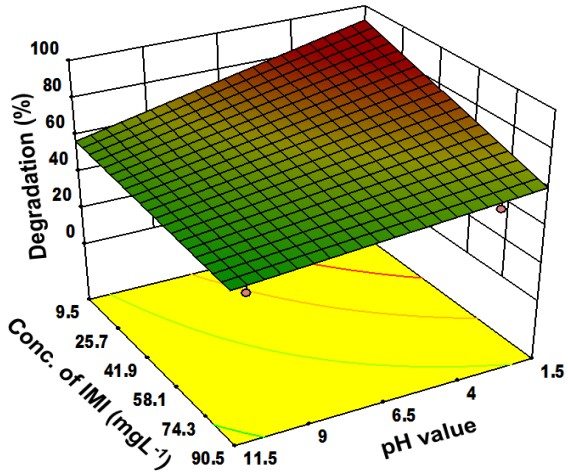

Fig. 3.47 Response surface graph for the interaction between pH and initial imidacloprid concentration at fixed depth of soil (0. 2cm) and light intensity 30 Wm^{-2}

Similarly, from the 3D response surface plot for pH and amount of soil (Fig. 3.48), it was visualized (increase in intensity of red colour) that decrease in these parameters resulted increase in the photodegradation of IMI. The maximum photodegradation of IMI determined experimentally (83%) at optimum pH = 3 and 0.2 cm of soil depth, is also in accordance to that determined from this response surface plot. The enhancement in the photodegradation of IMI in soil by increasing the acidity of soil and lowering of concentration of IMI could be ascribed to

the pH dependent surface properties of TiO_2 (Grover et al. 2013). The decrease in pH of soil resulted into TiO_2 surface to become cationic, causing increase in attractive interaction between the O atom (partially negative) of resonance stabilized (Fig. 3.49) $-NO_2$ group in IMI. Consequently, increase in adsorption of IMI favored more number of IMI molecules to be present at the interface of TiO_2 and hence the degradation efficiency. However, at pH = 9-11, reduction in degradation efficiency (50% to 15%) could be ascribed to the protonation of imidazole ring as also revealed by the dark adsorption studies. At low concentration, the degradation of IMI was found to be faster than at high concentration of IMI. The reason might be the dominance of screening effect due to increase in concentration of IMI which prevents the penetration of the light and hence reduction in the generation of $OH^{\cdot}$ radicals on the catalyst surface (Rauf et al. 2011).

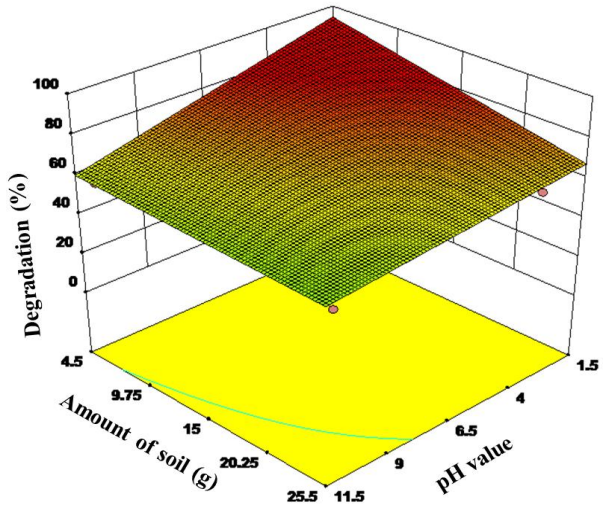

Fig. 3.48 Response surface graph for the interaction between pH and amount of soil at fixed conc. of IMI (10 mg kg^{-1}) and light intensity 30 Wm^{-2}

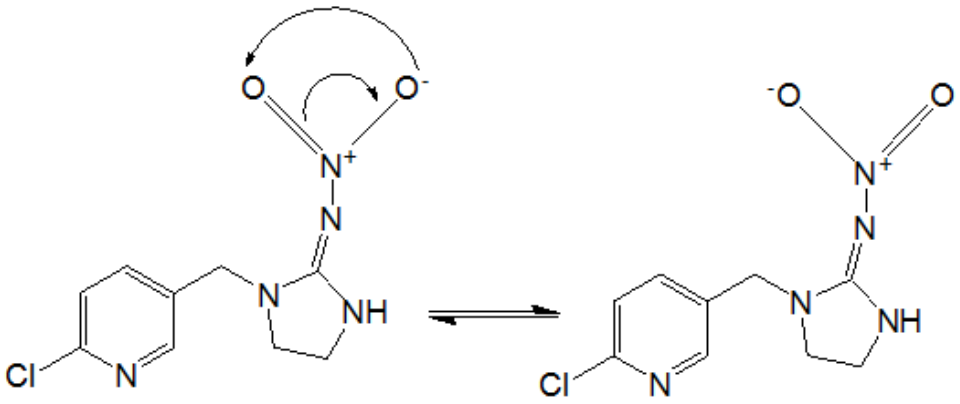

Fig. 3.49 Resonatic structure of NO_2

However, the response surface plots for the influence of intensity of light along with initial concentration of IMI (Fig. 3.50) and pH of soil (Fig. 3.51) on the degradation (%) of IMI were

also plotted which revealed that increase in UV light intensity caused increase in its photocatalytic degradation. This could be credited to more availability of photons for excitation of valance band electrons leading predominate formation of electron-hole pair and thereby diminishing the charge recombination process (Hebert and Miller, 1990; Wang et al. 2007; Dong et al. 2010). However, at lower light intensity, electron–hole pair separation competes with recombination which in turn decreases the formation of free radicals, thereby, causing less effect on the degradation of the IMI on soil surfaces (Dong et al. 2010 ; Bahnemann et al.2004).

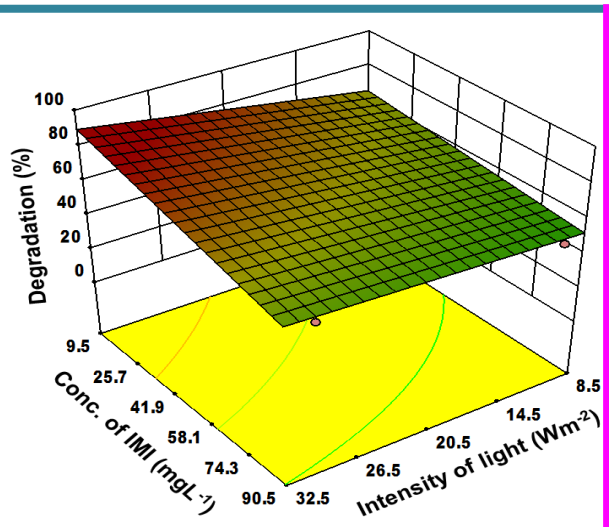

Fig. 3.50 Response surface graph for the interaction between light intensity and initial imidacloprid concentration at fixed depth of soil (0.2 cm) and pH= 3

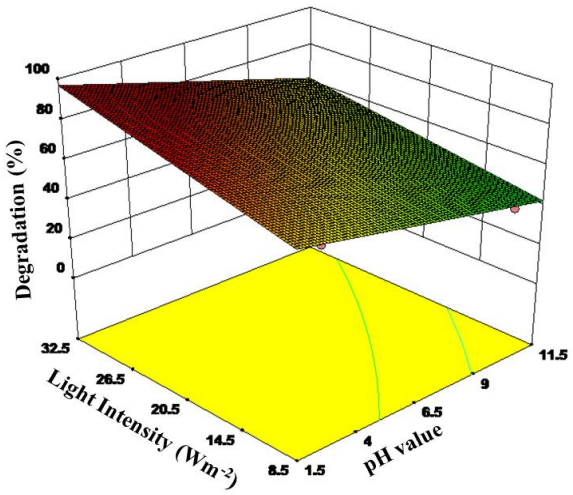

Fig. 3.51 Response surface graph for the interaction between light intensity and pH value at fixed depth of soil (0.2 cm) and initial conc. of IMI

The effect of soil depth (0.2-1cm) on degradation of IMI was also studied by plotting response surface plots with intensity of light (Fig. 3.52) and its initial concentration (Fig. 3.53). It has been observed that increase in the depth of soil render the degradation of IMI. This can be ascribed to the fact that required light cannot reach deep inside the soil and the necessary conditions for the photocatalytic degradation becomes absent in this part of soil, hence degradation decreases as the soil layer becomes thicker (Frank et al. 2002; Xu et al. 2011). Hence, the obtained experimental results yielding maximum degradation of 83% are found to be in agreement with the predicted response of 86% verified the validity of optimal point, indicating that CCD could be effectively used to optimize photocatalytic degradation of pollutants.

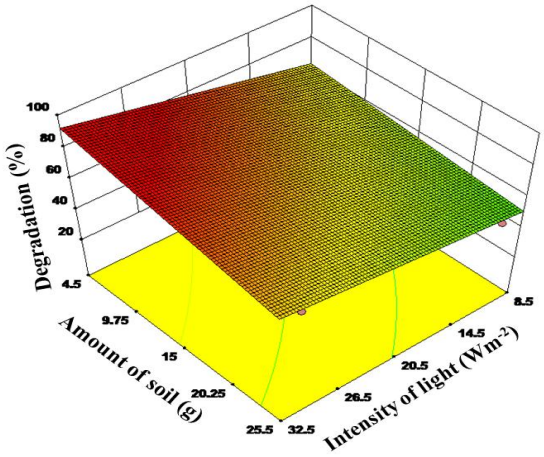

Fig. 3.52 Response surface graph for the interaction between depth of soil and initial imidacloprid concentration at fixed intensity of light 30 Wm^{-2} and pH = 3

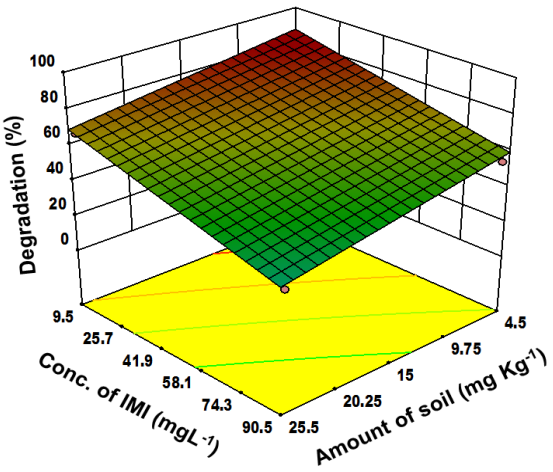

Fig. 3.53 Response surface graph for the interaction between depth of soil and initial imidacloprid concentration at fixed intensity of light 30 Wm^{-2} and pH = 3.

3.19 Degradation reaction mechanism under optimized conditions

In order to study the degradation mechanism of IMI under the optimized conditions, LC-MS analysis was carried out and compared to photolysis (Fig. 3.54 a&b). A clear contrast has been found for the LC chromatograms obtained for the photolysis and photodegradation of IMI. It can be clearly distinguished that the peak height of the IMI after 18 h of its photolysis was comparatively higher than that found after photodegradation of IMI. Moreover, some new peaks at R_t = 1.6, 1.9, 2.3 and 2.5 min have appeared for the sample after photodegradation while only peak at R_t = 1.6 min was found after photolysis sample. The various intermediate products identified by LC-MS analysis (Fig. 3.55-3.57) were compound B (R_t = 1.95min), C (R_t =1.63 min), D (R_t =2.09 min) and E (R_t =3.32 min).

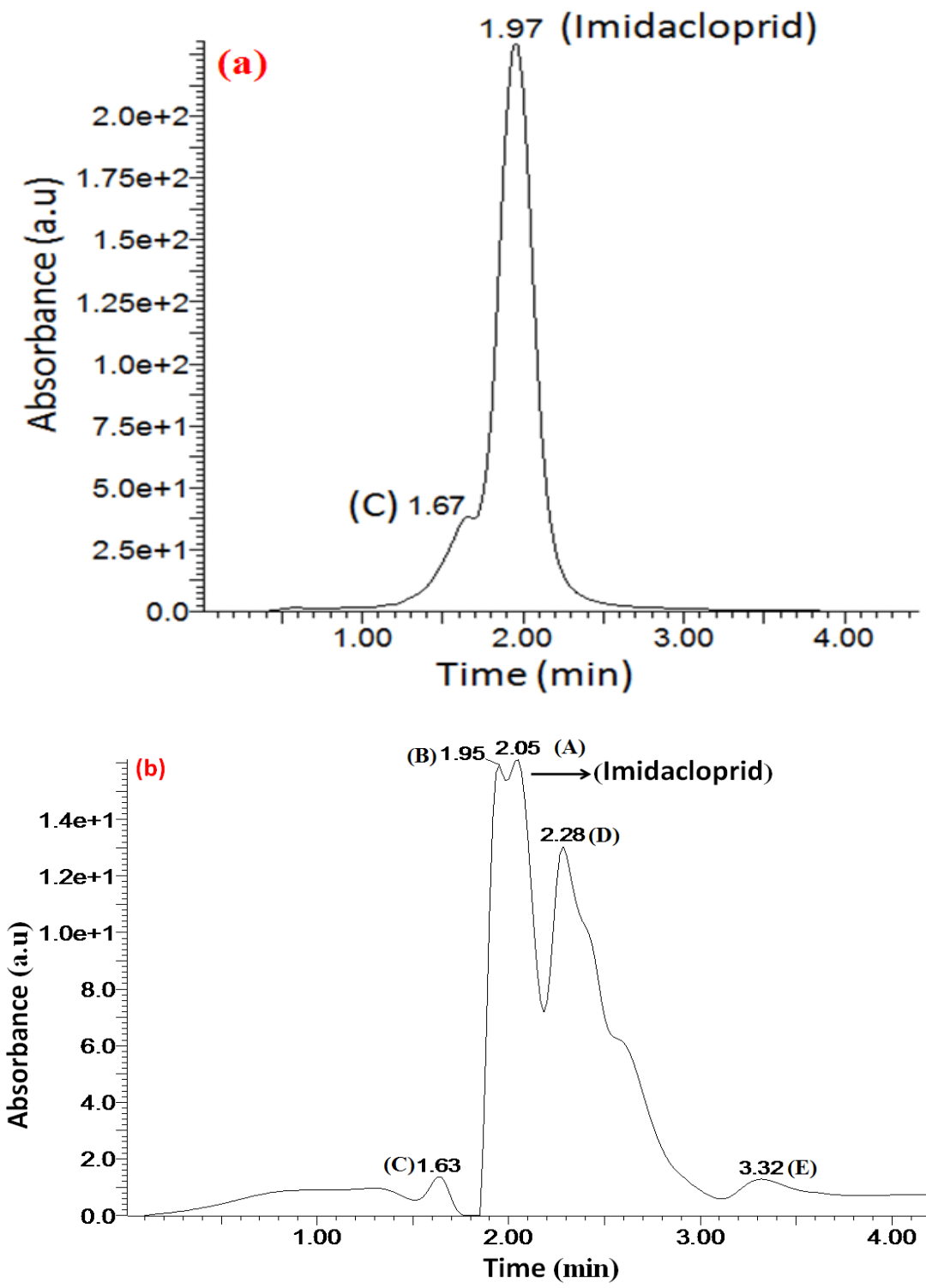

Fig. 3.54 LC Chromatogram of soil spiked with imidacloprid during (a) photolysis and (b) photocatalytic degradation after 18 h of UV irradiation

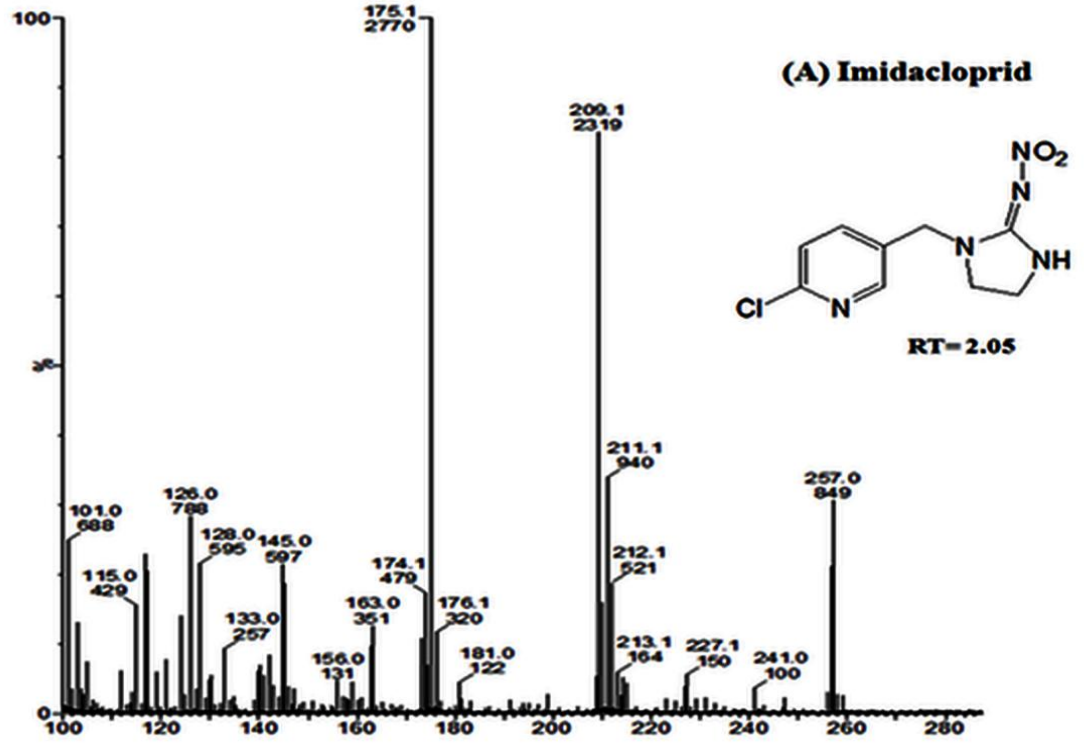

Fig. 3.55 Mass spectrum of standard imidacloprid (A); inset structural formula with its retention time (RT) as per LC chromatogram.

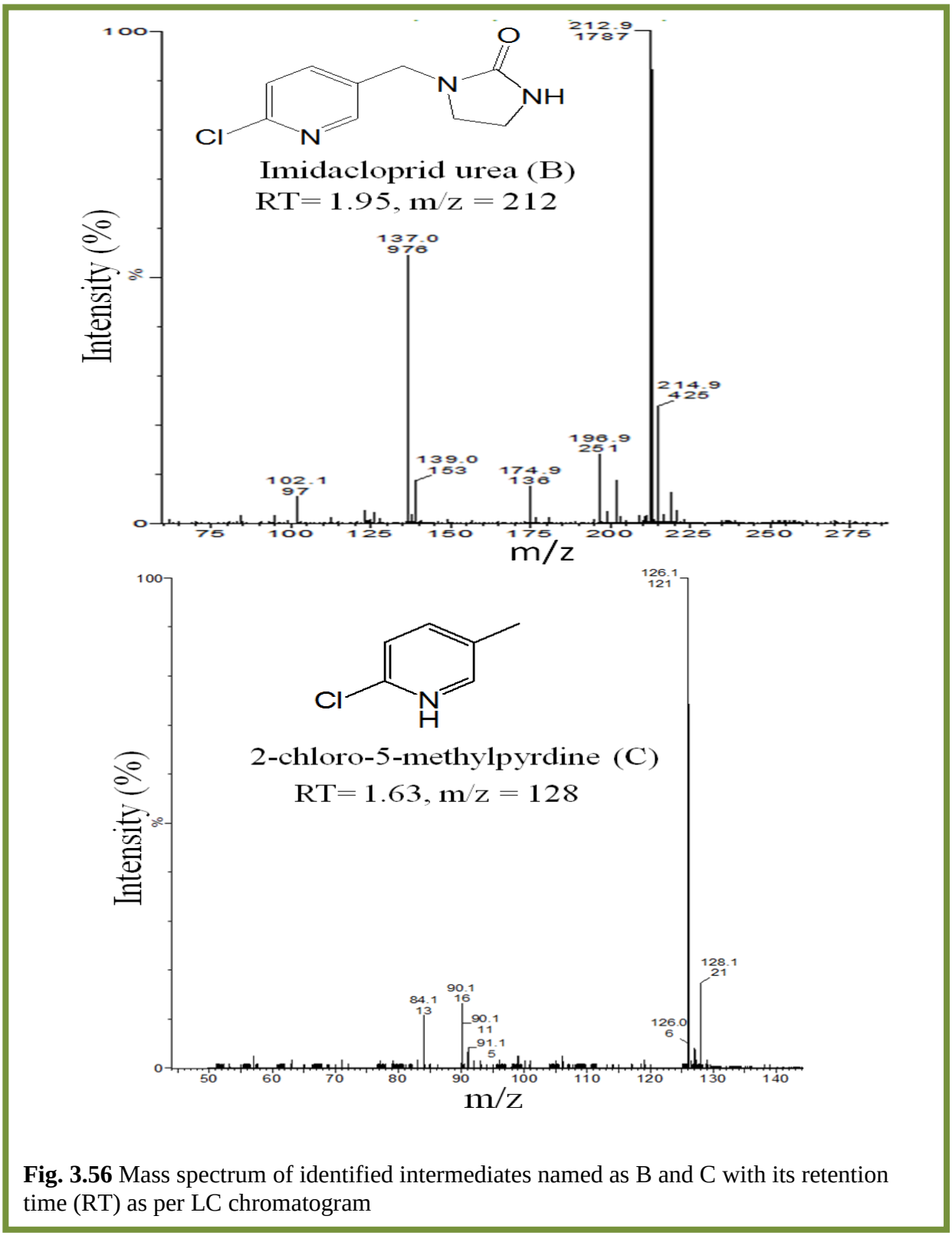

Fig. 3.56 Mass spectrum of identified intermediates named as B and C with its retention time (RT) as per LC chromatogram

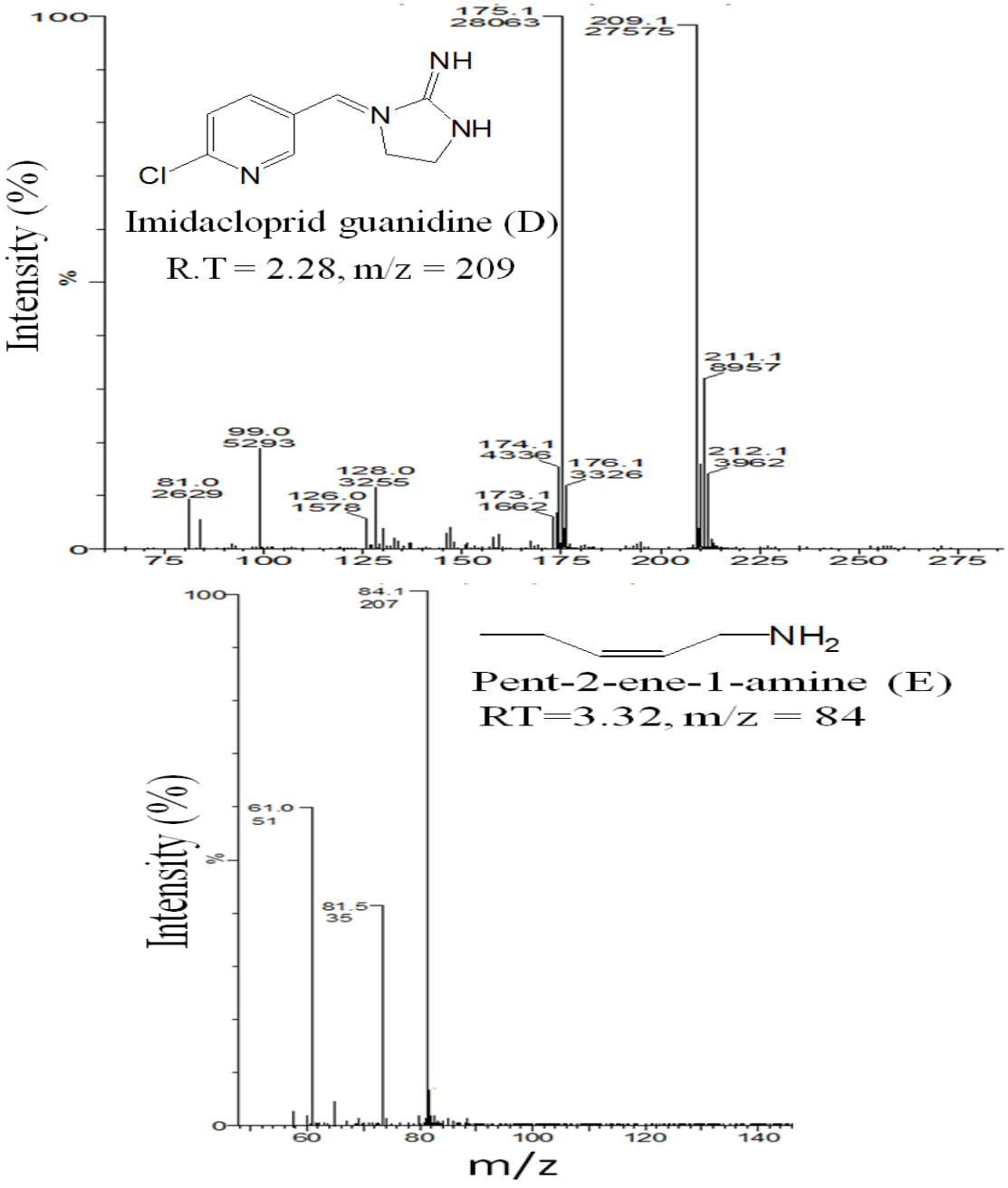

Fig. 3.57 Mass spectrum of identified intermediates named as D and E with its retention time (RT) as per LC chromatogram

The formation of these identified intermediates could be explained on the basis of proposed pathway (Fig. 3.58) suggested various possible attack positions by the hydroxyl radical at IMI. The preliminary attack of hydroxyl radicals at N-N in IMI expected to yield compound D which further degrade to compound E. The hydrolysis of IMI could resulted in the formation of intermediate compound B, which degraded to compound C via attack of hydroxyl radicals and was reported (Sharma et al., 2014) to be an intermediate product of IMI photooxidation. The formation of these identified intermediates during photolysis and photodegradation is in accordance to the previous reports (45) concerning the same in aqueous media.

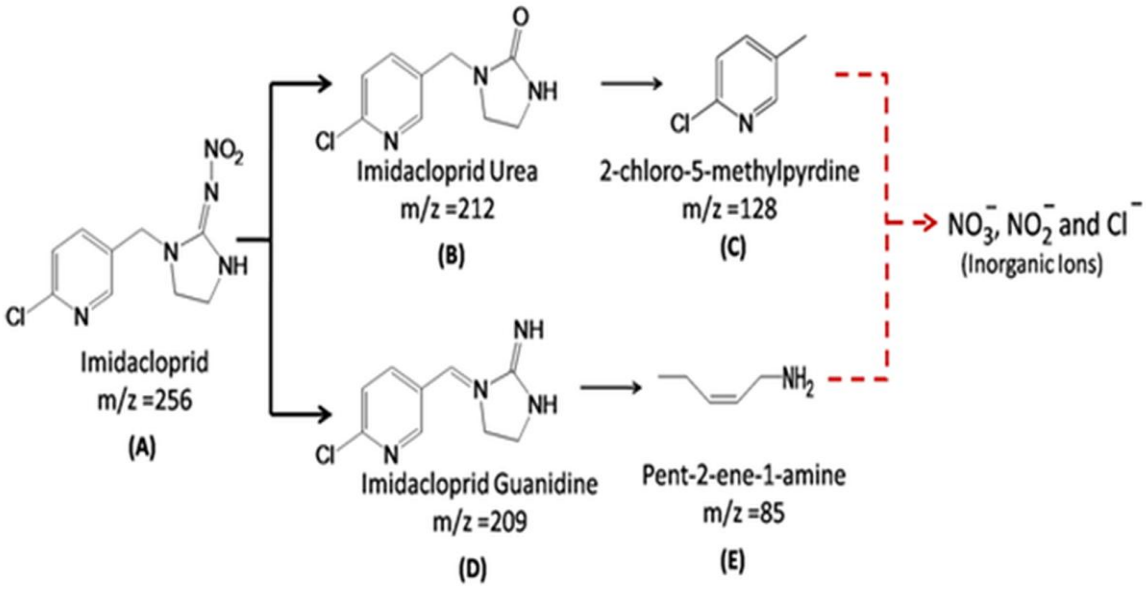

Fig. 3.58 Proposed pathway for the degradation of imidacloprid

3.20 Estimation of Inorganic ions

In order to confirm the mineralization of heteroatoms present in IMI to corresponding inorganic ions, ion chromatographic analysis was performed. It was observed that the amount of inorganic ions formed after 18h of photodegradation was notably higher than that found after photolysis of IMI, indication less mineralization in case of photolysis (Fig.3.59). The increases in formation of inorganic ions, with time of UV-light irradiation further confirmed the mineralization of IMI, during its photodegradation. The formulated (eq.3.4) balanced stoichiometric chemical equation for nitrate, nitrite and chloride ions during the photo degradation of IMI in present study found to deviate from the expected balance equation (eq. 3.5) after complete its degradation. The

existence of unidentified intermediates composing the heteroatoms accounts for the incomplete mineralization. The increase in the amount of nitrate ion formation with irradiation time is probably due to mineralization of the imidazole or pyridine-substituted ring(s). These results are in correlation with a previous study (Lhomme et al. 2007; Lambropoulou et al.2011) for the dissipation of cyrpoconazole and fenhexamid, where the nitrogen atoms present in the triazole moiety were found to decompose to nitrate and ammonium ions.

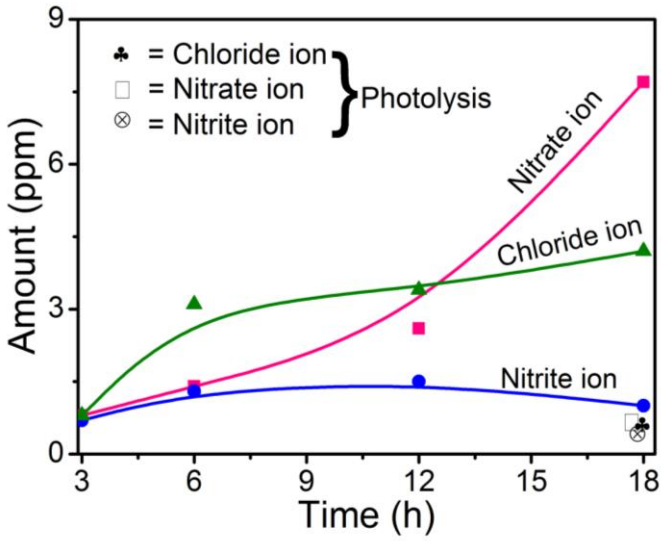

Fig. 3.59 Evolution of inorganic ions during photocatalytic degradation of imidacloprid

$$C_9H_{10}N_5O_2Cl + 3/2\ O_2 \xrightarrow[h\nu\ (18\ h)]{TiO_2} 0.10\ NO_2^- + 0.63\ NO_3^- + 0.57\ Cl^- + \text{Intermediate} \quad .....3.4$$

$$C_9H_{10}N_5O_2Cl + 33/2\ O_2 \longrightarrow 9\ CO_2 + 5\ NO_3^- + Cl^- + \text{Intermediate} \quad .....3.5$$

Thus, it is clear from these results that neither individual microbial degradation nor photocatalytic degradation has lead to the complete dissipation/mineralization of IMI in soil. Hence, another remediation strategy for destructive elimination of IMI and its metabolites from environment is required. An alternative for destructive removal of the IMI and its metabolites could be the microbial treatment combined with pre/post treatment of photocatalytic oxidation that could reduce its recalcitrant metabolites or improves its microbial degradation. In this context, both of these processes were coupled in two ways (i) microbial degradation followed by photocatalytic degradation (MP) and (ii) photocatalytic degradation followed by microbial degradation (PM), to achieve higher degradation of IMI in soil.

3.21 Sequential processes for degradation of imidacloprid

3.21.1 Photocatalytic-Microbial (PM) degradation

In this process the optimized conditions obtained from photocatalytic process (*section 2.2.10.5*) were used for degradation of IMI for 18 h. The soil obtained was further treated with strain ATA1 under the optimum conditions (*section 2.2.9.3*) and degradation of IMI was observed for 15 days.

During PM process (Fig. 3.60), it was observed that the initial decrease in residual amount of IMI taken place up to 18 h of photocatalytic degradation became almost stagnant during 15 d of microbial treatment. As it can be clearly visualized from Fig. 3.60a, the residual amount of IMI was calculated to be ~78% (11 mg L^{-1}) after photocatalytic degradation, served as control for microbial degradation. In microbial study, degradation of to ~ 86.2% (6.9 mgL^{-1}) was confirmed after 15 d of microbial degradation (Fig. 3.60b).

The time course UV-Vis absorption spectra (Fig. 3.61) for degradation of IMI during PM process showed that with increase in time of degradation, the peak corresponding to λ_{max} = 270 gradually decreases. A significant and noticeable decrease in peak height in comparison to standard IMI (absorbance = 1.9 a.u) has

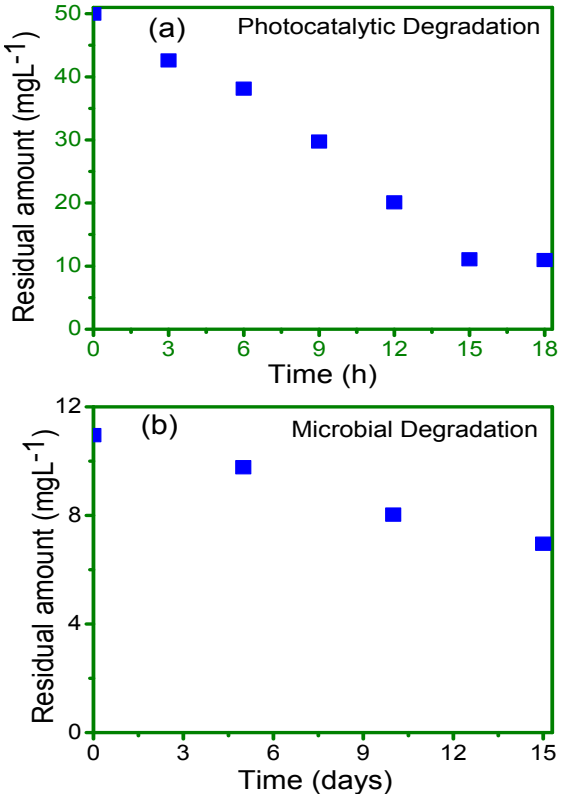

Fig. 3.60 Sequential process for degradation of IMI in soil by (a) photocatalytic degradation followed by (b) microbial degradation.

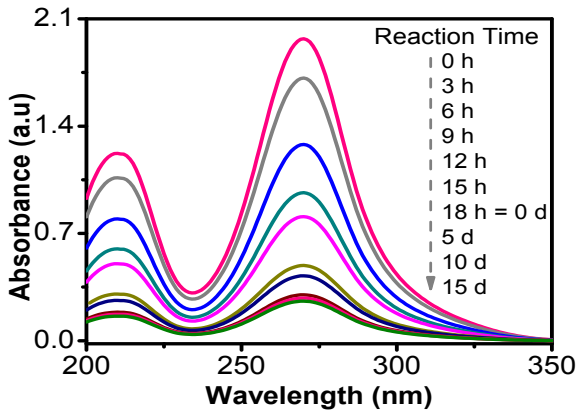

Fig. 3.61 Time course UV-vis spectra of imidacloprid (50 mg L^{-1}) during photocatalytic-microbial process

been taken place during 18 h of irradiation (0.48 a.u) and no notable change in peak height was found till 15 days (0.23 a.u) of microbial process.

3.21.2 Microbial-photocatalytic (MP) degradation

In MP process, degradation of IMI (50 mg kg^{-1}) was achieved by inoculating bacterial strain ATA1 for 15 days (section) and the same sample was further irradiated for 18 h for photocatalytic degradation under optimum conditions (section). It was observed that after 10 d of incubation, ~ 55.6% (22.2 mg L^{-1}) of IMI dissipated and became ~58.2 % (20.9 mg L^{-1}) after 15 d of microbial degradation (Fig. 3.62a). Afterwards, this amount (20.9 mg L^{-1}) served as the control of photocatalytic process (Fig. 3.62b) which was found to decrease significantly till 18 h of irradiation became 2.6 mg L^{-1} (~ 94.6 %).

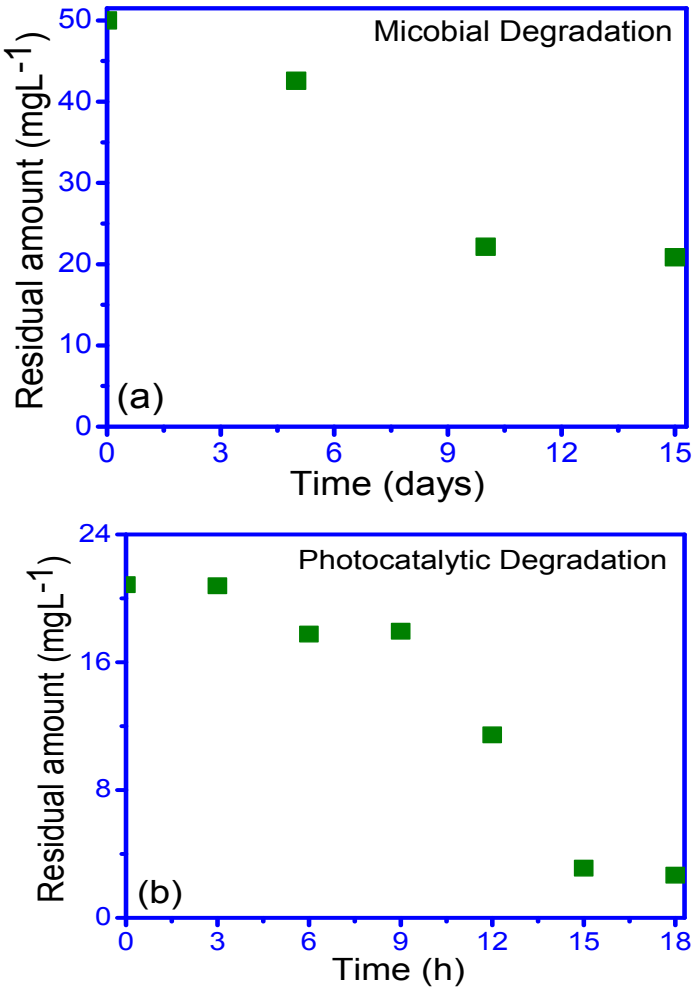

Fig. 3.62 Sequential process for degradation of IMI in soil by (a) Microbial degradation followed by (b) photocatalytic degradation

The UV-Vis. spectra (Fig.3.63) for MP process depicted decrease in peak height in comparison to standard IMI (absorbance = 1.9 a.u) after initial 5 d (0.93 a.u) that became almost constant till 15 d (0.81 a.u) of incubation. Thereafter, the photocatalytic degradation caused further decrease in peak height i.e., degradation.

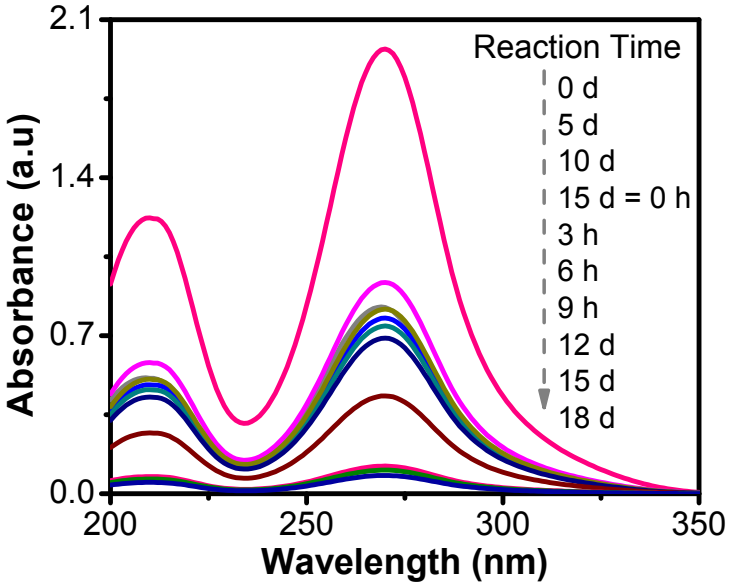

Fig. 3.63 Time course UV spectra of imidacloprid (50 mg L^{-1}) during Microbial- photocatalytic process

3.21.3 Comparison of photocatalytic-microbial and microbial-photocatalytic processes

Both the processes (PM & MP) were compared in terms of degradation and mineralization after 18 h + 15 d for PM and 15 d+ 18h for MP in the present study. Initially, residual amount of IMI for both were compared and it was concluded that among both of these processes, MP (degradation = 94.6%) process is better than PM process (degradation = 86.2%) by `~9%. This comparative high activity of MP process than PM process could be explained on the fact that, in PM process degradation of IMI by photodegradation could lead to the formation some intermediates that might be toxic to strain ATA1, resulting decrease in the enzymatic activity of microbes as the same was reported by the Jafari et al. (2011), Gonzalez et al. (2010) revealing reduction in activity of PM for the degradation of azo dye and chlorophenols, respectively. Another reason might be the higher concentration of IMI which did not favors the photocatalytic

process as pre-treatment for degradation and the same was supported by Suryaman et al. (2006), Balcioglu and Cecen (1999) and Li and Zhao (1999).

Although, the difference between the degradation efficiencies among these two processes seemed to be very small (~9%), yet was found to be very significant and supported by LC-MS analysis. It can be clearly seen in the LC chromatogram (Fig. 3.64) that the number of intermediates formed (corresponding to each peak) during MP process are almost double as compared to PM process. This further evidencing that MP process is better than PM process.

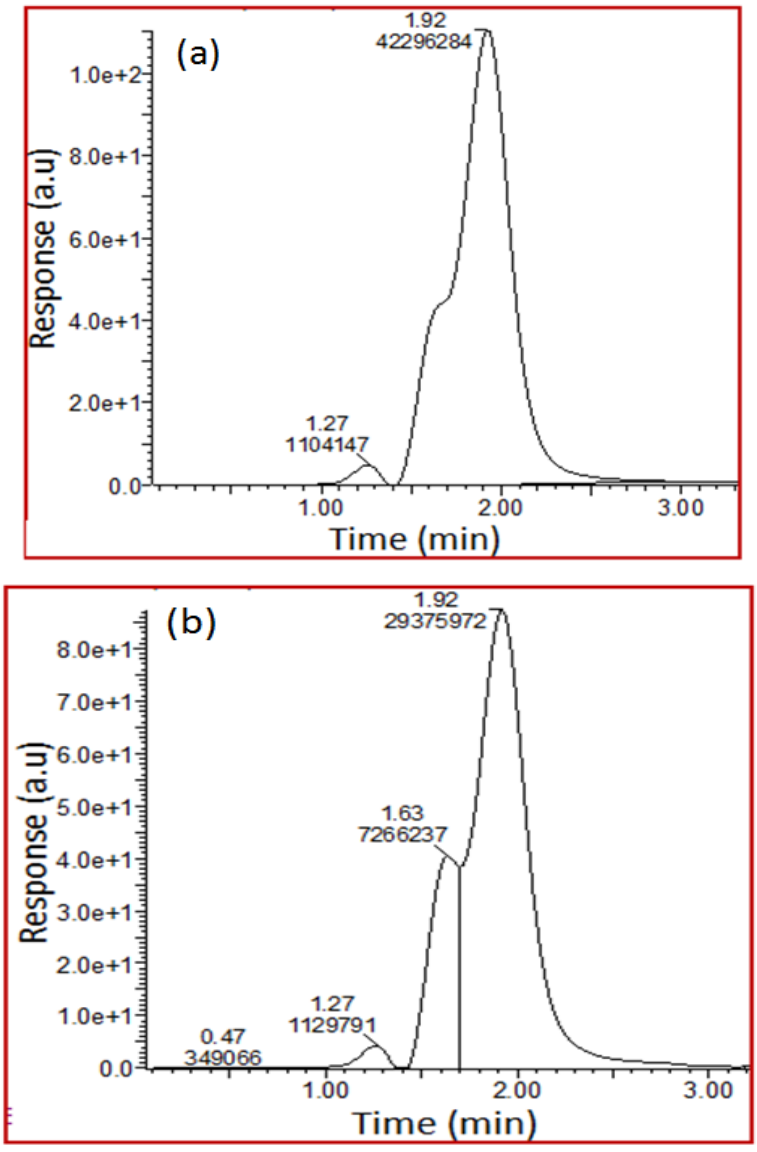

Fig 3.64 Sequential degradation of imidacloprid (50 $mgkg^{-1}$); (a) Photocatalytic-biological degradation at 18 h + 15 d time interval (b) Biological-photocatalytic degradation at 15 d+18 h time interval

In order to further support this, time course study of the intermediates was also carried out (Fig. 3.65). Among the identified intermediates two intermediates viz., I1 and I2 (Fig. 3.66) were found to be commonly formed during both of studied processes and were selected for this analysis. Since, the authentic samples for these intermediates were unavailable; therefore ratio of peak area at any time (Area $_{(t)}$)/maximum of peak area (Area $_{(max)}$) were plotted vs time. It was found that in MP process the amount of these two common intermediates (I1 & I2) maximized after initial 5 days of degradation and thereafter it reduced till 15 d + 18 h of incubation.

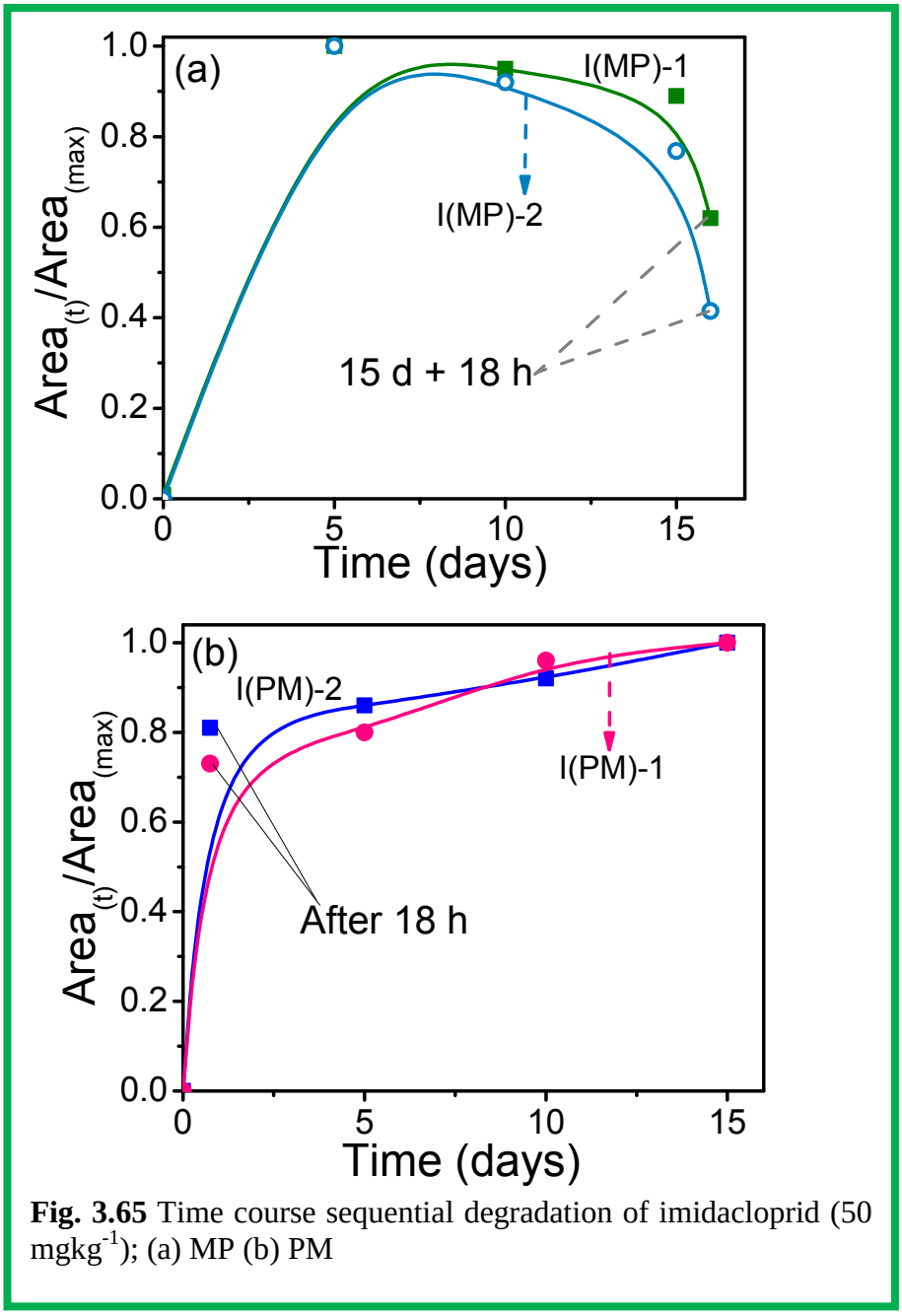

Fig. 3.65 Time course sequential degradation of imidacloprid (50 mgkg^{-1}); (a) MP (b) PM

However, in case PM process the formation of these intermediates continued until the maximum time (18 h + 15 d). These results clearly depicts that despite of insignificant increase in amount of degradation during the MP process a drastic change in-terms of number of intermediates produced and eventually their mineralization was observed conforming the superiority of this process as compared to PM .

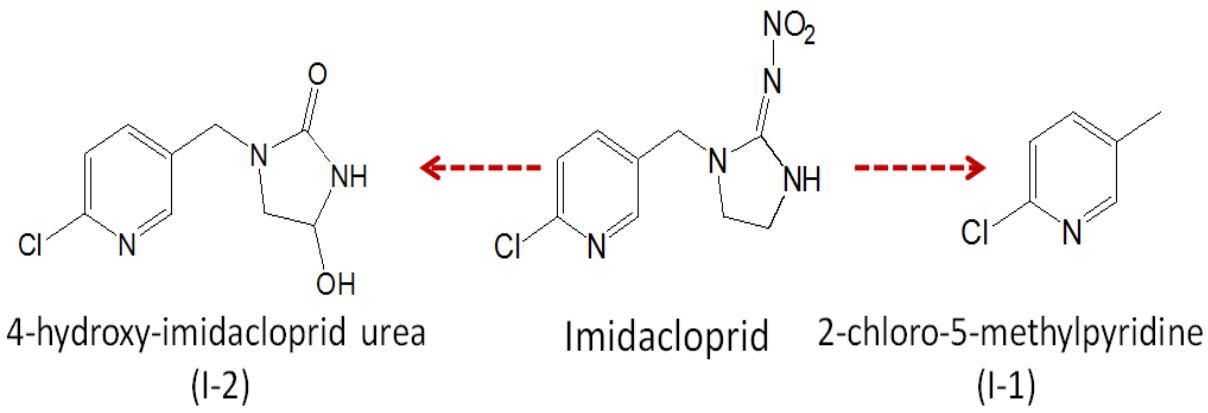

Fig. 3.66 Common identified intermediates of imidacloprid produced by MP and PM process

3.21.4 Comparison of degradation and mineralization (5th and 10th day) in Microbial-photocatalytic process

In MP process, residual amount of IMI after 10th (22.2 mgL^{-1}) and 15th (20.9 mgL^{-1}) day of biological degradation process were found to be not of any much difference. It was believed that same/better results could be obtained using photocatalytic process on 5th and 10th day instead of on 15th day of biological process. Thus, to verify this assumption, samples obtained after 5 d and 10 d were subjected to 18 h of photocatalytic degradation for IMI and obtained results are shown in Fig. 3.67. It was observed that the microbial degradation of IMI in

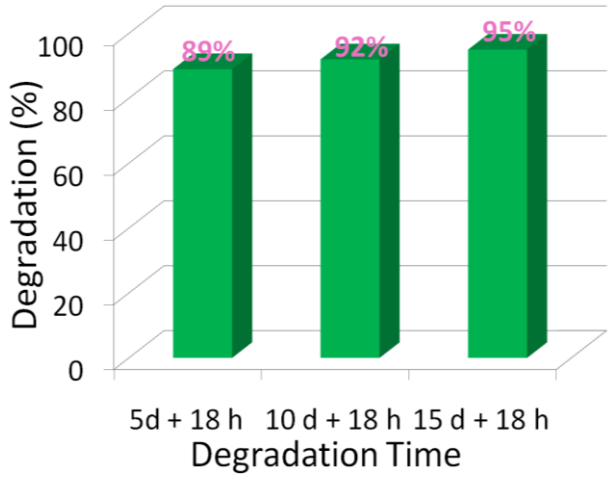

Fig. 3.67 Comparative degradation of IMI at various time intervals of MP Process

soil obtained after 5th day, 10th day, and 15th day was 89%, 92% and 95% respectively. The results showed that the difference in the final degradation after 5th /10th /15th day is not much which confirmed that the photocatalytic degradation cal be performed on the soil after 5th day of microbial degradation.

In order to verify these results, LC-MS (Fig. 3.68 a&b; Fig. 3.69-3.70) analysis was performed. It was found that only one intermediate was formed after 5 d + 18 h, whereas two intermediates in case of 10 d + 18h of reaction. Results from these two were compared with MP process of 15 d+ 18 h indicated later (15 d+18h) to be better than two processes (5 d + 18 h, 10 d + 18 h) where more than two intermediates were found to be formed.

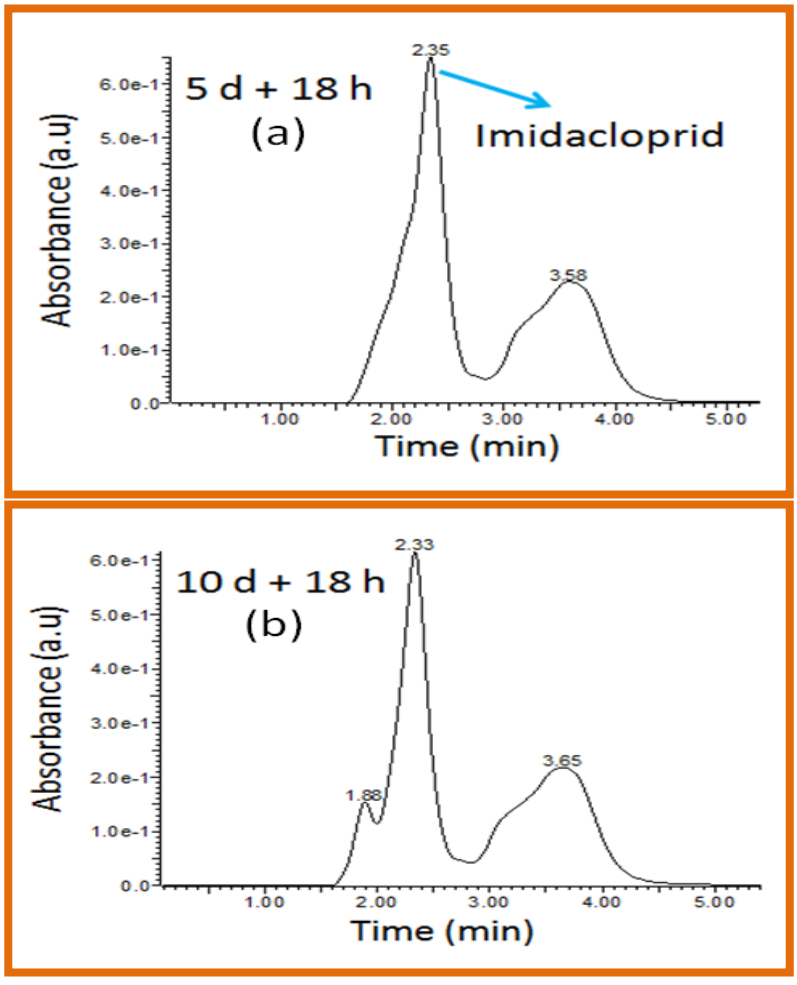

Fig. 3.68 LC chromatograms for degradation of imidacloprid in MP process obtained after (a) 5 d+18 h and (b) 10 d + 18 h

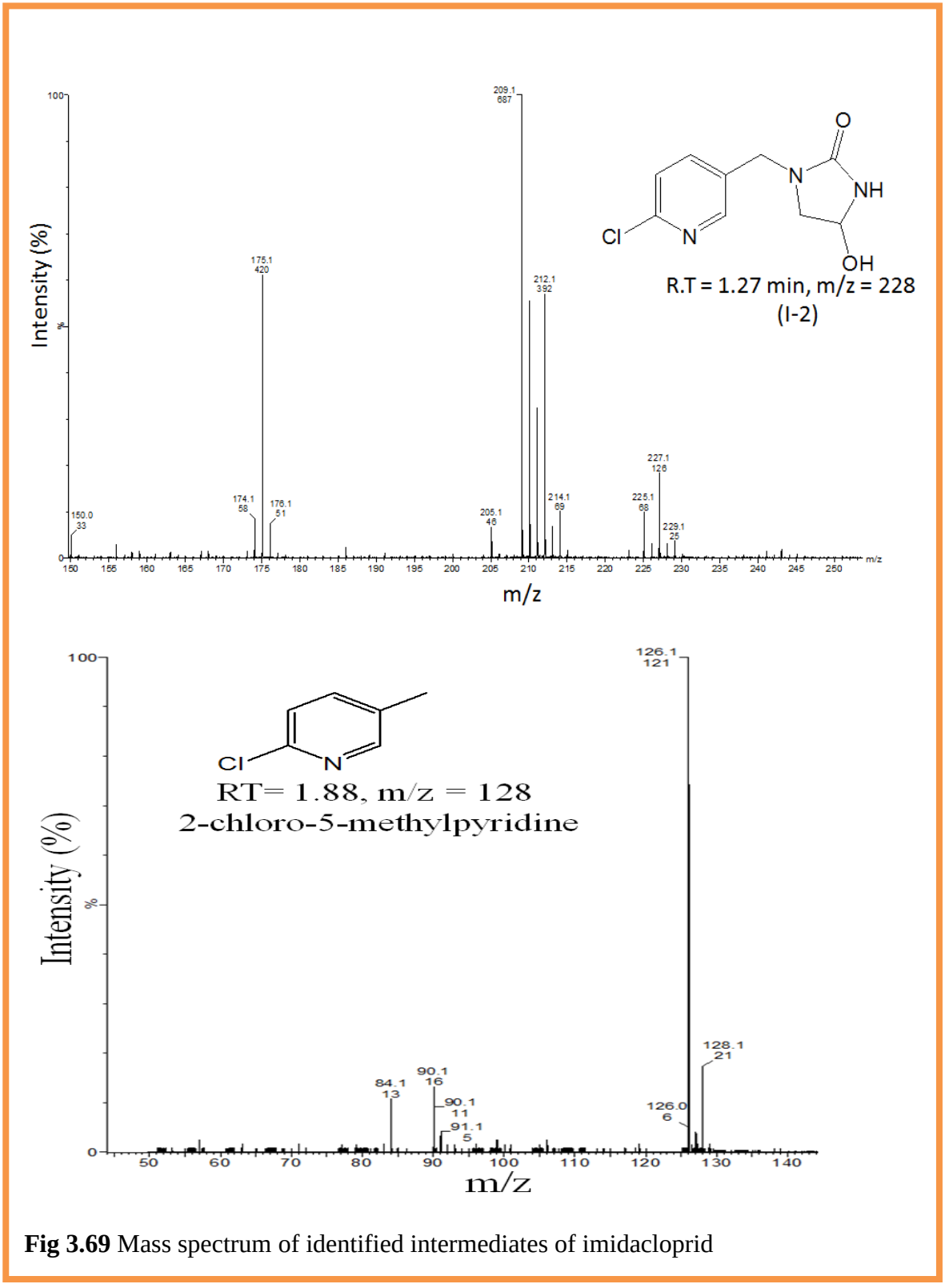

Fig 3.69 Mass spectrum of identified intermediates of imidacloprid

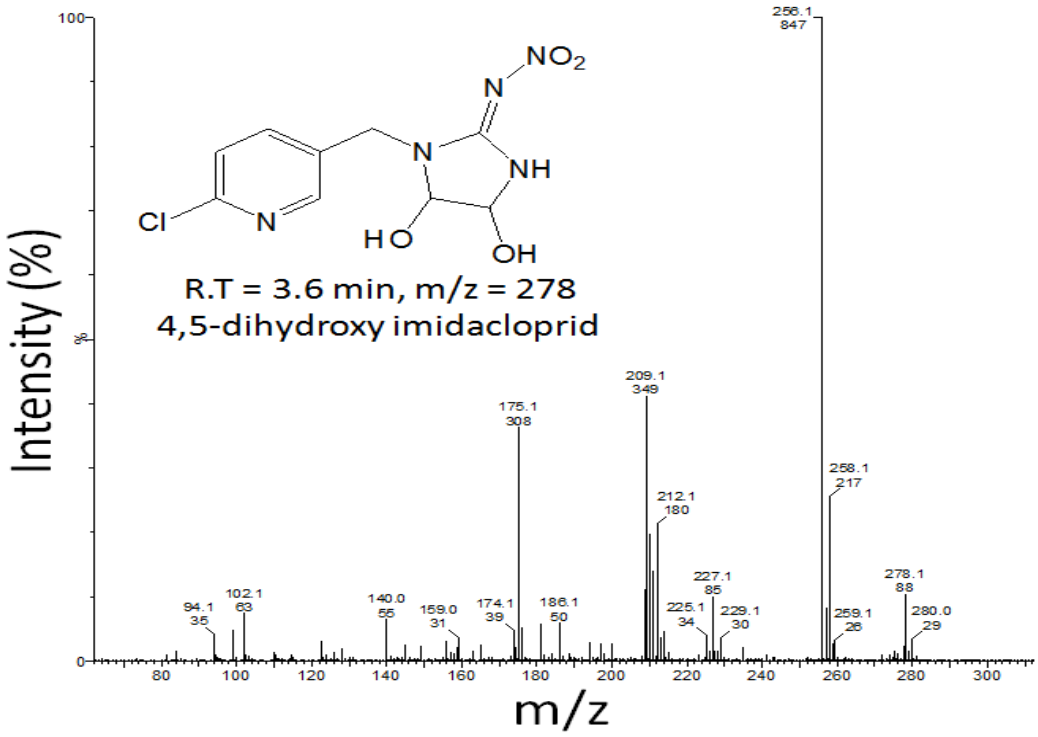

Fig 3.70 Mass spectrum of identified intermediates of imidacloprid

These above said results suggested that longer microbial process followed by photocatalytic process (18 h) can efficiently mineralizes the IMI and its intermediates. Hence, it can be concluded that although no notable difference after 5 d +18 h, 10 d + 18 h and 15 d + 18 h days of MP process was observed, yet the significant variation could be observed in terms of mineralization and truly signifies the removal of IMI from the soil.

CONCLUSIONS

In summary, the work aimed at examining the following objectives:

1. Isolation of neonicotinoid degrading bacteria from contaminated soil.
2. Optimization of conditions for maximum photocatalytic degradation using TiO_2.
3. Optimization of conditions for maximum degradation of pesticide by bacteria.
4. Studying sequential microbial-photocatalytic degradation of pesticide with optimum parameters.

The salient findings of above objectives are as follows:

Objective 1. Isolation of neonicotinoid degrading bacteria from contaminated soil

1. Five bacterial strains (T1-T5) were isolated initially on enrichment media (NB) containing 50 mgL^{-1} of IMI and secondary enrichment was done on minimal medium (50 mgL^{-1} of IMI) in order to study their efficiency for degradation of IMI.
2. Out of these five, strain T1 and T5 which exhibited the highest growth were further identified on the basis of morphological, biochemical, physiological characterization. Morphological and gram characteristics results revealed that both the strains were gram negative rods and showed the characteristics of member of *Enterobacter* species.
3. Molecular identification of both strain based upon 16S rRNA sequencing led to their characterization as *Enterobacter sp.* ATA1 and *Enterobacter sp.* ATA2, respectively.

Objective 2. Optimization of conditions for maximum degradation of pesticide by bacteria

1. The bacterial isolate *Enterobacter sp.* strain ATA1 selected for degradation of IMI was initially studied for its tolerance at various concentration of IMI (50-150 mgL^{-1}) as carbon source in minimal media. Growth of strain ATA1 was found to be more at IMI= 50 mgL^{-1} (absorbance = 0.028) as compared to 100 mgL^{-1} (absorbance = 0.019) and 150 mg L^{-1} (no growth) for 25 days of incubation.
2. Various carbon sources viz., Maltose, Sucrose, Fructose, Lactose and Glucose were used as co-metabolite to enhance growth and among these glucose (0.1% w/v) was observed to be effective carbon source than the others.

3. Under the optimized concentration of IMI (50 mgL^{-1}) in presence of glucose (0.1% w/v), co-metabolite degradation studies were performed in minimal media and it was found that degradation of ~ 45% achieved after 3 days of incubation. LC chromatogram analysis revealed decrease in peak height/peak area comparative to standard IMI (50 mgL^{-1}). Various new peaks were also appeared up to 15 days indicated the formation of intermediates/metabolites of IMI.
4. The identification of these intermediates was performed by their respective mass spectrum and concluded that disintegration of IMI takes place into imidacloprid urea (m/z = 212) and 4-hydroxy imidacloprid (m/z =271).
5. Microcosm study in the soil was performed under laboratory conditions for optimization of various parameters (pH, inoculums size, initial concentration of imidacloprid and flooding of soil) and concluded highest degradation (68%) was percieved at pH = 7 after 15 days of incubation.
6. Results obtained from effect of initial concentration of IMI (25-100 mg $kg^{-1}$of IMI) at pH = 7 showed that 50 $mgkg^{-1}$ of IMI lead to better degradation (74%) and hence considered as optimum. These results are supported by GC-MS chromatograms that have shown peak height/peak area for IMI is least while using its concentartion = 50 $mgkg^{-1}$, revealed it to be an optimum amount.
7. Effect of inoculum size on the degradation of IMI confirmed maximum degradation of IMI (74%) at 2×10^7 cfu g^{-1} soil. These results were found to correspond with the GC-MS chromatograms indicating 2×10^7 cfu g^{-1} to be an optimum inoculum size.
8. Influence of flooding/non-flodding conditions for maximum degradtion of IMI at optimized conditions of pH = 7, IMI concentartion = 50 $mgkg^{-1}$, inoculum size= 2×10^7 cfu g^{-1} soil was studied and it was found that IMI was degraded more efficiently in non-flooded (60%) conditions as compared to flooded (50%).

Objective 3. Optimization of conditions for maximum photocatalytic degradation using TiO_2

1. Photolysis and adsorption studies in soil confirmed that change in the concentration of IMI was not significant when kept under dark for 18 h. Soil having IMI when irradiated

with UV-light in presence of TiO_2 (0.1- 0.5gkg^{-1}), degradation increased with increase in photocatalyst doses and an amount of 0.3 gkg^{-1} TiO_2 was found to be an optimum.

2. Optimization of four experimental parameters (UV light intensity, initial conc. of IMI, pH, and depth of soil) was carried out using central composite design (CCD) based on response surface methodology (RSM). The 30 experiments obtained by Design-Expert Software (trial version 9.0.3.1, Stat-Ease, Inc., MN, USA) were performed on laboratory scale and the obtained results have been plotted for –ln(C/Co) vs. Time.
3. For all the experiments plots were straight line with R^2 = 0.993 to 0.974, indicated that degradation of IMI under the specified conditions follows the L-H kinetics and pseudo first-order kinetics.
4. Highest value of apparent rate constant (k) 15×10^{-4} min^{-1} was observed at pH = 3, intensity of light = 30 Wm^{-2} and initial IMI = 10 mgL^{-1}, followed by 9.3×10^{-3} min^{-1}, revealed the former as an optimum conditions for photocatalytic degradation of IMI in soil. It has also been found that amount of IMI photo-catalytically degraded (83%) complied with the theoretically determined (86%), not only for the optimized conditions but for all the experiments.
5. Adequacy and significance of the studied model was verified by applying ANNOVA test. The probability value (P) for A (pH) and D (concentration of IMI) were very low (<0.0001) in comparison to other parameters B (intensity of light) and C (depth of soil). The response factor of calculated residual values showed that all data points lie close to straight line and within 95% confidence intervals line with mean values near zero confirming the good correlation between experimental and predicted values.
6. Moreover, identification and probable mechanism involved for the formation of various intermediates with quantitative estimation of various ions (nitrate, nitrite, and chloride) was also carried out. Based upon the results obtained, a probable mechanism for conversion of one intermediate into another during decomposition of imidacloprid, and a stoichiometric mass balanced equation were being proposed.

Objective 4. Studying sequential microbial-photocatalytic degradation of pesticide with optimum parameters

1. In sequential studies, it was found that residual amount of IMI after 15 day + 18 h of degradation in microbial-photocatalytic process(MP) was ~2.6 mgL^{-1} (96%) significantly lower than that found in photocatalytic-microbial process (PM) ~7.0 mgL^{-1} (87%) confirming betterment of former process.
2. The results were verified by time course analysis of common metabolite (m/z = 128 & 228) found from both processes and it was observed that in case of MP process the metabolites becomes highest of their concentration and thereafter started degrading or inter-converting into other compounds. However, for PM process an opposite has been observed where the formation of these intermediates continues till 15 d + 18 h of degradation. These results confirmed that MP process was superior to the PM process.
3. For optimum degradation time for mineralization of IMI, samples obtained after 5^{th} and 10^{th} day of microbial degradation were subjected to the photocatalytic degradation under similar conditions and were analyzed for LC-MS spectrum. It was confirmed that more number of metabolites were formed (reflected by number of peaks) after 15 d + 18 h of degradation in relation with 5 d + 18 h and 10 d + 18 h. This clearly suggested that time of 15 d + 18 h is optimum for mineralization of IMI under the conditions specified in present study.

REFERENCES

Adams CD, Kuzhikanni JJ (2000). Effect of UV/H_2O_2 preoxidation on the aerobic biodegradability of quaternary amine surfactants. Water Research; 34:668–672.

Ahmed N, Kanan H, Inanaga S, Ma Y, Sugimoto Y (2001). Impact of pesticide seed treatments on aphid control and yield of wheat in the Sudan. Crop Protection; 20: 929–934.

Aislabie J, Jones GL (1995). A review of bacterial-degradation of pesticides. Australian Journal of Soil Research; 33:925–942.

Alexander M (1965). Biodegradation: problems of molecular recalcitrance and microbial fallibility. Advanced Applied Microbiology; 7:35–80.

Alletto L, Benoit P, Bergheaud V, Coquet Y (2008). Temperature and water pressure head effects on the degradation of the diketonitrile metabolite of isoxaflutole in a loamy soil under two tillage systems. Environmental Pollution; 156:678–688.

Alletto L, Coquet Y, Benoit P, Heddadj D, Barriuso E (2010). Tillage management effects on pesticide fate in soils: A review. Agronomy for Sustainable Development; 30:367–400.

Alsayeda H, Pascal-Lorber S, Nallanthigal C, Debrauwer L, Laurent F (2008). Transfer of the insecticide [14C] imidacloprid from soil to tomato plants. Environmental Chemistry Letters; 6: 229–234.

Amat AM, Arques A, Beneyto H, Garcia A, Miranda MA, Segui S (2003). Ozonisation coupled with biological degradation for treatment of phenolic pollutants: a mechanistically based study. Chemosphere; 53:79–86.

An T, An J, Yanga H, Li G, Feng X, Nie X (2011). Photocatalytic degradation kinetics and mechanism of antivirus drug-lamivudine in TiO_2 dispersion. Journal of Hazardous Materials; 197: 229–236.

Andreozzi R, Caprio V, Insola A, Martota R (1999). Advanced oxidation processes for water purification and recovery. Catalysis Today; 53:51–59.

Aneja K R (2003). Experiments in microbiology, plant pathology and biotechnology, New age international (p) Ltd. Publishers (4^{th} ed.), New Delhi.

Anhalat J, Moorman T, Koskinen W (2007). Biodegradation of imidacloprid by an isolated soil microorganism. Journal of Environmental Science and Health, Part B; 42: 509–514.

Anipsitakis GP, Dionysiou DD (2003). Degradation of organic contaminants in water with sulfate radicals generated by the conjunction of peroxymonosulfate with cobalt. Environmental Science and Technology; 37:4790–4797.

Anipsitakis GP, Dionysiou DD (2004). Radical generation by the interaction of transition metals with common oxidants. Environmental Science and Technology; 38:3705–3712.

Arancibia C, Bandala ER, Estrada C (2002). Radiation absorption and rate constants for carbaryl photocatalytic degradation in a solar collector. Catalysis Today; 76:149 – 159.

Arriaga FM, Esplugas S, Gimenez J (2010). Degradation of the emerging contaminant ibuprofen in water by photo-Fenton. Water Research; 44:589–595.

Asahi R, Morikawa T, Ohwaki T, Aoki K, Taga Y (2001). Visible-light photocatalysis in nitrogen-doped titanium dioxides. Science; 293:269–271.

Asghar MN, Ashfaq M, Ahmad Z, Khan IU (2006). 2-D PAGE analysis of pesticide-induced stress proteins of E. coli. Analytical and Bioanalytical Chemistry; 384: 946–950.

ASTM Standard D2434-68 (2006). Standard Test Method for Permeability of Granular Soils (Constant Head) ASTM International, West Conshohocken, PA, DOI: 10.1520/D2434-68R06, www.astm.org.

Awasthi N, Ahuja R, Kumar A (2000). Factors influencing the degradation of soil-applied endosulfan isomers, Soil Biology and Biochemistry; 32: 1697–1705.

Accinelli C, Screpanti C, Vicari A (2005). Influence of flooding on the degradation of linuron, isoproturon and metolachlor in soil; Agronomy for Sustainable Development; 25 : 401–406.

Badriyha BN, Song W, Ravindran V, Pirbazari M (2007). Advanced oxidation processes for destruction of endocrine disrupting chemicals in water treatment: Comparison of free-radical reaction mechanisms, pathways and kinetics. 2007 AIChE Annual Meeting.

Bahnemann D (2004). Photocatalytic water treatment: solar energy applications. Solar Energy; 77: 445–459.

Bajeer MA, Nizamani SM, Sherazi STH, Bhanger MI (2012). Adsorption and leaching potential of imidacloprid pesticide through alluvial soil. American Journal of Analytical Chemistry; 3: 604–611.

Balcioglu IA, Cecen F (1999). Treatability of kraft pulp bleaching wastewater by biochemical and photocatalytic oxidation. Water Science and Technology; 40:281–288.

Balmer ME, Goss KU, Schwarzenbach RP (2000). Photolytic transformation of organic pollutants on soil surfaces-an experimental approach. Environmental Science and Technology; 34:1240–1245.

Bandala ER, Dominguez Z, Rivas F, Gelover S (2007b). Degradation of atrazine using solar driven Fenton-like advanced oxidation technologies. Journal of Environmental Science and Health Part B; 42:21–26.

Bansal OP (2010). The Effects of Composts on Adsorption- Desorption of three carbamate pesticides in different soils of aligarh district. Journal of Applied Sciences & Environmental Management; 14:155–158.

Battu RS, Singh B, Kang BK (2004). Contamination of liquid milk and butter with pesticide residues in the Ludhiana district of Punjab state, India. Ecotoxicology and Environmental Safety; 59, 324–331.

Bayer Corp. (1998). Imidacloprid memo to U.S. EPA. June 5, 1998.

Beltran FJ (2004). Ozone reaction kinetics for Water and wastewater systems. Lewis Publishers.New York, USA.

Beltran FJ, Garcia AJF, Frades J, Alvarez P, Gimeno O (1999). Effects of single and combined ozonation with hydrogen peroxide or UV radiation on the chemical degradation and biodegradability of debittering table olive industrial wastewaters. Water Research; 33:723–732.

Bending GD, Lincoln SD, Sorensen SR, Morgan JAW, Aamand J, Walker A (2003). In-field spatial variability in the degradation of the phenyl-urea herbicide isoproturon is the result of interaction between degradative Sphingomonas sp. and soil pH. Applied and Environmental Microbiology; 69: 827–834.

Benitez FJ, Acero JL, Gonzalez T, Garcia J (2001). Ozonation and biodegradation process in batch reactors treating black table olive washing wastewater. Industrial Engineering and Chemistry Research; 40:3144–3151.

Benitez FJ, Beltran-Heredia J, Gonzalez T, Real F (1995). Photooxidation of carbofuran by a polychromatic UV irradiation without and with hydrogen peroxide. Industrial and Engineering Chemistry Research; 34: 4099–4105.

Bernardini C, Cappelletti G, Dozzi MV, Selli E (2010). Photocatalytic degradation of organic molecules in water: Photoactivity and reaction paths in relation to TiO_2

particles features. Journal of Photochemistry and Photobiology A Chemistry; 211: 185–192.

Black CA, Evans DD, White JL, Ensmingher LE, Clarke FE, Dinauer RC (1965). Methods of Soil Analysis Part 1-Physical and Mineralogical Properties Including Statistics of Measurement and Sampling, 9 Series Agronomy. American Society of Agronomy, Inc. Madison, Wisconsin, USA.

Blake DM (2000). Bibliography of work on the photocatalytic removal of hazardous compounds from water and air. Update number 3 to January 1999. National Technical Information Service. US Dept. of Commerce. Springfield, USA.

Blanco J, Malato S (2003). Solar Detoxification. UNESCO Publishing, ISBN 92-3-103916-4, France.

Blanco J, Fernandez P, Malato S (2007). Solar photocatalytic detoxification and disinfection of water: Recent overview. Journal of Solar Energy Engineering; 129:4–15.

Bollag JM, Liu SY (1990). Biological transformation processes of pesticides. In H.H. Cheng (ed.) Pesticides in the soil environment: Processes, impacts, and modeling. SSSA Book Ser. 2. SSSA, Madison, WI; 169-211.

Bolton JR (2001). Ultraviolet applications Handbook. Bolton Photosciences Inc. Ontario, Canada.

Brenner DJ, Mcwhorter AC, Arnold AK, Steigerwalt G, Farmer JJ (1986). *Enterobacter asburiae* sp. nov., a New species found in clinical specimens, and reassignment of erwinia dissolvens and erwinia nimipressuralis to the genus *Enterobacte*r as *Enterobacter dissolvens comb. nov.* and *Enterobacter nimipressuralis comb*. nov. Journal of Clinical Microbiology; 1114–1120.

Buchel KH (1983). Chemistry of Pesticides, John Wiley & Sons, Inc. New York, USA.

Cappuccino JG, Sherman N (1999). Microbiology: A laboratory manual (4th edition) Addison-Wesley Longman, Inc.

Capri E, Camisa MG, Cespedes FF, Glass CR, Pradas EG, Trevisan M (2001). Imidacloprid and pyrimethanil soil sorption. Agronomie; 2:5764.

Carey H (1990). An introduction to AOPs for destruction of organics in wastewater, In: Proceedings of the symposium on oxidation processes treatment contamination. Water Air Wastewater Technology Centre Adv. Paper No. 1, Burlington, Ontario, 13.

Carey JH, Lawerence J, Tosine HM (1976). Photodechlorination of PCB's in the presence of titanium dioxide in aqueous suspensions. Bulletin of Environmental Contamination and Toxicology; 16:697–701.

Casero I, Sicilia D, Rubio S, and Perez-Bendito D (1997). Chemical degradation of aromatic amines by fenton's reagent. Water Research; 31:1985–1995.

Cernigoj U, Stangar U L, Trebse P (2007). Evaluation of a novel Carberry type photoreactor for the degradation of organic pollutants in water. Journal of Photochemistry and Photobiology A Chemistry; 188:169–176.

Cernigoj U, Stangar UL, Trebse P, Ribic PR (2006). Comparison of Different Characteristics of TiO2 Films and Their Photocatalytic Properties. Acta Chimica Slovenica; 53:29–35.

Chahal, KK, Singh B, Kang BK, Battu RS, Joia BS (1997). Insecticide residues in farmgate vegetable samples in Punjab. Pesticide Research Journal; 9: 256–260.

Chan CY, Tao S, Dawson R, Wong PK (2004). Treatment of atrazine by integrating photocatalytic and biological processes**.** Environmental Pollution; 131:45–54.

Chen S, Alexander M (1989). Reasons for the acclimation of 2, 4-D biodegradation in lake water, Journal of Environmental Quality: 18: 153–156.

Chen X, Mao SS (2007). Titanium dioxide nanomaterials: synthesis, properties, modifications, and applications. Chemical Reviews;107:2891–2959.

Chiron S, Fernandez A, Rodriguez A, Calvo EG (2000). Pesticide chemical oxidation: State-of-the-art. Water Research; 34:366 –377.

Chopra SL, Kanwar JS (1991). Analytical agricultural chemistry. Kalyani Publishers, New Delhi; 309-310.

Choudhury PP, Dureja P (1997). Studies on photodegradation of chlorimuron-ethyl in soil. Journal of Pesticide Science; 51:201–205.

Coleman H M, Vimonses V, Leslie G, Amal R (2007). Removal of contaminants of concern in water using advanced oxidation techniques. Water Science & Technology 55; 12: 301-306.

Comeau Y, Greer CW, Samson R (1993). Role of inoculums preparation and density on the bioremediation of 2, 4-D contaminated soils, Applied Microbiology and Biotechnology; 38: 681–687.

Cox L, Hermosin MC, Koskinen WC, Cornejo J (2001). Interactions of imidacloprid with organic-and inorganic-exchanged smectites. Clay Minerals; 36: 267–274.

Corpet F (1988). Multiple sequence alignment with hierarchical clustering. Nucleic Acids Research; 16:10881–10890.

Cox L, Koskinen WC, Celis R, Yen PY, Hermosin MC, Cornejo J (1998a). Sorption of imidacloprid on soil clay mineral and organic components. Soil Science Society of America Journal; 62:911–915.

Cox L, Koskinen WC, Yen PY (1998b). Changes in sorption of imidacloprid with incubation time. Soil Science Society of America Journal; 62:342–347.

Craigmill AL, Winterlin WL (1985). Pesticide wastewater disposal: Biological Methods, In Proceedings of the National Workshop on Pesticide Waste Disposal. 54–59.

Deshpande NM, Sarnaik SS, Paranjpe SA, Kanekar PP (2004). Optimization of dimethoate degradation by *Brevundimonas* sp. MCM B-427 using factorial design: studies on interactive effects of environmental factors. World Journal of Microbiology and Biotechnology; 20: 455–462.

Devi LG, Murthy BN (2009). Structural characterization of Th-doped TiO_2 photocatalyst and its extension of response to solar light for photocatalytic oxidation of oryzalin pesticide: A comparative study. Central European Journal of Chemistry; 1:118–129.

Dieckmann Y, Christian F, Ishaque M, Kerl W, Kohle H (2010a). Agrochemical formulations comprising co-polymers based on ethylenically unsaturated dicarboxylic mono and diesters. Patent No. US 2010/0063167 A1: 1–14.

Digrak M, Kazanici F (2001). Effect of some organophosphorus insecticides on soil microorganisms. Turkish Journal of Biology; 25: 51–58.

Domenech X, Jardim WF, Litter MI (2004). Advanced oxidation processes for contaminant removal. In: Contaminants removal by heterogeneous photocatalysis, Blesa M.A., Sanchez B. (Ed). Editorial CIEMAT, Madrid, Spain (In Spanish).

Dong D, Li P , Li X , Zhao Q, Zhang Y, Jia C, Li P (2010). Investigation on the photocatalytic degradation of pyrene on soil surfaces using nanometer anatase TiO_2 under UV-irradiation. Journal of Hazardous Materials; 174: 859–863.

Doong R, Chang W (1997). Photoassisted titanium dioxide mediated degradation of organophosphorus pesticides by hydrogen peroxide. Journal of Photochemistry and Photobiology A Chemistry; 107:239–244.

Drum C (1980). Soil Chemistry of Pesticides, PPG Industries, Inc. USA.

Duetz WA, Marques S, de-Jong C, Ramos JL, Van-Andel JG (1994). Inducibility of the TOL catabolic pathway in *Pseudomonas putida* (pWW0) growing on succinate in

continuous culture: Evidence of carbon catabolite repression control. Journal of Bacteriology; 176:2354-2361.

Elbert A, Buchholz A, Ebbinghaus KU, Erdelen C, Nauen R, Schnorbach HJ (2001). The biological profile of thiacloprid – A new chloronicotinyl insecticide. Pflanzenschutz-Nachrichten Bayer (English edition); 54: 185–208.

Emmanuelle V, Chovelon JM, Guillard C, Herrmann JM (2003). Factors influencing the photocatalytic degradation of sulfonyurea herbicides by TiO_2 aqueous suspension. Journal of Photochemistry and Photobiology A Chemistry; 159:71–79.

Esplugas S, Contreras S, Ollis DF (2004). Engineering aspects of the integration of chemical and biological oxidation: simple mechanistic models for the oxidation treatment. Journal of Environmental Engineering; 9:967–974.

Estevez MA, Periago EL, Carballo EM, Gandara JS, Mejuto JC, Rio LG (2008). The mobility and degradation of pesticides in soils and the pollution of groundwater resources. Agriculture, Ecosystems and Environment; 123: 247–260.

Felsot AS, Racke KD, Hamilton DJ (2003). Disposal and degradation of pesticide waste. Reviews of Environmental Contamination and Toxicology; 177:123–200.

Feng C, Xu G, Liu X (2013). Photocatalytic degradation of imidacloprid by composite catalysts $H_3PW_{12}O_{40}$/La-TiO_2. Journal of Rare Earths; 31:44–48.

Fernandez BJD, Nogales R, Romero E (2007). Improved retention of imidacloprid (Confidor ((R))) in soils by adding vermicompost from spent grape marc. Science of the Total Environment; 378:95–100.

Florencio MH, Pires E, Castro AL, Nunes MR, Borges C, Costa FM (2004). Photodegradation of diquat and paraquat in aqueous solutions by titanium dioxide: Evolution of degradation reactions and characterisation of intermediates. Chemosphere; 55: 345–355.

Ford KA, Casida JE (2006). Unique and common metabolites of thiamethoxam, clothianidin, and dinotefuran in mice. Chemical Research in Toxicology; 19:1549–1556.

Frank MP, Graebing P, Chib JS (2002). Effect of soil moisture and sample depth on pesticide photolysis, Journal of Agricultural and Food Chemistry; 50: 2607–2614.

Fujishima A, Honda K (1972). Electrochemical photolysis of water at a semiconductor electrode. Nature; 238:37–38.

Galli C (2002). Degradación por medios bacterianos de compuestos químicos tóxicos. Comisión Técnica Asesora en: Ambiente y desarrollo sostenible, Buenos Aires, Argentina.

Gavrilescu M (2005). Fate of pesticides in the environment and its bioremediation. Engineering in Life Sciences; 5:497–526.

Gish TJ, Shirmohammadi A, Vyravipillai R, Wienhold BJ (1995). Herbicide leaching under tilled and no-tillage fields. Soil Science Society of America Journal; 59:895–901.

Glaze WH, Kwang JW, Chapin DH (1987). Chemistry of water treatment processes involving ozone, hydrogen peroxide and ultraviolet radiation. Ozone Science and Engineering; 9:335–352.

Goi A, Trapido M, Tuhkanen T (2004). A study of toxicity,biodegradability, and some by-products of ozonised nitrophenols. Advances in Environmental Research; 8:304–311.

Gong A,Ye CM, Wang XJ, Lei ZF, Liu, JM (2001). Dynamics and mechanism of ultraviolet photolysis of atrazine on soil surface. Pest Managment Science; 57:380–385.

Gonzalez LF, Sarria V, Sanchez OF (2010). Degradation of chlorophenols by sequential biological-advanced oxidative process using *Trametes pubescens* and TiO_2/UV. Bioresource Technology; 101:3493–3499.

Goswami DY, Blake DM (1996). Cleanup with sunshine. Mechanical Engineering; 118:56–59.

Grover IS, Singh S, Pal B (2013). The preparation, surface structure, zeta potential, surface charge density and photocatalytic activity of TiO_2 nanostructures of different shapes. Applied Surface Sciences; 280:366-372.

Grover IS, Singh S, Pal B (2014). Photodegradation of imidacloprid insecticide by Ag-deposited titanate nanotubes: A study of intermediates and their reaction pathways. Journal of Agriculture and Food Chemistry; doi.org/10.1021/jf5041614.

Guillard C, Pichat P, Huber G, Van CH (1996). The GC-MS analysis of organic intermediates from the TiO_2 photocatalytic treatment of water treatment contaminate by lindane (2,3,4,5,6-hexachlorocyclohexane). Journal of Advanced Oxidation Technologies; 1:53–60.

Habisreutinger SN, Mende LS, Stolarczyk JK (2013). Photocatalytic reduction of CO_2 on TiO_2 and othr semiconductors. Angewandte Chemie International Edition; 52:7372–7408.

Hebert VR, Miller GC (1990). Depth dependence of direct and indirect photolysis on soil surfaces. Journal of Agricultural and Food Chemistry; 38: 913–918.

Helble A, Schlayer W, Liechti P, Jenny R, Mobius C (1999). Advanced effluent treatment in the pulp and paper industry with a combined process of ozonation and fixed bed biofilm reactors. Water Science and Technology; 40:343–350.

Hennebole J (1998). Aerobic metabolism of imidacloprid, ^{14}C-NTN 33893, in an aquatic model ecosystem under xenon light and sunlight conditions. Bayer AG, Institute for Metabolism Research and Residue Analysis, Leverkusen-Bayerwerk, Germany. Report No. PF 4337.

Herrmann JM (1999). Water treatment by heterogeneous catalysis. Catalysis Science and Service, 1 (Environmental Catalysis); 171–194.

Herrmann JM, Guillard C, Arguello M, Aguera A, Tejedor A, Piedra L, Fernandez-Alba A (1999). Photocatalytic degradation of pesticide pirimiphos-methyl: Determination of the reaction pathway and identification of intermediate products by various analytical methods. Catalysis Today; 54:353–367.

Higarashi MM, Jardim WF (2002). Remediation of pesticide contaminated soil using TiO_2 mediated solar light. Catalysis Today; 76:201–207.

Hilarides RJ, Gray KA, Gurzetta J, Cortellucci N, Sommer C (1994). Radiolytic degradation of 2,3,7,8-TCDD in artificially contaminated soils. Environmental Science & Technology; 28:2249–2258.

Hindumathy CK, Gayathri V (2013). Effect of pesticide (chlorpyrifos) on soil microbial flora and pesticide degradation by strains isolated from contaminated soil. Journal of Bioremediation & Biodegradation; doi: 10.4172/2155-6199.1000178

Hong Q, Zhang Z, Hong Y, Shunpeng L (2007). A microcosm study on bioremediation of fenitrothion contaminated soil using *Burkholderia* sp. FDS-1, International Biodeterioration and Biodegradation; 59: 55–61.

Houston PL, Pignatello J (1999). Degradation of selected pesticide active ingredients and commercial formulations in water by the photo-assisted Fenton reaction. Water Research; 33:1238–1246.

Hu G, Y Zhao, B Liu, F Song, M You (2013). Isolation of an indigenous imidacloprid-degrading bacterium and imidacloprid bioremediation under simulated in situ and ex situ conditions. Journal of Microbiology and Biotechnology; 23:1617–1626.

Huang CP, Dong C, Tang Z (1993). Advanced chemical oxidation: its present role and potential future in hazardous waste treatment. Waste Management; 13:361–377.

Hustert K, Moza PN, Kettrup A (1999). Photochemical degradation of carboxin and oxycarboxin in the presence of humic substances and soil. Chemosphere; 38:3423–3429.

Ihara T, Miyoshi M, Iriyama Y, Matsumoto O, Sugihara S (2003). Visible-light-active titanium dioxide photocatalyst realized by an oxygen-deficient structure and by nitrogen doping. Applied Catalysis B Environmental; 42:403–409.

Ikehata K, El-Din MG (2005b). Aqueous pesticide degradation by ozonation and ozonebased advanced oxidation proceses: A review (Part II). Ozone Science and Engineering ; 27: 173–202.

Ikehata K, El-Din MG (2006). Aqueous pesticide degradation by hydrogen peroxide/ultraviolet irradiation and Fenton type advanced oxidation processes: a review. Journal of Environmental Engineering and Sciences; 5:81–135.

Ismail BS, Shamsuddin N (2005). Effects of alachlor and metolachor on microbial populations in the soil. Malaysian Journal of Microbiology; 1: 36–41.

Iwaya K, Kagabu S (1998). Biological properties of the chloronicotinyl insecticide imidacloprid: high selectivity and safer use in practice. Reviews in Toxicology; 2:121–132.

Jackson ML (1967). Soil Chemical Analysis, Asia Publishing House, Bombay; 498

Jadhav JP, Phugare SS, Dhanve RS, Jadhav SB (2010). Rapid biodegradation and decolorization of Direct Orange 39 (Orange TGLL) by an isolated bacterium Pseudomonas aeruginosa strain BCH. Biodegradation; 21:453–463.

Jafari N, Kermanshahi RK, Soudi MR, Mahvi AH, Gharavi S (2012). Degradation of a textile reactive azo dye by a combined biological-photocatalytic process: Candida tropicalis Jks2 -TiO_2/UV. Iranian Journal of Environmental Health Sciences & Engineering; 9: 33–35.

Janke D, Fritsche W (1985). Nature and significance of microbial cometabolism of xenobiotics. Journal of Basic Microbiology; 25:603–619.

Jansen M, Letschert HP (2000). Inorganic yellow-red pigments without toxic metals. Nature; 404:980–982.

Jeschke P, Nauen R, Schindler M, Elbert A (2011). Overview of the status and global strategy for neonicotinoids. Journal Agriculture and Food Chemistry; 59:2897–2908.

Jodeh S, Khalaf O, Obaid A, Hammouti B, Hadda T, Jadeh W, Hadded M, Iarad W (2014). Adsorption and kinetics of abamectin and imidacloprid in greenhouse soil in palestine. Journal of Materials and Environmental Science; 2: 571–580.

Johnsen K, Nielsen P (1999). Diversity of *Pseudomonas* strains isolated with King's B and Gould's S1 agar determined by repetitive extragenic palindromic-polymerase chain reaction, 16S rDNA sequencing and fourier transform infrared spectroscopy characterisation. FEMS Microbiology Letters; 173:155–162

Joia BS, Jaswinder K, Udean AS (2001). Persistence of ethion residues on/in chilli. Paper presented in the National Symposium on Integrated Pest Management (IPM) in horticulturalcrops, Bangalore, 17^{th}–19^{th} October 2001.

Joseph JM, Jacob TA, Manoj VM, Aravindakumar CT (2000). oxidative degradation of triazine derivatives in aqueous medium: A radiation and photochemical study. Journal of Agricultural and Food Chemistry; 48:3704–3709.

Kamble ST, Saran RK (2005). Effect of concentration on the adsorption of three termiticides in soil. Bulletin of Environmental Contamination and Toxicology; 75:1077–1085.

Kampfer P, Ruppel S, Remus R (2005). *Enterobacter radicincitans* sp. nov., a plant growth promoting species of the family Enterobacteriaceae. Systematic and Applied Microbiolog; 28: 213–221.

Kansal SK, Kundu P, Sood S, Lamba R, Umar A, Mehta, SK (2014). Photocatalytic degradation of the antibiotic levofloxacin using highly crystalline TiO_2 nanoparticles. New Journal of Chemistry; 38:3220–3226.

Karpouzas D G, Walker A (2000). Factors influencing the ability of *Pseudomonas putida* strains epI and II to degrade the organophosphate ethoprophos, Journal of Applied Microbiology; 89: 40–48.

Karunya S, Reetha D (2012). Biological degradation of chlorpyrifos and monocrotophos by bacterial isolates. International Journal of Pharmaceutical and Biological Archives; 3: 685–691.

Khan SUM, Al-shahry M, Ingler JWB (2002). Efficient photochemical water splitting by a chemically modified n-TiO_2. Science; 297:2243–2245.

Khodja AA, Sehili T, Pilichowski JF, Boule P (2001). Photocatalytic degradation of 2-phenylphenol on TiO_2 and ZnO in aqueous suspensions. Journal of Photochemistry and Photobiology A Chemistry; 141:231–239.

Kimura M, (1980). A simple method for estimating evolutionary rates of base substitutions through comparative studies of nucleotide sequences. Journal of Molecular Evolution; 16:111–120.

Kish H (1989). What is photocatalysis? In: Serpone N., Pelizzetti E. (Eds.) Photocatalysis fundamentals and applications. John Wiley and Sons. ISBN 0471626031. New York,USA.

Kitsiou V, Filippidis N, Mantzavinos D, Poulios I (2009). Heterogeneous and homogeneous photocatalytic degradation of the insecticide imidacloprid in aqueous solutions. Applied Catalysis B Environment; 86:27–35.

Koch R, Burkness E, Hutchison W, Rabaey T. Efficacy of systemic insecticide seed treatments for protection of early-growth-stage snap beans from bean leaf beetle (Coleoptera: Chrysomelidae) foliar feeding. Crop Protection; 24:734–742.

Koltzenburg S, Dombo P, Oetter G, Bratz M (2010). Comb polymers and use thereof for the production of active or effective ingredient formulations. USA.

Krohn J, Hellpointner E (2002). Environmental fate of imidacloprid. Pflanzenschutz-Nachrichten Bayer (Special edition); 55:1–25.

Ku Y, Jung I (1998). Decomposition of monocrotophos in aqueous solution by UV irradiation in the presence of titanium dioxide. Chemoshere; 37: 2589–2597.

Kulkarni AG, Kaliwal BB (2012). Proteomic Profiling of *Escherichia coli* in Response to Carbamate Pesticide–Methomyl. Insecticides Basic and Other Applications. Assessed at http://cdn.intechopen.com/pdfs-wm/27805.pdf on 28th May 2015.

Kumar J, Bansal A (2012). Photodegradation of amaranth in aqueous solution catalyzed by immobilized nanoparticles of titanium dioxide. International Journal of Environment Science and Technology; 9:47–484.

Kumar J, Bansal A (2013). A comparative study of immobilization techniques for the photocatalytic degradation of Rhodamine B using nanoparticles of titanium dioxide. Water Air Soil Pollution; 224: 1452–1462.

Lambropoulou DA, Konstantinou IK, Albanis TA, Fernandez-Alba AR (2011). Photocatalytic degradation of the fungicide fenhexamid in aqueous TiO_2 suspensions: identification of intermediates products and reaction pathways. Chemosphere; 83:367–378.

Lapertot M, Pulgarin C, Fernandez-Ibanez P, Maldonado MI, Perez-Estrada L, Oller I, Gernjak W, Malato S (2006b). Enhancing biodegradability of priority substances (pesticides) by solar photo-Fenton. Water Research; 40:1086–1094.

Laurent FM, Rathahao E (2003). Distribution of [(14)C]imidacloprid in sunflowers (Helianthus annuus L.) following seed treatment. Journal of Agricultural Food Chemistry; 51:8005–8010.

Ledakowicz S, Solecka M, Zylla R (2001). Biodegradation, decoourization and detoxification of textile wastewater enhanced by advanced oxidation processes. Journal of Biotechnology; 89:175–184.

Legrini O, Oliveros E, Braun AM (1993). Photochemical process for water treatment. Chemical Reviews; 93:671–698.

Lehto KM, Vuorimaa E, Lemmetyinen, H (2000). Photolysis of polycyclic aromatic hydrocarbons (PAHs) in dilute aqueous solutions detected by fluorescence. Journal of Photochemistry and Photobiology A Chemistry; 136:53–60.

Lhomme L, Brosillon S, Wolbert D (2007). Photocatalytic degradation of a triazole pesticide,cyproconazole, in water. Journal of Photochemistry and Photobiology A: Chemistry; 188: 34– 42.

Li XY, Zhao YG (1999). Advanced treatment of dyeing wastewater for reuse. Water Science and Technology; 39:249-255.

Liu L, Zhao GH, Pang YN, Lei YZ, Gao JX, Liu MC (2010). Integrated biological and electrochemical oxidation treatment for high toxicity pesticide pollutant. Industrial & Engineering Chemistry Research; 49:5496–5503.

Liu WP, Zheng W, Ma Y, Liu KK (2006). Sorption and degradation of imidacloprid in soil and water. Journal of Environmental Science and Health Part B; 41:623–634.

Liu Z, Dai Y, Huan Y, Liu Z, Sun L, Zhou Q, Zhang W, Sang Q, Wei H, Yuan S (2013). Different utilizable substrates have different effects on cometabolic fate of imidacloprid in *Stenotrophomonas maltophilia*. Applied Microbiology and Biotechnology; 97:6537–6547

Liu Z, Dai Y, Huang G, Gu Y, Ni J, Wei H, Yuan S (2011). Soil microbial degradation of neonicotinoid insecticides imidacloprid, acetamiprid, thiacloprid and imidaclothiz and its effect on the persistence of bioefficacy against horsebean aphid Aphis craccivora Koch after soil application. Pest Management Sciences; 67:1245–1252.

Lu LA, Ma YS, Kumar M, Lin JG (2011b). Photochemical degradation of carbofuran and elucidation of removal mechanism. Chemical Engineering Journal; 166: 150–156.

Litter MI (1999). Heterogeneous photocatalysis transition metal ions in photocatalytic systems. Applied Catalysis B Environmental; 23:89 –114.

Macrae IC, Alexander M (1965). Microbial degradation of selected herbicides in soil. Journal of Agricultural and Food Chemistry; 13:72–76.

Madhuban G, Dutta D, Jha SK, Kalra S, Bandyopadhyay S, and Das SK (2011). Biodegradation of imidacloprid and metribuzin by Burkholderia cepacia strain CH9. Pesticide Research Journal; 23:36–40.

Maheshwari M, Vyas, RK, Sharma M (2013). Kinetics, equilibrium and thermodynamics of ciprofloxacin hydrochloride removal by adsorption on coal fly ash and activated alumina. Desalination and Water Treatment; 51: 7241–7254.

Malato S, Blanco J, Richter C, Milow B, Maldonado MI (1999a). Solar photocatalytic mineralization of commercial pesticides: methamidophos. Chemosphere; 38:1145–1156.

Malato S, Blanco J, Vidal A, Richter C (2002a). Photocatalysis with solar energy at a pilot plant-scale: An overview. Applied Catalysis Environment Part B; 37:1–15.

Malato S, Caceres J, Aguera A, Mezcua M, Hernando D, Vial J, Fernandez-Alba AR (2001). Degradation of imidacloprid in water by photo-fenton and TiO_2 photocatalysis at a solar pilot plant: A comparative study. Environmental Science & Technology; 35: 4359–4366.

Mamy L, Vrignaud P, Cheviron N, Perreau F, Belkacem M, Brault A, Breuil S, Delarue G, Petraud, JP, Touton I, Mougin C, Chaplain V (2011). No evidence for the effect of soil compaction on the degradation and impact of isoproturon. Environmental Chemistry Letters; 9:145–150.

Mapa RB, Green RE, Santo L (1986). Temporal variability in soil hydraulic properties with wetting and drying subsequent to tillage. Soil Science Society of America Journal; 50: 1133–1138.

Marco A, Esplugas S, Saum G (1997). How and why to combine chemical and biological processes for wastewater treatment. Water Science and Technology; 35:321–327.

Martinez-Huitle CA, De-Battisti A; Ferro S, Reyna S, Cerro M, Quiroz MA (2008). Removal of the methamidophos pesticide from aqueous solution by electrooxidation using Pb/PbO_2, Ti/SnO_2 and Si/BDD electrodes. Environmental Science and Technology; 42:6929–6935.

Masten SJ, Davies SH (1994). The use of ozonation to degrade organic contaminants in wastewaters. Environmental Science and Technology; 28:180–185.

Miethling R, Karlson U (1996). Accelerated mineralization of pentachlorophenol in soil upon inoculation with *Mycobacterium chlorophenolicum* PCP I and *Sphingomonas chlorophenolica* RA 2, Applied and Environmental Microbiology; 62: 4361–4366.

Miller RM, Singer GM, Rosen JD, Bartha R (1988). Sequential degradation of chlorophenols by photolytic and microbial treatment. Environmental Science and Technology; 22:1215–1219.

Moring JB, Kennedy JH, Wiggins JH (1992). Assessment of the potential ecological and biological effects of NTN 33893 on aquatic ecosystems as measured in fibreglass pond systems. Report prepared by Miles Inc., Agriculture Division. Bayer Crop Science Report No. 102600.

Muhamad SG (2010). Kinetic studies of catalytic photodegradation of chlorpyrifos insecticide in various natural waters, Arabian journal of Chemistry; 3:127–133.

Mukherjee I, Gopal M (2000). Environmental behaviour and translocation of imidacloprid in eggplant, cabbage and mustard. Pest Management Science; 56: 932–936.

Muller P (1994). Glossary of terms used in physical organic chemistry (IUPAC recommendation 1994). Pure and Applied Chemistry; 66:1077–1184.

Mulye HS (1995). Environmental evaluation of imidacloprid insecticide and the end-use product Admire 240F. Submission Numbers: 94-1706 and 94-1705. Pesticides Division, Commercial Chemicals Evaluation Branch, Environmental Protection Service, Environment Canada.

Muszkat L, Bi L, Feigelson L (1995). Solar photocatalytic mineralization of pesticides in polluted waters. Journal of Photochemistry and Photobiology A Chemistry; 87:85–88.

Muszkat L, Bir L, Feigelson L (1992). Solar photodegradation of xenobiotic contaminants in polluted well water. Journal of Photochemistry and Photobiology A Chemistry; 65: 409–417.

Nagaveni K, Sivalingam G, Hegde MS, Madras G (2004b). Solar photocatalytic degradation of dyes: High activity of combustion synthesized nano-TiO_2. Applied Catalysis B Environmental; 48:83–93.

Nakata K, Fujishima A(2012). TiO_2 photocatalysis: Design and applications. Journal of Photochemistry and Photobiology C Photochemistry Reviews; 13:169–189.

Naldoni A, Arienzo MD, Altomare M, Marelli M, Scotti R, Morazzoni F, Selli E, Santo VD (2013). Pt and Au/TiO_2 photocatalysts for methanol reforming: Role of metal

nanoparticles in tuning charge trapping properties and photoefficiency**.** Applied Catalysis B Environmental; 130–131:239 – 248.

Nauen R, Hungenberg H, Tollo B, Tietjen K, Elbert A (1998). Antifeedant-effect, biological efficacy and high affinity binding of imidacloprid to acetylcholine receptors in tobacco associated Myzus persicae (Sulzer) and Myzus nicotianae Blackman (Homoptera: Aphididae). Pesticide Science; 53:133–140.

Nishino SF, Spain JC (1993). Degradation of nitrobenzene by a *Pseudomonas pseudoalcaligenes.* Applied and Environmental Microbiology; 59:2520–2525.

Nemeth-Konda L, Füleky G, Morovjan G, Csokan P (2002). Sorption behaviour of acetochlor, atrazine, carbendazim, diazinon,imidacloprid and isoproturon on Hungarian agricultural soil Chemosphere; 48: 545-552.

Oi M (1999). Time-dependent sorption of imidacloprid in two different soils. Journal of Agricultural and Food Chemistry; 47:327–332.

Oller I, Gernjak W, Perez L, Sanchez JA, Malato S (2006). Solar photocatalytic degradation of some hazardous water-soluble pesticides at pilot-plant scale. Journal of Hazardous Materials; 138:507– 517.

Olsen SR, Cole CV, Watanabe FS, Dean LA (1954). Estimation of available phosphorous by extraction with sodium bicarbonate, USDA Circ, 939; 1–19.

Ortiz-Hernandez ML, Sanchez-Salinas E, Olvera-Velona A, Folch-Mallol JL (2011). Pesticides in the Environment: Impacts and its Biodegradation as a Strategy for Residues Treatment, Pesticides - Formulations, Effects, Fate, Margarita Stoytcheva (Ed.), Intech. doi: 10.5772/13534.

Orme S, Kegley S (2003). PAN Pesticide Database, Pesticide Action Network. Imidacloprid. www.pesticideinfo.org. Accessed: 30 May 2015.

Pandey G, Dorrian SJ, Russell RJ, Oakeshott JG (2009). Biotransformation of the neonicotinoid insecticides imidacloprid and thiamethoxam by *Pseudomonas sp*. 1G. Biochemical and Biophysical Research Communications; 380:710–714.

Paszko T (2006). Sorptive behavior and kinetics of carbendazim in mineral soils. Polish Journal of Environmental Studies; 15:449–456.

Pathirana HMKK, Maithreepala RA (1997). Photodegradation of 3,4-dichloropropionamide in aqueous TiO_2 suspensions. Journal of Photochemistry and Photobiology A Chemistry; 102:273–277.

Peris CE, Terol J, Mauri AR, Guardia M, Pramauro E (1993). Continuous flow photocatalytic degradation of carbaryl in aqueous media. Journal of Environmental Science and Technology Health Part B; 28:431–440.

Peyton GR, Huang FY, Burleson JL, Glaze WH (1982). Destruction of pollutants in water with ozone in combination with ultraviolet radiation. General principles and oxidation of tetrachloroethylene. Environmental Science and Technology; 16:449–453.

Phugare S, Kalyani D, Gaikwad Y, and Jadhav J, (2013). Microbial degradation of imidacloprid and toxicological analysis of its biodegradation metabolites in silkworm (Bombyx mori). Chemical Engineering Journal; 230, 27-35.

Ping L, Zhang C, Zhu Y, Wu M, Dai F, Hu X, Zhao H, Li, Z (2010). Imidacloprid adsorption by soils treated with humic substances under different pH and temperature conditions. African Journal of Biotechnology; 9:1935–1940.

Pierobon M, Bouillo N, Lange RFM, Meyer K, Kolter K (2008) Use of amphiphilic copolymers as solubilising agents.http://www.google.com/patents/US20080153925.

Pirkanniemi K, Sillanpaa M (2002). Heterogeneous water phase catalysis as an environmental application: A review. Chemosphere; 48:1047–1060.

PMRA (Pest Management Regulatory Agency) (2001). Imidacloprid. Regulatory Note. REG2001-11. Ottawa: Health Canada, Pest Management Regulatory Agency. Assessed at http://www.pmra-arla.gc.ca/english/pdf/reg/reg2001-11-e.pdf on 26th May 2015.

PPDB (2012) Pesticide properties database. Accessed at http://sitem.herts.ac.uk/aeru/ppdb/en/index.htm on 21st May, 2015

Pusino, Fiori MG, Braschi I, Gessa, C (2003). Adsorption and desorption of triasulfuron by soil. Journal of Agriculture and Food Chemistry; 51:5350–5354.

Rabindranathan S, Devipriya S, Yesodharan S (2003). Photocatalytic degradation of phosphamidon on semiconductor oxides. Journal of Hazardous Materials; 102:217–29.

Radwan A (2005). Water treatment by heterogeneous photocatalysis: An Overview. SWCC acquired experience symposium.

Rajeshwar K (1996). Photochemical strategies for abating environmental pollution. Chemistry and Industry; 12:454–458.

Ramadan M A, El-Tayeb OM, Alexander M (1990). Inoculum size as a factor limiting success of inoculation for biodegradation, Applied and Environmental Microbiology; 56: 1392–1396.

Rauf MA, Meetani MA, Hisaindee S (2011). An overview on the photocatalytic degradation of azo dyes in the presence of TiO_2 doped with selective transition metals. Desalination; 276: 13–27.

Redlich D, Shahin N, Ekici P, Friess A, Parlar H (2007). Kinetic study of the photoinduced degradation of imidacloprid in aquatic media. Clean; 35: 452–458.

Roberts TR, Hutson DH (1999). Imidacloprid. Metabolic Pathways of Agrochemicals - Part 2: Insecticides and Fungicides, The Royal Society of Chemistry: Cambridge, UK: 111–120.

Rojo F (2010). Carbon catabolite repression in Pseudomonas: Optimizing metabolic versatility and interactions with the environment. FEMS Microbiology Reviews; 34:658–684**.**

Romero E, Dios G, Mingorance MD, Matallo MB, Pena A, Sanchez-Rasero F (1998). Photodegradation of mecoprop and dichlorprop on dry, moist and amended soil surfaces exposed to sunlight. Chemosphere; 37:577–589.

Rouchaud J, Gustin F, Wauters A (1994). Soil Biodegradation and Leaf Transfer of Insecticide Imidacloprid Applied in Seed Dressing in Sugar Beet Crops. Bulletin of Environmental Contamination and Toxicology; 53: 344–350.

Rousseaux S, Hartmann A, Soulas G (2001). Isolation and characterisation of new gram-negative and gram-positive atrazine degrading bacteria from different French soils. Microbiology Ecology; 36: 211–222.

Sabbagh GJ, Lenz MF, Fisher JM, Arthur EL (2002). Significance of binding on imidacloprid degradation in soils, and effects of soil characteristics on imidacloprid adsorption capacity. Report No. 200327. Bayer CropScience, Stilwell, Kansas.

Sabourmoghaddam N, Zakaria MP, Omar D (2014). Evidence for the microbial degradation of imidacloprid in soils of Cameron Highlands. Journal of the Saudi Society of Agricultural Sciences; doi:10.1016/j.jssas.2014.03.002.

Sadeghi AM, Isensee AR, Shelton DR (1998). Effect of tillage age on herbicide dissipation: A side-by-side comparison using microplots. Soil Sciences; 163:883–890.

Sahoo MK, Sinha BM, Marbaniang, Naik DB (2011). Degradation and mineralization of Calcon using UV365/H2O2 technique: Influence of pH. Desalination; 280:266–272.

Saien J, Khejrianjoo S (2008). Degradation of the fungicide carbendazim in aqueous solutions with UV/TiO_2 process: optimization, kinetics and toxicity studies. Journal of Hazardous Materials; 157: 269–276.

Saitou N, Nei M (1987). The neighbor-joining method: A new method for reconstructing phylogenetic trees. Molecular Biology and Evolution; 4:406–425.

Sakkas VA, Islam MA, Stalikas, Albanis TA (2010). Photocatalytic degradation using design of experiments: A review and example of the congo red degradation; Journal of Hazardous Materials; 175: 33–44.

Sarkar MA, Biswas PK, Roy S, Kole RK, Chowdhury A (1999). Effect of pH and type of formulation on the persistence of imidacloprid in water. Bulletin of Environmental Contamination and Toxicology; 63: 604–609.

Sarkar MA, Roy S, Kole RK, Chowdhury A (2001). Persistence and metabolism of imidacloprid in different soils of West Bengal. Pest Management Science; 57: 598–602.

Sarria V, Parra S, Adler N, Peringer P, Benitez N, Pulgarin C (2002). Recent developments in the coupling of photoassisted and aerobic biological processes for the treatment of biorecalcitrant compounds. Catalysis Today; 76:301-315.

Schmuck R, Stadler T, Schmidt HW (2003). Field relevance of a synergistic effect observed in the laboratory between an EBI fungicide and a chloronicotinyl insecticide in the honey bee (Apis mellifera L., Hymenoptera). Pest Management Science; 59: 279–286.

Scholz K, Spiteller M (1992). Influence of groundcover on the degradation of ^{14}C imidacloprid in soil. Brighton Crop Protection Conference: Pests and Diseases; 2: 883–888.

Scott JP, Ollis DF (1995). Integration of chemical and biological oxidation processes for waste water treatment: Review and Recommendations. Environmental Progress; 14: 88–103.

Scott JP, Ollis DF (1995). Integration of chemical and biological oxidation processes for waste water treatment: Review and Recommendations. Environmental Progress; 14: 88–103.

Shah MP (2013). Combined Application of Biological-Photocatalytic Process in Degradation of Reactive lack Dye: An Excellent Outcome. American Journal of Microbiological Research; 4:92–97.

Shahgholi H. (2014). Factors controlling degradation of pesticides in the soil environment: A Review Agriculture Science & development; 3: 273-278.

Sharma AK, Lee BK (2013). Lead sorption onto acrylamide modified titanium nanocomposite from aqueous media. Journal of Environmental Management; 128:787–797.

Sharma S, Singh B, and Gupta VK (2014). Biodegradation of imidacloprid by consortium of two soil isolated *Bacillus* sp. Bulletin of Environmental Contamination and Toxicology; 93:637–642.

Sharma T, Rajor A, Toor AP (2015). Potential of *Enterobacter* sp. strain ATA1 on imidacloprid degradation in soil microcosm: Effects of various parameters. doi:10.1002/ep.12115.

Shetti A, Kaliwal B (2012). Imidacloprid induced intoxication in soil isolate *Brevundimonas* Sp. Mj.15. International Journal of Life Sciences and Pharmaceutical Research; 2: 105–117.

Shetti AA, Kaliwal BB (2012). Biodegradation Of Imidacloprid By Soil Isolate *Brevundimonas* sp. MJ15. International Journal of Current Research; 10:100–106.

Shetti AA, Kaliwal RB, Kaliwal BB (2014). Imidacloprid induced intoxication and its biodegradation by soil isolate *Bacillus weihenstephanensis*. British Biotechnology Journal; 4: 957–969.

Si YB, Yue YD, Chen HM, Zhou DM (2004). Photodegradation of bensulfuron-methyl on soil surface. Pest Managment Science; 60:286–290.

Singh BK, Walker A, Wright DJ (2006). Bioremedial potential of fenamiphos and chloropyrifos degrading isolates: influence of different environmental conditions. Soil Biology and Biochemistry; 38: 2682–2693.

Singh DK (2008). Biodegradation and bioremediation of pesticide in soil: Concept, method and recent developments. Indian Journal of Microbiology; 48:35–40.

Sinha AK, Jana S, Pande S, Sarkar S, Pradhan M, Basu M, Saha S, Pal A, Pal T (2009). New hydrothermal process for hierarchical TiO_2 nanostructures. CrystEngComm; 11:1210–1212.

Sivalingam G, Nagaveni K, Hegde MS, and Madras G (2003). Photocatalytic degradation of various dyes by combustion synthesized nano anatase TiO_2. Applied Catalysis B Environmental; 45:23–38.

Sood S, Mehta SK, Umar A, Kansal SK (2014). The visible light-driven photocatalytic degradation of Alizarin red S using Bi-doped TiO_2 nanoparticles New Journal of Chemistry; 38:3127–3136.

Spiteller M (1993). Aerobic metabolism of imidacloprid, ^{14}C-NTN 33893, in an aquatic model ecosystem. Bayer AG, Institute for Metabolism Research, Leverkusen-Bayerwerk, Germany. Report No. PF 3950.

Starner K, Goh KS (2012). Detection of the neonicotinoid insecticide imidacloprid in surface waters of three agricultural regions of California, USA, 2010–2011. Bulletin of Environmental Contamination and Toxicology; 88:316–321.

Stenrod M, Charnay MP, Benoit P, Eklo OM (2006). Spatial variability in microbial soil characteristics in two sandy loam norvegian soils as affected by surface topographical variability. Soil Biology & Biochemistry; 38:962–971.

Stephan R, Trappen S, Cleenwerck I, Vancanneyt M, Vos P, Lehner A (2007). *Enterobacter* turicensis sp.nov. and *Enterobacter* heleticus sp. nov. Isolated from fruit powder. International Journal of Systematic and Evolutionary Microbiology; 57:820-826.

Strong DT, Sale PWG, Helyar KR (1998). The influence of the soil matrix on nitrogen mineralisation and nitrification (II) The pore system as a framework for mapping the organisation of the soil matrix. Australian Journal of Soil Research; 36:855–872.

Suryaman D, Hasegawa K, Kagaya S (2006). Combined biological and photocatalytic treatment for the mineralization of phenol in water. Chemosphere; 65:2502–2506.

Tamer E, Aly AM, Ossama ET, Bo M, Benoit G (2007). Sequential photochemicalbiological degradation of chlorophenols. Chemosphere; 66:2201–2209.

Tamer E, Hamid Z, Aly AM, Ossama ET, Mattiasson B, Benoit G (2006). Sequential UV–biological degradation of chlorophenols. Chemosphere; 63: 277-284.

Tamimi M, Qourzal S, Assabbane A, Chovelon JM, Ferronato C, Ait-Ichou Y (2006). Photocatalytic degradation of pesticide methomyl: Determination of the reaction pathway and identification of intermediate products. Photochemical & Photobiological Sciences; 5:477–482.

Tanaka K, Robeldo SM, Hisanaga T, Ramli ZA, Bakar WA (1995). Photocatalytic degradation of 3,4-xylyl N-methylcarbamate (MPMC) and other carbamate pesticides in aqueous TiO_2 suspensions. Journal of Molecular Catalysis A; 144:425–430.

Texier I, Ouazzani J, Delaire J, Giannotti C (1999). Study of the mechanisms of the photodegradation of atrazine in the presence of two photocatalysts: TiO_2 and $Na_4W_{10}O_{32}$. Tetrahedron; 55:3401–3412.

Thuyet DQ, Yamazaki K, Phong TK, Watanabe H, Nhung DTT, Takagi K (2010). determination of imidacloprid in paddy water and soil by liquid chromatography electrospray ionization-tandem mass spectrometry., Journal of Analytical Chemistry; 65: 843–847.

Tixier C, Sancelme M. Ait AS. Widehem P, Bonnemoy F, Cuer A, Truffaut A, Veschambre H (2002). Biotransformation of phenylurea herbicides by a soil bacterial strain, Arthrobacter sp. N2: structure, ecotoxicity and fate of diuron metabolite with soil fungi. Chemosphere; 46:519–526.

Tomizawa M, Casida JE (2003). Selective toxicity of neonicotinoids attributable to specificity of insect and mammalian nicotinic receptors. Annual Review of Entomology; 48:339–364.

Tomizawa M, Casida JE (2005). Neonicotinoid insecticide toxicology: mechanisms of selective action. Annual Review of Pharmacology and Toxicology; 45:247–268.

Toor AP, Verma A, Jotshi C, Bajpai PK, Singh V (2005). Photocatalytic degradation of 3, 4 Dichlorophenol using TiO_2 in a shallow pond slurry reactor. Indian Journal of Chemical Technology; 12:75–81.

Toor AP, Verma A, Singh V, Jotshi CK, Bajpai PK (2006). Photocatalytic degradation of Direct Yellow 12 dye using UV/TiO_2 in a shallow pond slurry reactor. Dyes and Pigments; 68:53–60.

Tomlin CDS (Ed.) (2000). The Pesticide Manual, 12th Edition. British Crop Protection Council, Surrey, United Kingdom.

Topp E, Vallayes T, Soulas G (1997). Pesticides: Microbial degradation and effects on microorganisms. Modern Soil Microbiology; 547–575.

United States Environmental Protection Agency (2005). Pesticide Fate Database. Environmental Fate and Effects Division of the Office of Pesticide Programs. Accessed at http://cfpub.epa.gov/pfate/home.cfm on 22nd May 2015.

Valente JS, Tzompantzi F, Prince J, Cortez JGH, Gomez R (2009). Adsorption and photocatalytic degradation of phenol and 2,4 dichlorophenoxiacetic acid by Mg-Zn-Al layered double hydroxides. Applied Catalysis B Environmental; 90:330–338.

Van Dijk TC, Marja A, V Staalduinen, Jeroen PVS (2013). Macro-Invertebrate decline in surface water polluted with imidacloprid. doi:10.1371/journal.pone.0062374.

Van Eerd L, Hoagland RE, Zablotowicz RM, Hall JC (2003). Pesticide metabolism in plants and microorganisms. Weed Science; 51:472–495.

Verma A, Sheron M, Toor AP (2013). Titanium dioxide mediated photocatalytic degradation of malathion in aqueous phase. Indian Journal of Chemical Technology; 20:46–51.

Vieuble-Gonod L, Chenu C, Soulas G (2003). Spatial variability of 2,4-Dichlorophenoxyacetic acid (2,4-D) mineralisation potential at a millimetre scale in soil. Soil Biology & Biochemistry; 35:373–382.

Villaverde J, Maqueda C, Undabeytia T, Morillo E (2007). Effect of various cyclodextrins on photodegradation of a hydrophobic herbicide in aqueous suspensions of different soil colloidal components. Chemosphere; 69:575–584.

Viswanathan B (2003). Photocatalytic processes – Selection criteria for the choice of materials. Bulletin Catalysis Society of India; 2:71–74.

Vikelsoe J, Johansen E (2000). Estimation of dioxin emission fire from chemicals. Chemosphere; 40:165–175.

Walker A, Exposito MJ, Bending GD, Smith VJR (2001). Spatial variability in the degradation rate of isoproturon in soil. Environmental Pollution; 111:407–415.

Walkley A, Black C.A, (1934). An examination of the Degtjareff method for determining soil organic matter and a proposed modification of the chromic acid titration method. Soil Science; 37: 29-38.

Wang G, Yue W, Liu Y, Li F, Xiong M, Zhang H (2013). Biodegradation of the neonicotinoid insecticide acetamiprid by bacterium *Pigmentiphaga* sp. strain AAP-1 isolated from soil. Bioresource Technology; 138:359–368.

Wang G, Zhang J, Wang L, Liang B, Chen KLS, Jiang J (2010). Co-metabolism of DDT by the newly isolated bacterium *Pesudoxanthomonas* sp.wax. Brazilian Journal of Microbiology; 41:431–438.

Wang J, Chen S, Quan X, Zhao H, Zha Y (2007). Enhanced Photodegradation of PNP on soil surface under UV irradiation with TiO_2. Soil & Sediment Contamination; 16, 413–421.

Wang J, Hirai H, Kawagishi H (2012). Biotransformation of acetamiprid by the white-rot fungus Phanerochaete sordida YK-624. Applied Microbiology and Biotechnology; 93:831–835.

Westwood F, Bean KM, Dewar AM, Bromilow RH, Chamberlain K (1998). Movement and persistence of [14C] imidacloprid in sugarbeet plants following application to pelleted sugar-beet seed. Pesticide Science; 52: 97–103.

Xu X, Ji F, Fan Z, He L (2011). Degradation of Glyphosate in Soil Photocatalyzed by $Fe_3O_4/SiO_2/TiO_2$ under Solar Light. International Journal of Environmental Research and Public Health; 8:1258–1270.

Xu Z, Xie Q, Shuo C, Hui-min Z, Yu L (2007). Photocatalytic remediation of hexachlorocyclohexane contaminated soils using TiO_2 and montmorillonite composite photocatalyst. Journal of Environmental Sciences; 19:358–361.

Yamamoto I, Casida JE (1999). Neonicotinoid Insecticides and the Nicotinic Acetylcholine Receptor, Springer-Verlag,Tokyo, Japan.

Yao XH, Min H (2006). Isolation, characterization and phylogenetic analysis of a bacterial strain capable of degrading acetamiprid. Journal Environmental Sciences–China; 18:141–146.

Yeber MC, Rodriguez J, Freer J, Baeza J, Duran N, Mancilla HD (1999). Advanced oxidation of a pulp mill bleaching wastewater. Chemosphere; 39:1679–1688.

Yoshida H (1989). Hydrolysis of NTN 33893. Yuki Institute, Ibaraki, Japan. 34 pp. Miles Report No. 99708.

Yu JC, Yu JG, Ho WK, Jiang ZT, Zhang LZ (2002). Effects of F-doping on the photocatalytic activity and microstructures of nano crystalline TiO_2 powders. Chemistry of Materials; 14:3808–3816.

Yun Q, Lin Z, Xin T (2009). Cometabolism and immobilized degradation of monochlorobenzoate by Rhodococcus erythropolis. African Journal of Microbiology; 9: 482–486.

Zabar R, Komel T, Fabjan J, Kralj MB, Trebse P (2010). Photocatalytic degradation with immobilised TiO_2 of three selected neonicotinoid insecticides: Imidacloprid, thiamethoxam and clothianidin. Chemosphere; 89:293–301.

Zaleska A, Hupka J, Wiergowski M, Bizuik M (2000). Photocatalytic degradation of lindane, p,p'-DDT and methoxychlor in an aqueous environment. Journal of Photochemistry and Photobiology A Chemistry; 135:213–220.

Zeng Y, Hong PKA, Wavrek DA (2000). Integrated Chemical–biological treatment of benzo(a)pyrene. Environmental Science & Technology; 34:854–862.

ZhaoYJ, DaiYJ, Yu CG, Luo J, Xu WP, Ni JP (2009). Hydroxylation of thiacloprid by bacterium *Stenotrophomonas maltophilia* CGMCC1.1788. Biodegradation; 20:761–768.

Zheng W, W Liu (1999). Kinetics and mechanism of the hydrolysis of imidacloprid. Pesticide Science; 55: 482–485.

Zhou G, Wang Y, Zhai S, Ge F, Liu Z, Dai Y, Yuan S, and Hou J (2013). Biodegradation of the neonicotinoid insecticide thiamethoxam by the nitrogen-fixing and plant-growth-promoting *Rhizobacterium Ensifer adhaerens* strain TMX-23. Applied Microbiology Biotechnology; 97:4065–4074.

Bioremediation Journal, 18:227–235, 2014

ISSN: 1088-9868 print / 1547-6529 online
DOI: 10.1080/10889868.2014.918575

Taylor & Francis

Degradation of Imidacloprid in Liquid by *Enterobacter* sp. Strain ATA1 Using Co-Metabolism

Teena Sharma,[1] Anita Rajor,[1] and Amrit Pal Toor[2]
[1]Department of Biotechnology and Environmental Science, Thapar University, Patiala, Punjab, India
[2]University Institute of Chemical Engineering and Technology, Panjab University, Chandigarh, India

ABSTRACT Imidacloprid (IMI), a potent insecticide, belongs to the neonicotinoid family and is of great concern due to the fact that its persistence in the soil is a threat to both plants and vertebrates. The present study was aimed at the isolation and characterization of a bacterial strain from paddy field soil at Punjab (India), which has a history of 9–10 years of imidacloprid contamination. Among the various isolates, a soil bacterium was selected and identified by 16S rRNA gene sequencing as *Enterobacter* sp. strain ATA1. It grew well in pH ranging from 6.0 to 7.0 at 37°C, and it was found to be a competent bacterium for the degradation of IMI. The presence of glucose in minimal salt medium (MMG; 0.1% w/v) as compared with any other co-substrate provokes the dissipation of IMI as a co-metabolite. Initially, incubation of IMI for 72 h in the MMG resulted in 30–40% degradation; thereafter, no significant change in its amount was found until 15 days of incubation, which explains the disappearance of any viable cells in the medium. Among the various identified metabolites, imidacloprid urea ($m/z = 212$) and imidacloprid guanidine ($m/z = 211$) were found to be the end products of IMI degradation, whereas others remained unidentified ($m/z = 99$ and $m/z = 119$).

KEYWORDS co-metabolism, *Enterobacter* sp. strain ATA1, imidacloprid, metabolites, microbial degradation

INTRODUCTION

Insecticides are necessary for the protection of crops from unwanted insects, which affects the production of food worldwide (Tomlin 1997). An increase in the demand for agro-products has resulted in greater and greater application of insecticides to crops. Imidacloprid [(*EZ*)-1-(6-chloro-3-pyridylmethyl)-*N*-nitroimidazolidin-2-ylideneamine; IMI] (Figure 1a) was the first member of the neonicotinoid family to be launched in 1991 and was registered globally in approximately 120 countries, including India (Krohn and Helliponter 2002). It is a systemic chloronicotinyl insecticide that is used for soil, seed, and foliar applications for the control of sucking insects, including aphids, thrips,

Address correspondence to Amrit Pal Toor, University Institute of Chemical Engineering and Technology, Panjab University, Chandigarh, 160014 India. E-mail: aptoor@yahoo.com

Color versions of one or more of the figures in the article can be found online at www.tandfonline.com/lbrm.

Potential of *Enterobacter* sp. Strain ATA1 on Imidacloprid Degradation in Soil Microcosm: Effects of Various Parameters

Teena Sharma,[a] Anita Rajor,[a] and Amrit Pal Toor[b]

[a]School of Energy and Environment, Thapar University, Patiala, 147004 Punjab, India

[b]Dr. S.S.Bhatnagar University Institute of Chemical Engg. & tech., panjab University, Chandigarh, 160014 India; aptoor@yahoo.com (for correspondence)

Published online 00 Month 2015 in Wiley Online Library (wileyonlinelibrary.com). DOI 10.1002/ep.12115

Previously isolated strain ATA1 of Enterobacter *sp. was used in this work to study various factors affecting degradation of IMI in soil microcosm. Minimal salt medium containing 1% (w/v) glucose was found to be suitable as carbon source for inoculums preparation. Effect of various parameters including soil pH, inoculum size, initial concentration of IMI and flooding of soil for the degradation of imidacloprid in soil were investigated. Strain ATA1 has effectively degraded imidacloprid of range 25–50 mg kg^{-1} when soil was spiked with different initial concentration of IMI (25–100 mg kg^{-1}) as verified by HPLC analysis. Degradation rate was slower in soil with lower pH compare to neutral pH of soil. An inoculums size of 2×10^7 CFU g^{-1} of soil was found to be suitable at pH 7 for degrading IMI of 50 mg kg^{-1}. Flooding of IMI spiked soil has also shown significant degradation as compare to nonflooded soil. Metabolites produced after IMI degradation under optimized parameters were identified by GC-MS analysis. This model study could be used for removal of toxic compounds in field experiments.* © 2015 American Institute of Chemical Engineers Environ Prog, 00: 000–000, 2015

Keywords: imidacloprid, Enterobacter sp. strain ATA1, bioremediation, soil, factors

INTRODUCTION

Excessive and continuous dispersion of insecticides in the environment results in pollution of air, water, soil, and therefore is a threat to the mammals, since some of them are reported to be toxic in nature. Hence, a new class of insecticide namely neonicotenoid was introduced in 1984, which is found to exhibit comparative less toxicity towards the mammals. Among variety of members in this family, [(6-chloro-3-pyridylmethyl) -*N*-nitro-2-imidazolidinimine; (Figure 1) i.e., Imidacloprid (IMI) used to control a wide spectrum of insects on a broad range of crops and thus admitted over 120 nations world-wide [1]. Its continuous utilization for the past two decades, half life over 100 days results into accumulation of the IMI in the soil, therefore making it a hazard for environment [2,3]. This attracts the research interest regarding its dissipation (in soil slurry), parameters affecting its degradation and determination of its various metabolites, where some of them are found to be more toxic than IMI itself. Parameters which play a crucial role in the dissipation of IMI of soil such as pH, temperature, moisture content, presence of microorganism amount of organic matter, etc.

Regarding its degradation two major routes have been reported viz photocatalytically [4–6] and biologically [7,8]. However later approach is found to be more effective, since its easy operation, low cost, and complete destruction of pollutants. Both success and failure have been observed, when pure bacterial isolates capable of degrading pesticides in liquid media introduced into the soil [9,10]. Few reports have been published where degradation of IMI was done using various bacterial strains such as *Pseudomonas sp., Ieifsonia. sp., Burkholderia cepacia., Pseudomonas and Bacillaceae., Stenotrophomonas maltophilia* [7,11–14] in liquid media. However, very limited studies have been investigated regarding IMI biodegradation in soil and recently genus *Ochrobactrum* strain BCL1 degraded ~ 60 % IMI within 20 days for ex-situ bioremediation [15]. Hence a bacterial strain exhibiting higher activity for the IMI degradation in minimum time in soil is highly desirable.

In the previous work, isolation of bacterium *Enterobacter sp.* strain ATA1 (Gen Bank no. JX233483) was done which was used for co-metabolic degradation of IMI in liquid media [16]. No research has been done on IMI degradation using *Enterobacter sp.* strain in soil. Therefore, in the present work we have developed an effective technology for bioremediation of IMI contaminated soil where influence of various factors such as pH, initial concentration of IMI, inoculums size, and flooding in the soil have examined. In addition degradation of IMI was qualitatively studied in terms of metabolites formed through GC-MS technique.

MATERIALS AND METHODS

Chemicals and Media Used for Cultivation

Technical grade Imidacloprid (purity 99%) was obtained as gift sample from Bayer crop science India. All solvents (acetonitrile and methanol) used in the experimental were of HPLC grade, purchased from Merck. All other chemicals for minimal media preparation used were of high analytical

Additional Supporting Information may be found in the online version of this article.

RSC Advances

PAPER

View Article Online
View Journal | View Issue

Cite this: RSC Adv., 2015, 5, 25059

Photocatalytic degradation of imidacloprid in soil: application of response surface methodology for the optimization of parameters†

Teena Sharma,[a] Amrit Pal Toor*[b] and Anita Rajor[a]

The photocatalytic mineralization of imidacloprid (IMI) in soil to inorganic ions and the formation of various intermediates using TiO_2 as the photocatalyst have been investigated under UV light. Various parameters, *viz.*, catalyst concentration, soil depth and pH, intensity of light and initial concentration of IMI were optimized theoretically by using a central composite design based on a response surface methodology and were correlated with experimental results. The statistical analysis from the modelling results indicates that the degradation efficiency of IMI is affected by the depth of soil and the intensity of light, but the effects of the pH and the initial concentration of imidacloprid are more dominant. The optimum conditions obtained for the maximum degradation of imidacloprid were at pH = 3, intensity of UV light = 30 W m^{-2}, soil depth = 0.2 cm and initial concentration of imidacloprid = 10 mg kg^{-1} of soil. Under these optimum conditions, the highest degradation efficiency of 83% was achieved after 18 h of UV light irradiation. The identification of various photoproduced intermediates of IMI by LC-MS analysis revealed its degradation, whereas the increase in the formation of inorganic ions with time of UV light irradiation confirms its mineralization.

Received 4th February 2015
Accepted 25th February 2015

DOI: 10.1039/c5ra02224j

www.rsc.org/advances

1. Introduction

Soil, the ultimate sink for the accumulation of applied pesticides has attracted current research interest in-terms of the analysis of leaching behaviour, formation of intermediate products and the role of parameters affecting the degradation of pesticides. Upon contact, binding between the pesticide and the soil takes place, the extent of which depends on the nature, composition, texture, organic matter, pH, cation exchange capacity, electrical conductance and moisture of the soil.[1] The adsorption of pesticides into soil is a crucial factor, as it is well known to influence[2] their persistency, degradation and fate in the soil. For instance, adsorption and desorption processes have been reported[3] to determine the mobility of pesticides and were found to be influenced by the physico-chemical properties of soil. Some studies have shown that organic matter affects the binding of pesticide molecules to soil[4] and it is reported as a major controller component in the sorption, transformation, and transport of many organic pollutants in soil.[5]

Imidacloprid (IMI), part of the neonicotinoid family of insecticides and effective on insects that are resistant to carbamates, organophosphates and pyrethroids, has been used from the past two decades over 120 crops worldwide. Due to its high water solubility, leaching behaviour and half-life, this insecticide has contaminated the soil and water reservoirs nearby agricultural fields, and is of concern for the environment.[6] Its natural degradation is slow in soil under natural conditions, decomposing into, sometimes, more toxic and persistent intermediates than IMI itself. Therefore, efforts have been made to study the degradation and formation of metabolites from IMI biologically[7–11] in soil and broth. The degradation of IMI has also been studied photocatalytically in water[12,13] using TiO_2 as the photocatalyst. The available reports reveal that approx 95% degradation of IMI can be achieved by photocatalysis in water.[14] No studies have been reported on the photocatalytic degradation of IMI in soil; however, for other molecules such diuron,[15] PNP and polycyclic aromatic hydrocarbons,[16,17] the same process has been well reported. Therefore, using TiO_2 as the photocatalyst in the soil could be useful for the mineralization of IMI, which seems to be an unexplored concept. Hence, degradation of IMI using commercially available Degussa P25–TiO_2 as the photocatalyst under UV light irradiation in soil has been studied.

Generally, a single-variable-at-a-time (SVAT) method is used to study photocatalytic processes,[18,19] however, it suffers from some disadvantages such as time consumption and incapability to account for interactions between different variables and, hence, to predict optimum conditions.[20] On the contrary, central composite design (CCD) based on response surface methodology (RSM) has been found to be more convenient, as it

[a]School of Energy & Environment, Thapar University, Patiala 147004, Punjab, India
[b]Dr S. S. Bhatnagar University Institute of Chemical Engg & Tech., Panjab University, Chandigarh, 160014, India. E-mail: aptoor@pu.ac.in; Tel: +91-172-253-4904

† Electronic supplementary information (ESI) available. See DOI: 10.1039/c5ra02224j